APRIL 2023 DIAGNOSIS LIST

23-0401: malignant sarcomatoid neoplasm (bladder; GU path)
23-0402: epithelioid angiomyolipoma (kidney; GU path)
23-0403: HSV syringitis with CD30+ lymphoid infiltrate (skin; dermpath and ID path)
23-0404: vasitis nodosa (testis; GU path)
23-0405: rectal tonsil (large bowel; hemepath)
23-0406: intrahepatic cholangiocarcinoma with ductal plate malformation-like features
23-0407: myelokathexis (bone marrow; hemepath)
23-0408: artifactual cystic spaces in TURP (prostate; GU path)

23-0401

Ingold Huang/Emily Chan; UCSF

80ish M with remote h/o prostatic adenocarcinoma treated with radiation and androgen deprivation therapy. Now undergoes radical cystoprostatectomy for 12cm urinary bladder mass.

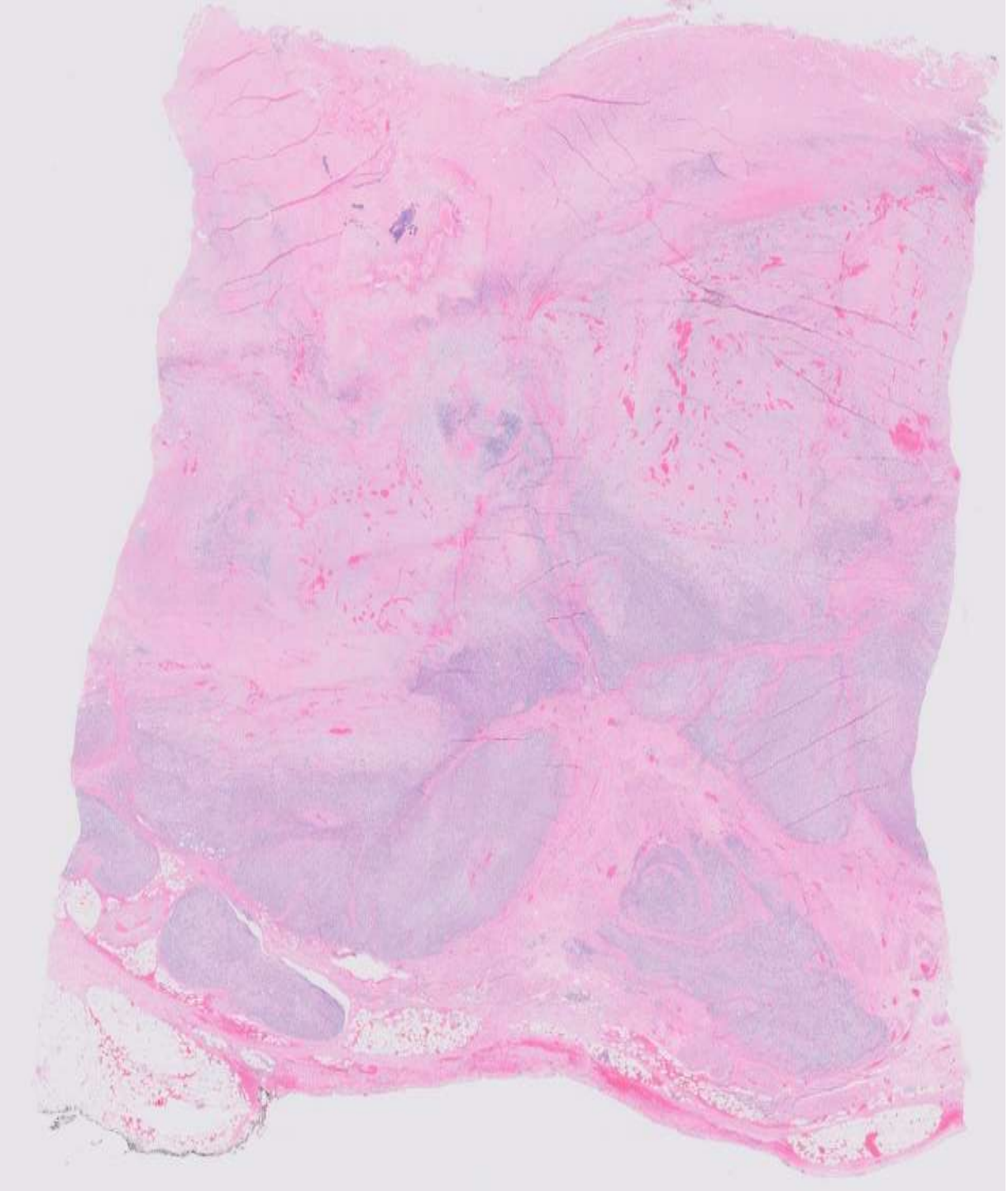

Urinary bladder, full-thickness cross section

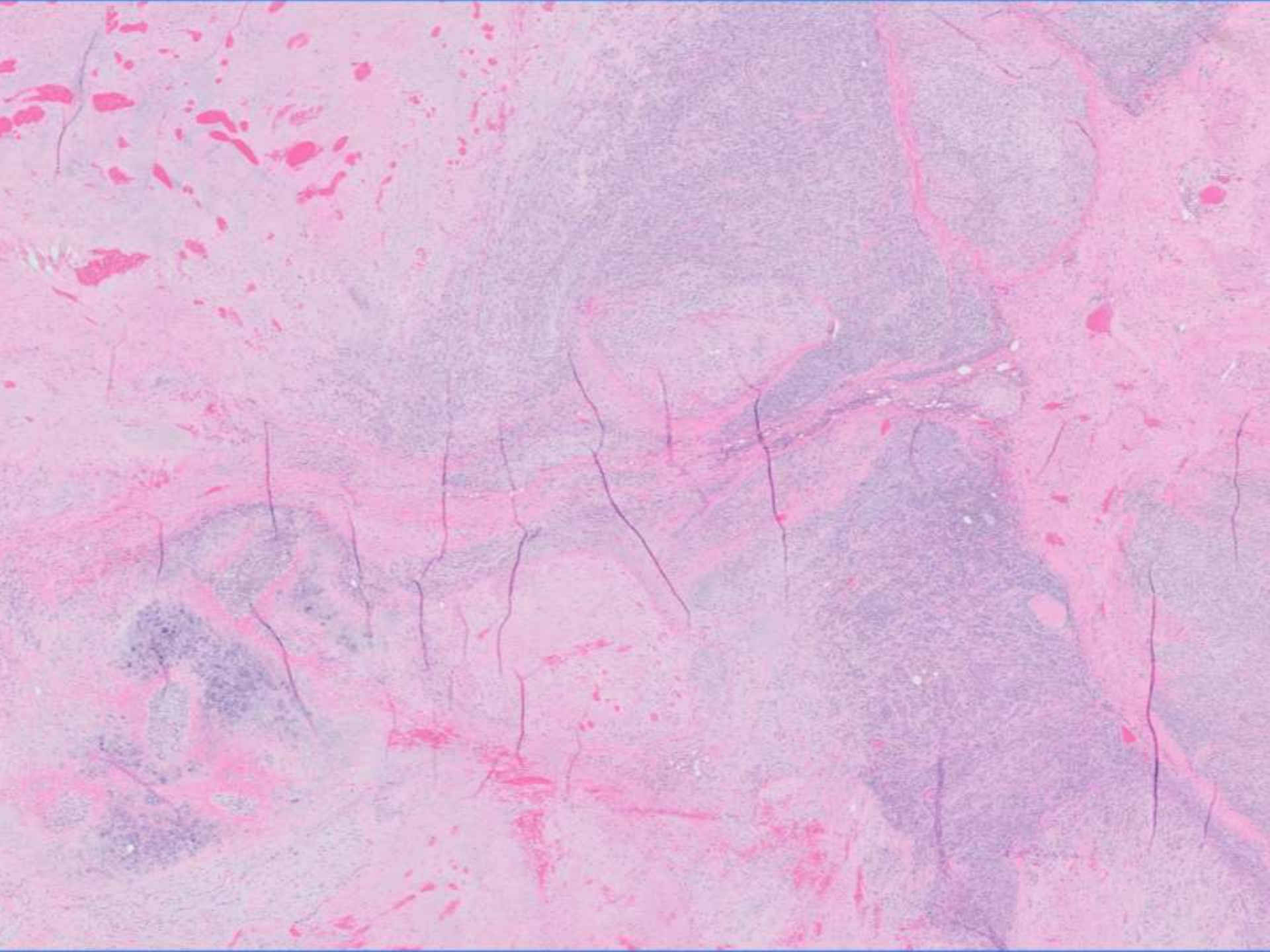

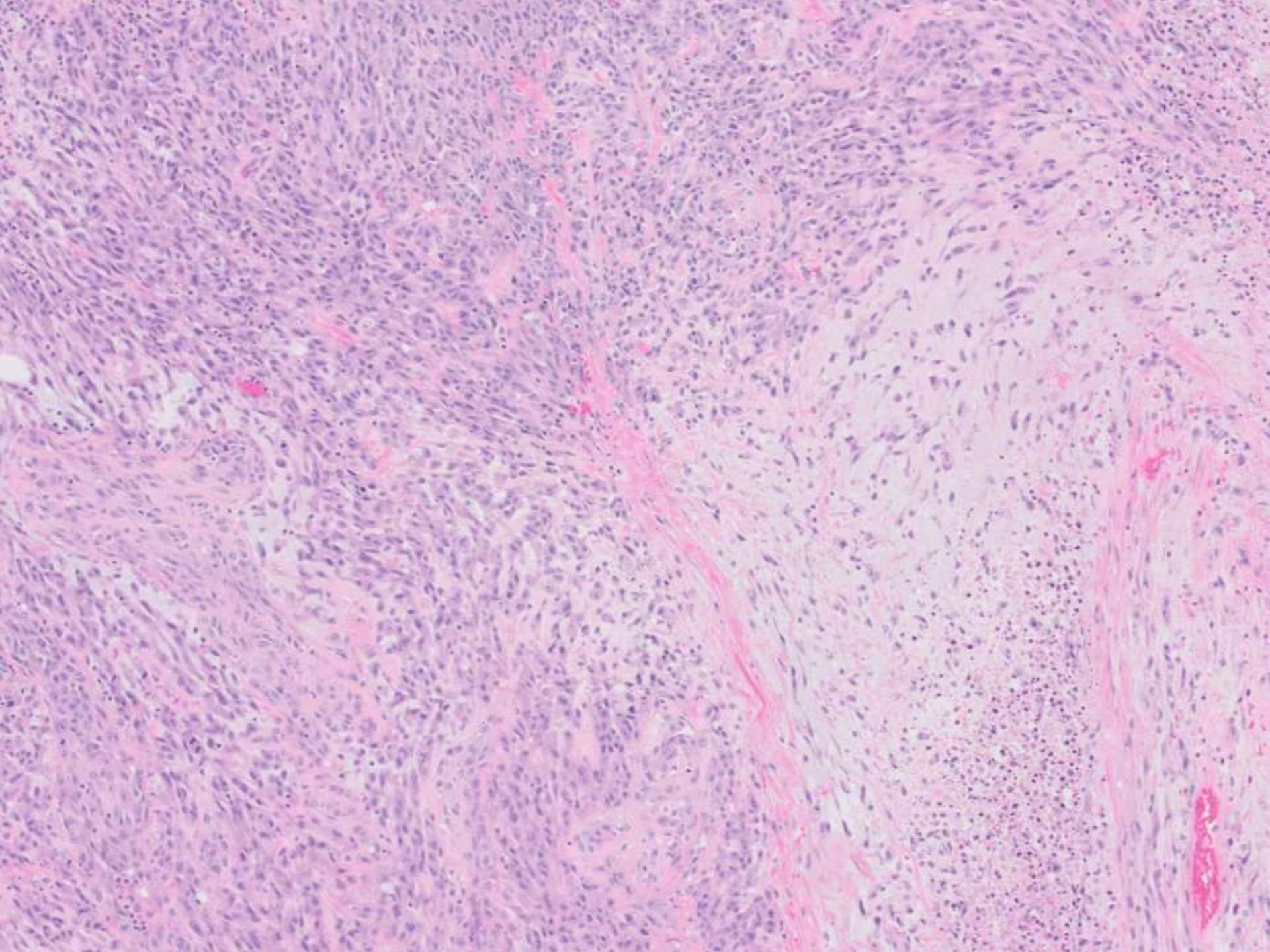

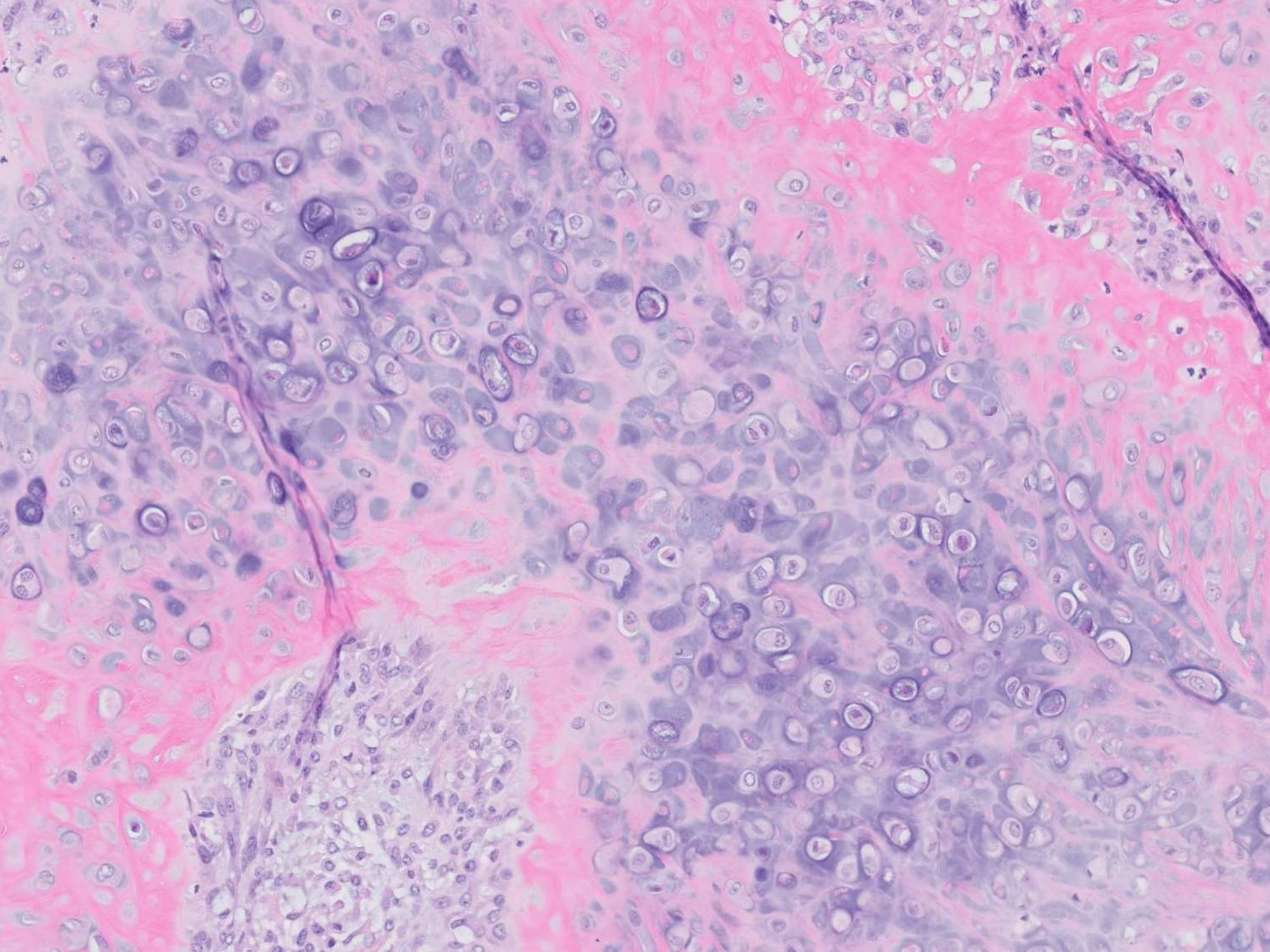

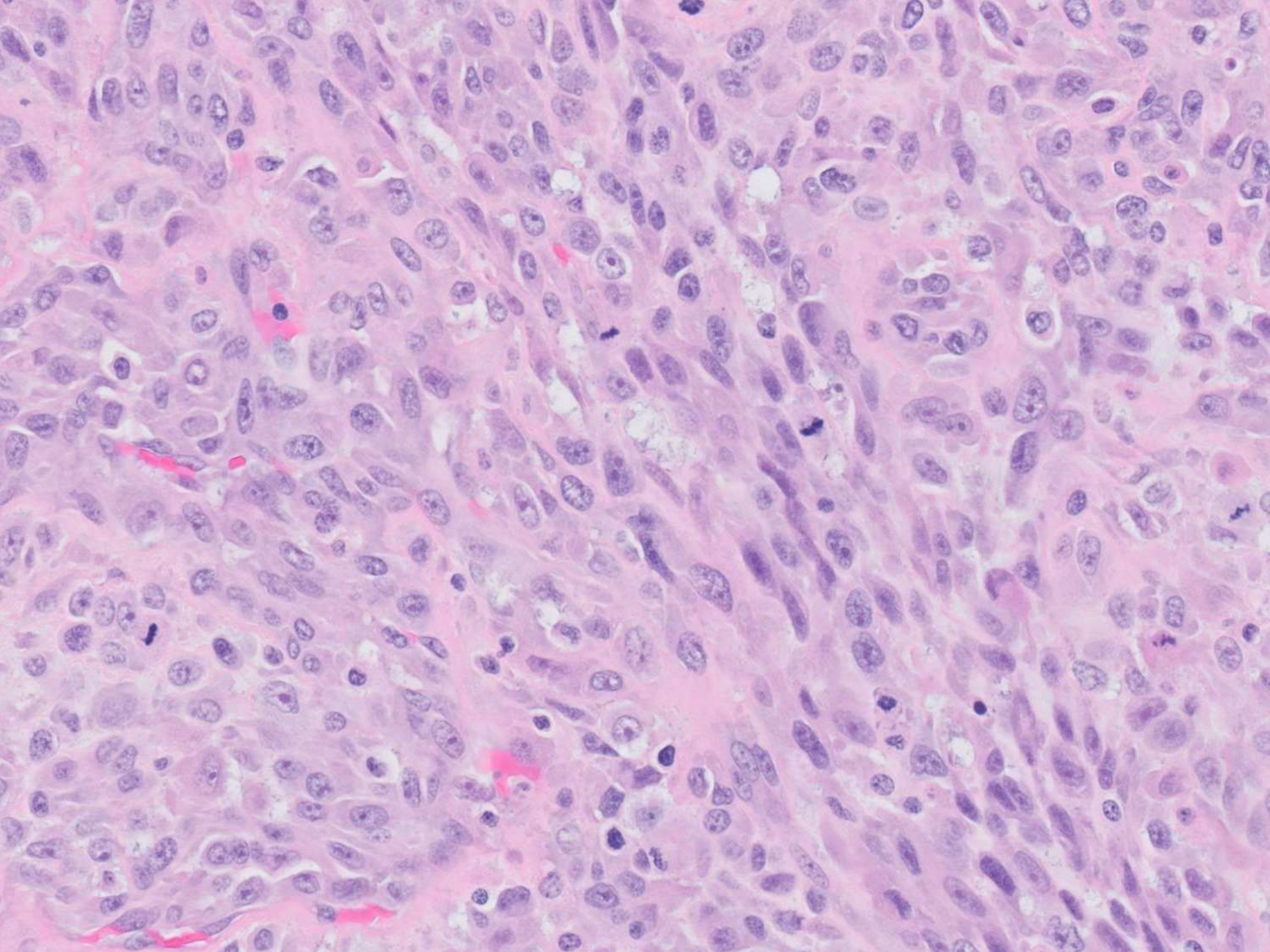

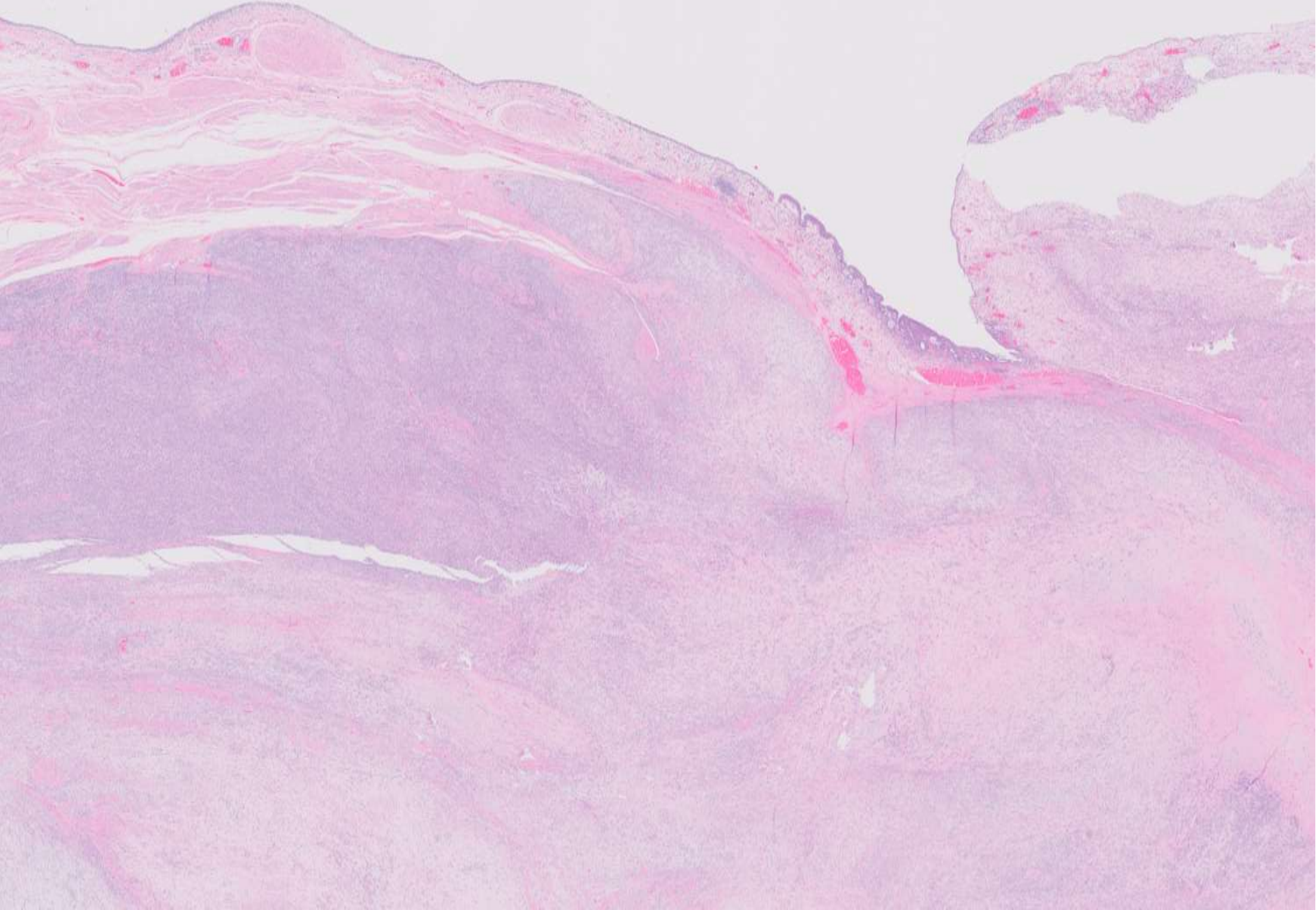

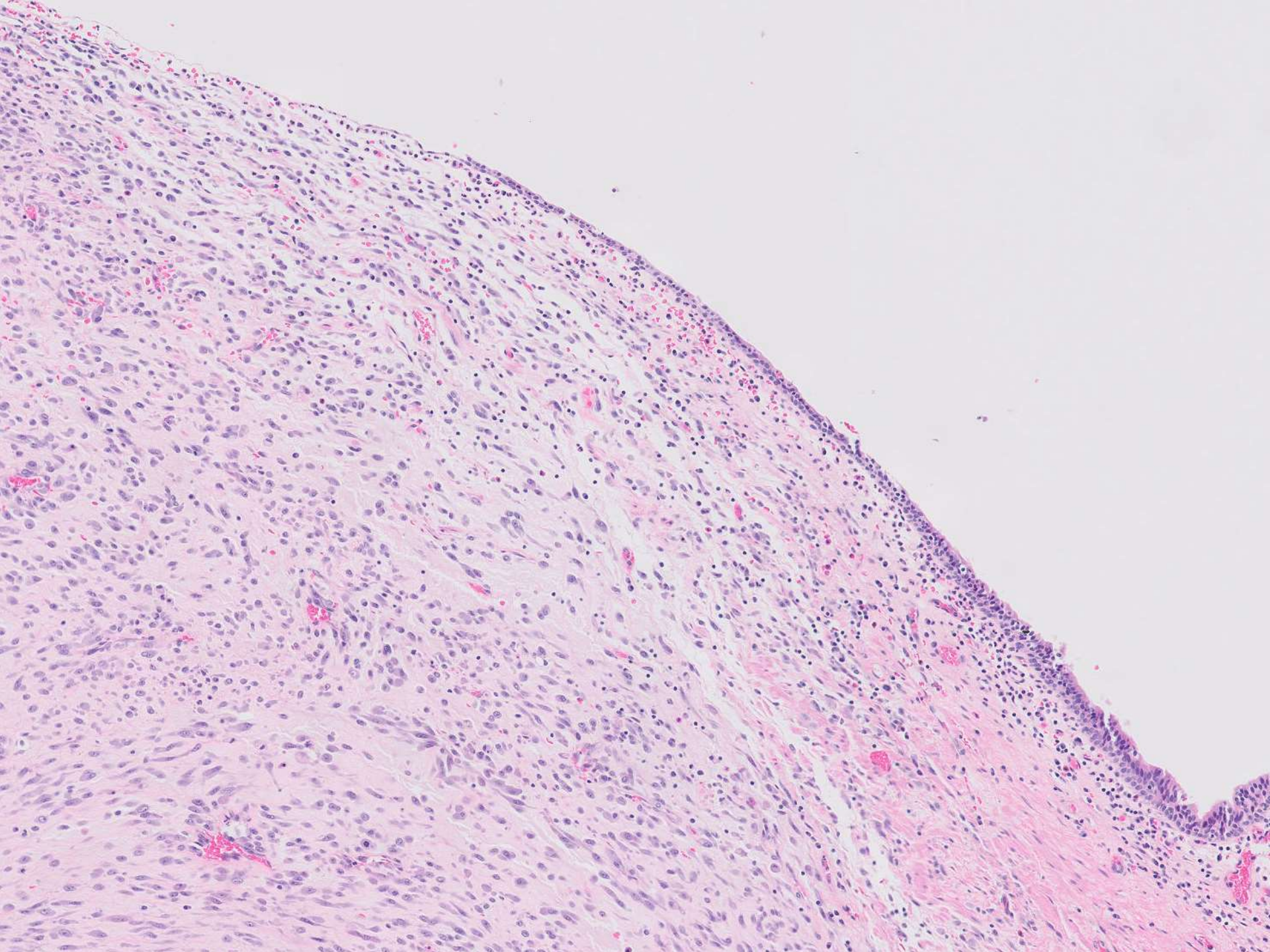

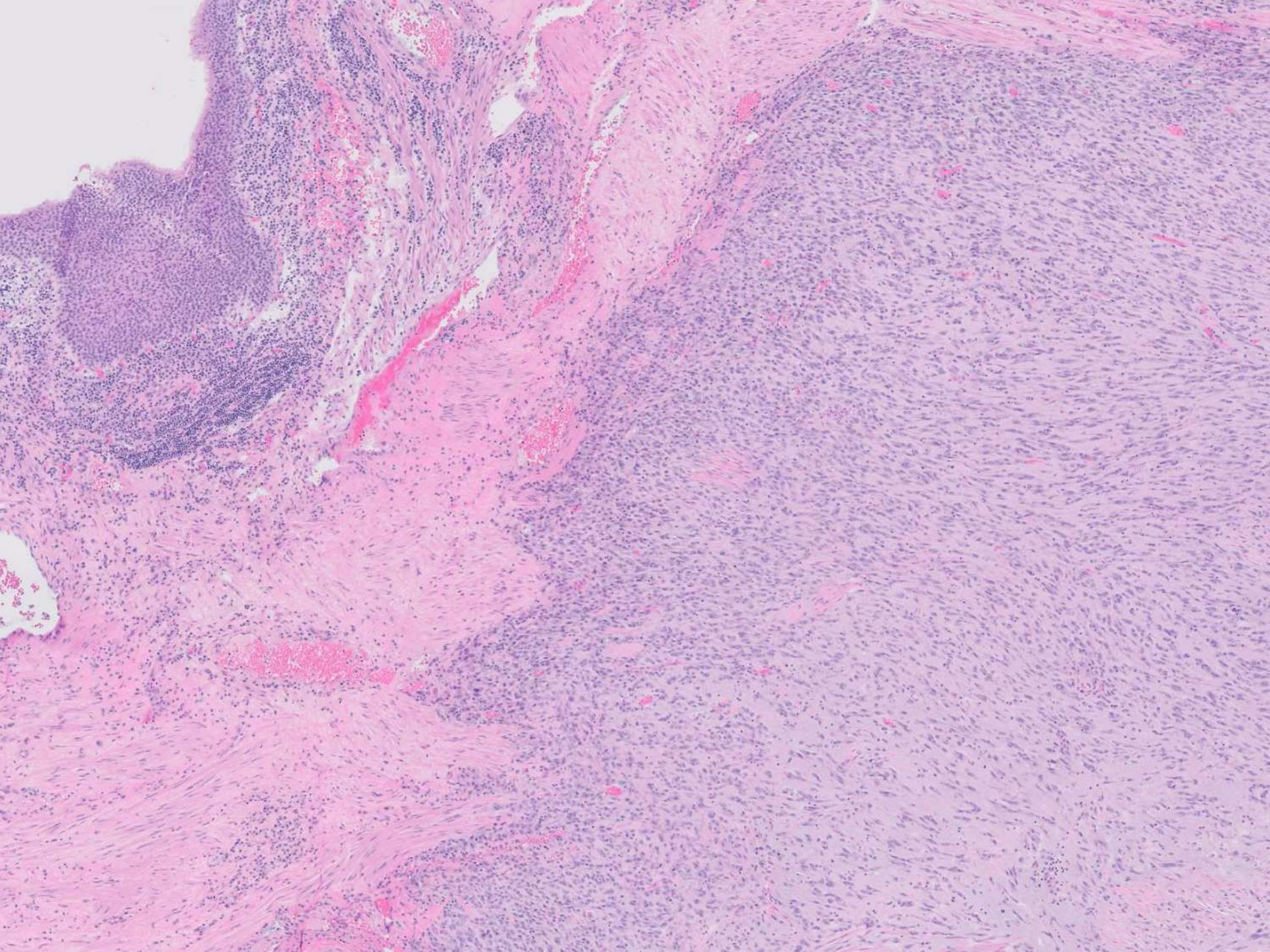

Urinary Bladder Mass: Summary Slides

Ingold Huang/Emily Chan; UCSF

- 80ish M, remote prostatic adenocarcinoma, treated with radiation and androgen deprivation therapy
- Now 12 cm urinary bladder mass → radical cystoprostatectomy

Notes on H&E findings

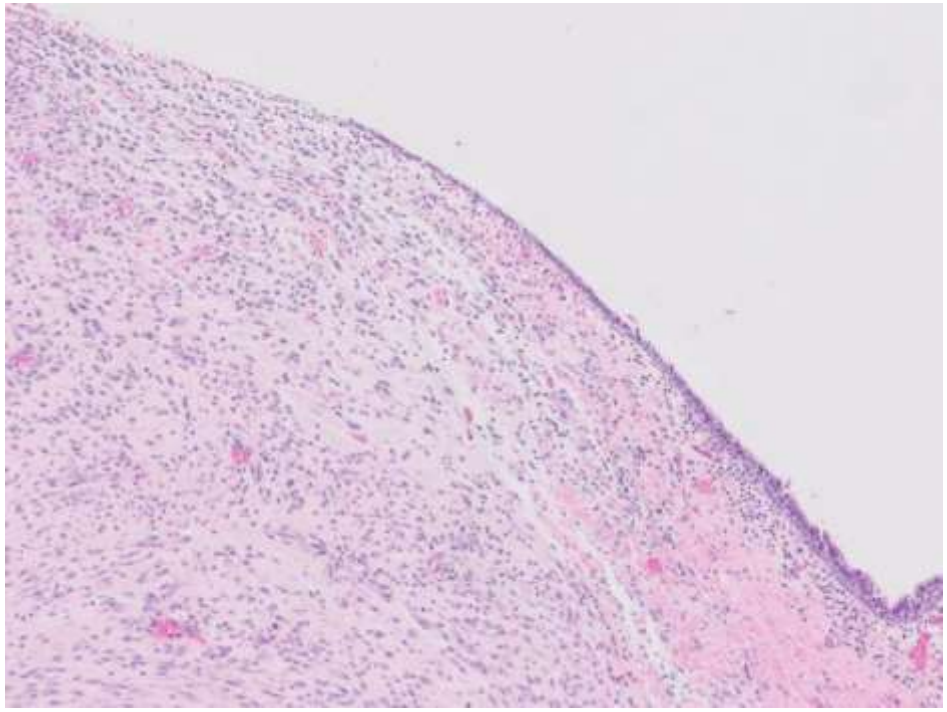

1. No involvement of urothelium by tumor after extensive sampling.
2. No evidence of tumor invasion from outside the urinary bladder.

Differential diagnosis & considerations

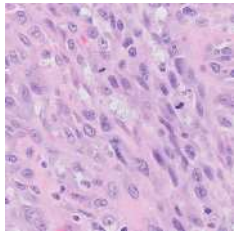
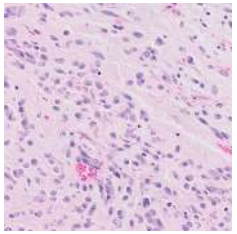
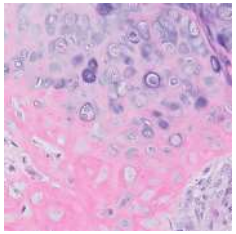
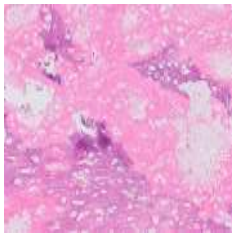

- Urothelial carcinoma with extensive sarcomatoid variant histology and heterologous elements (osteosarcoma and chondrosarcoma) (*i.e.*, carcinosarcoma, sarcomatoid carcinoma)
- Sarcoma
  - Primary/de novo versus radiation induced??
- Sarcomatoid transformation of prostate cancer (*i.e.*, carcinosarcoma, sarcomatoid carcinoma)
- Metastasis

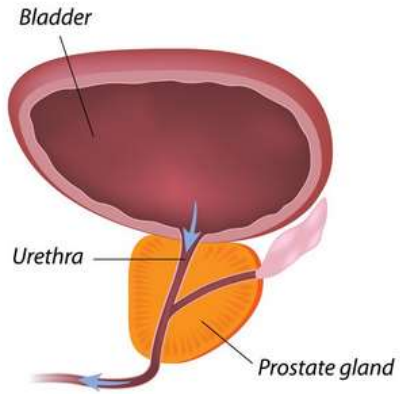

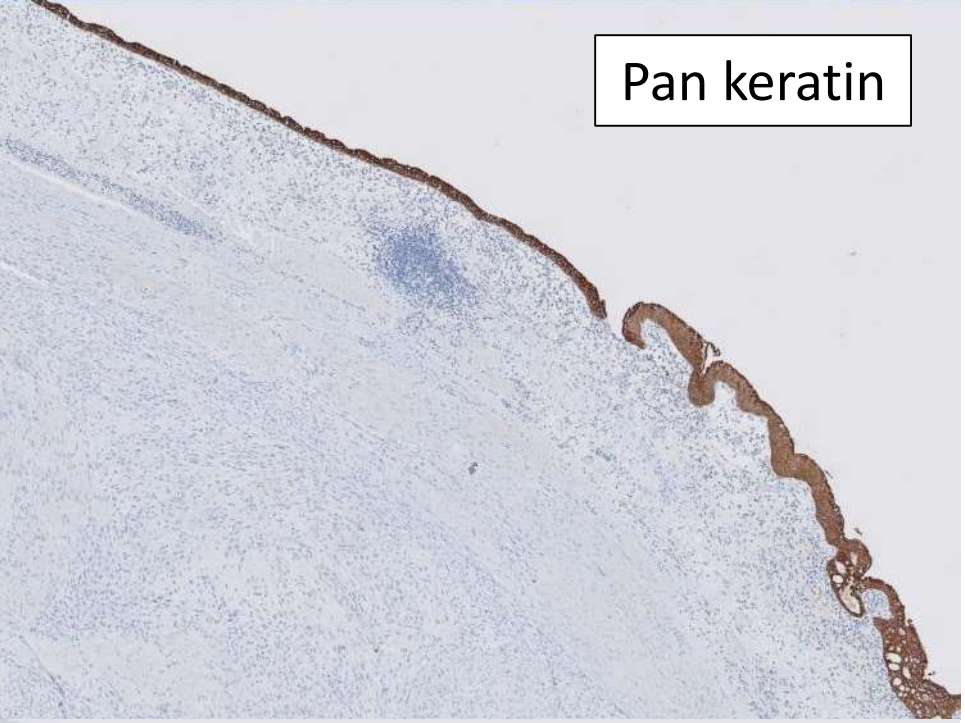

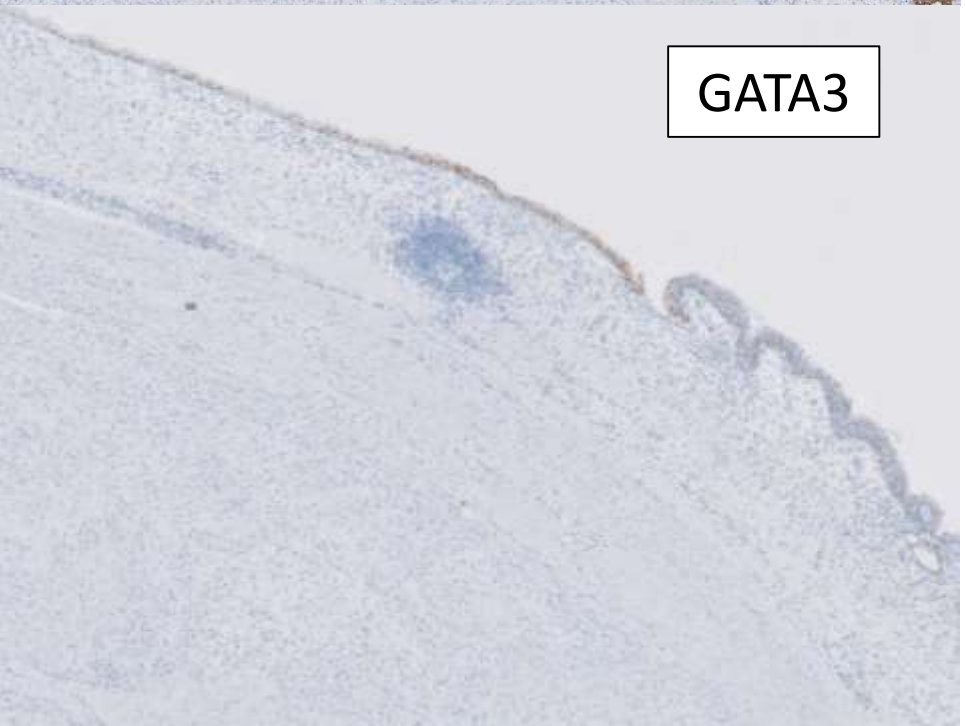

Other negative IHC

- p40
- CAM5.2
- CK7
- CK20
- NKX3.1
- PSA
- S100
- CD34
- ERG
- Desmin

Signed out as:
Malignant sarcomatoid neoplasm; see comment

Submitted sample of tumor for
UCSF500 next-gen sequencing

Comparison of molecular alterations

Urothelial carcinomas

- *TERT* promoter (85%)*
- *TP53* (49%)
- *CDKN2A* (CNA 47%)
- *KMT2D/MLL2* (27%)
- *ARID1A* (25%)
- *PIK3CA* (20%)

*(% mutated or copy number alteration)

Radiation-associated secondary malignancies

- High rate of deletions (esp small deletions)
- Balanced inversions
- Low overall rate of single nucleotide variants
- High numbers of segmental copy gains and losses involving many chromosomes

Liu *Front Immun* 2023; TCGA *Nature* 2014; Robertson *Cell* 2017; Behjati *Nat Comm* 2016

Comparison of molecular alterations

Urothelial carcinomas

- *TERT* promoter
- *TP53*
- *CDKN2A*
- *KMT2D/MLL2*
- *ARID1A*
- *PIK3CA*

Radiation-associated secondary malignancies

- High rate of deletions (esp small deletions)
- Balanced inversions
- Low overall rate of single nucleotide variants
- High numbers of segmental copy gains and losses involving many chromosomes

Seen in this case

Sarcomatoid and urothelial components from the same muscle-invasive bladder cancer shared truncal somatic mutations

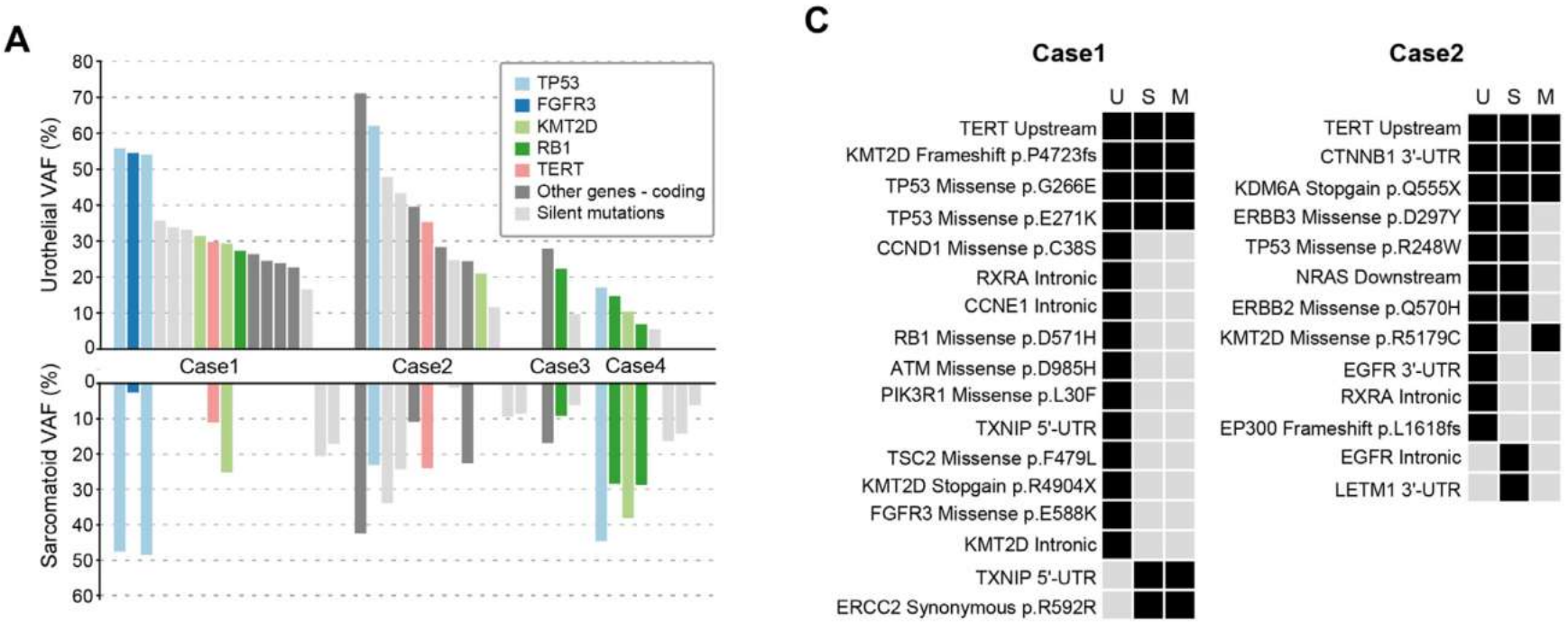

Genitsch *Uro Oncol* 2019

PATHOGENIC AND LIKELY PATHOGENIC ALTERATIONS

VARIANT	TRANSCRIPT ID	CLASSIFICATION	READS	MUTANT ALLELE FREQUENCY
CDKN2B,CDKN2A homozygous/biallelic deletion	All	Pathogenic	N/A	N/A
KMT2C p.P1838fs	NM_170606.2	Pathogenic	1270	53%
KMT2C p.Q1764*	NM_170606.2	Pathogenic	941	30%
KMT2D p.L3818fs	NM_003482.3	Pathogenic	1705	33%
PIK3CA p.E542K	NM_006218.2	Pathogenic	733	33%
PTEN p.Q171*	NM_000314.4	Pathogenic	153	72%
TERT c.-124C>T	NM_198253.2	Pathogenic	700	59%
ARHGAP35 p.Q1482fs	NM_004491.4	Likely Pathogenic	880	89%
FBXW7 p.R479G	NM_033632.3	Likely Pathogenic	635	45%

'Reads' indicates the number of unique DNA molecules sequenced. 'Mutant Allele Frequency' indicates the percentage of the reads with the respective 'Variant' and is affected by the degree of normal cell contamination of the sample and whether the variant is fully clonal or subclonal. 'Pathogenic' and 'Likely Pathogenic' classifications are based on CCGL molecular pathologist/geneticist interpretation of data from somatic and germline databases and published literature. Variants classified as 'Possibly Pathogenic' have unknown significance but occur in genes or molecular pathways known to be recurrently altered in the tumor type.

2 of 86 tested microsatellites (2.33%) were found to be unstable. This is interpreted as Microsatellite Stable (MSS).

Assessment of microsatellite instability (MSI) by percentage of unstable sites:
<20%: MSI absent (MSS) | 20-30%: MSI equivocal | >30%: MSI present (MSI-High)

UCSF500 tumor mutation burden: 16.5 mutations/Mb

UCSF500 Report Interpretation:

Molecular signature of this tumor favors a *urothelial carcinoma or carcinosarcoma* over a radiation-induced sarcoma

Treatment strategies: urothelial carcinoma vs sarcoma

- Different chemotherapy agents
- Adjuvant radiation considerations

Take home points

- Consider in the differential diagnosis of a sarcomatoid neoplasm in the urinary bladder:
  - Urothelial carcinoma with sarcomatoid differentiation
  - Primary sarcoma
  - Radiation-induced sarcoma (if hx of radiation)
- Molecular studies may provide evidence to suggest a primary site of origin or whether a tumor may be secondary to ionizing radiation

References

1. Liu T, Li S, Xia C, Xu D. *TERT* promoter mutations and methylation for telomerase activation in urothelial carcinomas: New mechanistic insights and clinical significance. Front Immunol. 2023 Jan 12;13:1071390. doi: 10.3389/fimmu.2022.1071390. PMID: 36713366; PMCID: PMC9877314.
2. The TCGA Network. Comprehensive molecular characterization of urothelial bladder carcinoma. Nature 2014;507:315. PubMed PMID: 24476821.
3. Robertson AG et al., Comprehensive molecular characterization of muscle-invasive bladder cancer. Cell. 2018 Aug 9;174(4):1033. PubMed PMID: 28988769.
4. Behjati S et al., Mutational signatures of ionizing radiation in second malignancies. Nat Commun. 2016 Sep 12;7:12605. PMID: 27615322; PMCID: PMC5027243.
5. Genitsch V et al. Morphologic and genomic characterization of urothelial to sarcomatoid transition in muscle-invasive bladder cancer. Urol Oncol. 2019 Sep;37(9):573.e19-573.e29. doi: 10.1016/j.urolonc.2019.06.021. Epub 2019 Jul 26. PMID: 31358384.

23-0402

Andrew Xiao/Emily Chan; UCSF

50ish F with 12.5cm left inferior pole renal mass.

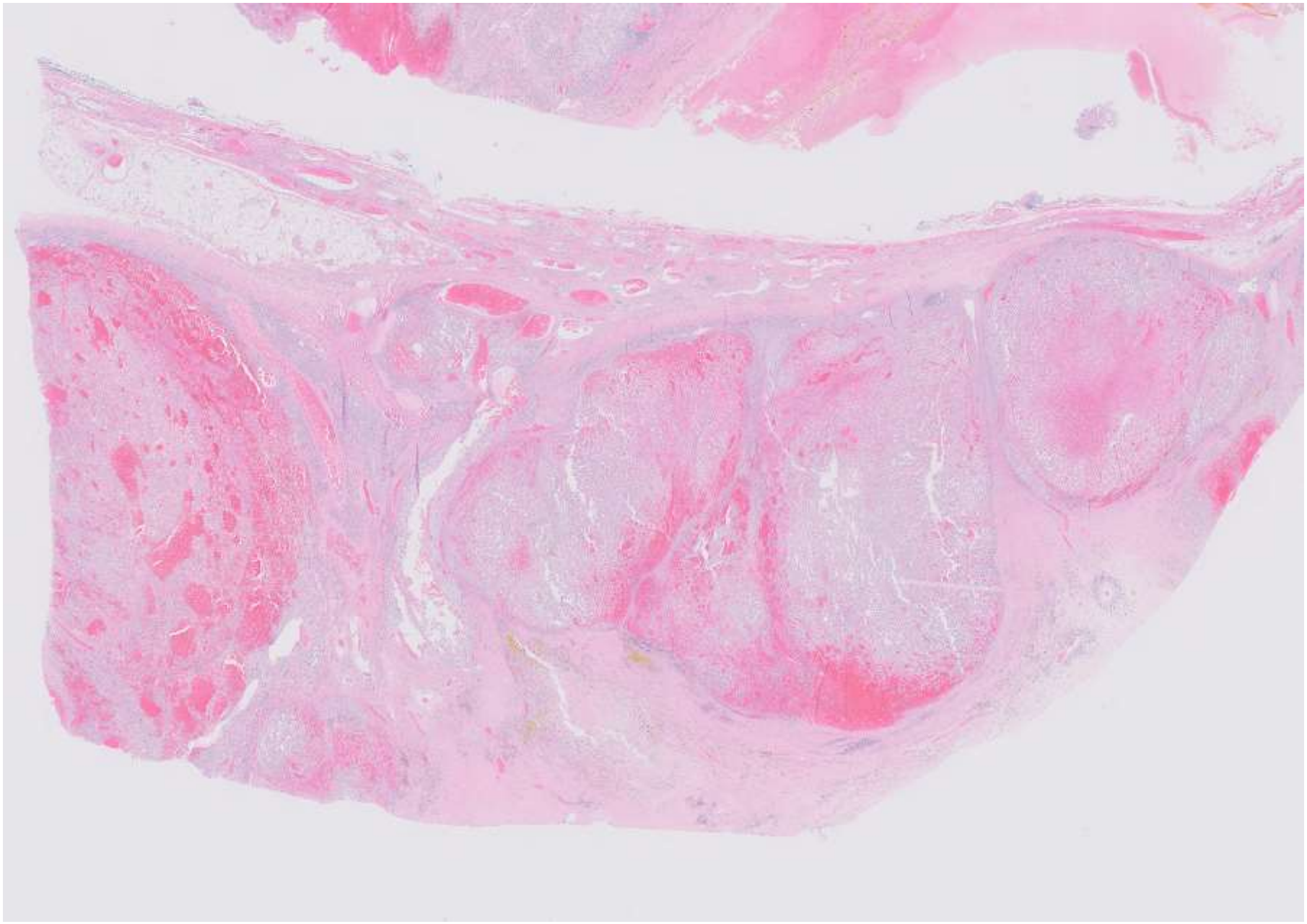

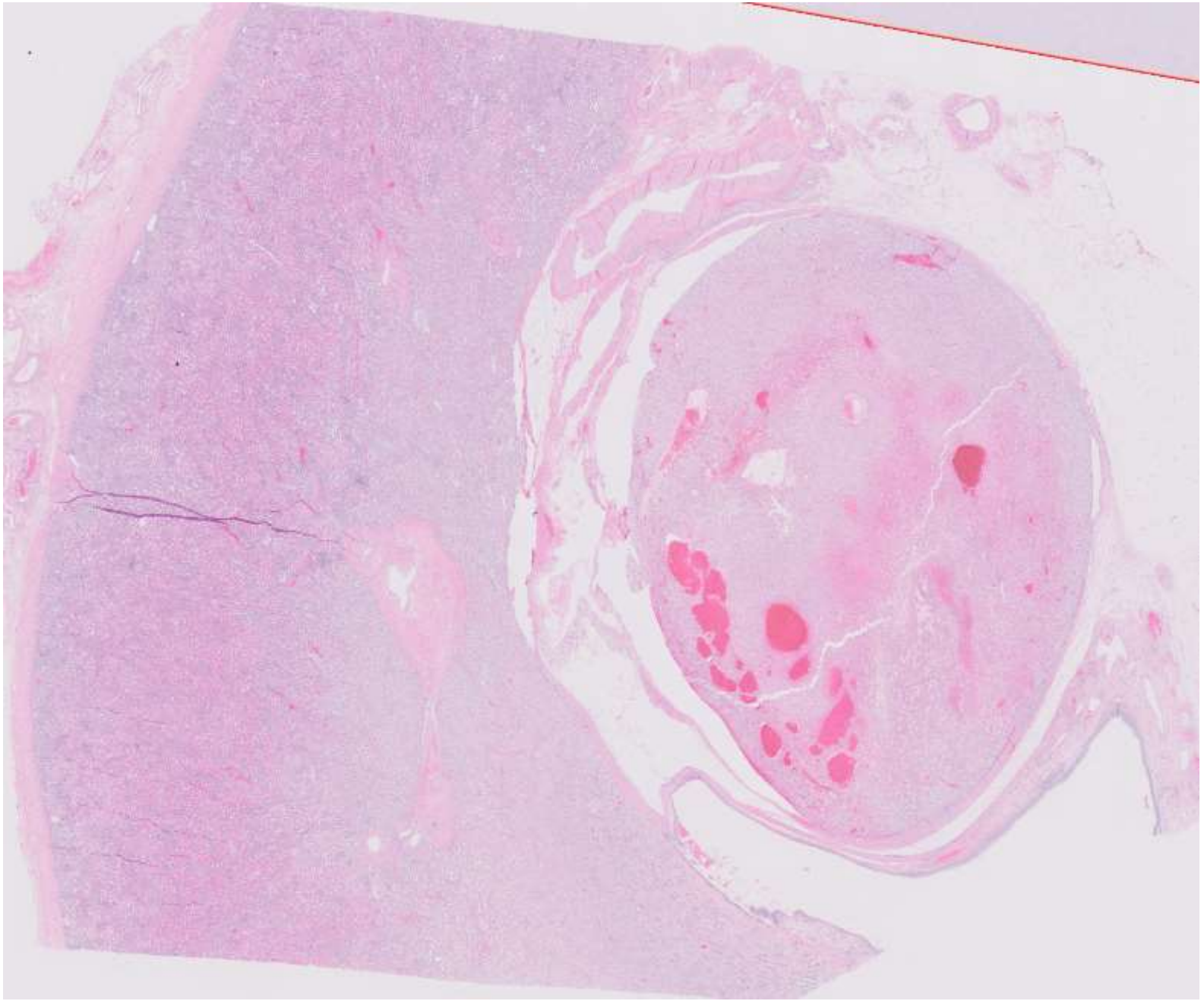

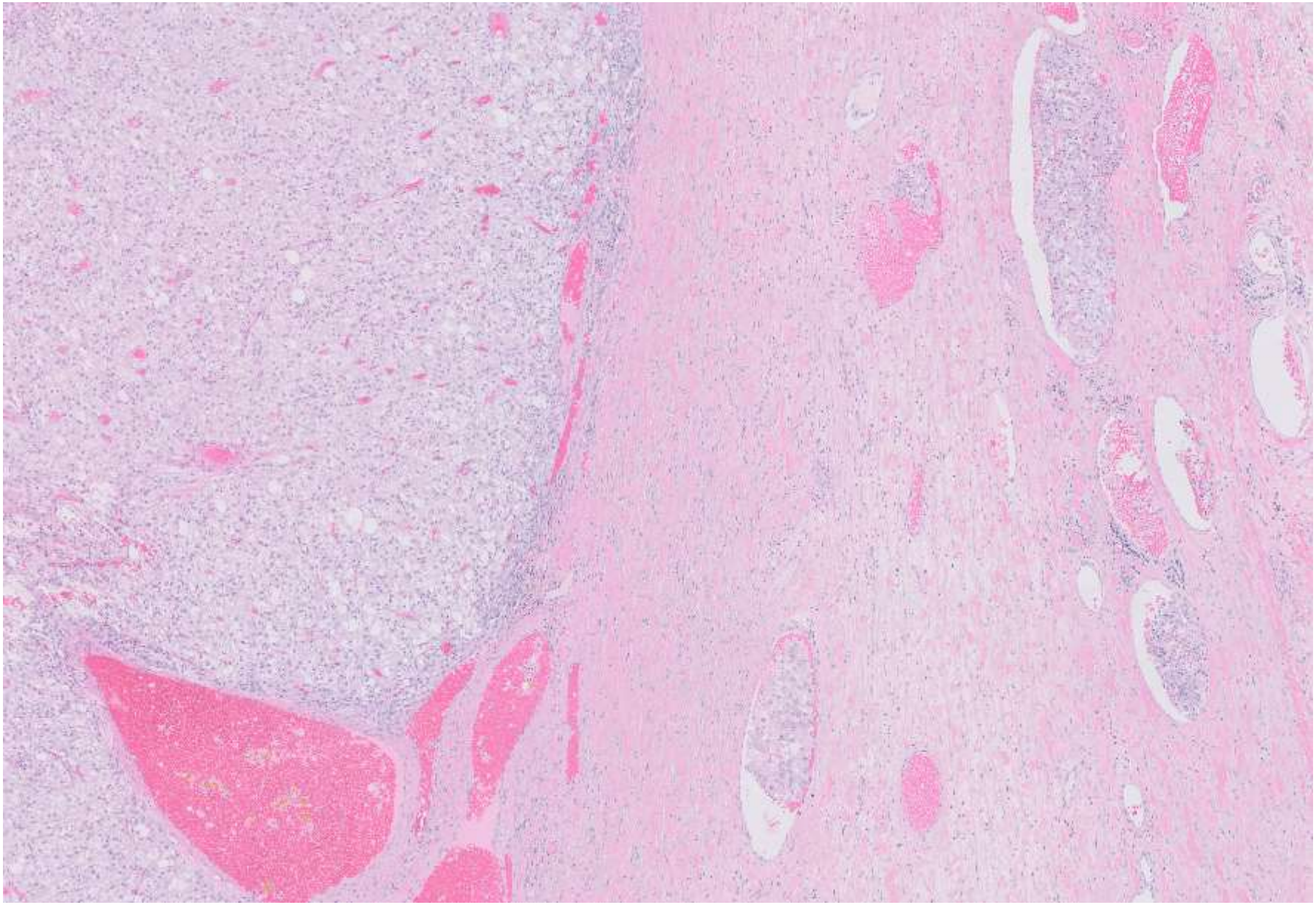

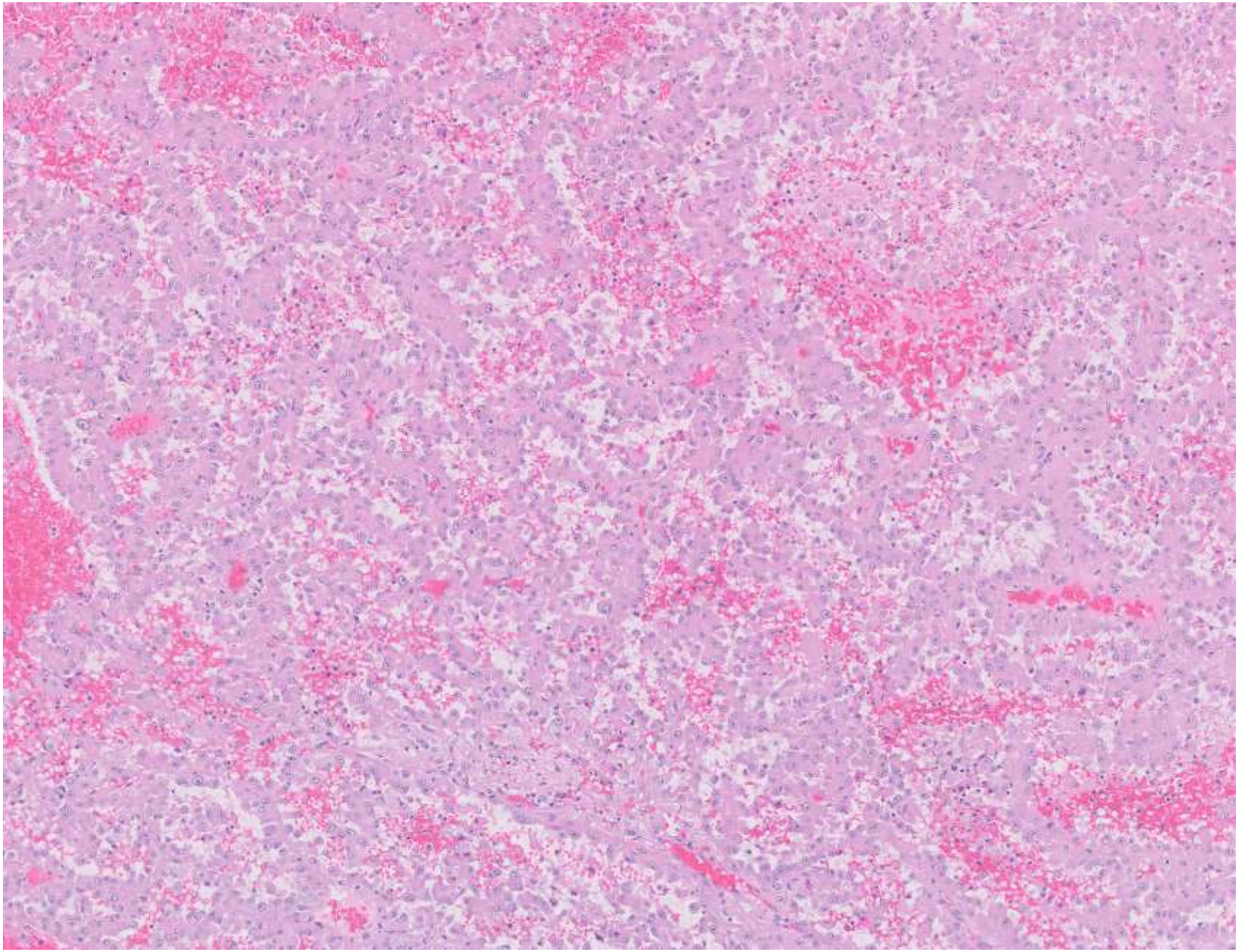

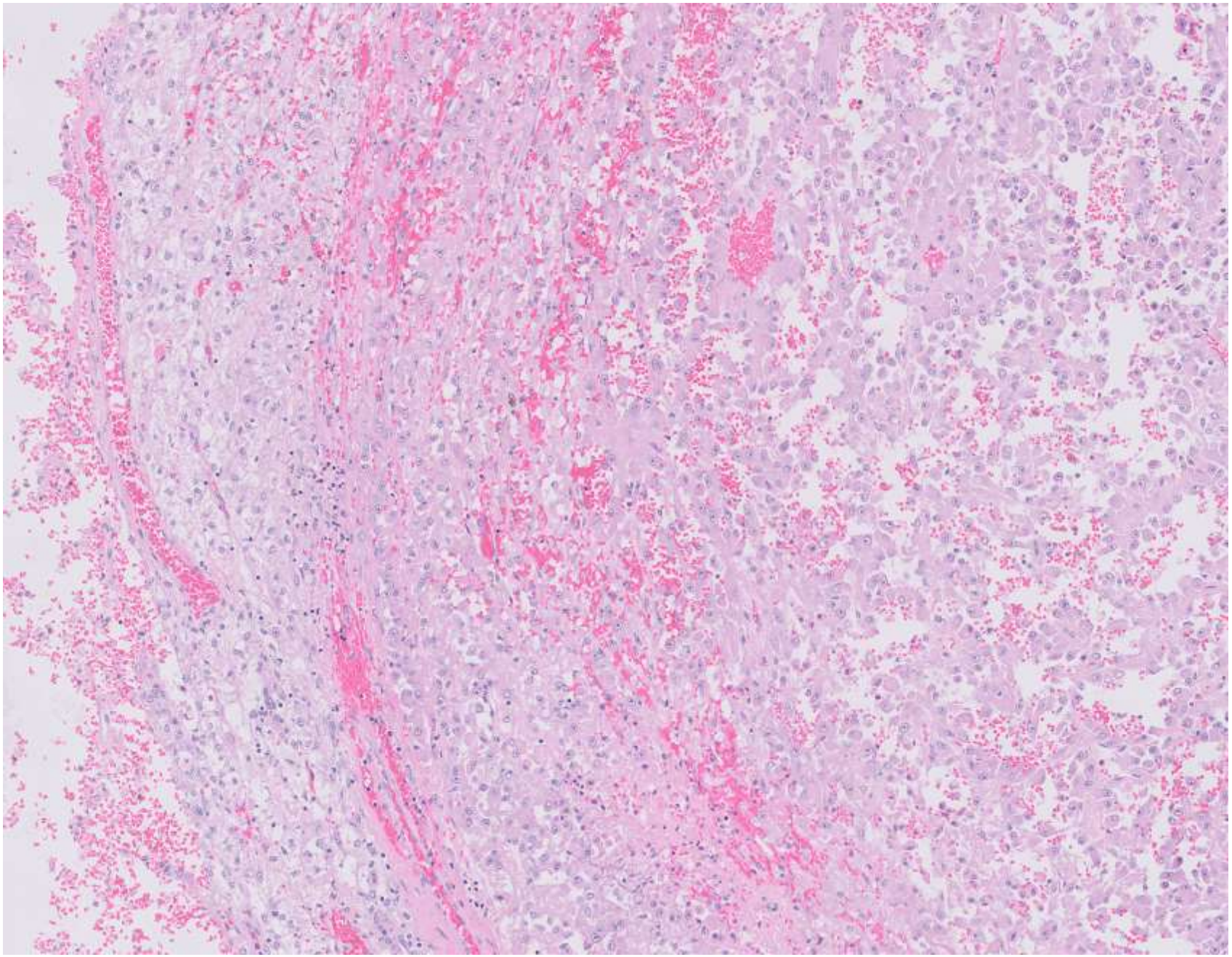

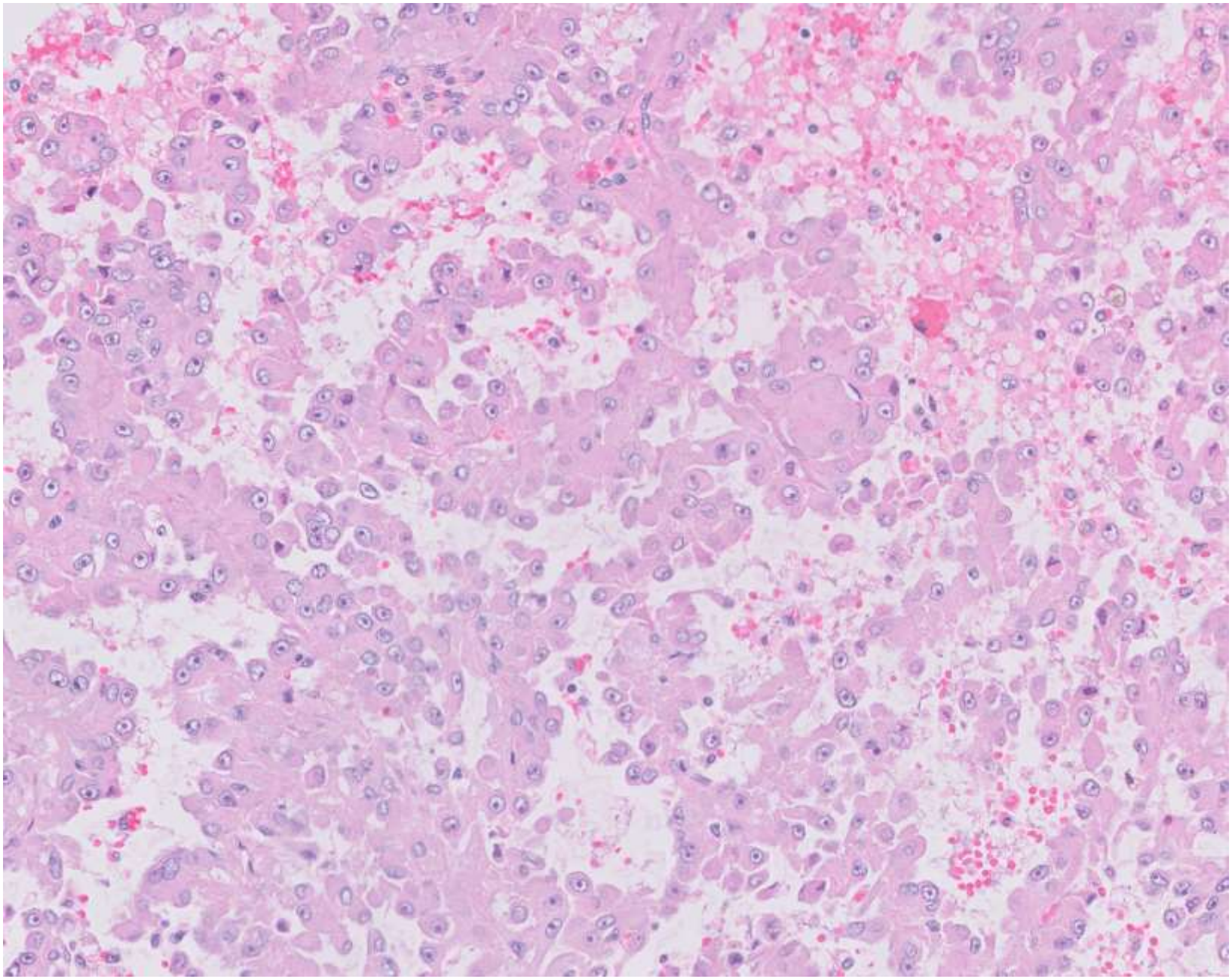

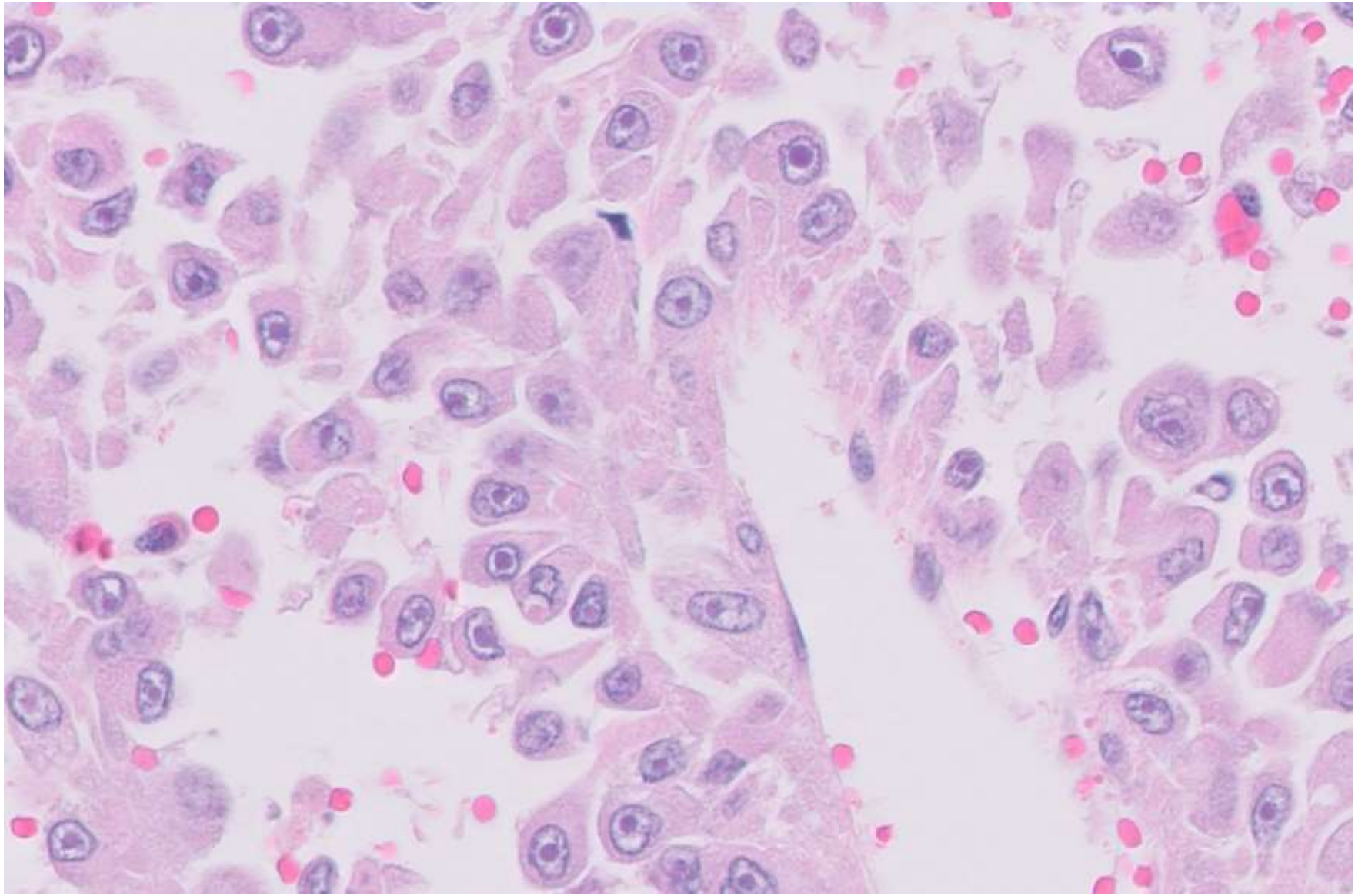

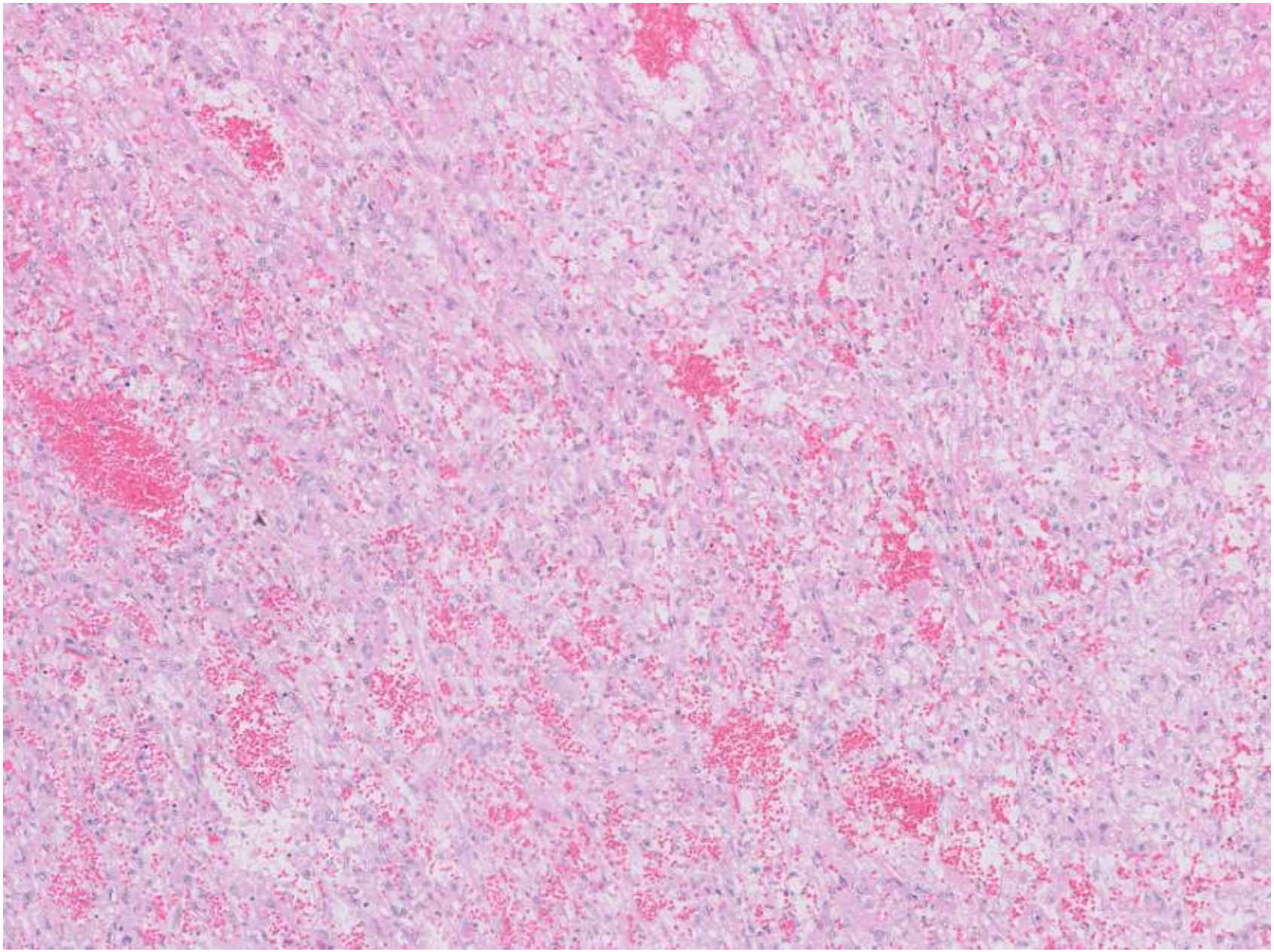

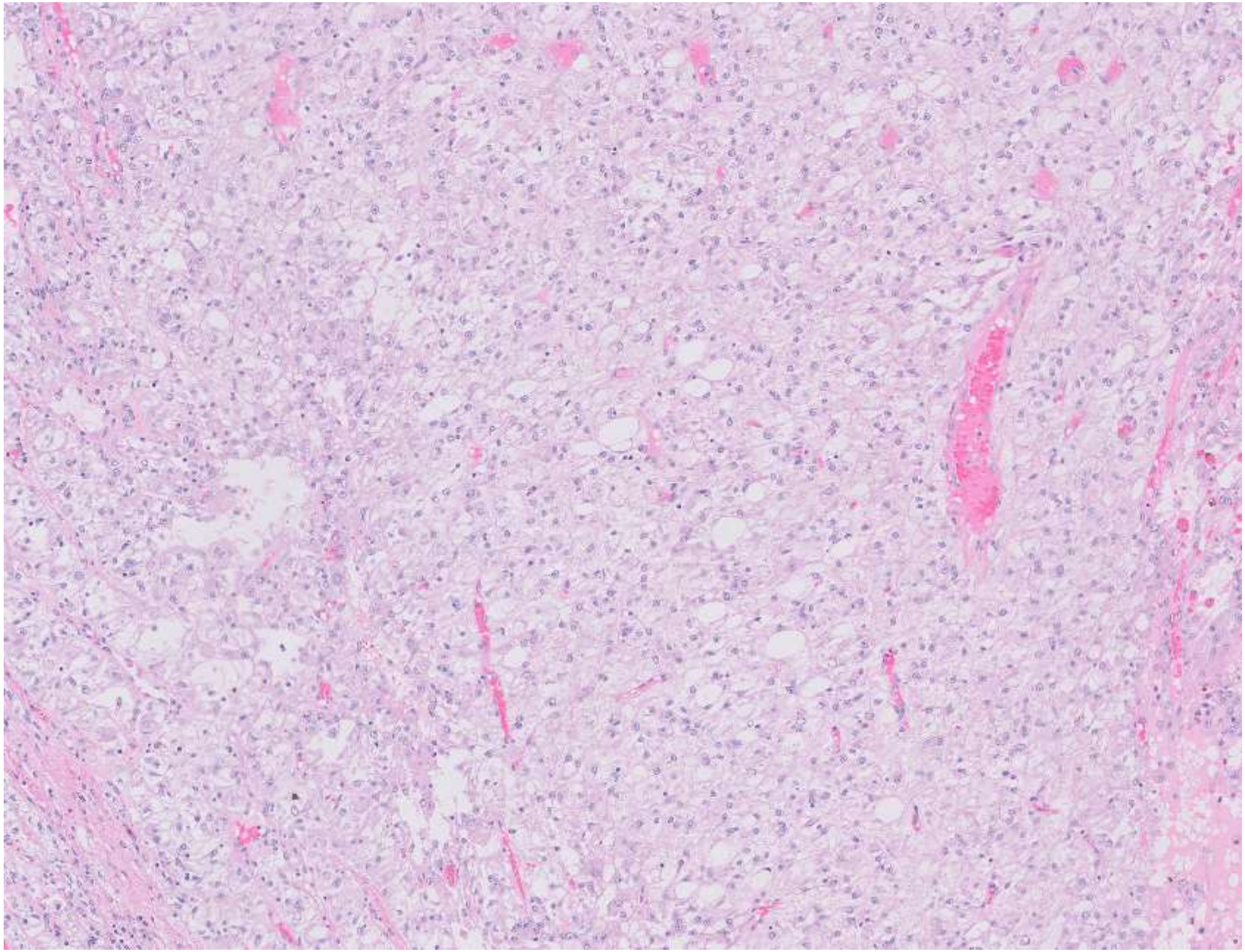

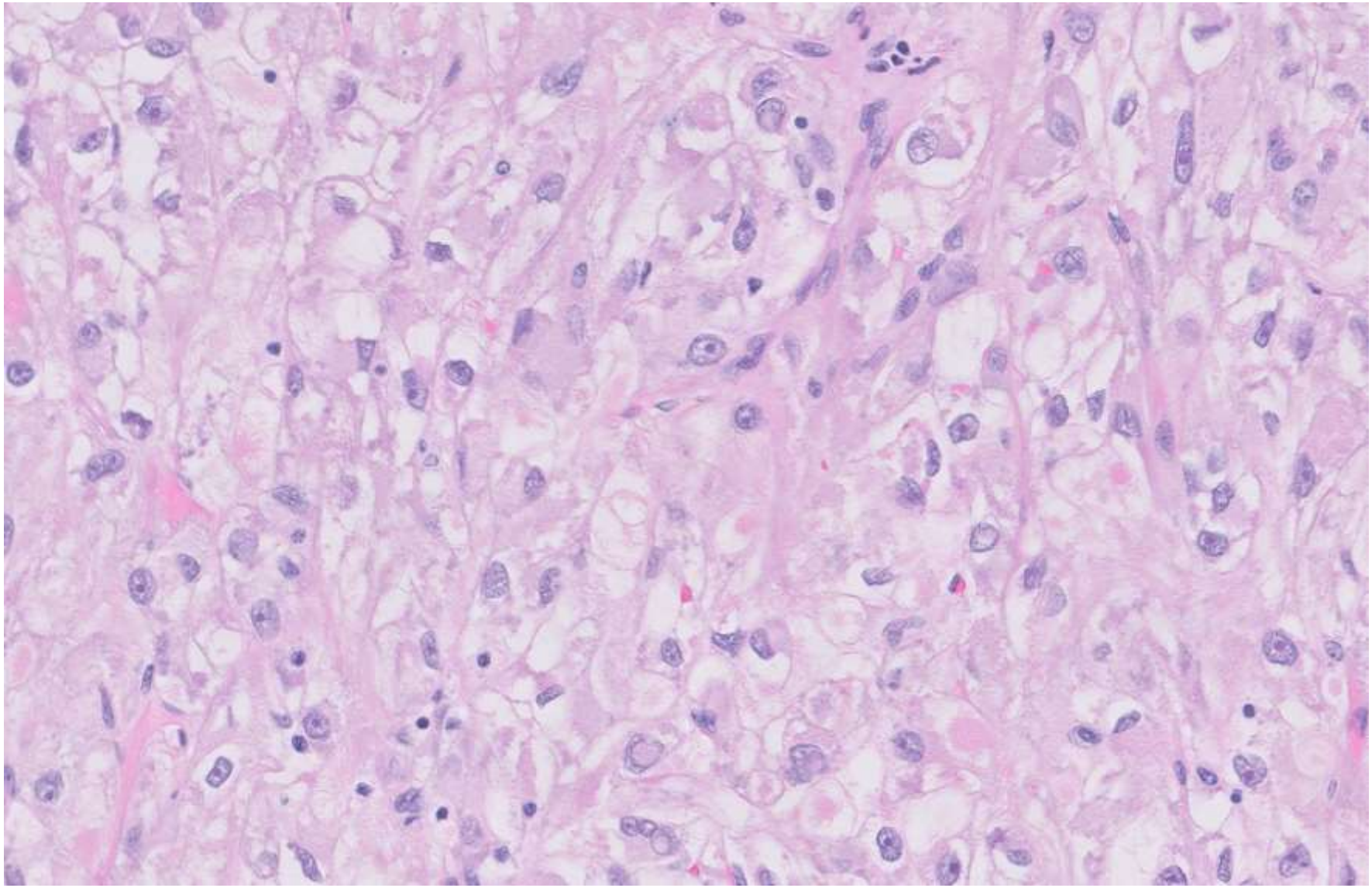

Microscopic features

- Carcinoma-like areas
  - Papillary architecture:
    - Epithelioid cells containing abundant eosinophilic cytoplasm
    - Prominent cherry-red nucleoli

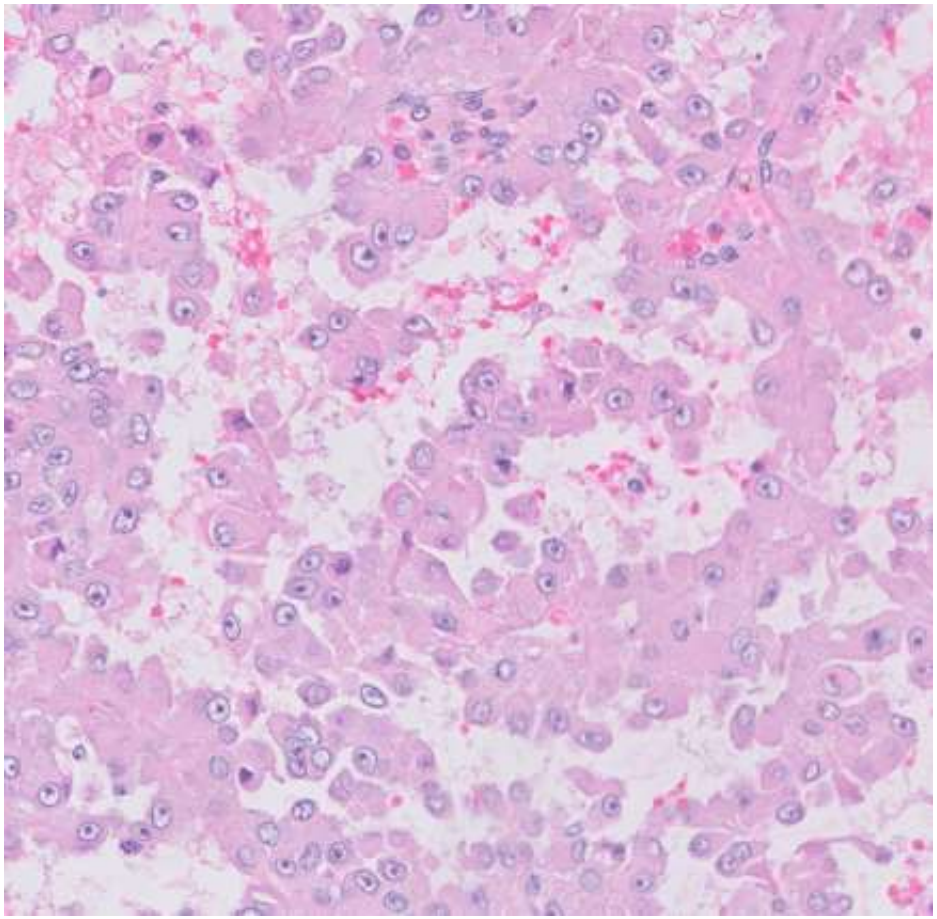

Microscopic features

- Epithelioid and plump spindle cells in diffuse growth
  - Intranuclear inclusions

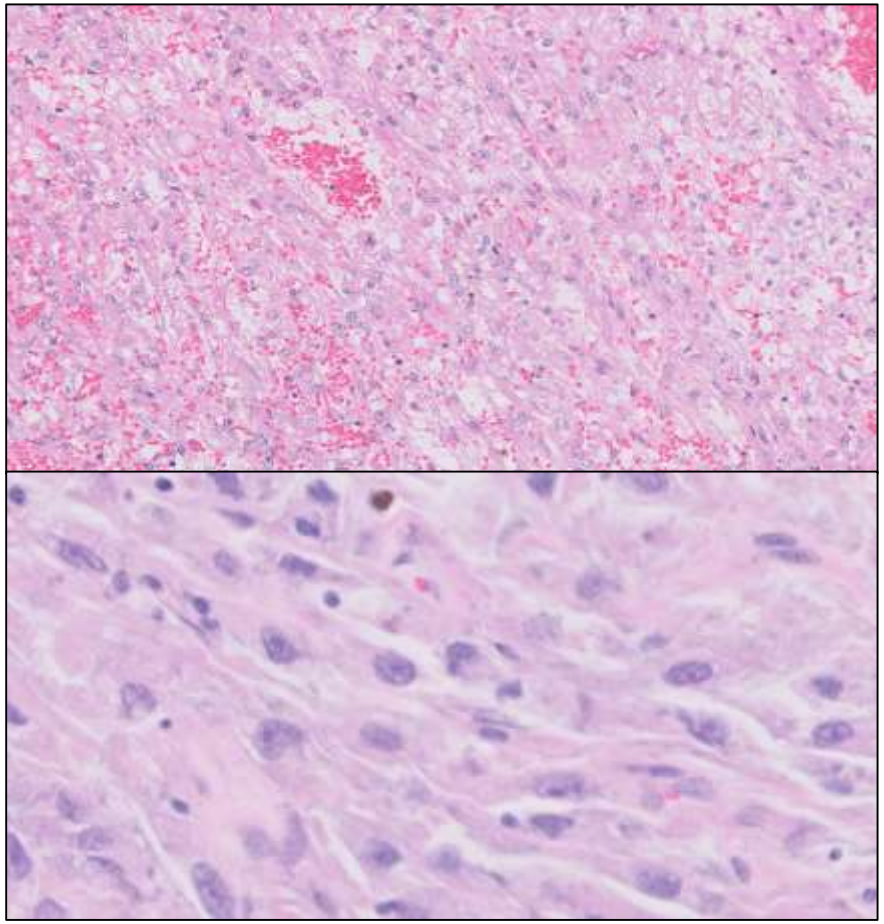

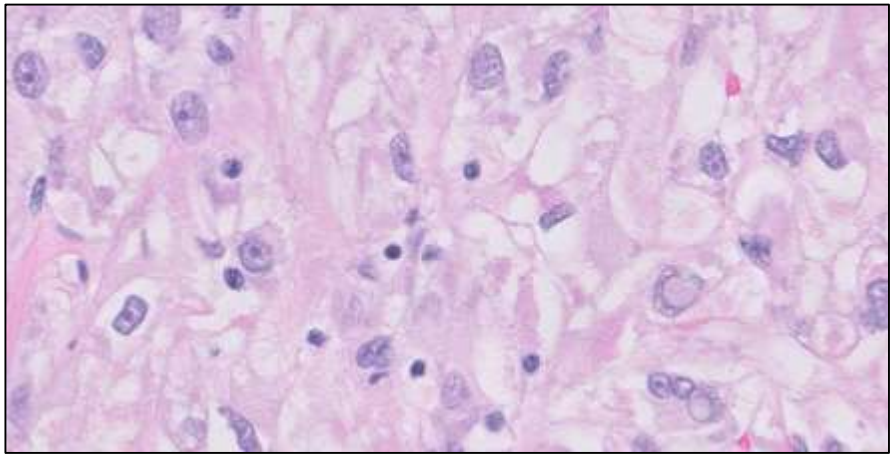

Differential Diagnosis

- Renal cell carcinoma with sarcomatoid features
  - Fumarate hydratase-deficient
  - *MITF*-altered (*TFE3*- or *TFEB*-altered)
  - Eosinophilic and vacuolated
  - ALK-rearranged
  - Succinate dehydrogenase-deficient
  - Chromophobe
  - Clear cell
- Epithelioid angiomyolipoma
- Urothelial carcinoma with extensive sarcomatoid differentiation
- Melanoma

Stains in solid/spindled & papillary areas

- Negative
  - Pan-Keratin
  - PAX8
  - CK7
  - CD10
  - CAIX
  - TFE3
  - ALK
- Retained
  - Fumarate hydratase
  - Succinate dehydrogenase
  - INI1

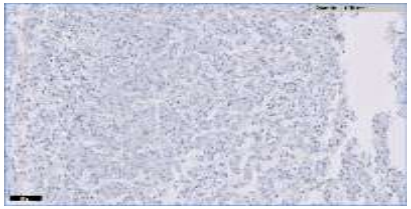

Pan-Keratin

PAX8

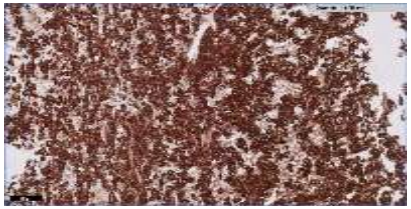

Fumarate hydratase

Stains in solid/spindled & papillary areas

- Positive
  - Melan A
  - HMB45
  - SMA

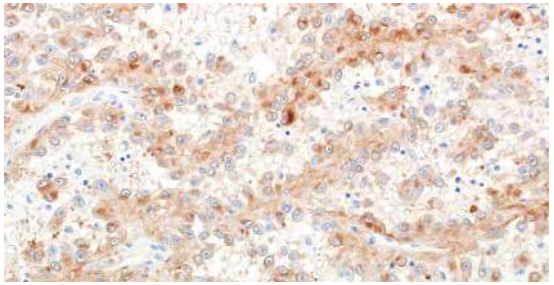

Melan A

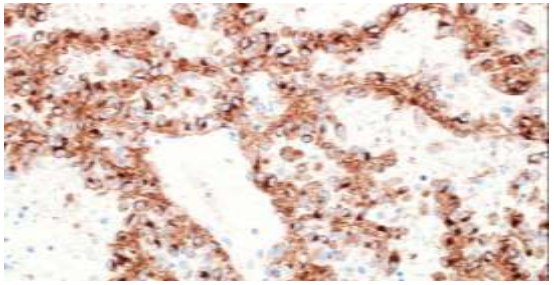

HMB45

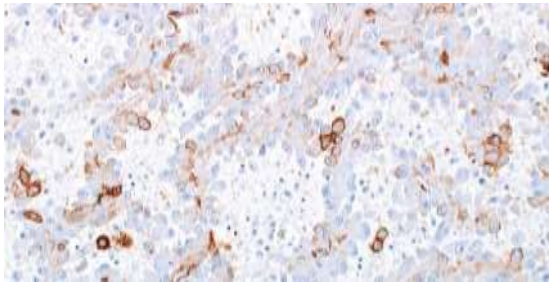

SMA

Diagnosis

- Epithelioid angiomyolipoma (EAML)
  - Also known as: epithelioid PEComa of the kidney

EAML

- Mesenchymal tumor thought to originate from perivascular epithelioid cells with predominant epithelioid features
  - Closely related to usual AML
  - Associated with alterations in Tuberous Sclerosis Complex genes (TSC1 & TSC2)
  - Variable cut-off for percent epithelioid histology, most studies using ≥70-80%

- Two histologic patterns:
  - Cells arranged as cohesive nests, broad alveoli, and sheets separated by thin vascular septa
    - Unusual feature: Papillary architecture
  - Plump spindled and epithelioid cells arranged in diffuse sheets with less prominent vascularity

EAML

- IHC stains:
  - Positive
    - Melanocytic markers (HMB45, MelanA)
    - Smooth muscle markers (may be focal)
    - CathepsinK
    - CD68
  - Negative
    - Epithelial markers
    - PAX8
- May have malignant potential

UCSF 500 Next Generation Sequencing

PATHOGENIC AND LIKELY PATHOGENIC ALTERATIONS				
VARIANT	TRANSCRIPT ID	CLASSIFICATION	READS	MUTANT ALLELE FREQUENCY
TERT promoter rearrangement	NM_198253.2	Pathogenic	191	N/A
TSC2 p.I1357fs	NM_000548.3	Pathogenic	1610	34%
TSC2 p.G1577fs	NM_000548.3	Pathogenic	1561	31%

contamination of the sample and whether the variant is fully clonal or subclonal. 'Pathogenic' and 'Likely Pathogenic' classifications are based on CCGL molecular pathologist/geneticist interpretation of data from somatic and germline databases and published literature. Variants classified as 'Possibly Pathogenic' have unknown significance but occur in genes or molecular pathways known to be recurrently altered in the tumor type.

0 of 84 tested microsatellites (0.00%) were found to be unstable. This is interpreted as Microsatellite Stable (MSS).

Assessment of microsatellite instability (MSI) by percentage of unstable sites:
<20%: MSI absent (MSS) | 20-30%: MSI equivocal | >30%: MSI present (MSI-High)

UCSF500 tumor mutation burden: 8.9 mutations/Mb

INTERPRETATION

Tumor-only sequencing of this malignant epithelioid neoplasm demonstrates two inactivating frameshift mutations in TSC2. Also identified is a structural rearrangement involving the TERT promoter.

Copy number analysis reveals chromosome 1p loss, 2 loss, 4q loss, 6q loss with interstitial 6q gain, 7p gain, 8p loss, 16q loss, 17p loss, 19 loss, 22q loss. Also identified is copy neutral loss of heterozygosity of chromosome 5.

TSC2 has been reported to be altered in kidney neoplasms including unclassified renal cell carcinomas (Ref. 1), papillary renal cell carcinomas (Ref. 2) renal cell carcinomas with eosinophilic and vacuolated cytoplasm (RCC-EVC) (Ref. 3), as well as renal angiomyolipoma (Ref. 7-8). Structural rearrangement involving the TERT promoter has been shown to result in increased transcription due to acquisition of an enhancer element (Ref. 4-5). TERT promoter mutations are identified in various cancer types, including in renal neoplasms (Ref. 6).

Malignant Potential

- Malignancy criteria
  - ≥ 70% atypical epithelioid cells
  - ≥ 2 mitoses/10 HPF (≥ 1 mitosis/mm2)
  - Atypical mitotic figures
  - Necrosis

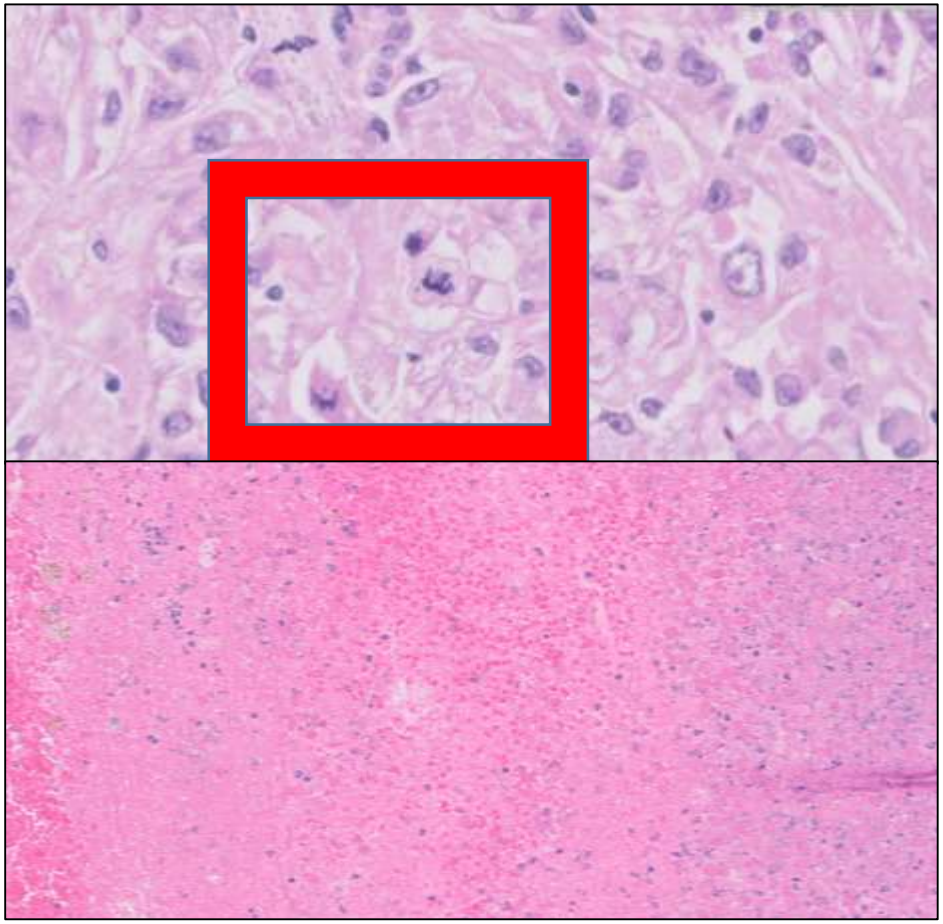

Brimo F, Robinson B, Guo C, Zhou M, Latour M, Epstein JI. Renal epithelioid angiomyolipoma with atypia: a series of 40 cases with emphasis on clinicopathologic prognostic indicators of malignancy. Am J Surg Pathol. 2010 May;34(5):715-22. doi: 10.1097/PAS.0b013e3181d90370. PMID: 20410812.

Take Home Points

- Consider an EAML when you see a tumor with carcinoma-like and spindle cell-like morphology
  - Rare papillary architecture can be seen
  - Mimics renal cell carcinoma
- Useful IHC includes positive HMB45, MelanA, SMA, CathepsinK, and negative PAX8
- Assess for malignant potential

23-0403

Hubert Lau; VA Palo Alto

80ish M with h/o melanoma and several non-melanoma skin cancers presents with 3cm pink plaque with overlying scale and hemorrhagic crust in postauricular area for 2-3 months. The lesion is tender and growing. Clinical DDx: SCC, less likely AK, trauma.

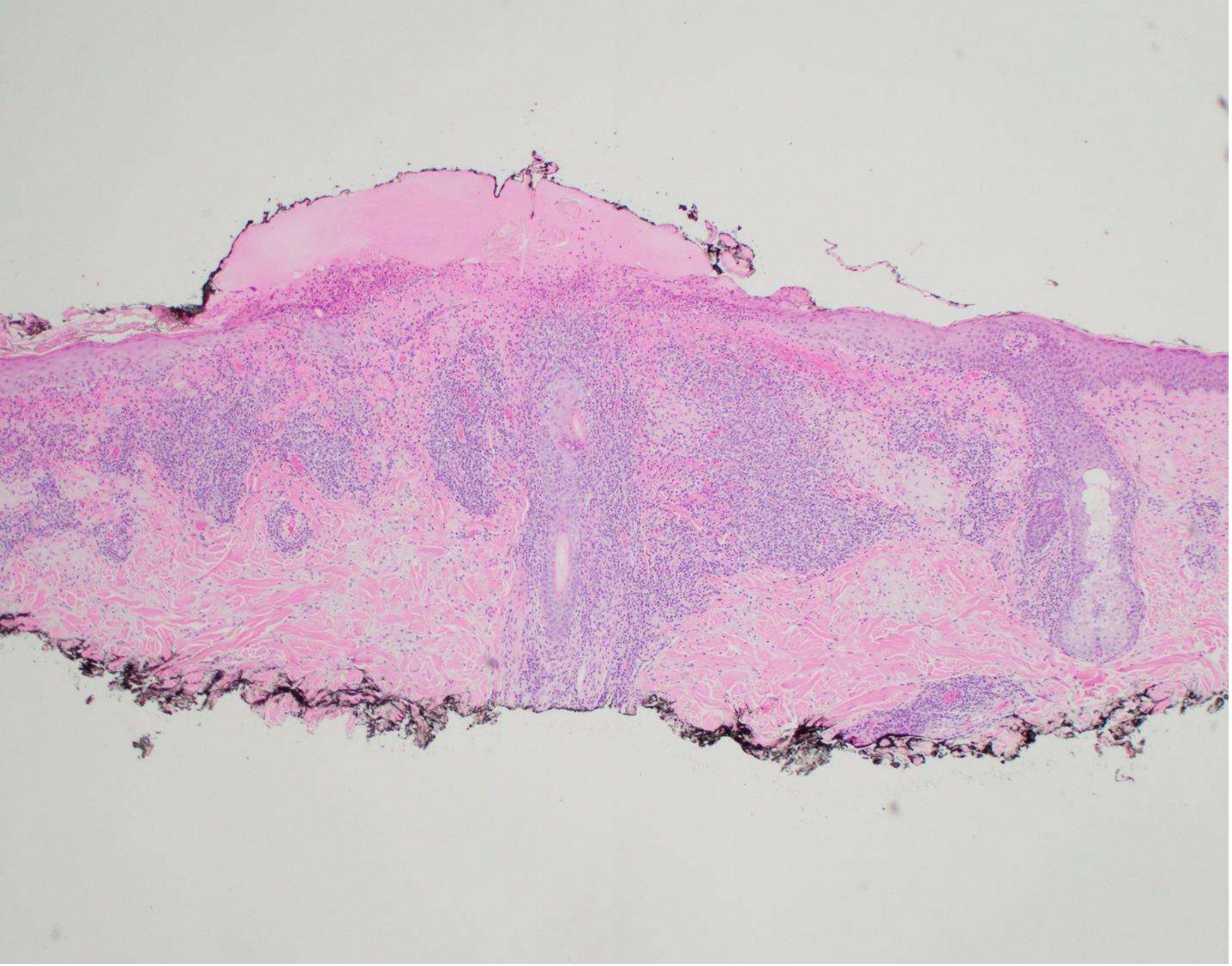

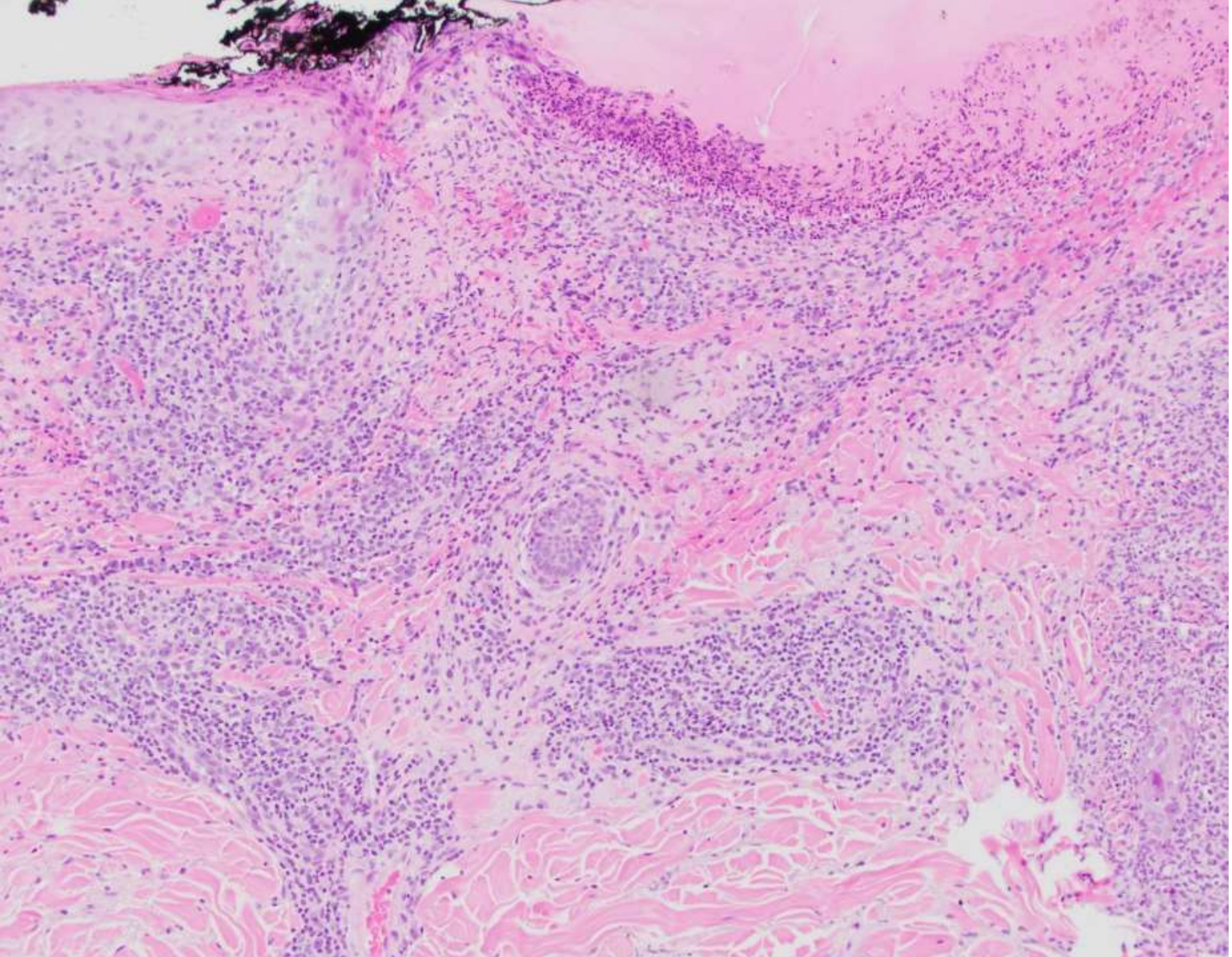

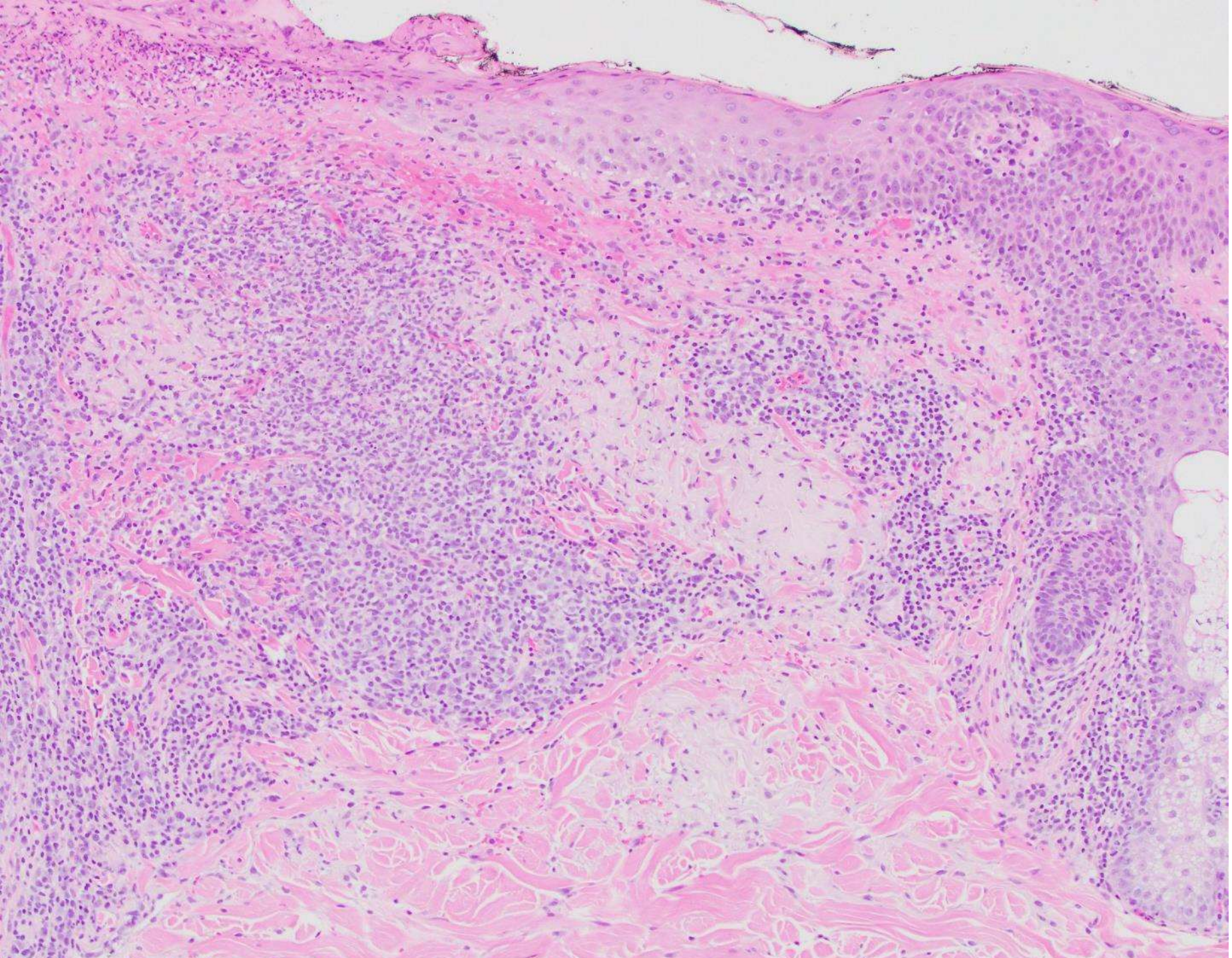

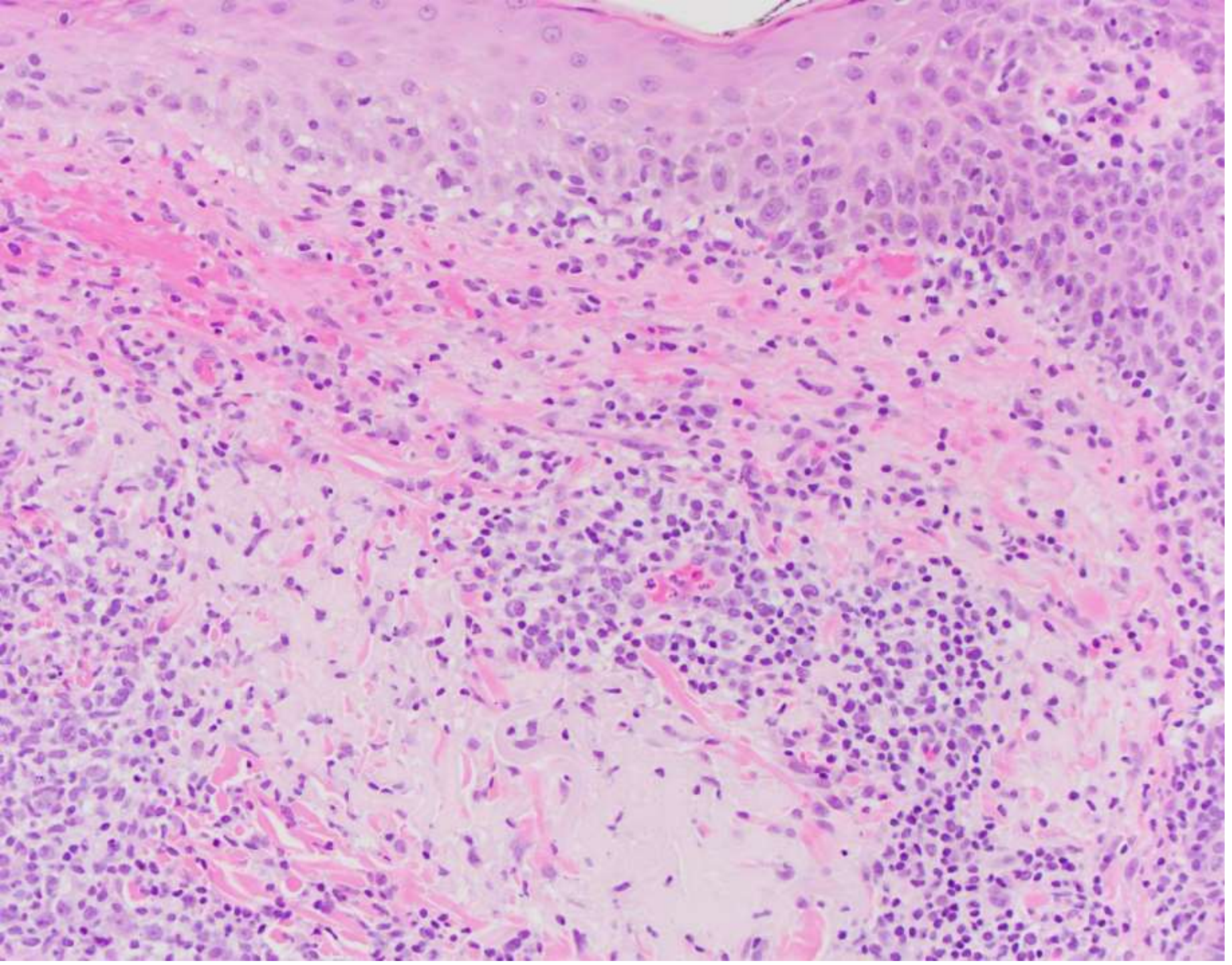

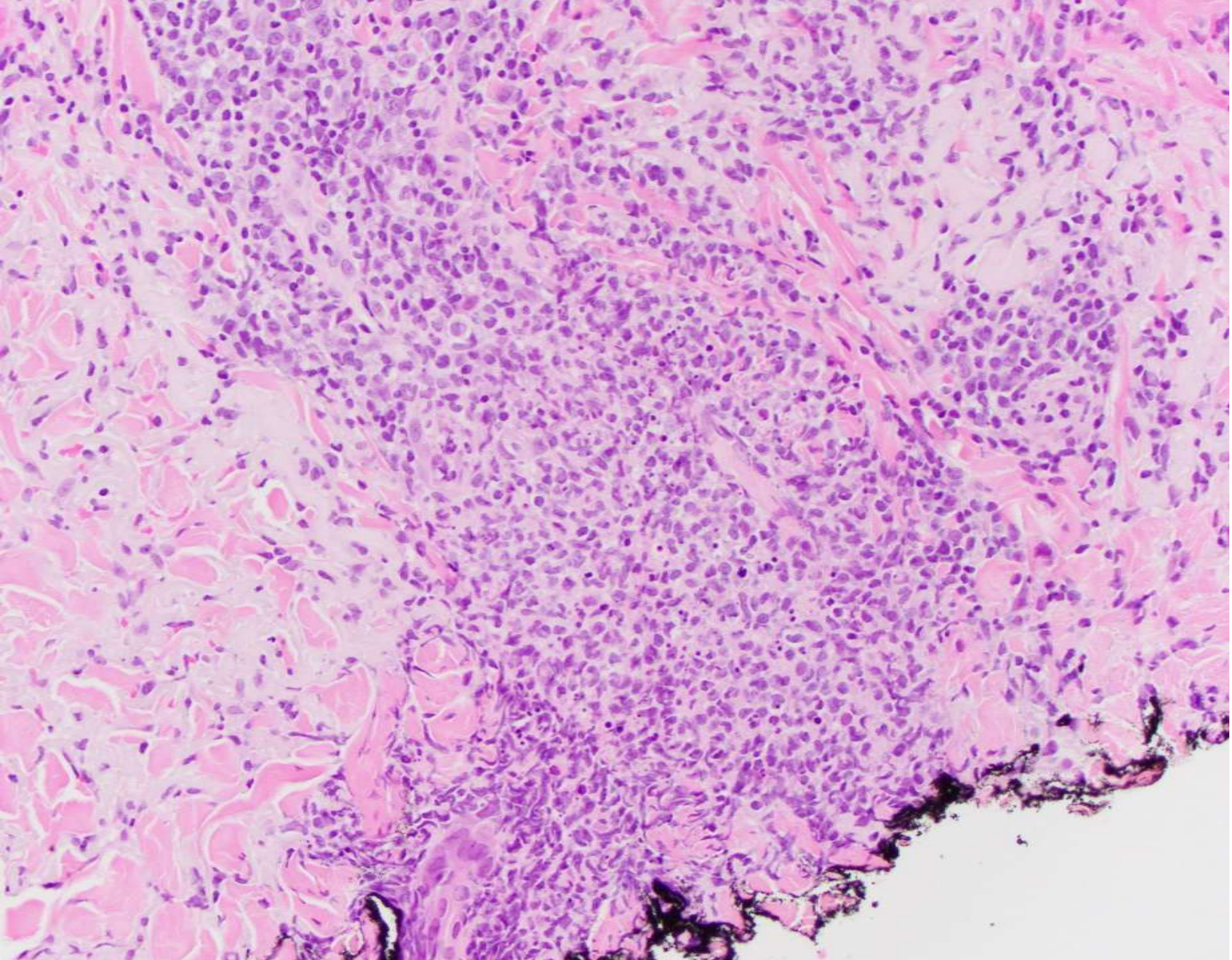

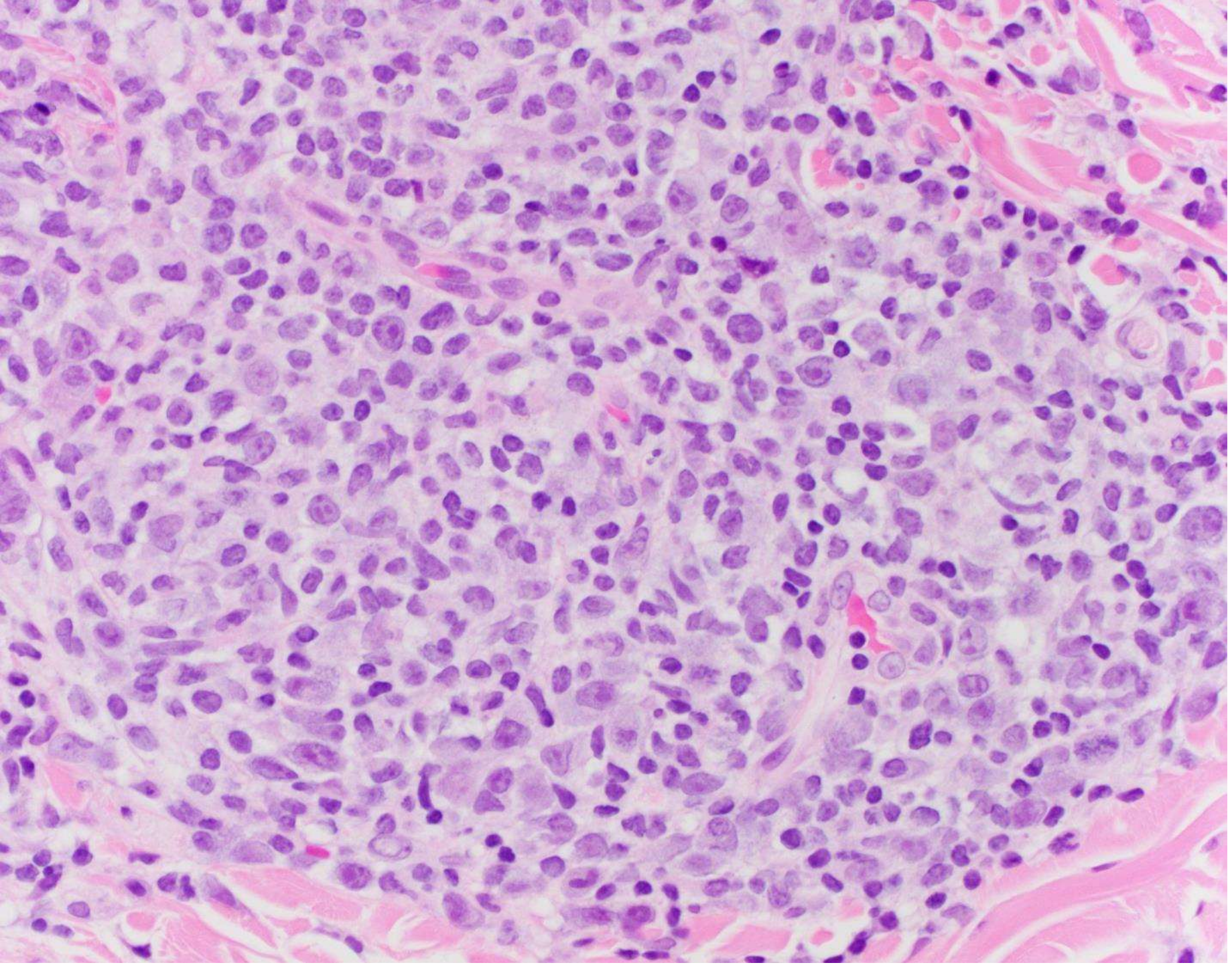

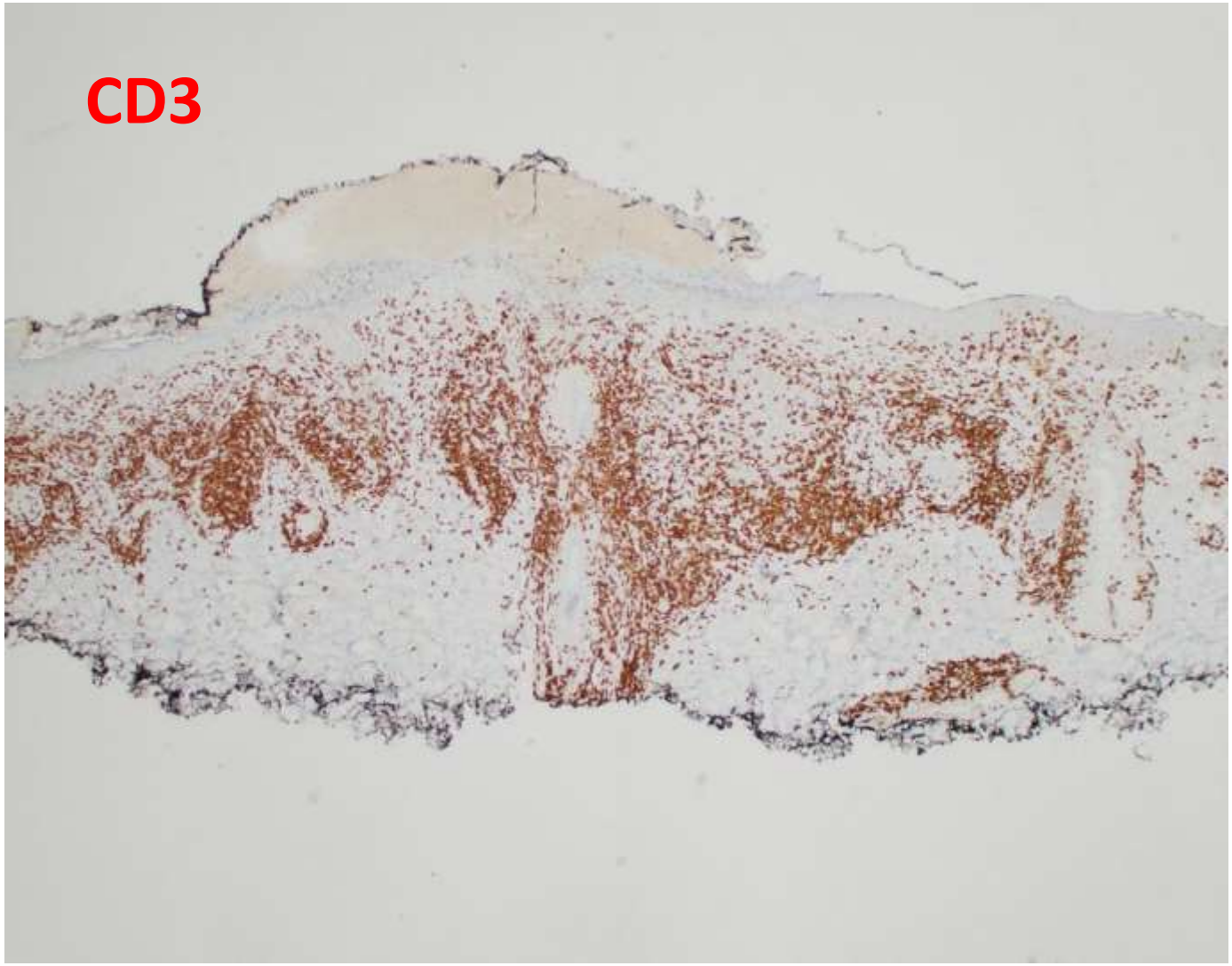
CD3

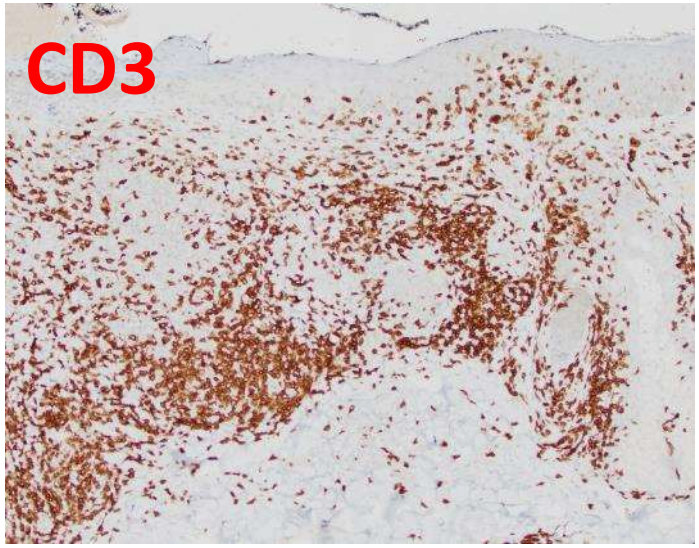
CD3

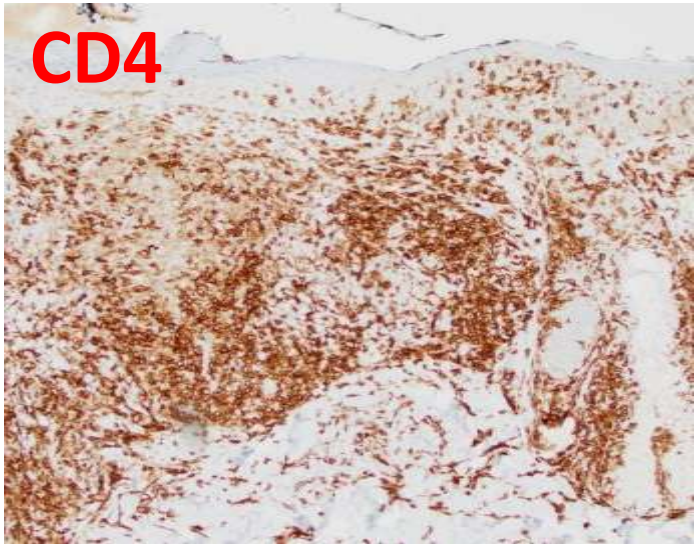
CD4

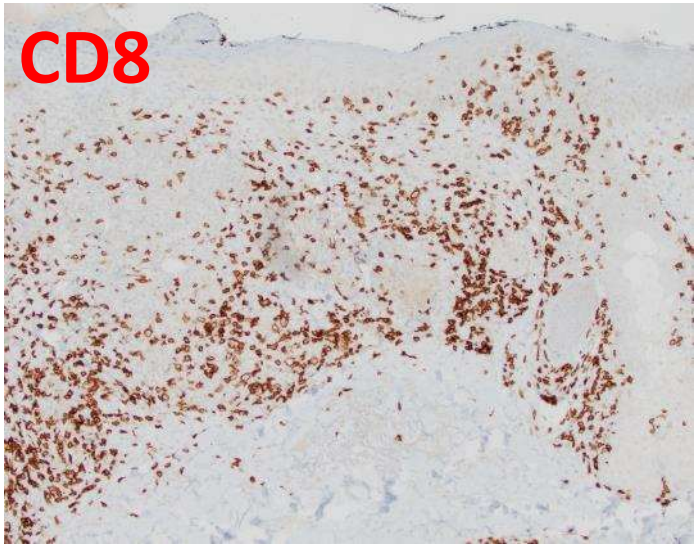
CD8

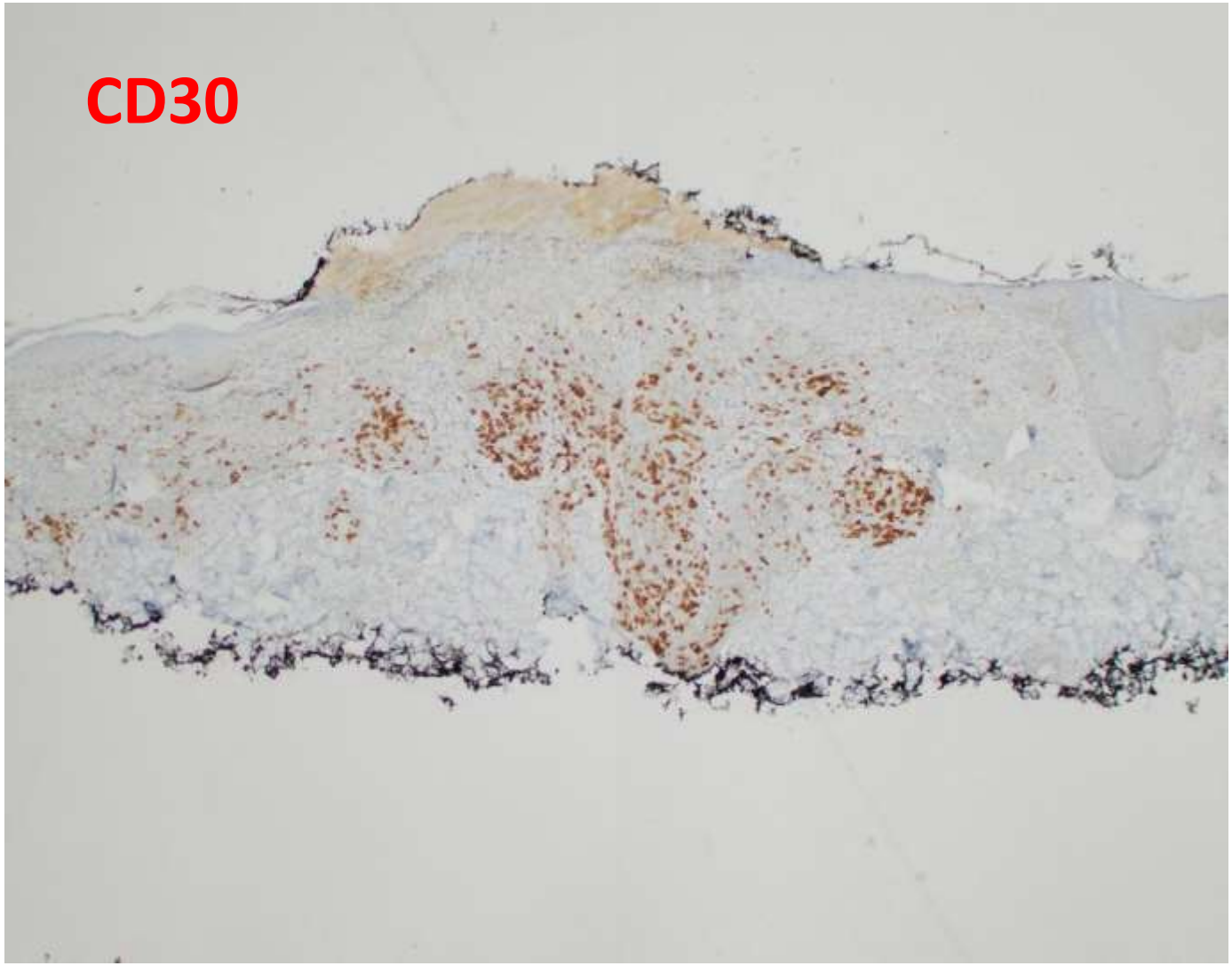
CD30

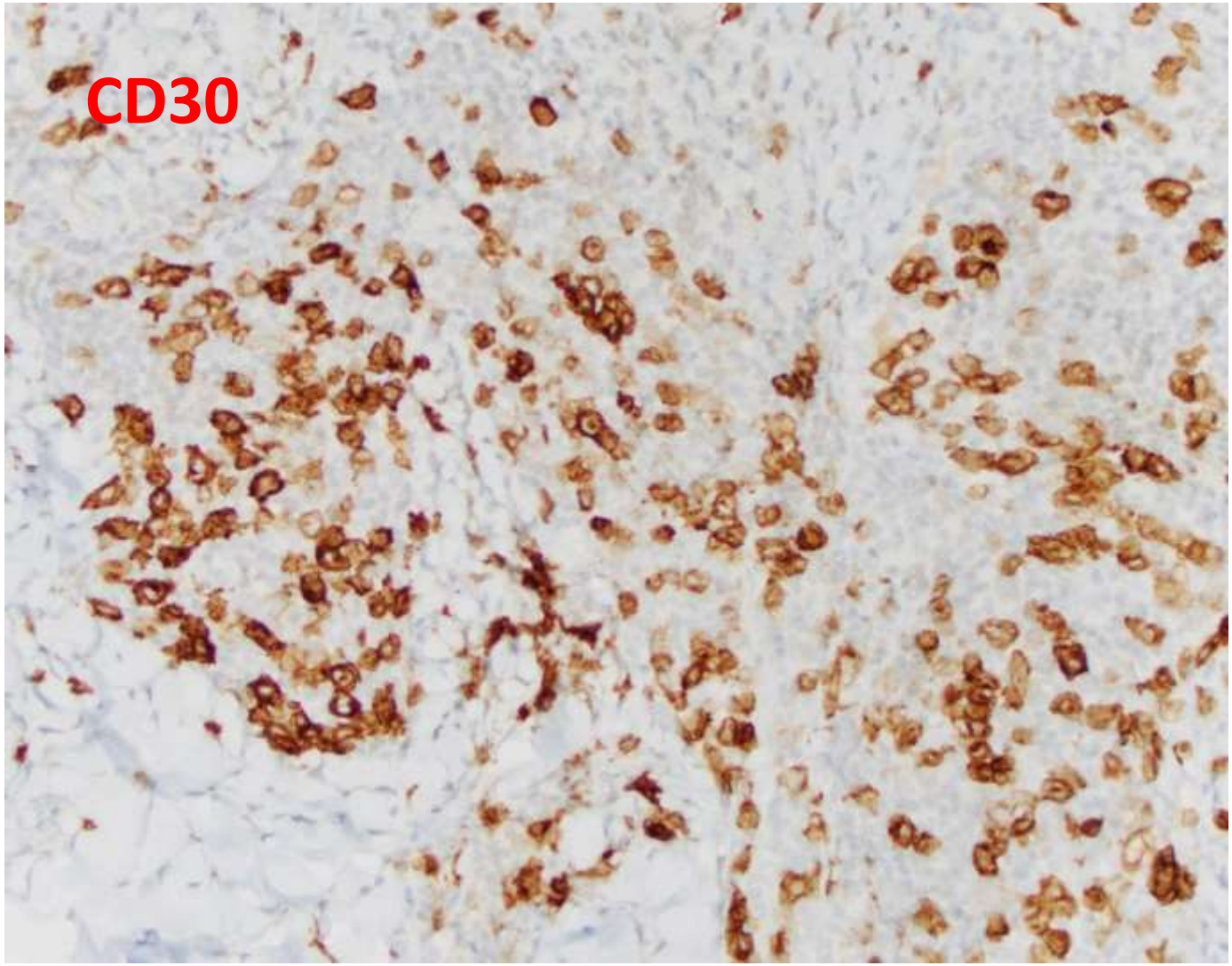
CD30

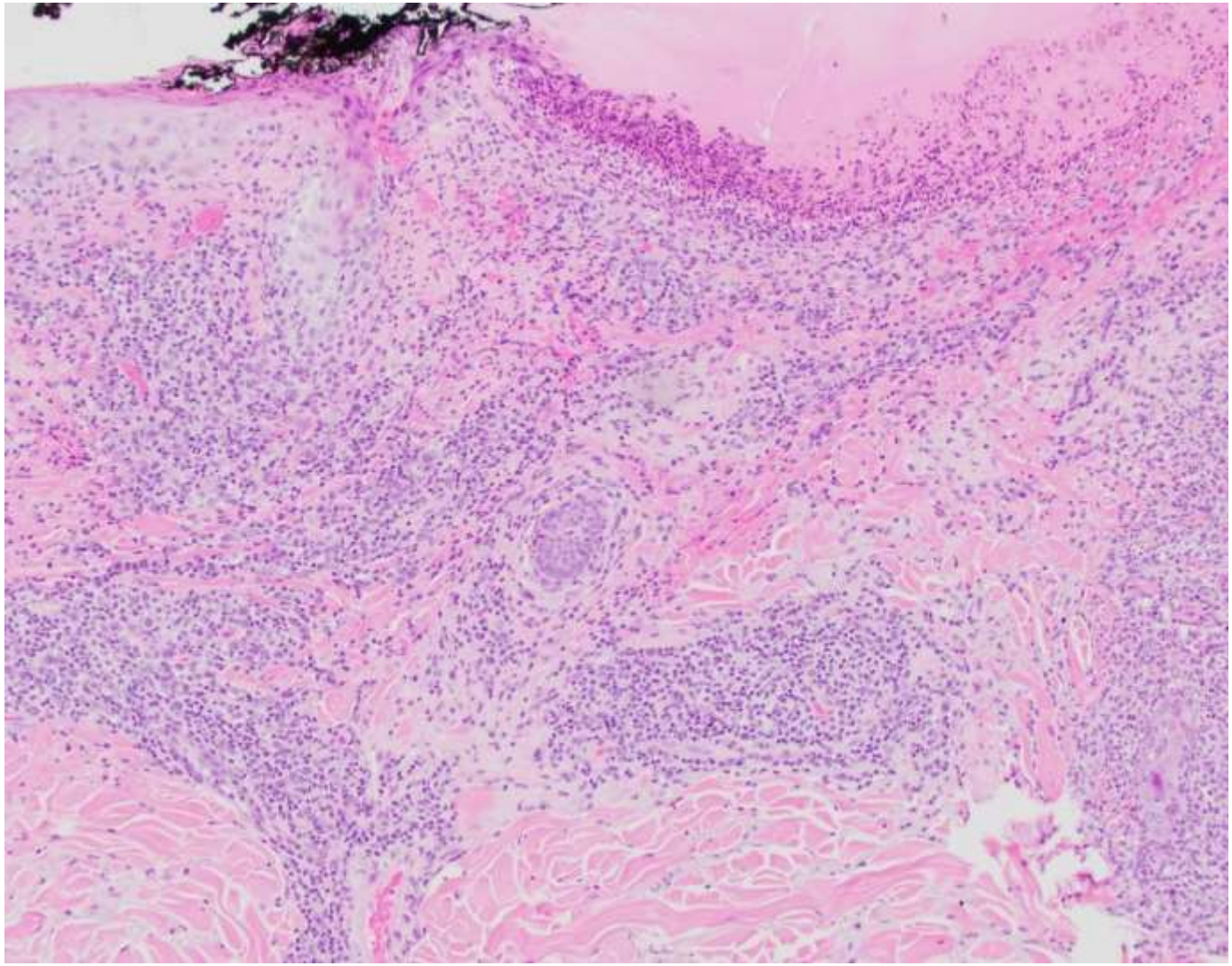

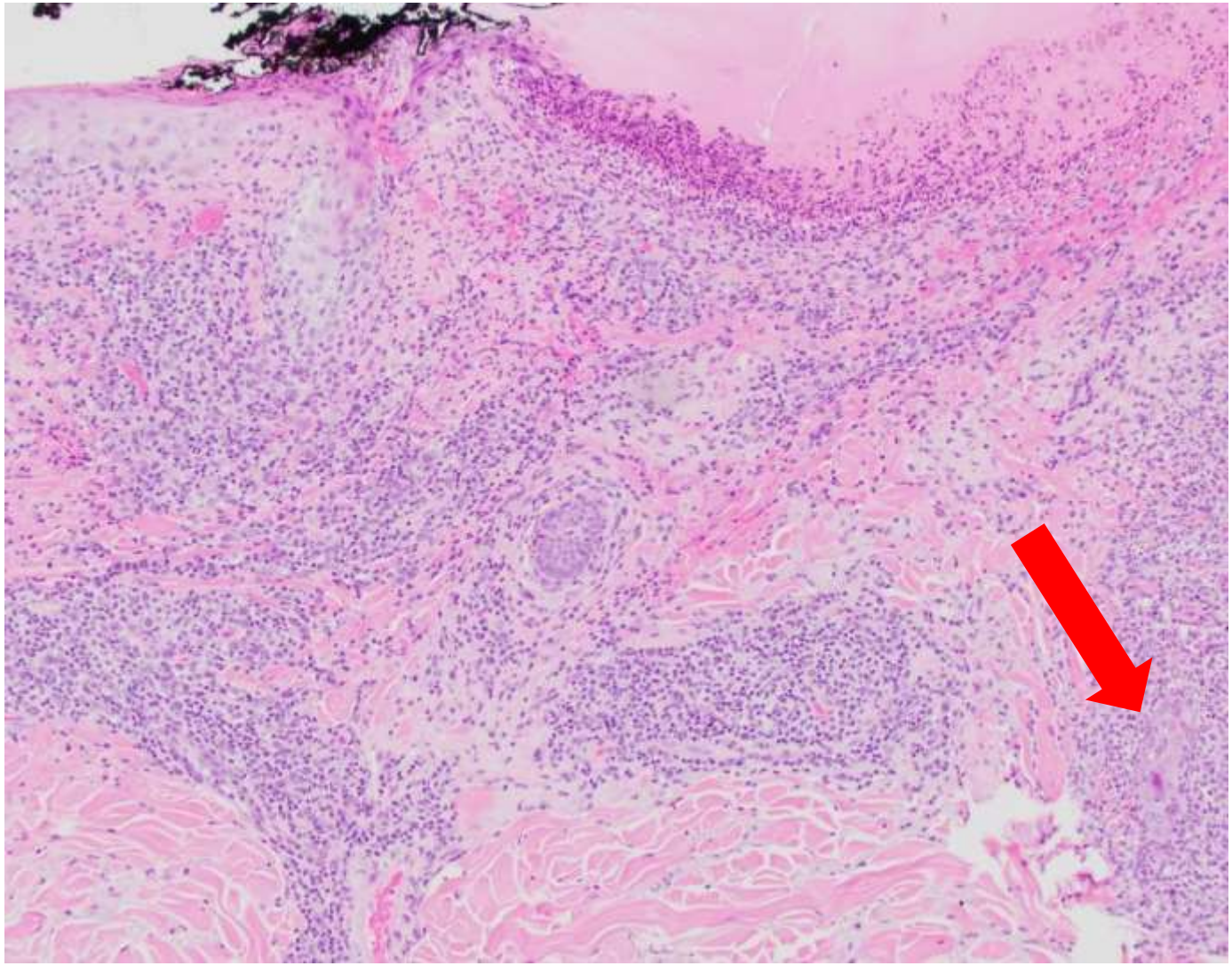

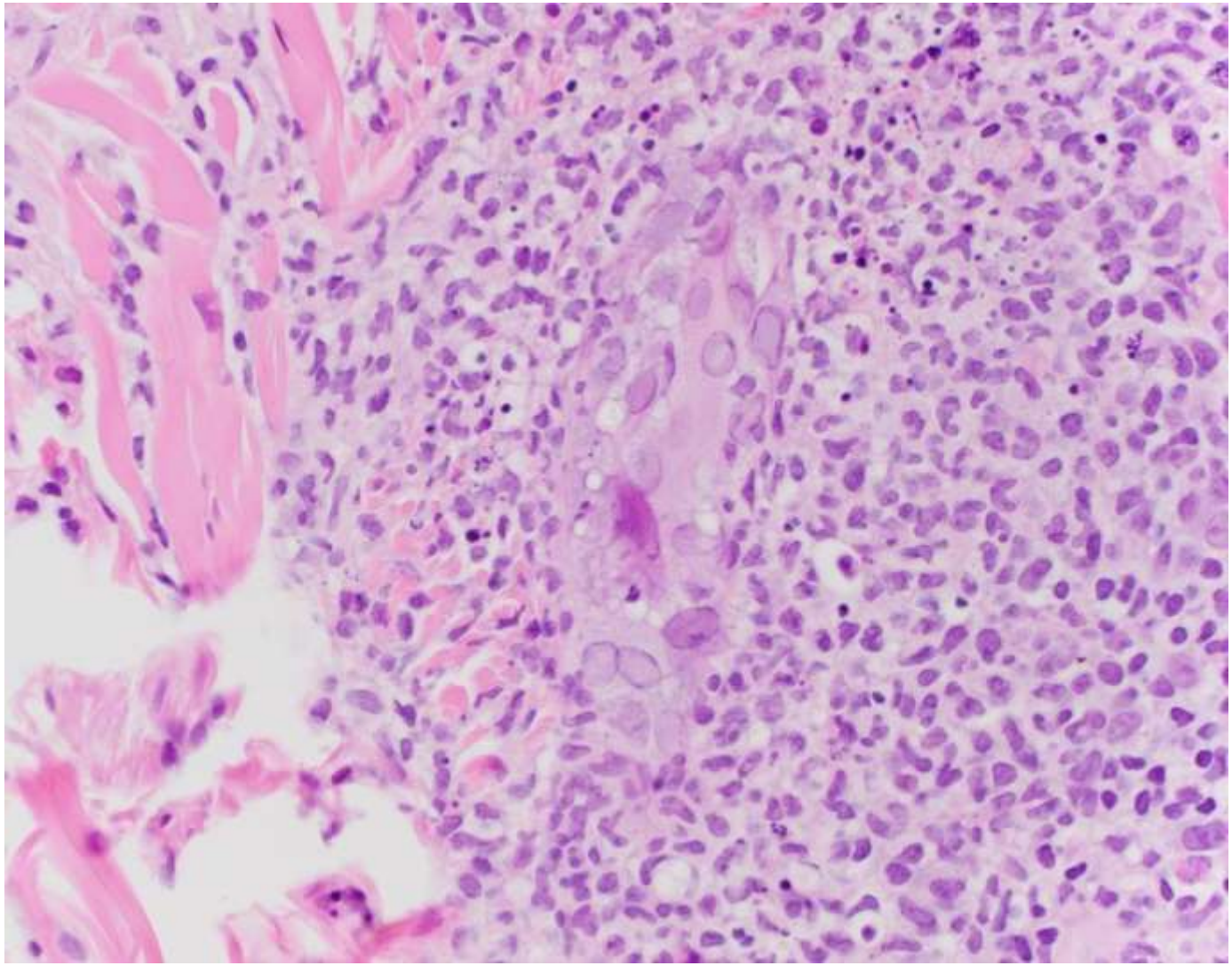

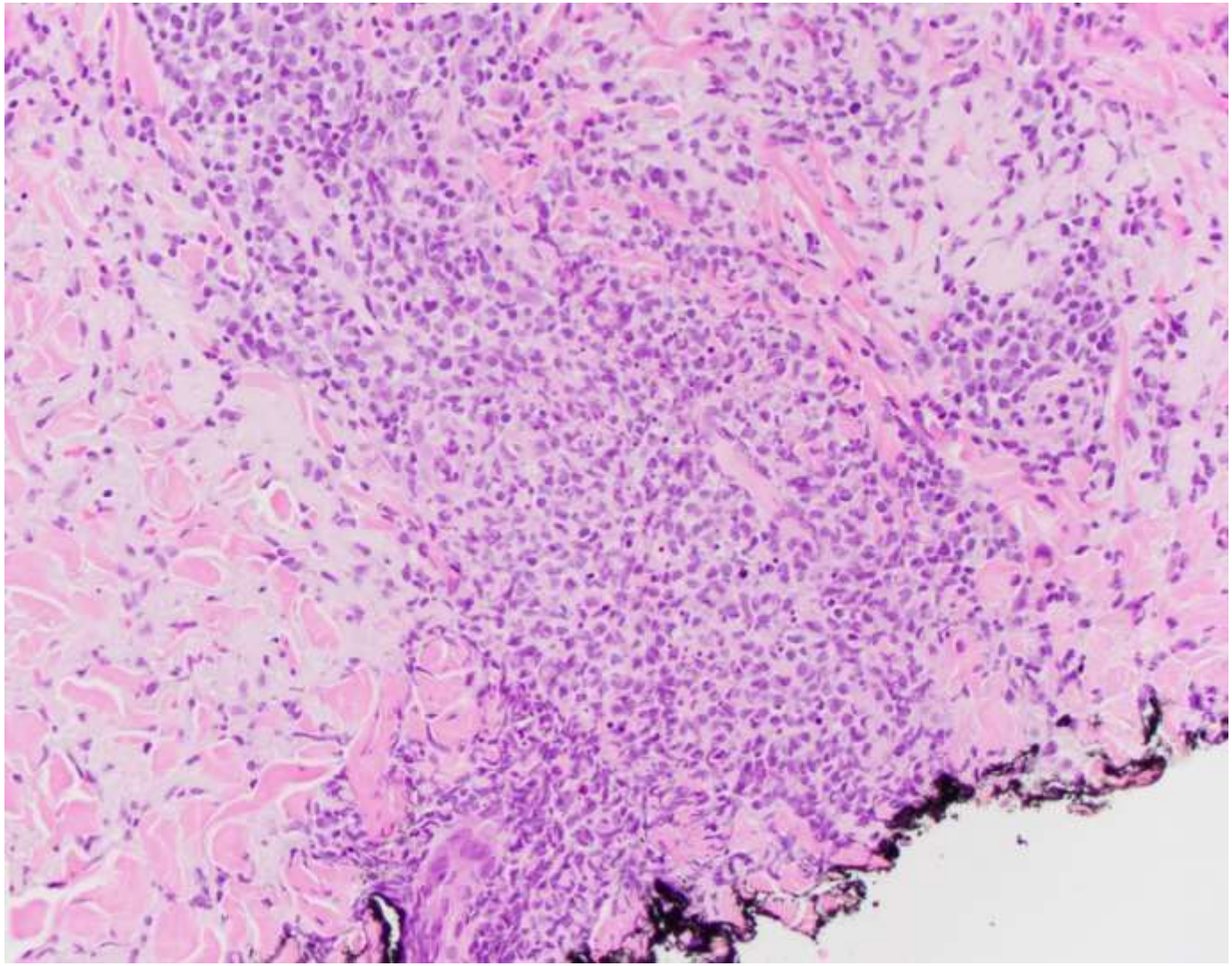

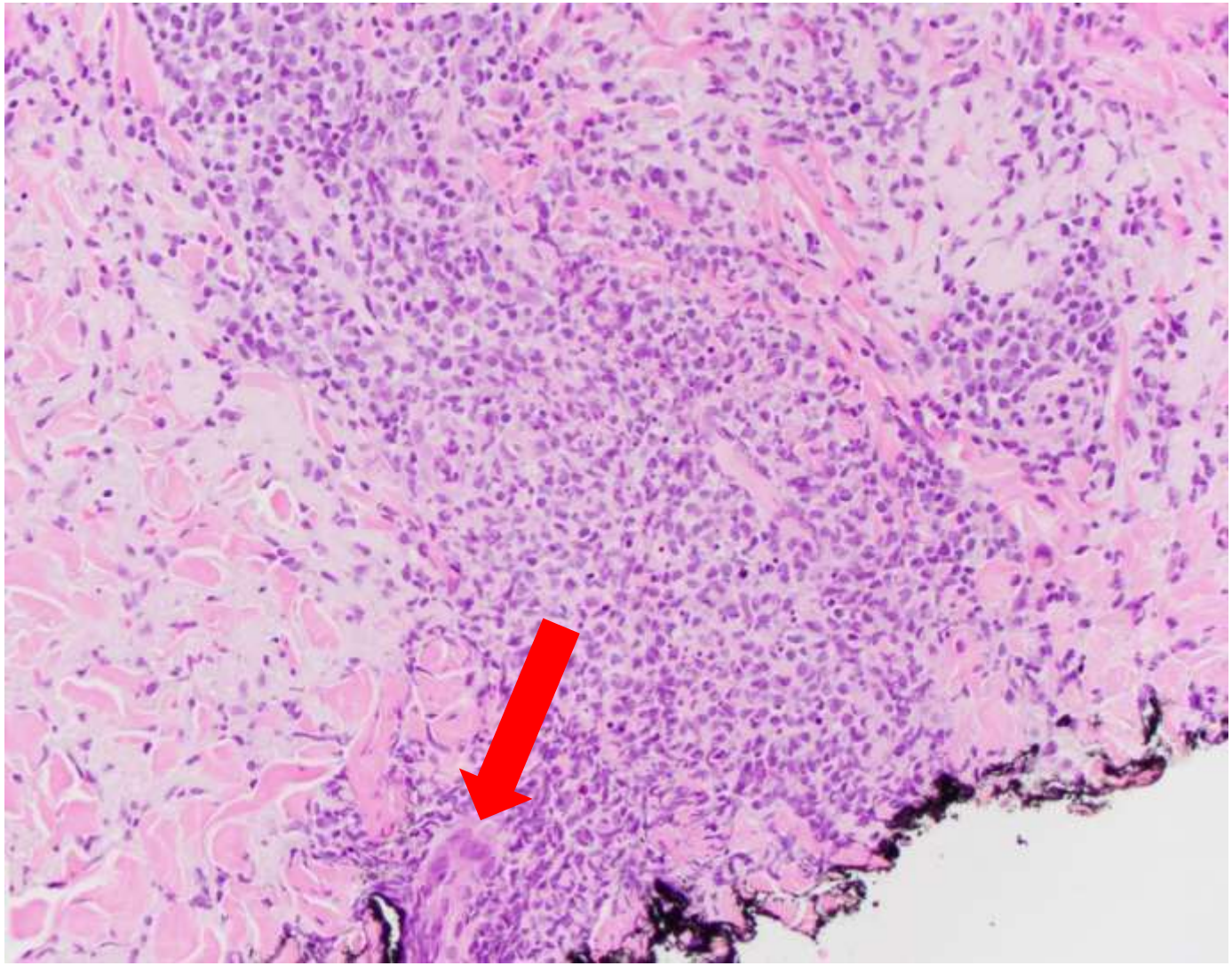

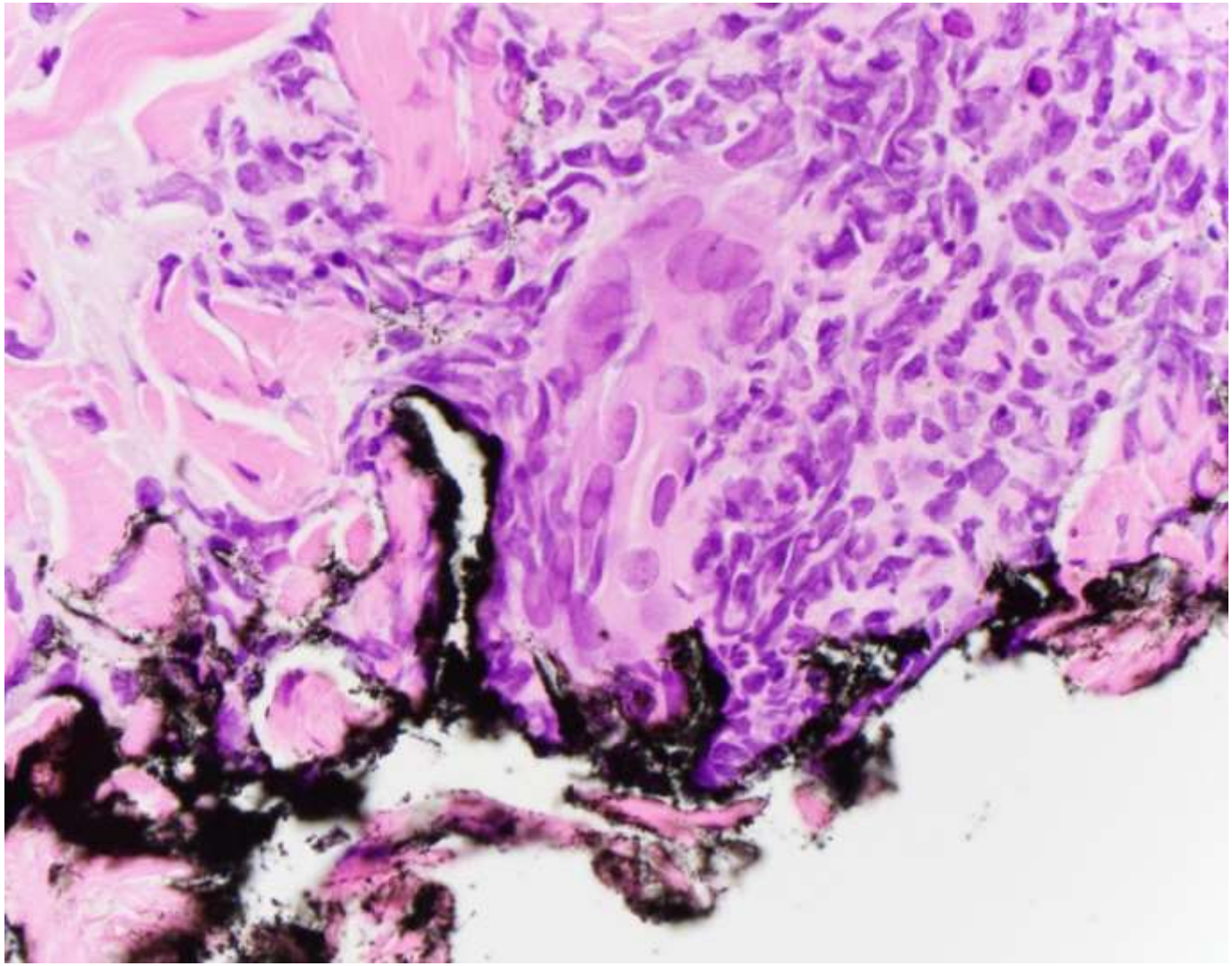

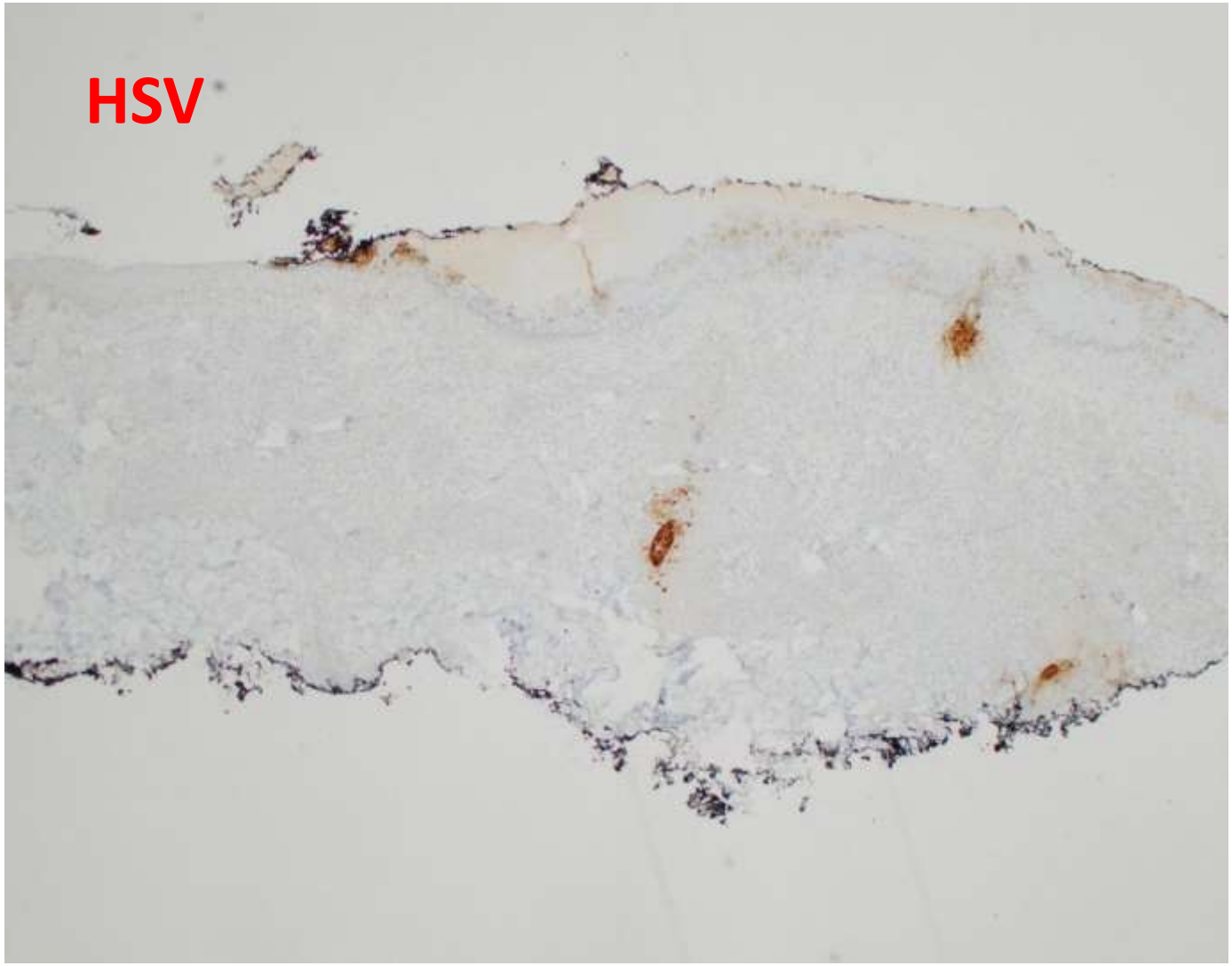
HSV

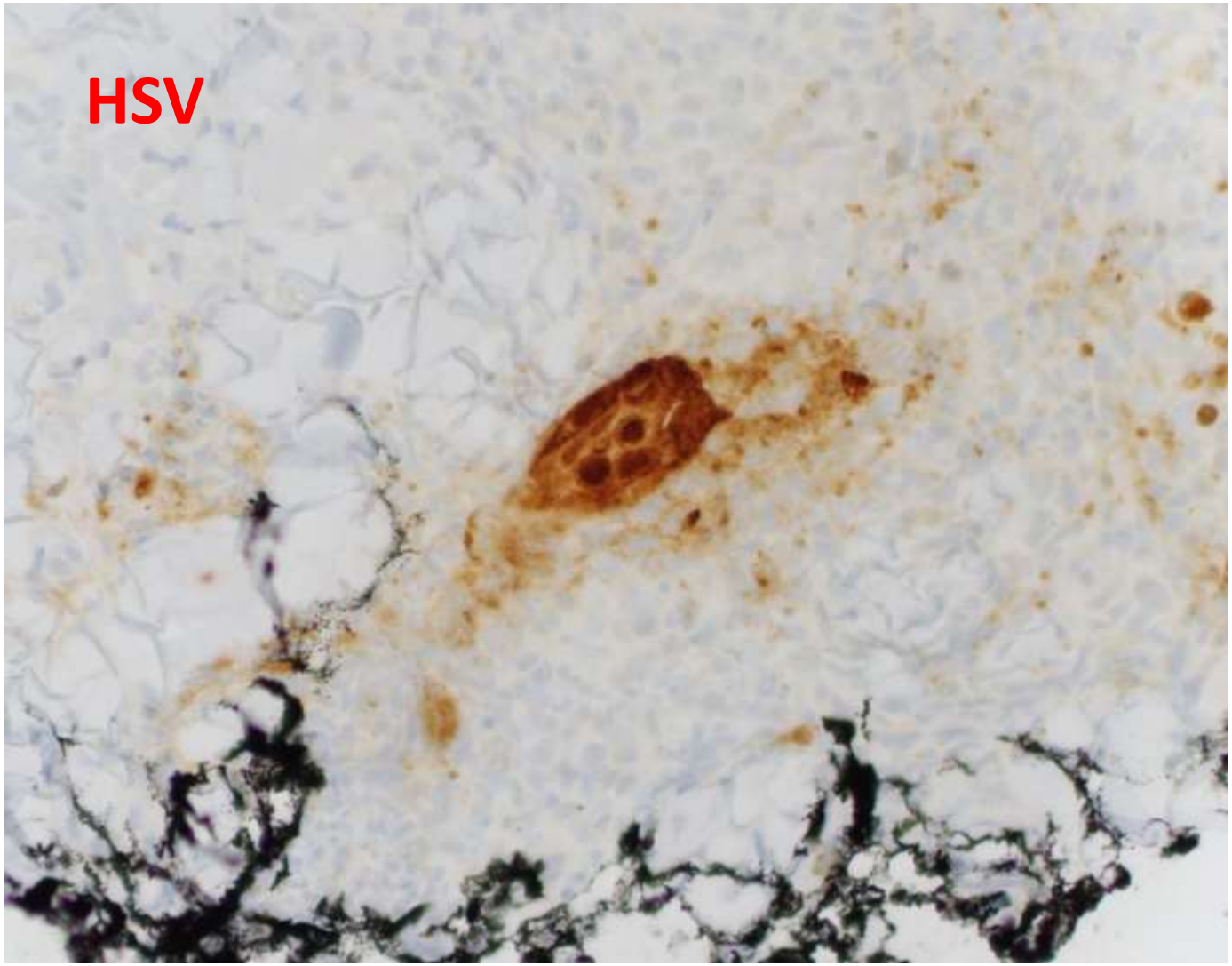
HSV

Differential diagnosis of CD30+ cutaneous infiltrate

- Primary cutaneous CD30+ T cell lymphoproliferative disorder
  - Lymphomatoid papulosis
  - Primary cutaneous anaplastic large cell lymphoma
- Mycosis fungoides/Sézary syndrome in transformation
- Secondary involvement by lymphoma with CD30+ cells, such as systemic anaplastic large cell lymphoma, Hodgkin lymphoma, adult T-cell lymphoma/leukemia, others
- Reactive conditions

Large CD30-positive cells in reactive infiltrates of the skin

- Large CD30-positive cells are not exclusive to malignancy
- Also reported in:
  - Viral infection, including EBV, HPV, HSV/VZV, Molluscum contagiosum, parapoxvirus (milker's nodule)
  - Other infectious causes, including syphilis, mycobacteria, and leishmaniasis
  - Arthropod bite, scabies
  - Drug reaction
  - Other various inflammatory conditions (gold acupuncture, scar following excision, etc.)
- They can be seen in clusters and as single cells with membranous and Golgi CD30 positivity, mimicking malignancy

23-0404

Ankur Sangoi; El Camino Hospital

70ish M presenting with right testicular pain, epididymal mass excision submitted.

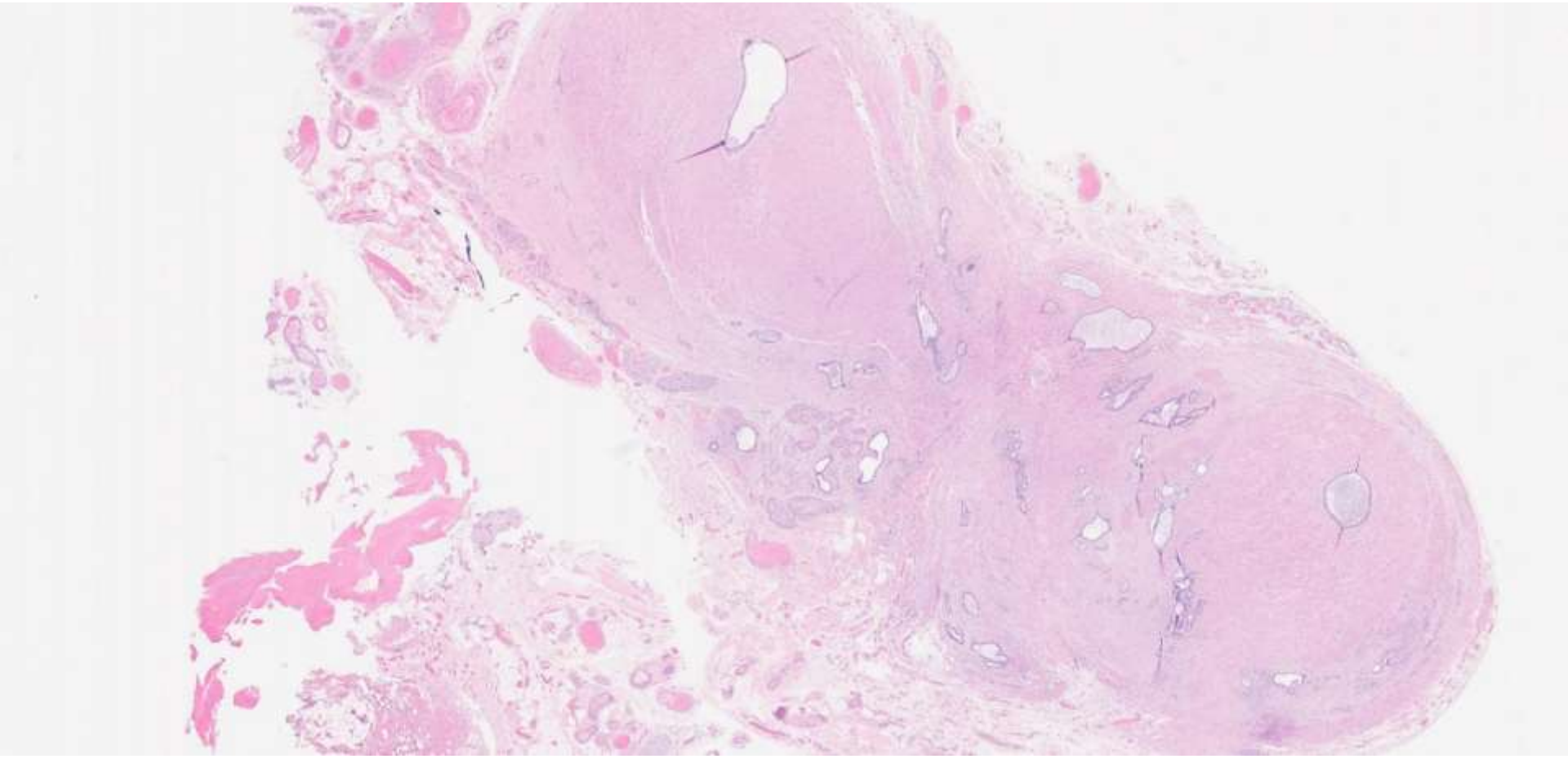

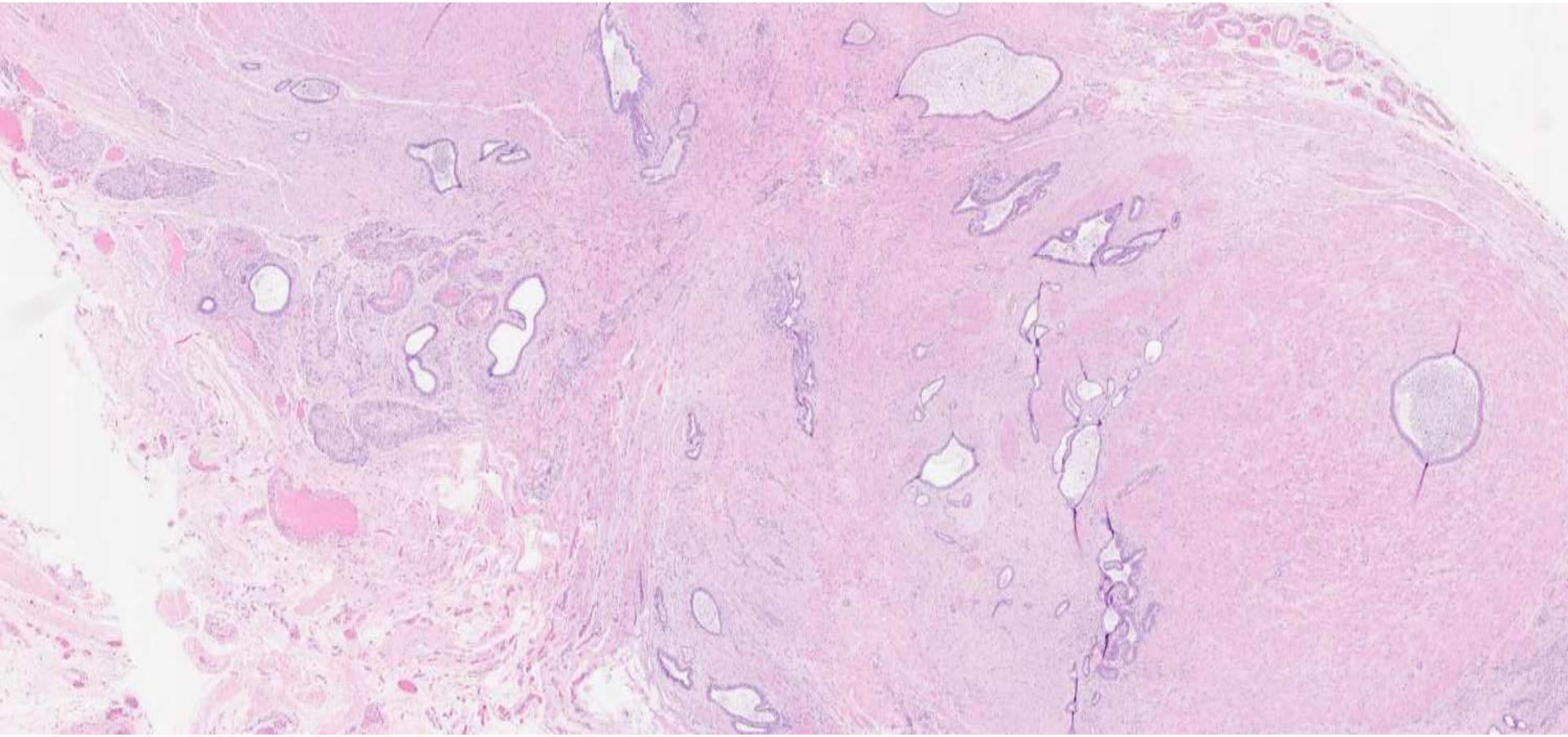

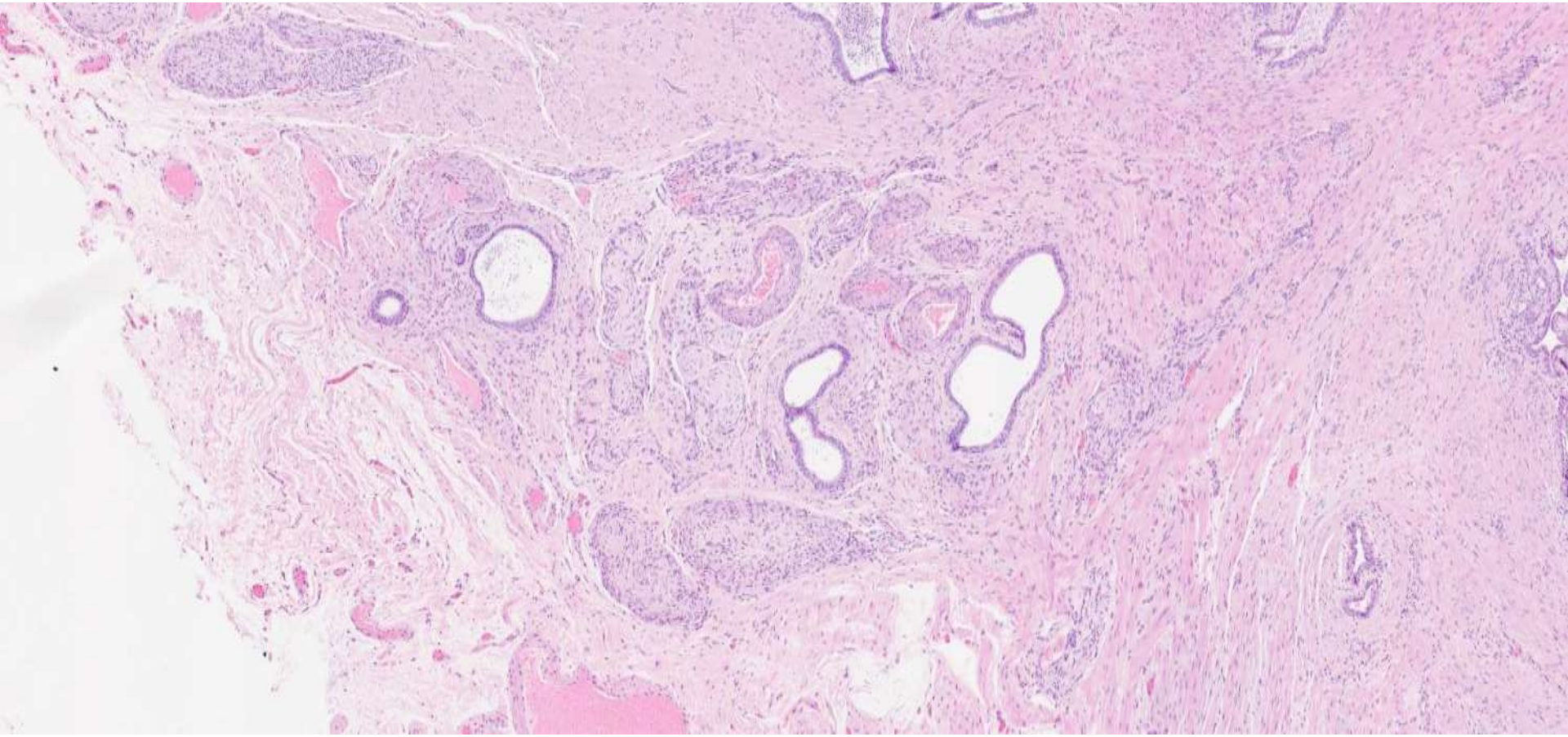

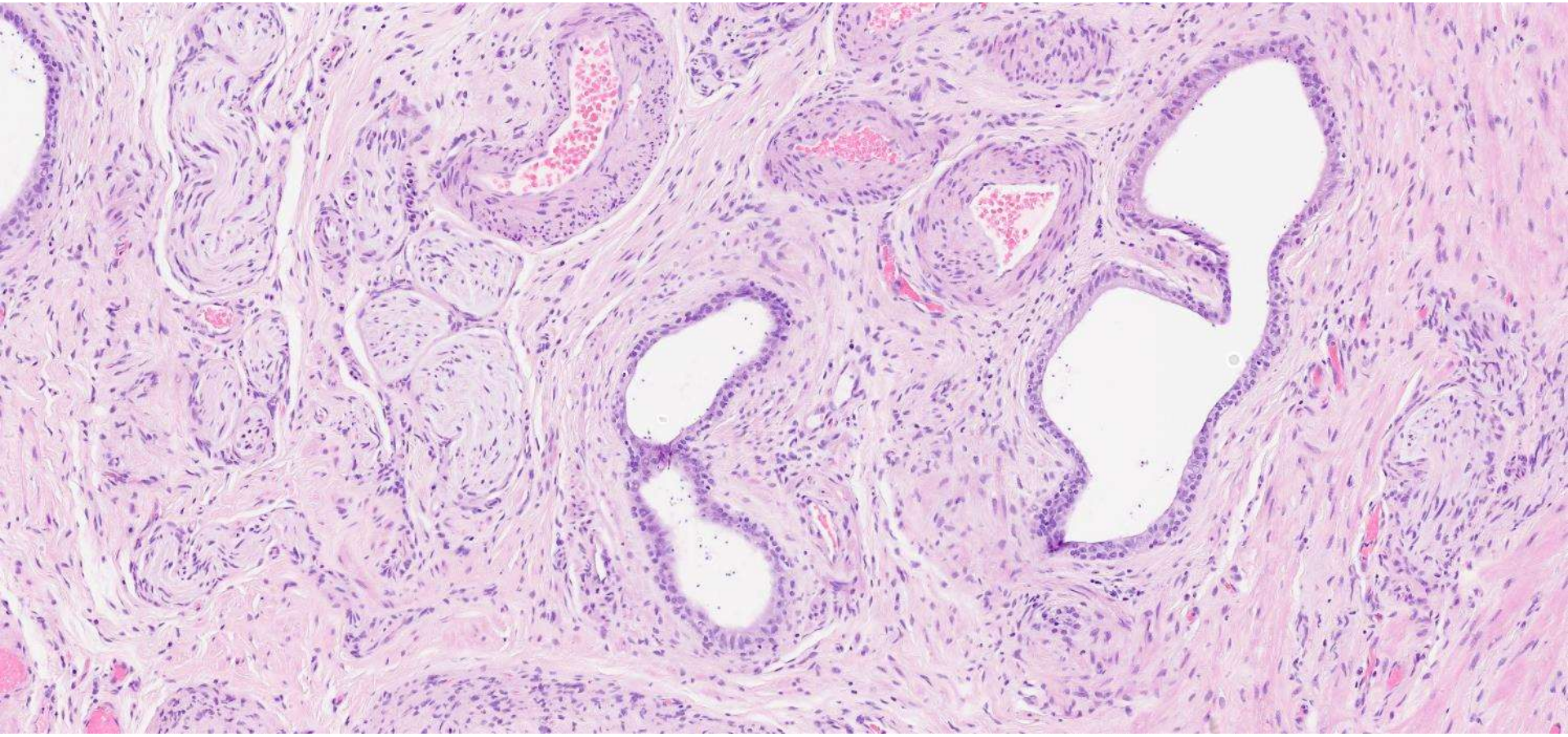

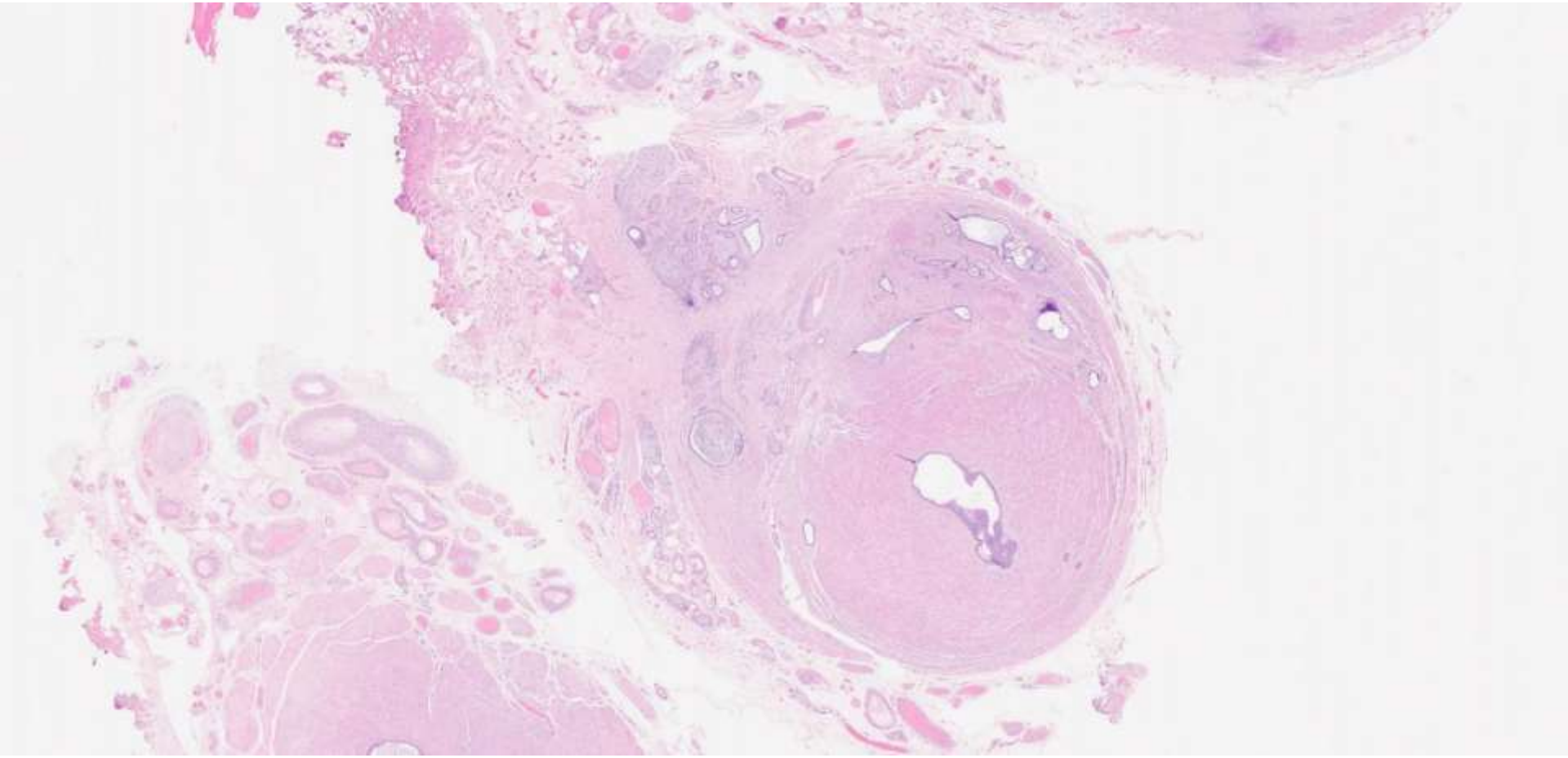

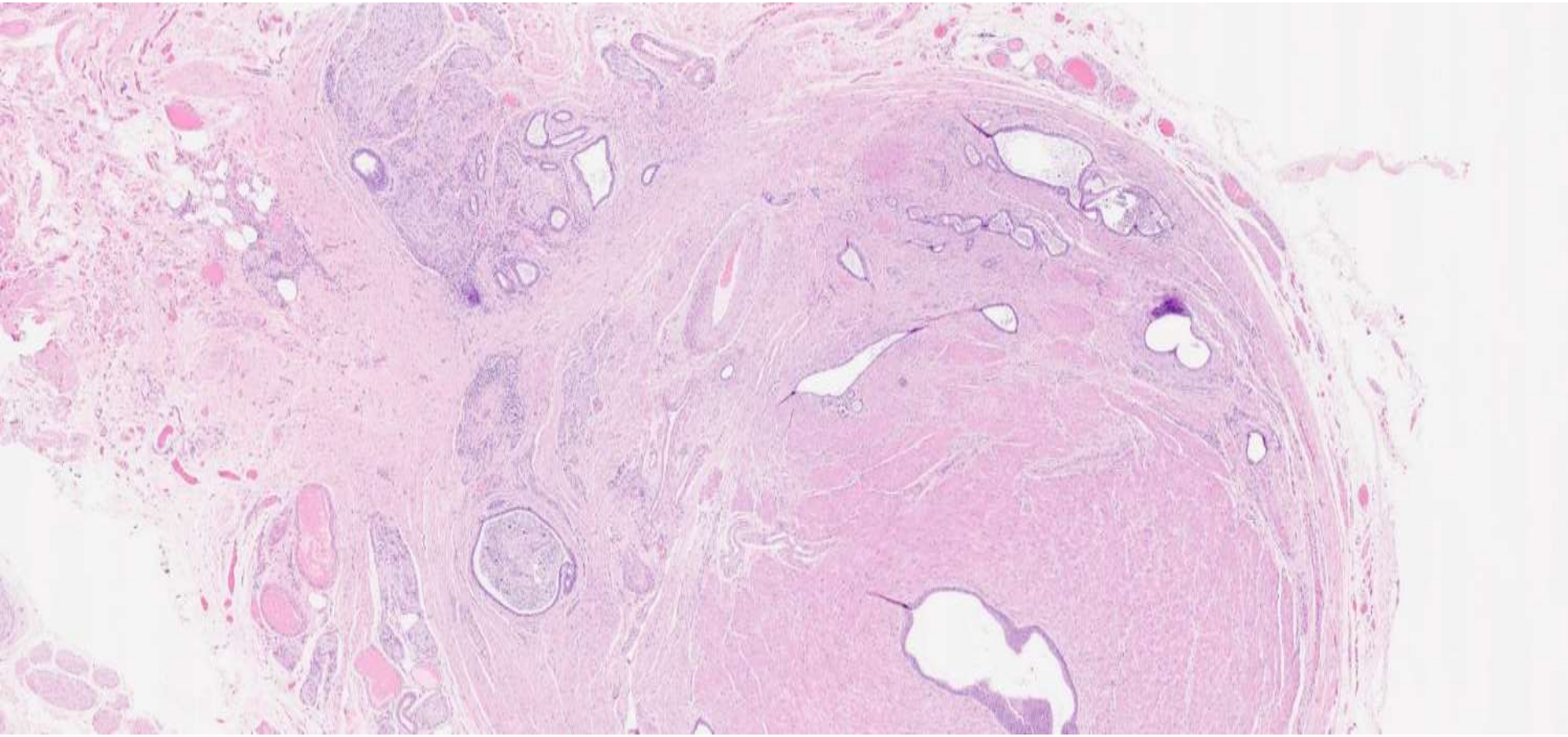

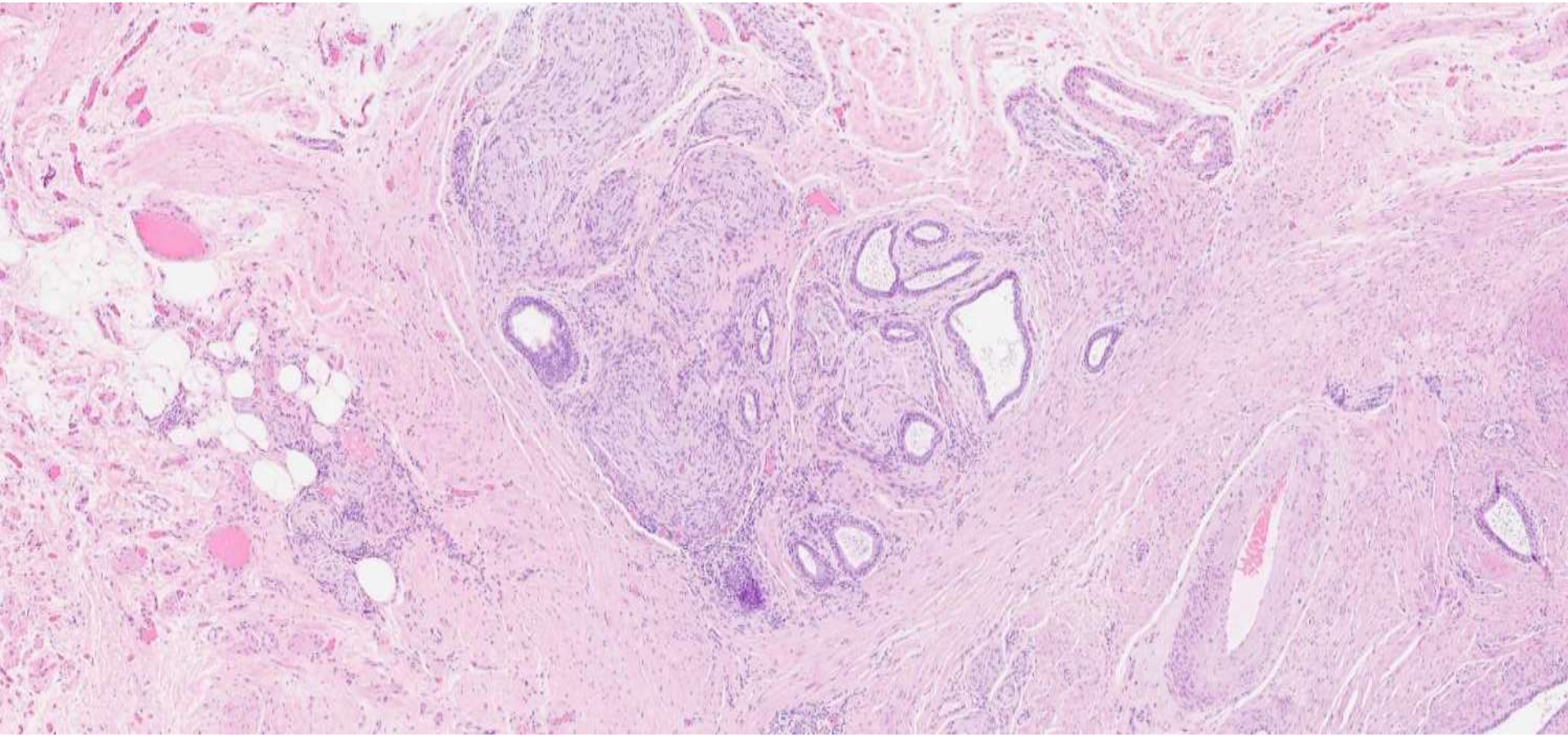

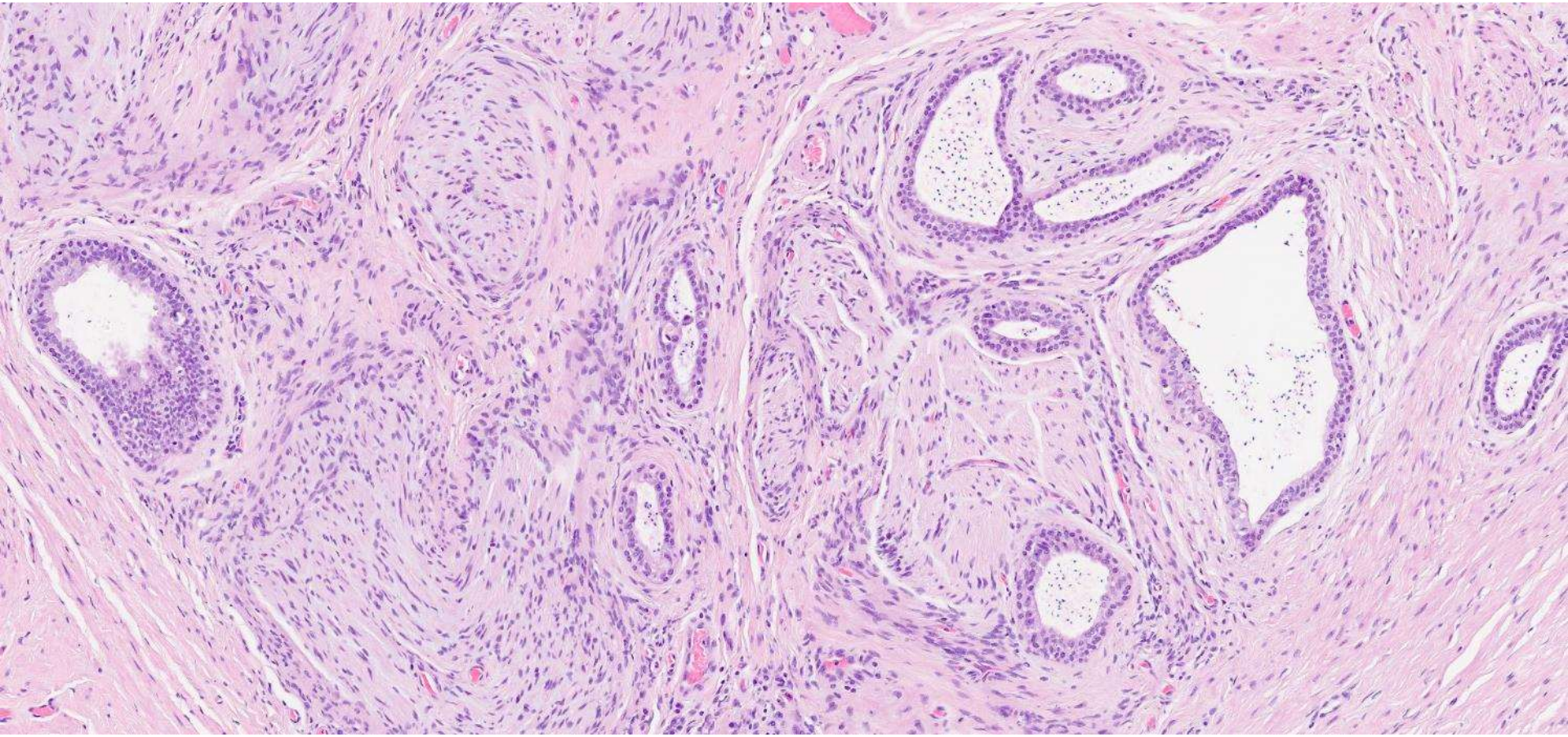

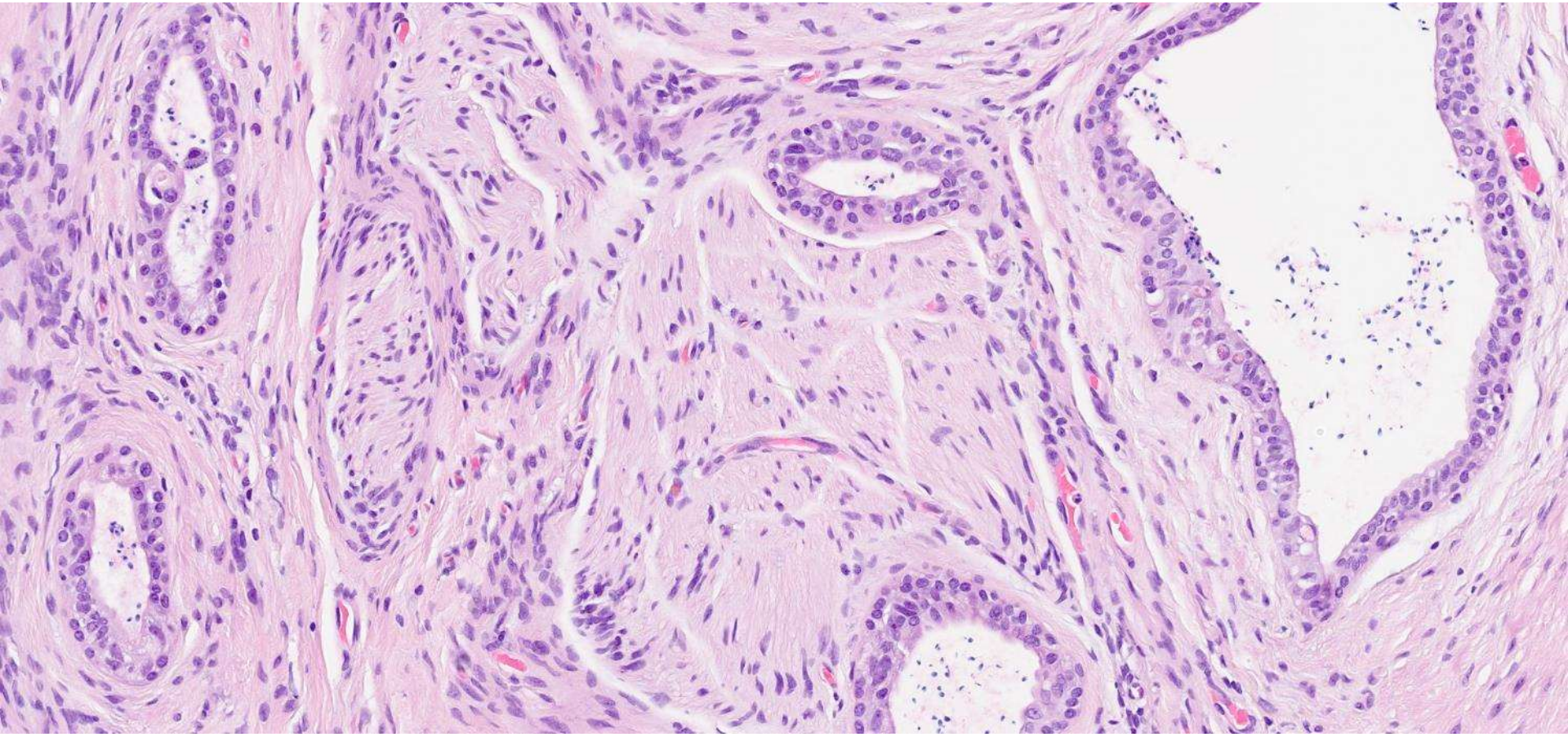

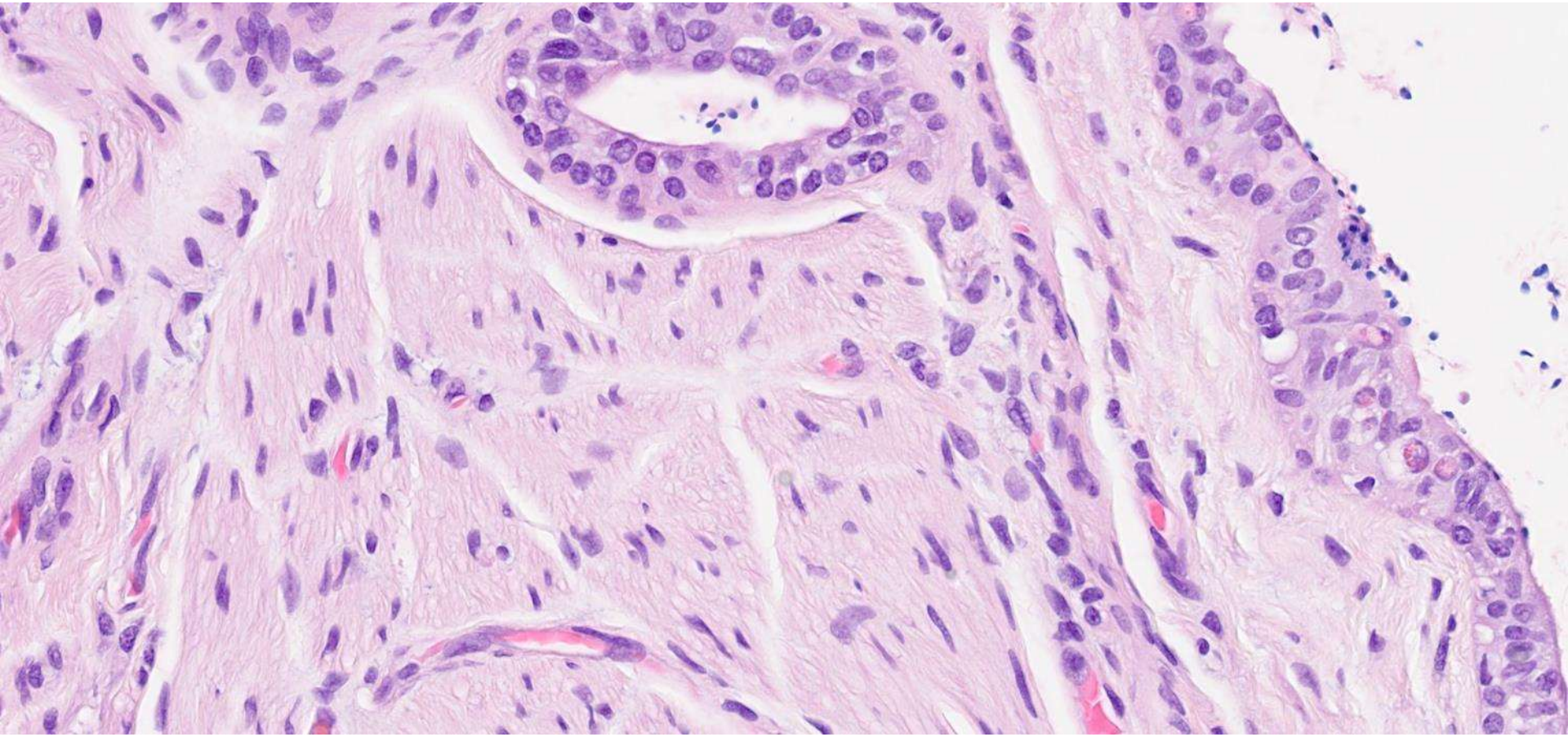

Human Pathology (2018) 73, 164–170

ELSEVIER

Human PATHOLOGY

www.elsevier.com/locate/humpath

Original contribution

Vasitis nodosa and related lesions: a modern immunohistochemical staining profile with special emphasis on novel diagnostic dilemmas ☆

Brie E. Kezlarian MD[a], Liang Cheng MD[b,c], Nilesh S. Gupta MD[a], Sean R. Williamson MD[a,d,*]

[a]*Department of Pathology and Laboratory Medicine and Henry Ford Cancer Institute, Henry Ford Health System, Detroit, MI 48202, USA*
[b]*Department of Pathology and Laboratory Medicine, Indiana University School of Medicine, Indianapolis, IN 46202, USA*
[c]*Department of Urology, Indiana University School of Medicine, Indianapolis, IN 46202, USA*
[d]*Department of Pathology, Wayne State University School of Medicine, Detroit, MI 48201, USA*

Received 17 August 2017; revised 16 November 2017; accepted 1 December 2017

Keywords:
Vasitis nodosa;
Immunohistochemistry;
Prostate cancer;
GATA3;
PAX8;
NKX3.1

Summary Vasitis nodosa is a benign proliferation of vas deferens epithelium, thought to be a response to trauma or obstruction, usually vasectomy. Although histologic features mimic malignancy, diagnosis is usually straightforward due to the clinical context. We analyzed 21 specimens with vasitis or epididymitis nodosa with antibodies to PAX8, CD10, p63, α-methyl-acyl-coA-racemase (AMACR), GATA3, prostein, NKX3.1, and prostate-specific antigen (PSA). Two diagnostically problematic cases included (1) florid bladder muscle involvement after prostatectomy and (2) involvement of the ampulla and ejaculatory duct in a radical prostatectomy specimen. Vasitis nodosa was excluded in 3 additional histologic mimics (2 post-treatment prostate cancers and 1 bladder cancer). PAX8 yielded consistent positive (100%) nuclear staining in the proliferative glands of vasitis nodosa, often stronger and more uniform than native vas deferens. CD10 labeling was common but also labeled secretions and other structures. Labeling for p63 was often basally located in glands with a multilayered appearance, but often markedly attenuated or lacking in the proliferative glands compared to native epithelium. AMACR positivity was variable but often present (19/21). PSA, prostein, and NKX3.1 were consistently negative. Rare problematic cases of vasitis nodosa include "invasion" of the ejaculatory duct at the prostate and involvement of bladder muscle after prostatectomy. The proliferative vasitis nodosa glands often have a prostate cancer–like staining pattern with variable AMACR positivity and negative or patchy p63. However, reliable positivity for PAX8, patchy GATA3, and negative staining for PSA, NKX3.1, and prostein aid in distinguishing from prostate cancer and tubular variants of bladder cancer.

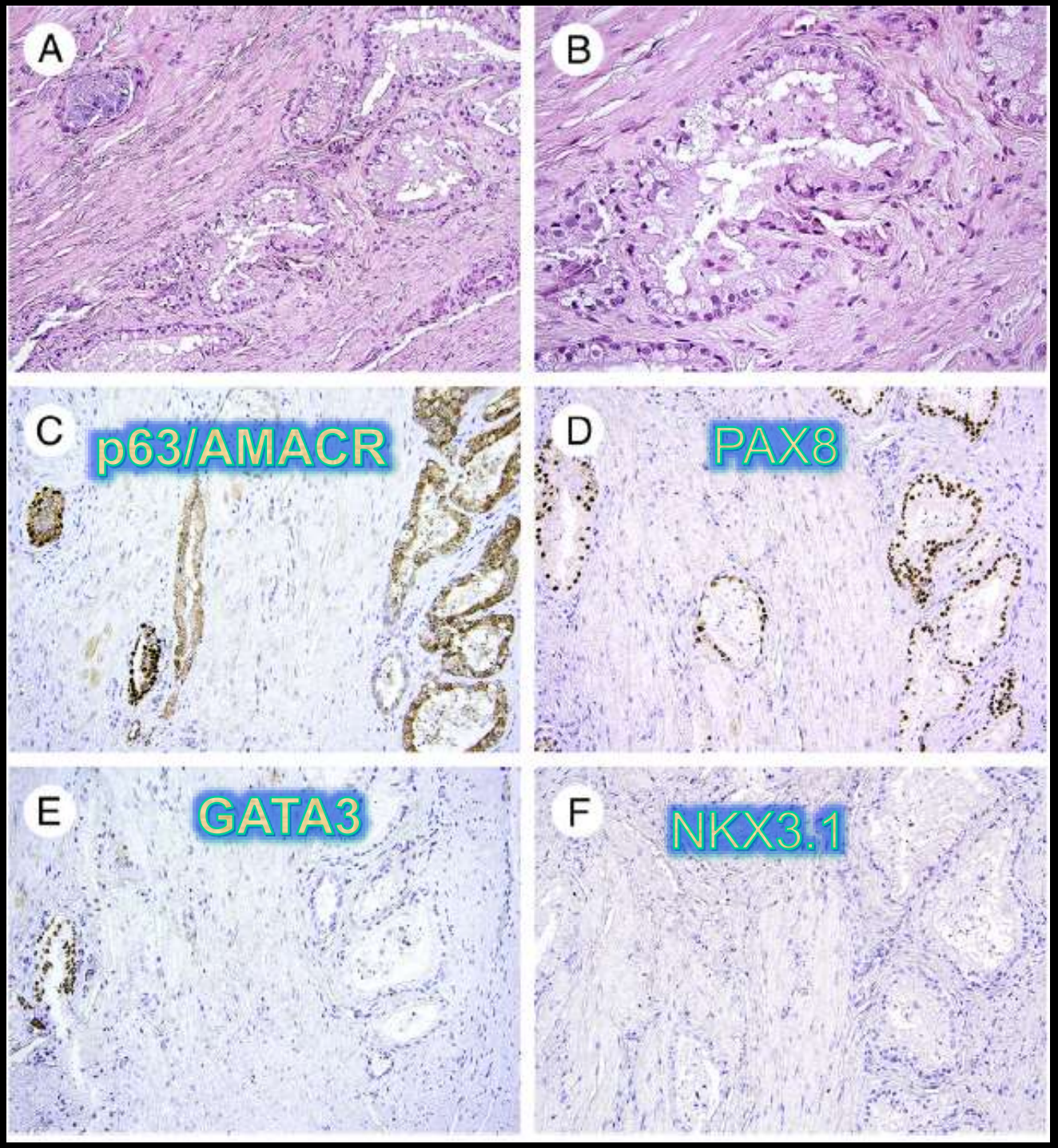
A
B
C
p63/AMACR
D
PAX8
E
GATA3
F
NKX3.1

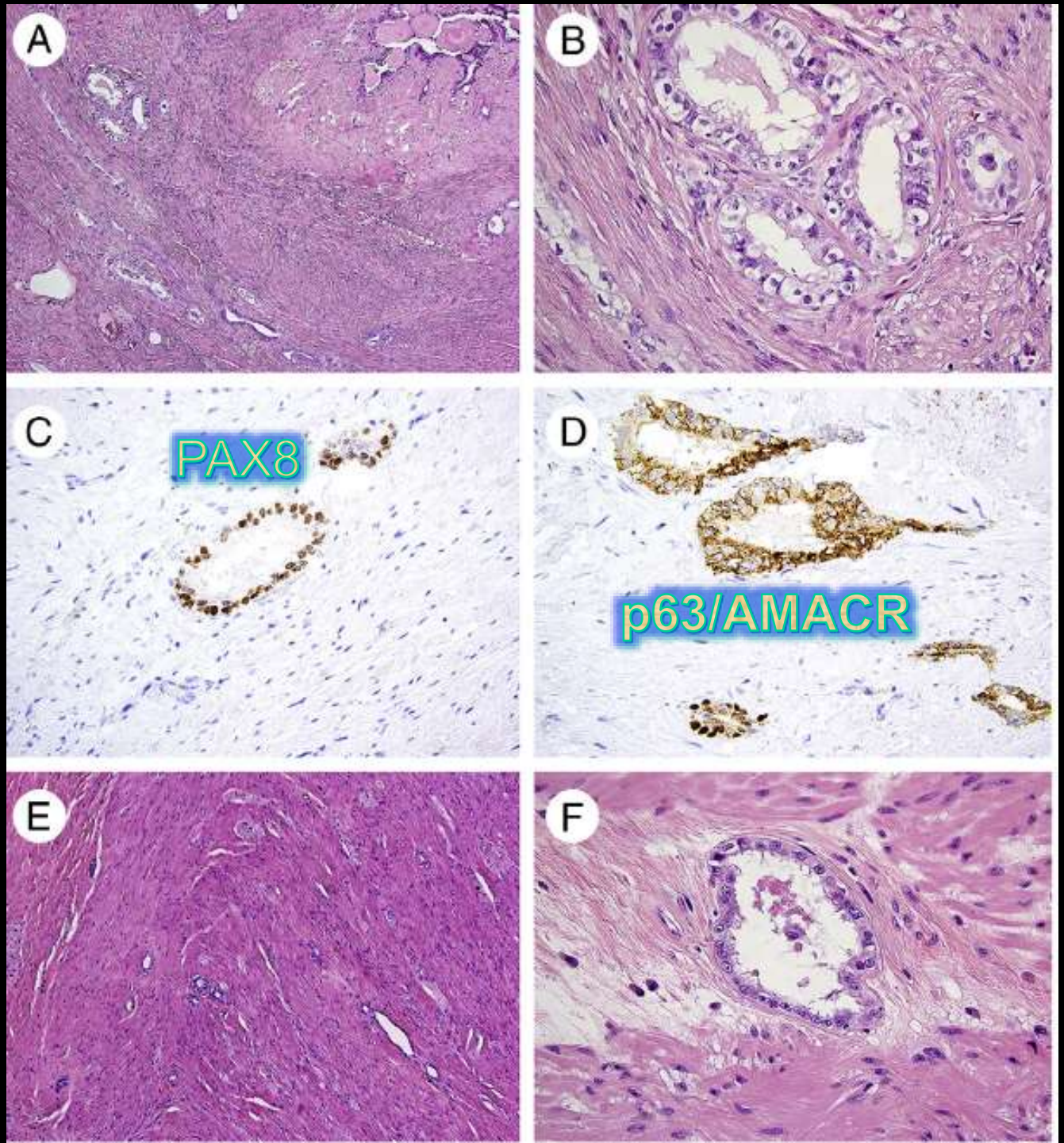
A
B
C
PAX8
D
p63/AMACR
E
F

Table Summary of immunohistochemical markers in vasitis nodosa and mimics

	Vasitis nodosa	Prostate cancer mimicking vasitis nodosa	Urothelial carcinoma mimicking vasitis nodosa
p63	12/21, often basally located	0/2	1/1, patchy
AMACR	18/21, variable, weak to strong	2/2, strong	ND
GATA3	10/18, patchy or basal	ND	1/1, patchy, nonbasal
PAX8	21/21, more uniform in vasitis nodosa than normal lining	0/2	0/1
CD10	21/21, diffuse in glands and secretions	ND	1/1, patchy but some cuboidal glands entirely negative
PSA	0/20	2/2	0/1
Prostein	0/20	1/1	0/1
NKX3.1	0/20	ND	ND

Abbreviations: AMACR, α-methylacyl-CoA racemase; PSA, prostate-specific antigen; ND, not done.

VASITIS NODOSA: potential pitfalls

- IHC: prostate cancer-like staining
  → AMACR+ neg/patchy p63 but PAX8+

- "pseudo" invasive histology
  → encroaching into soft tissues/nerves
  → rare can involve ejac duct, bladder muscle after prostatectomy

23-0405

Anjanaa Vijayanarayanan/Sonam Prakash; UCSF

30ish F who presented with rectal and abdominal pain. Rectal biopsy performed.

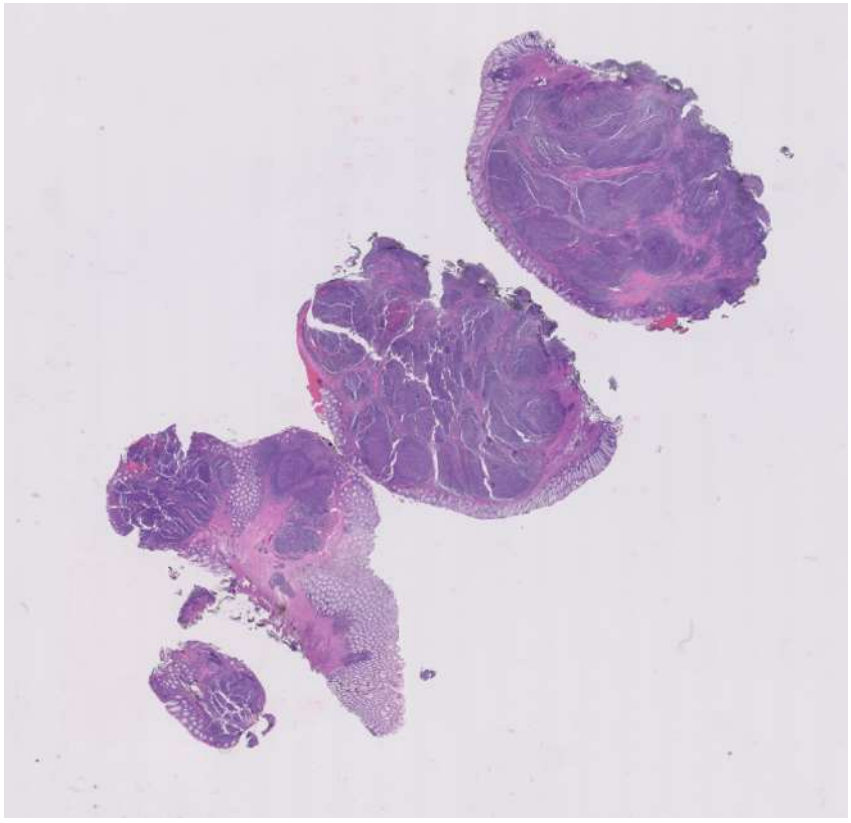

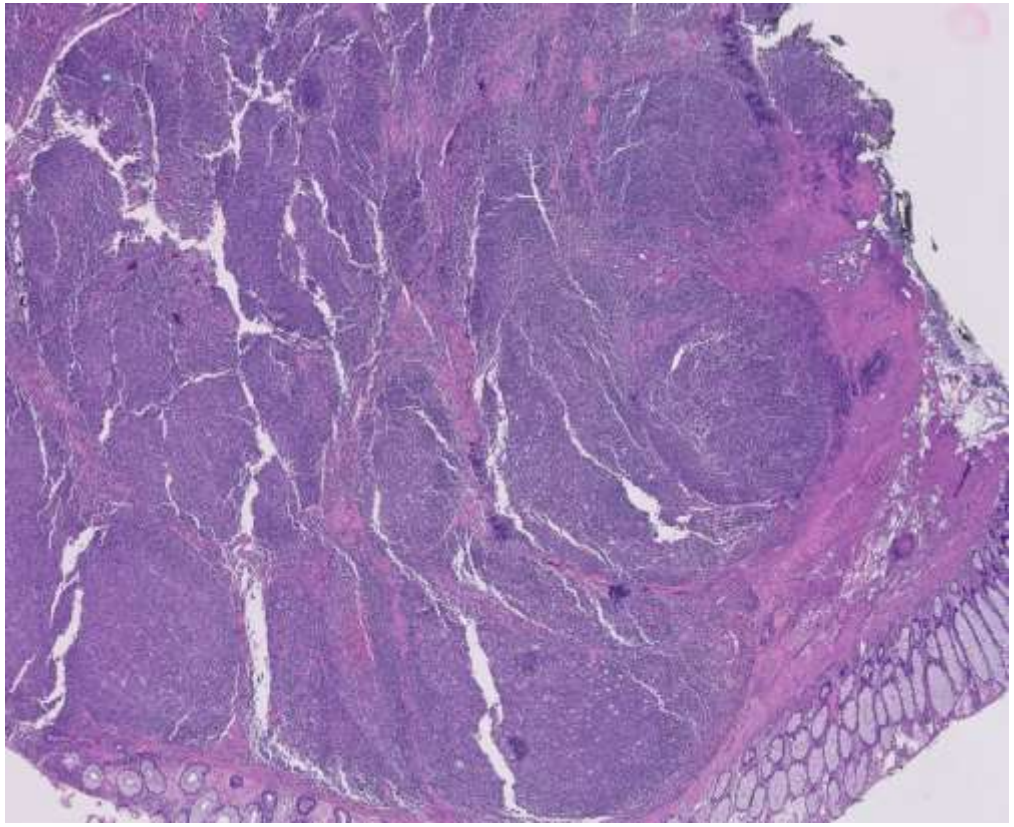

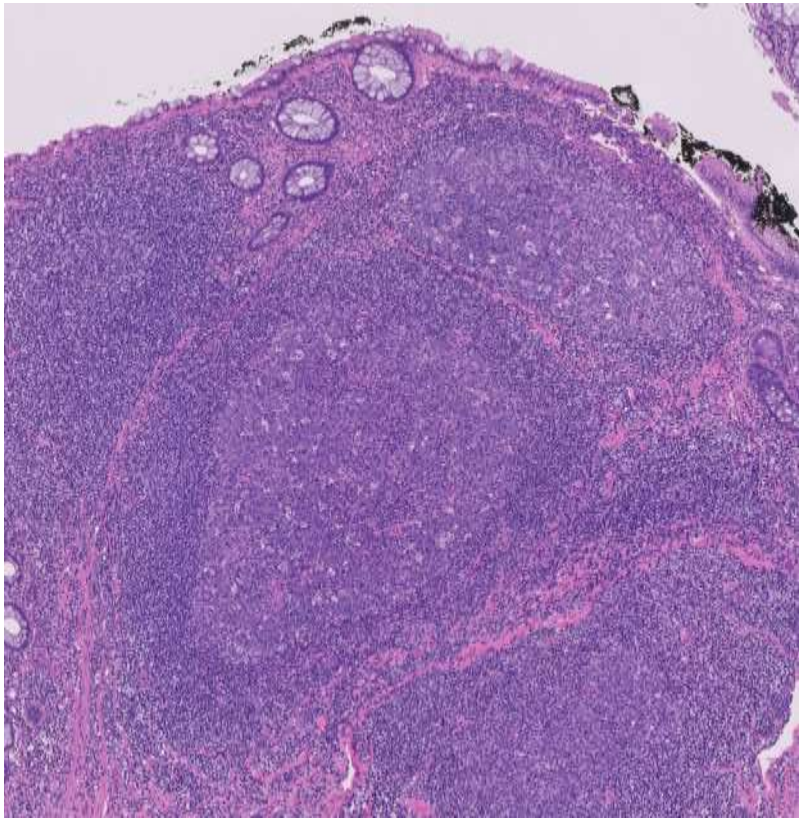

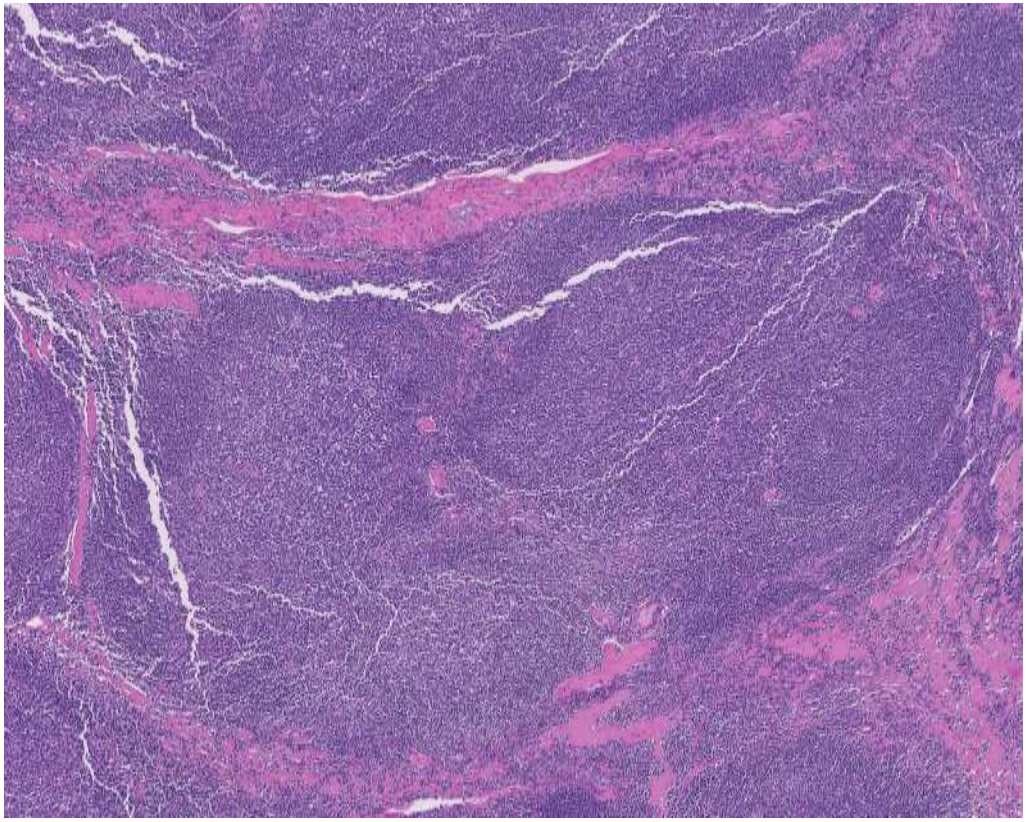

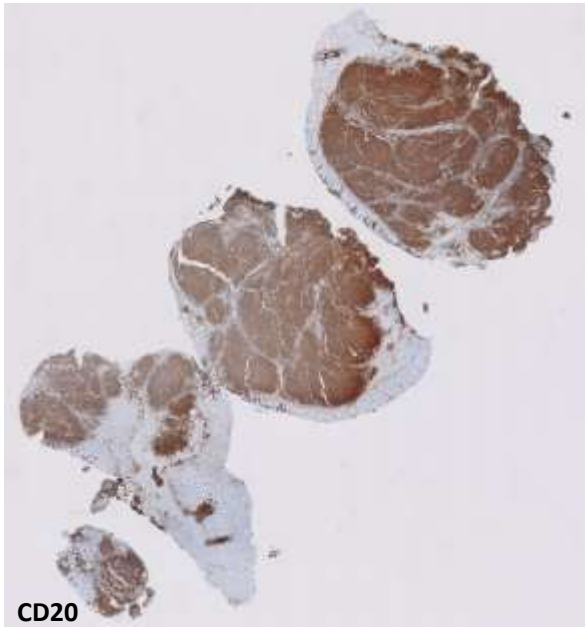
CD20

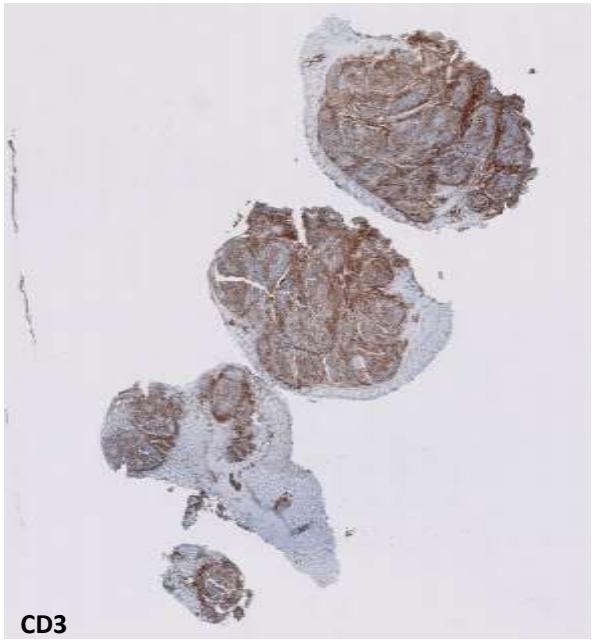
CD3

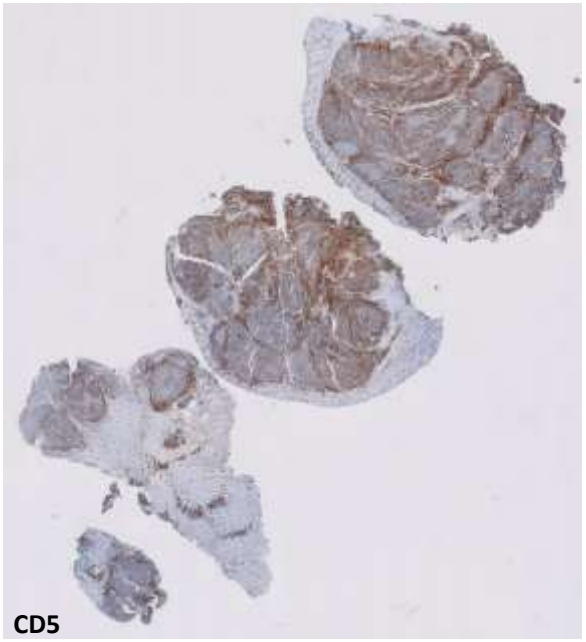
CD5

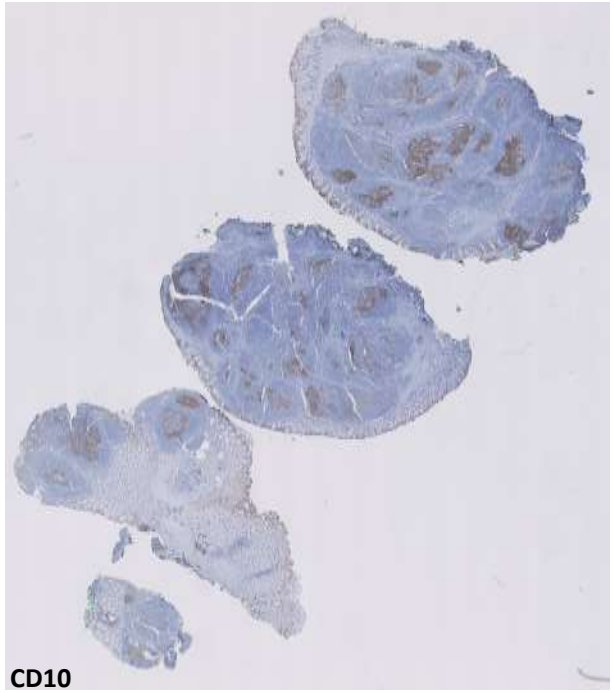

CD10

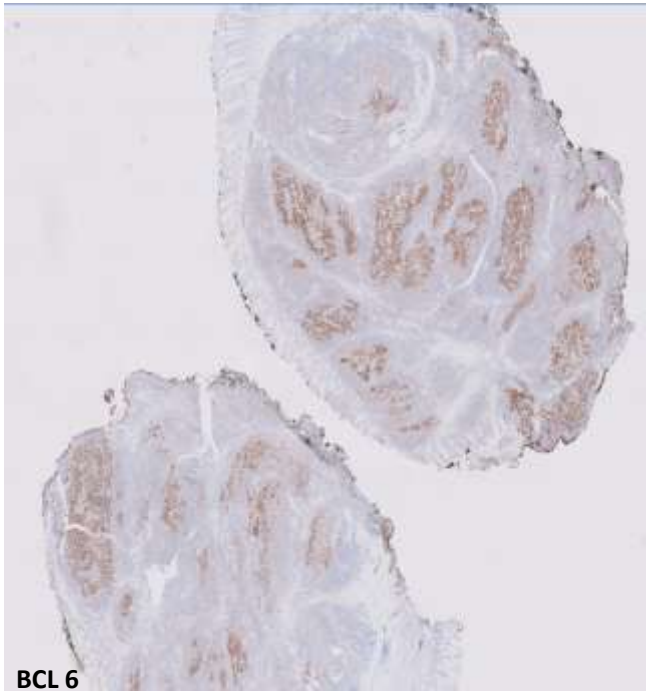

BCL 6

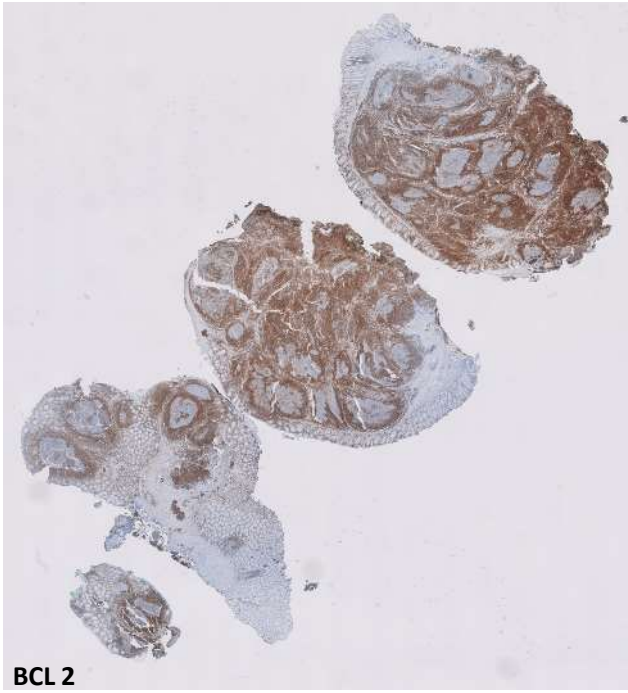

BCL 2

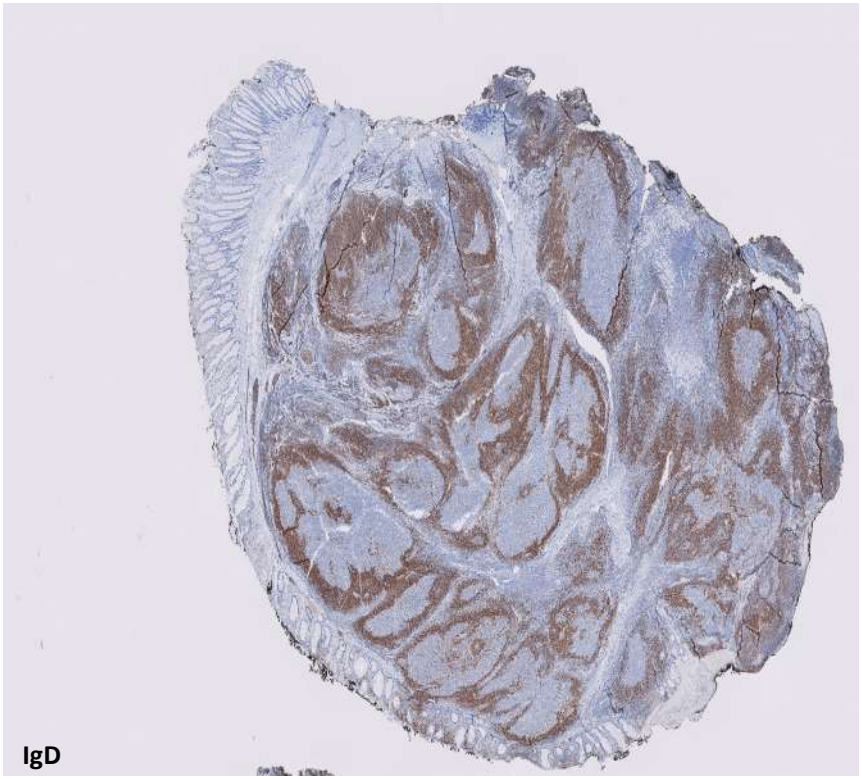
IgD

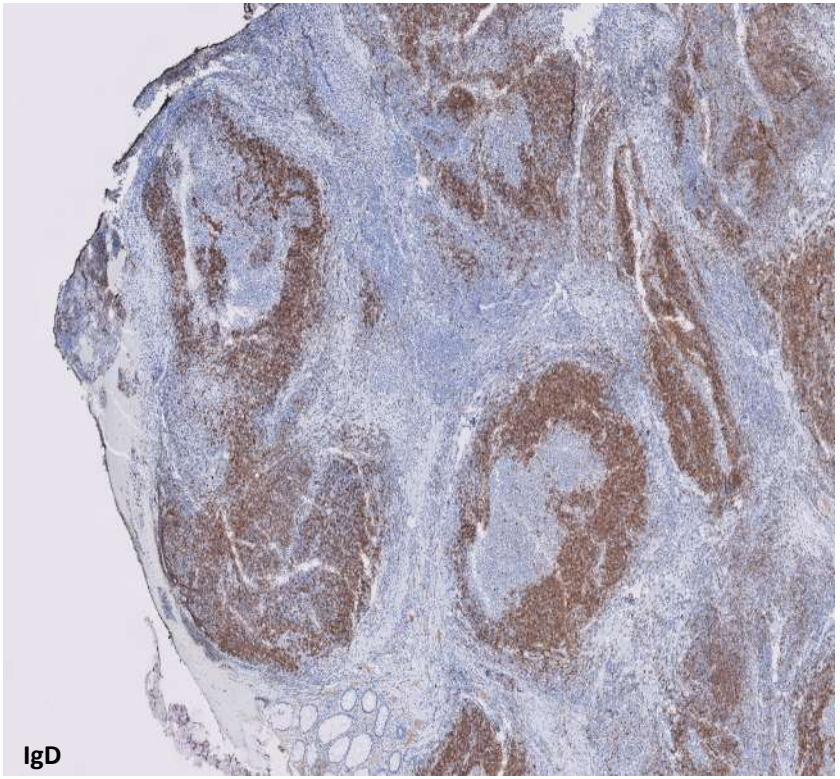
IgD

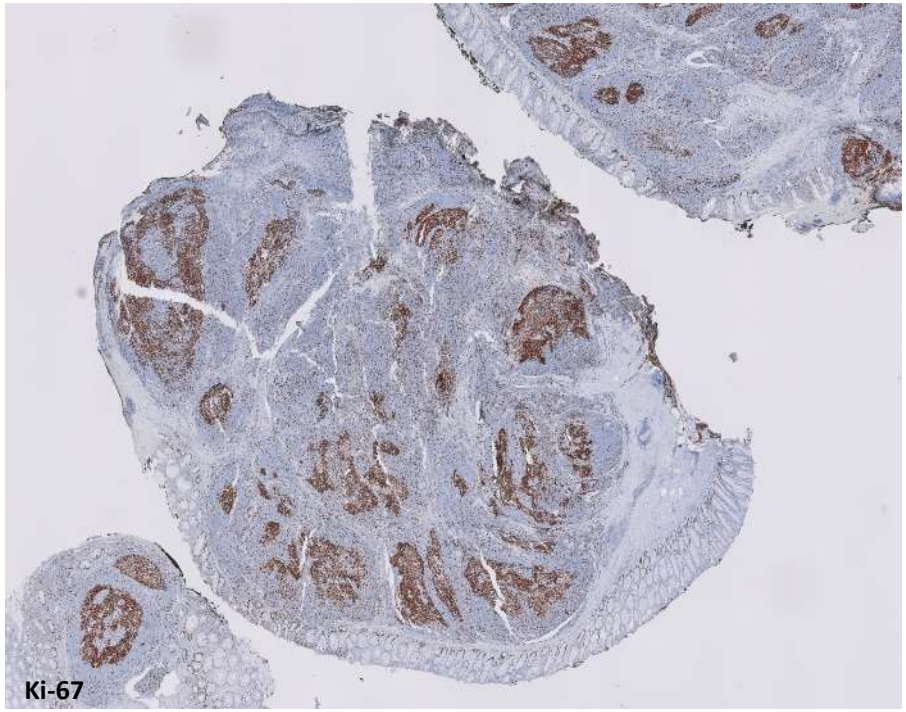
Ki-67

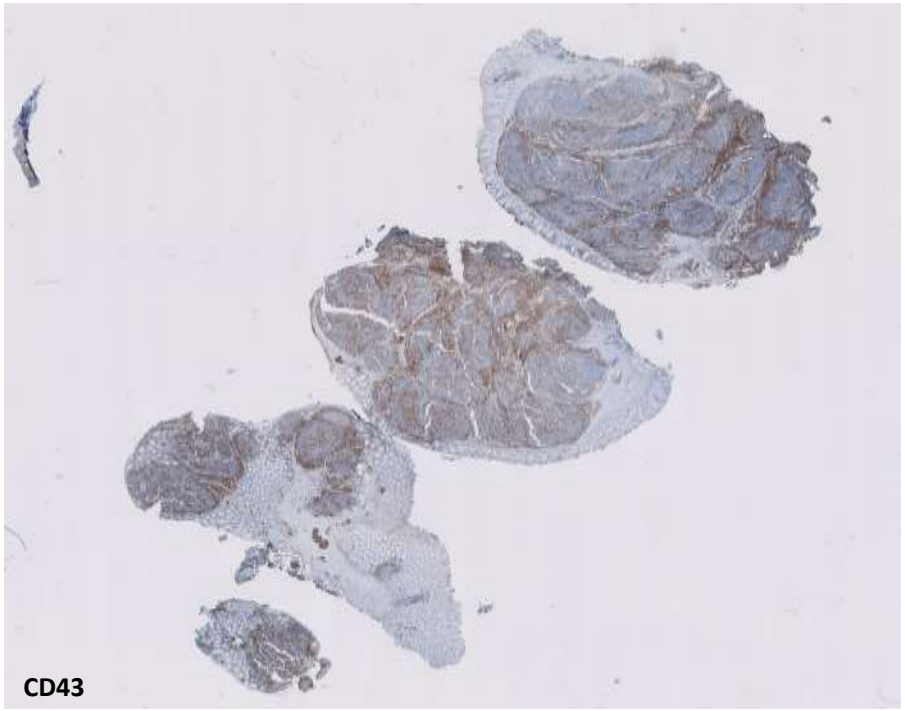
CD43

- The patient is a 30ish woman who presented to an OSH with rectal and abdominal pain.
- She underwent colonoscopy and was found to have a 7 mm semi-pedunculated nodule in the rectosigmoid colon.
- She underwent biopsy of this nodule

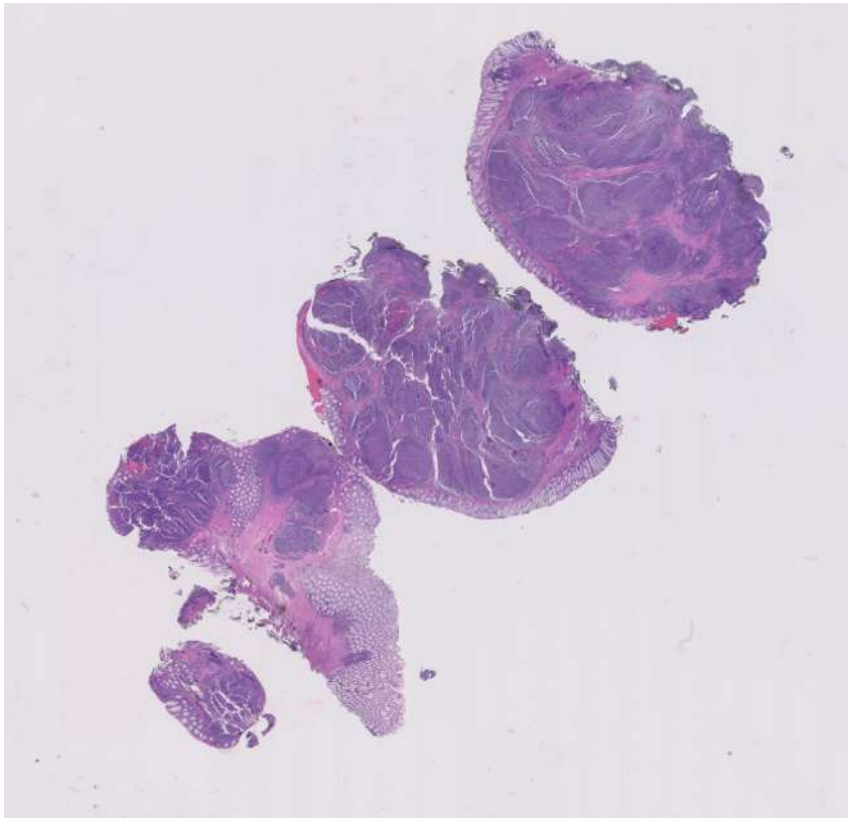

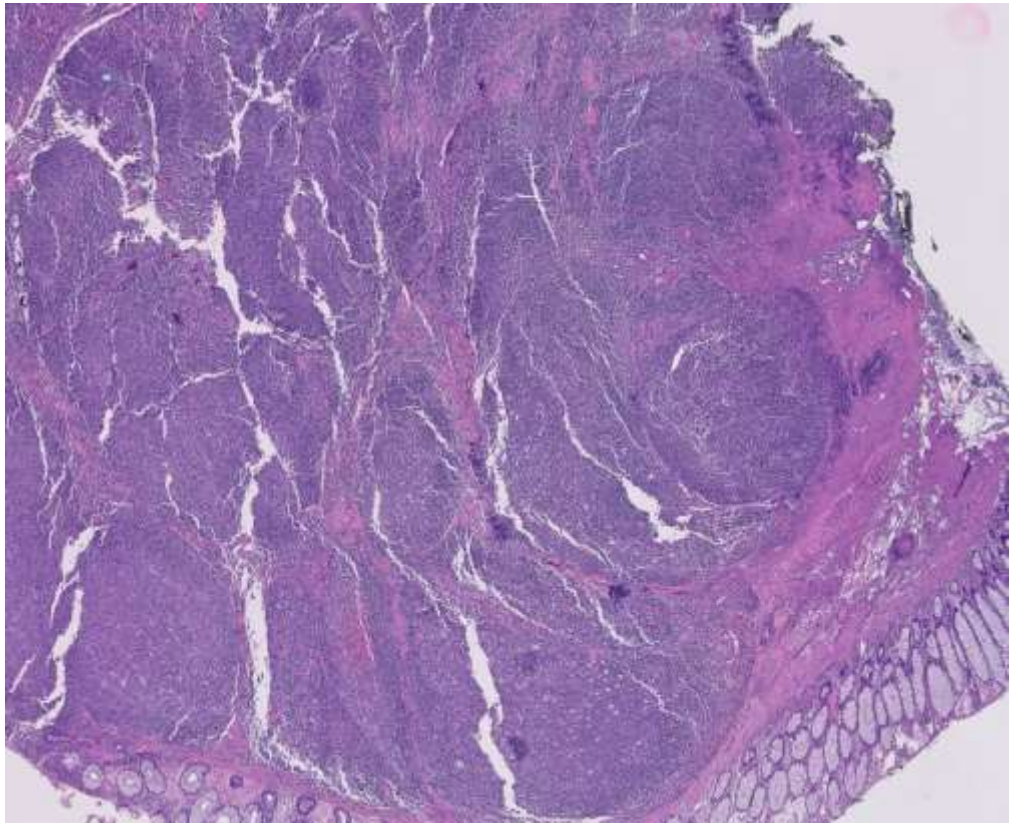

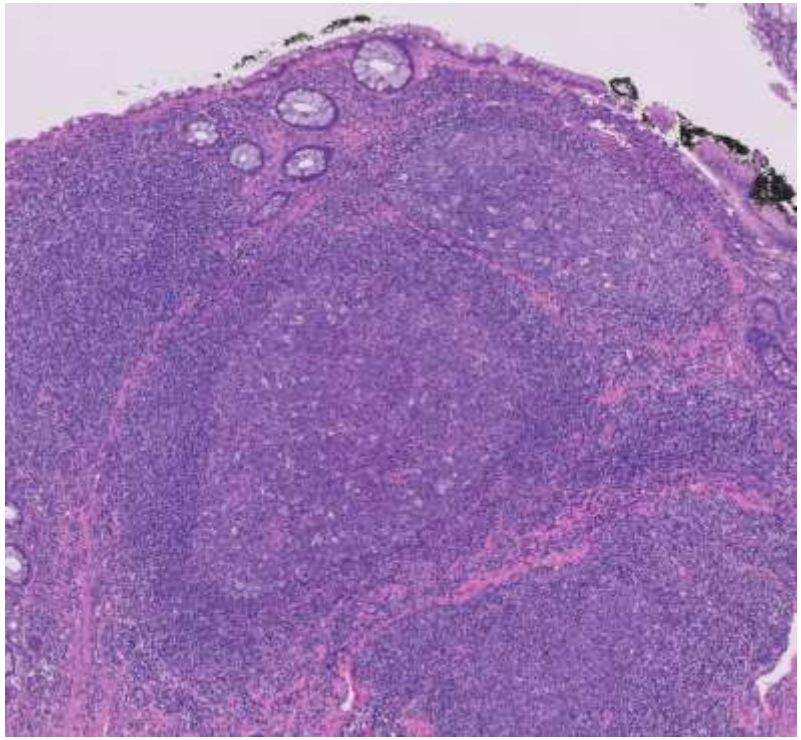

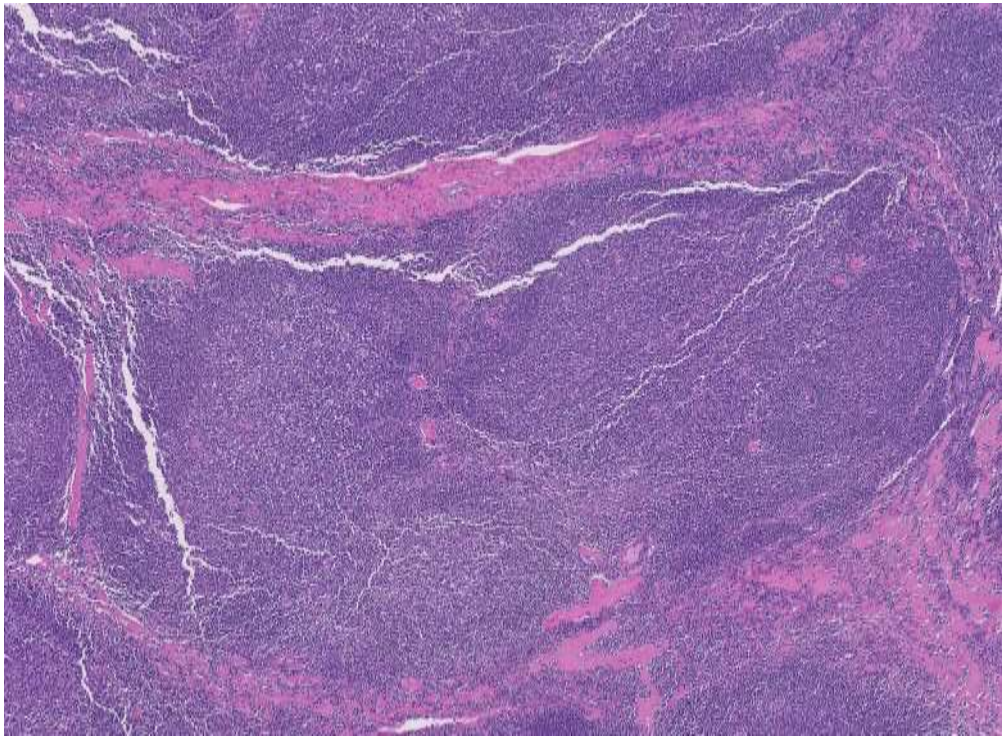

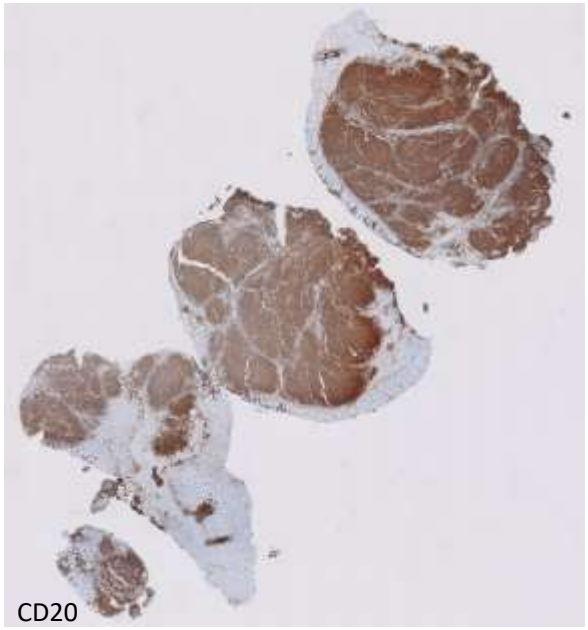
CD20

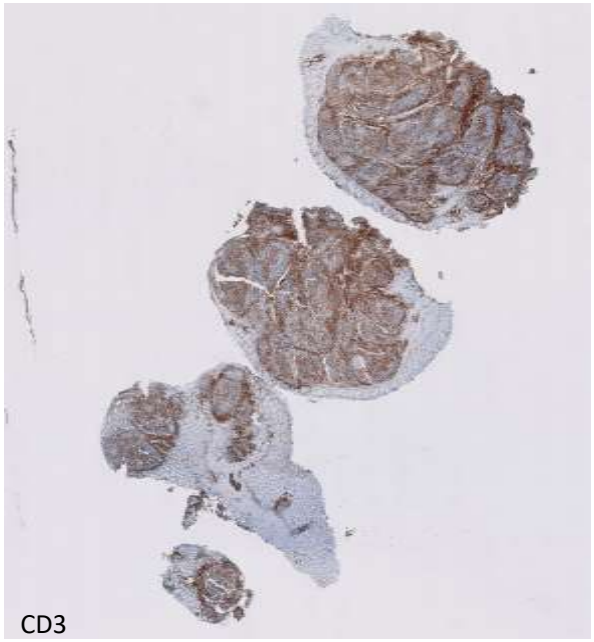
CD3

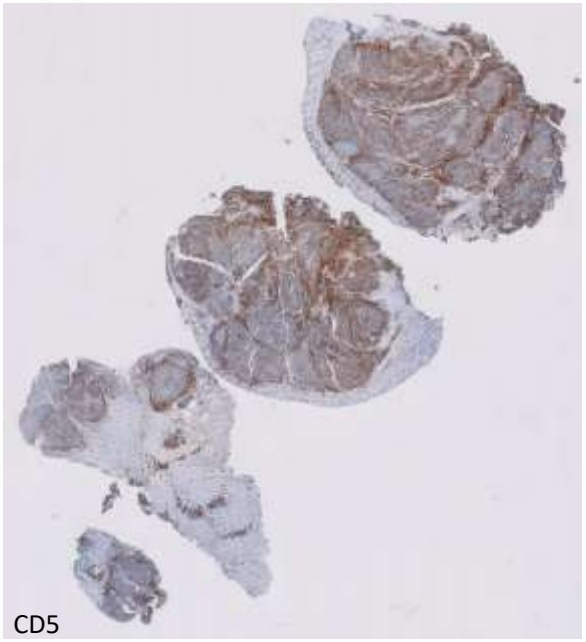
CD5

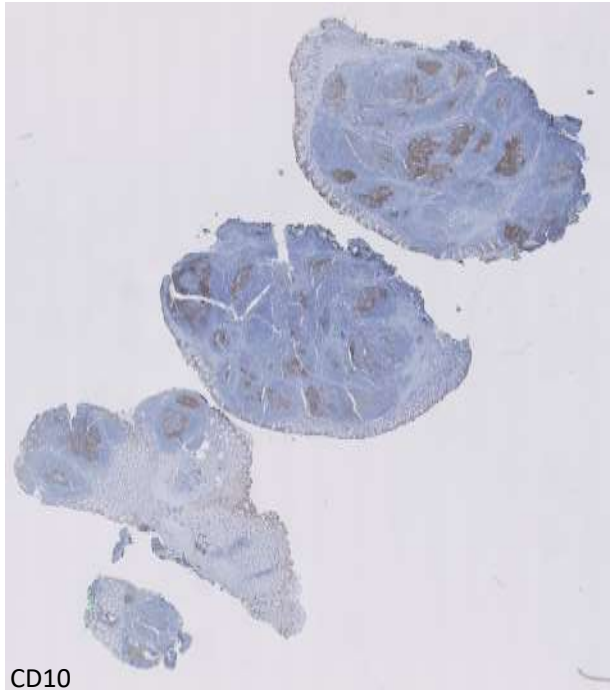
CD10

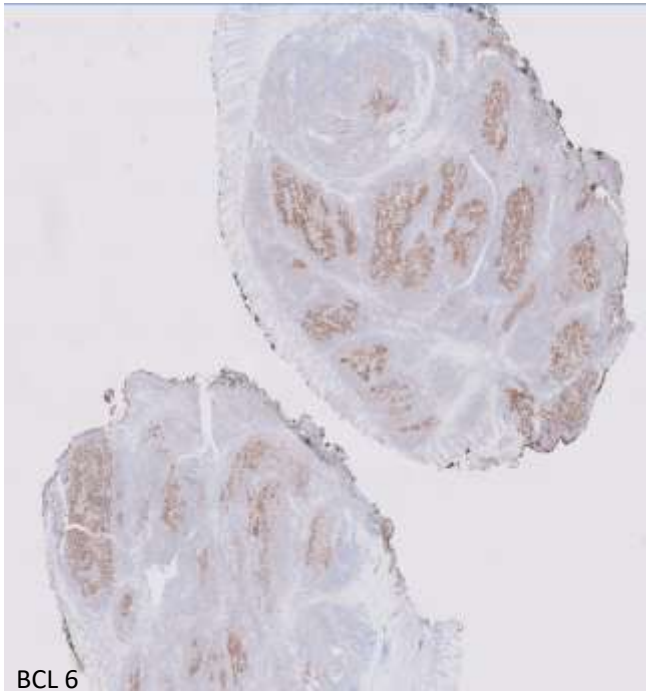
BCL 6

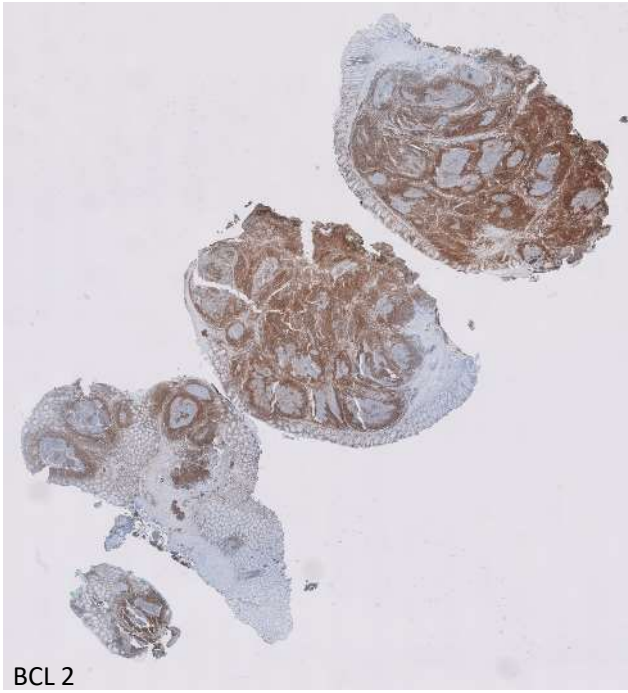
BCL 2

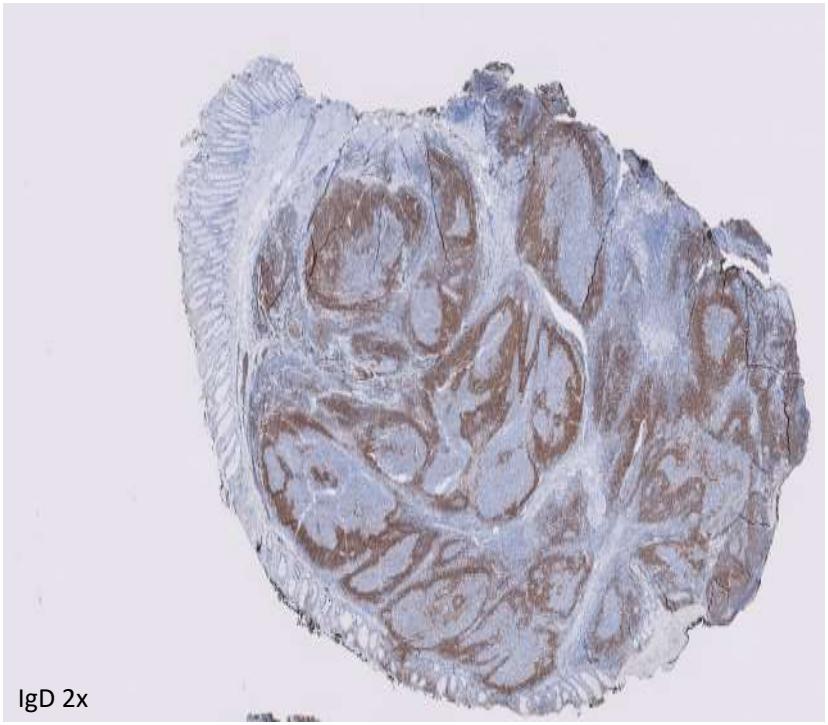

IgD 2x

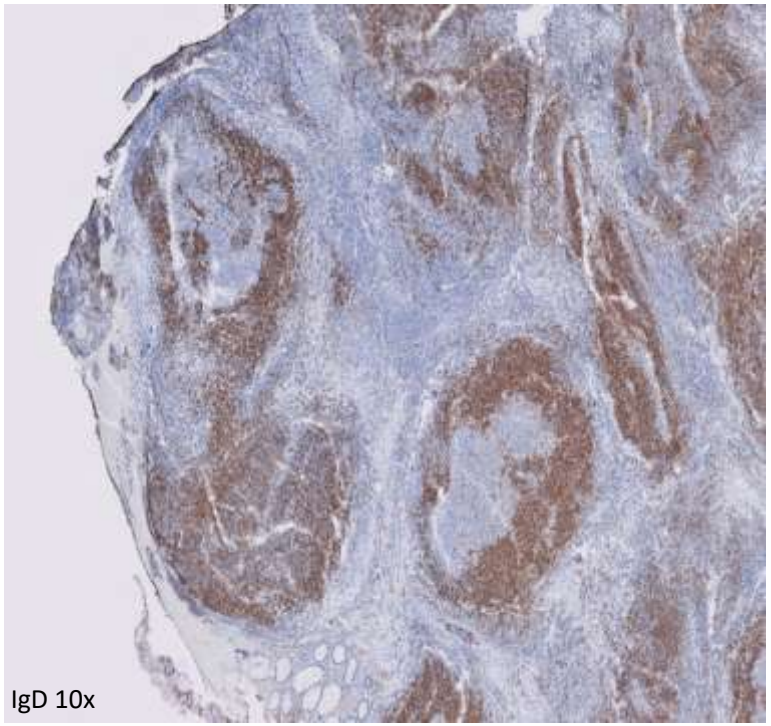

IgD 10x

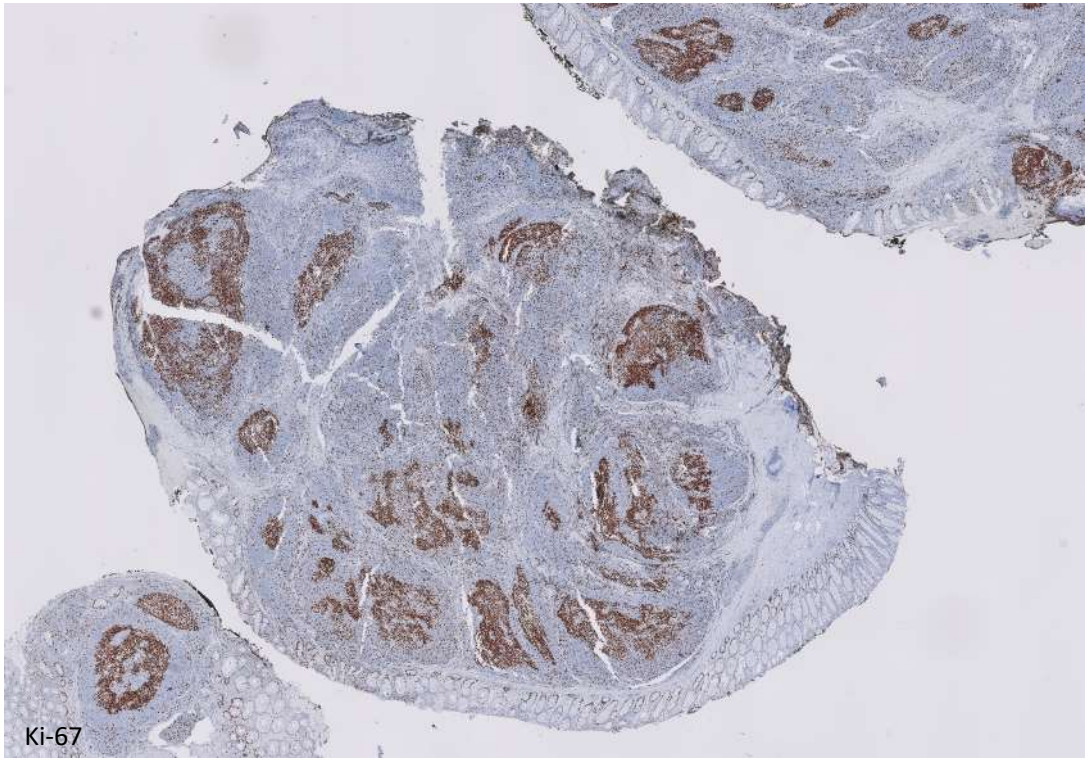
Ki-67

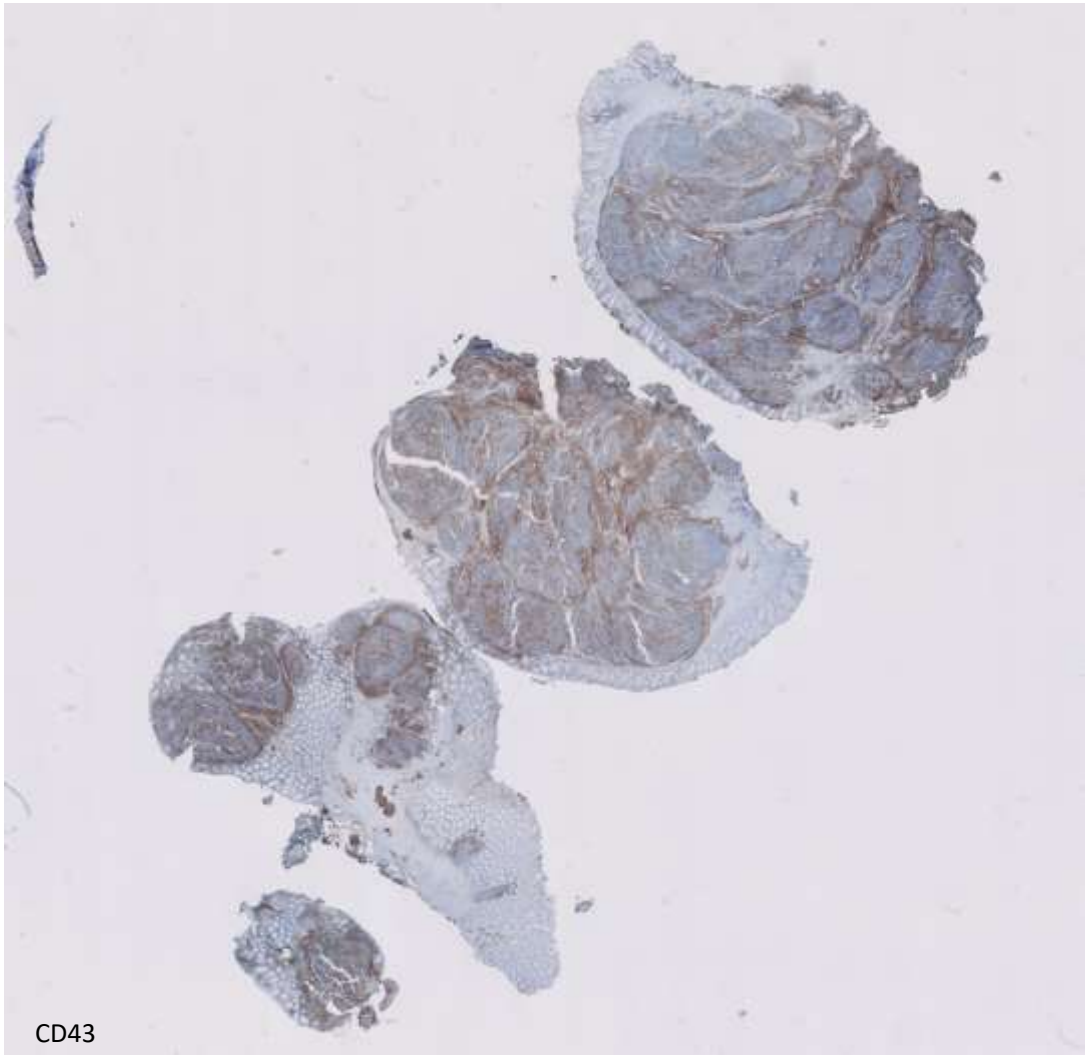
CD43

Ancillary tests

Not sent for flow

FISH performed at an outside lab showed no evidence of IgH/BCL2 t(14;18) or API2/MALT1 t(11;18) fusions.

Rectal tonsil

Rare, benign lymphoid proliferation which is most often found just above the dentate line and can mimic low-grade B-cell lymphoma.

Close differential is Marginal zone lymphoma (MALT lymphoma) with follicular growth pattern

ORIGINAL ARTICLES

The Rectal Tonsil: A Reactive Lymphoid Proliferation That May Mimic Lymphoma

Farris, Alton B. MD[*†]; Lauwers, Gregory Y. MD[*†]; Ferry, Judith A. MD[*†]; Zukerberg, Lawrence R. MD[*†]

Author Information

The American Journal of Surgical Pathology 32(7):p 1075-1079, July 2008. | **DOI:** 10.1097/PAS.0b013e318162c3ec

Abstract

The rectal tonsil (RT), a localized reactive proliferation of lymphoid tissue occurring in the rectum, can cause diagnostic difficulty; and awareness of this entity can prevent a misdiagnosis of lymphoma. A clinicopathologic analysis of 11 cases of RT was performed to determine the features that can aid in the recognition of this entity. The patients (6 males and 5 females) were middle-aged adults, except for 1 case affecting a young boy (age range, 1 to 62 y; mean, 49 y). All presented with either rectal bleeding or abdominal pain, or had the lesion found on routine screening. Endoscopic descriptions, available in all cases, reported a raised, polypoid lesion in 8 cases, a nodule in 2 cases, and a “mass” in 1 case. Histologically, all cases were composed of a lymphoid proliferation involving the lamina propria or submucosa. Lymphoid follicles could be identified in all cases, although some were difficult to appreciate without immunostains for follicular dendritic cells. Five cases showed overlying cryptitis and mild architectural distortion, but no cases showed crypt obliteration or crypt abscesses. Intraepithelial lymphocytes were present in 9 cases, and 5 cases showed nondestructive lymphoepithelial lesions. During a mean follow-up of 5.8 years, none showed a recurrence or developed lymphoma. In conclusion, RT, with its distinctive features, is an important entity to recognize. Familiarity with the range of histologic features characteristic of the RT is critical in avoiding misinterpretation as lymphoma.

J Clin Exp Hematopathol
Vol. 49, No. 1, May 2009

Original Article

Histological Variety of Localized Lymphoid Hyperplasia of the Large Intestine : Histopathological, Immunohistochemical and Genotypic Findings of 16 Cases

Masaru Kojima,[1] Naoya Nakamura,[2] Hideaki Itoh,[3] Tadashi Motoori,[4] Kazue Hoshi,[5] Yasunari Enomoto,[6] Takashi Johshita,[7] and Hirokazu Nakamine[8]

Previous reports emphasized that localized lymphoid hyperplasia (LLH) of the large intestine is usually histologically characterized by large lymphoid follicles with striking enlarged germinal centers, and a narrow surrounding mantle zone and marginal zone (MZ). To clarify the histological varieties of LLH of the large intestine, 16 such cases have been studied. The present study demonstrated histological diversity of the LLH of the large intestine including (i) reactive follicular hyperplasia (RFH) (n = 8), (ii) RFH with progressive transformation of the germinal center (PTGC) (n = 3), (iii) RFH with MZ hyperplasia (n = 3) and (iv) RFH with PTGC and MZ hyperplasia (n = 2). Overall histomorphological findings of the present series appear quite different from previous descriptions of LLH of the large intestine. The present study showed histological variety of the LLH of the large intestine. Moreover, LLH of the large intestine should be differentiated from extranodal marginal zone B-cell lymphoma and nodular lymphocyte predominant Hodgkin lymphoma as well as follicular lymphoma. Immunohistological studies demonstrated the reactive nature of all 16 lesions. However, three cases showing RFH demonstrated immunoglobulin heavy chain gene rearrangement by polymerase chain reaction study in 12 cases examined. It remains unclear whether these three cases showing RFH could be a sign of the prelymphomatous stage (incipient follicular lymphoma) or representing merely an exaggeration of normal B-cell clonal response in the germinal centers. [*J Clin Exp Hematopathol 49(1) : 15-21, 2009*]

Keywords: localized lymphoid hyperplasia, large intestine, histological findings, progressive transformation of the germinal center, marginal zone hyperplasia

Table 1. Summary of the clinicopathological findings of 16 cases

Case No.	Age/ Sex	Site	Main clinical finding	Main endoscopic finding	Therapy	Follow-up (months)	Histological findings	IHC	PCR	EBER
1	19/F	Rectum	Anal bleeding	Confluence of multiple small nodules, up to 5 mm	None (biopsy only)	72, A	RFH	P	NE	−
2	45/F	Rectum	Anal bleeding	Confluence of multiple small nodules, up to 5 mm	None (biopsy only)	2, A	RFH	P	M	−**
3	46/F	Rectum	Screening	Solitary SMT (ϕ = 5 mm)	Polypectomy	48, A	RFH with MZE*	P	P	−
4	50/F	Rectum	Screening	Solitary polyp (ϕ = 5 mm)	Polypectomy	16, A	RFH with PTGC*	P	NE	+
5	58/F	Rectum	Anal bleeding	Solitary polyp (ϕ = 10 mm)	Polypectomy	25, A	RFH	P	P	−
6	60/F	Cecum	Occult bleeding	Solitary polyp (ϕ = 4 mm)	Polypectomy	10, A	RFH	P	P	−
7	64/F	Rectum	Anal bleeding	Multiple SMT (n = 30, ϕ = 6 mm)	Polypectomy + radiotherapy	38, A	RFH with MZE*	P	P	−
8	64/F	Rectum	Anal bleeding	Solitary polyp (ϕ = 5 mm)	Polypectomy	Lost	RFH	P	P	−
9	65/M	Rectum	Constipation	Solitary SMT (ϕ = 4 mm)	Polypectomy	28, A	RFH with PTGC*	P	P	−
10	66/F	Rectum	Occult anal bleeding	Multiple SMT (n = 5, ϕ = 6 mm)	Polypectomy	61, A	RFH with MZE*	P	P	−
11	69/F	Rectum	Occult anal bleeding	Multiple SMT (n = 2, ϕ = 5 mm)	Polypectomy	60, A	RFH	P	M	−
12	71/F	Rectum	Screening	Solitary polyp (ϕ = 5 mm)	Polypectomy	14, A	RFH with PTGC*	P	NE	+
13	71/F	Rectum	Occult anal bleeding	Multiple SMT (n = 3, ϕ = 3 mm)	EMR	31, A	RFH	P	P	−
14	72/M	Rectum	Occult anal bleeding	Confluence of multiple small nodules, up to 5 mm	None (biopsy only)	23, A	RFH	P	M	−**
15	72/M	Rectum	Unknown	Solitary SMT (ϕ = 10 mm)	EMR	Recent case	RFH with PTGC and MZE	P	NE	−
16	73/F	Ascending colon	Unknown	Solitary polyp (ϕ = 3 mm)	Polypectomy	Lost	RFH with PTGC and MZE	P	P	−

23-0406

Sanjay Kakar; UCSF

>60F with NASH cirrhosis and 3cm liver mass, biopsied.

History

- >60 year old woman with NASH cirrhosis
- 3 cm mass, imaging indeterminate, findings not typical of HCC

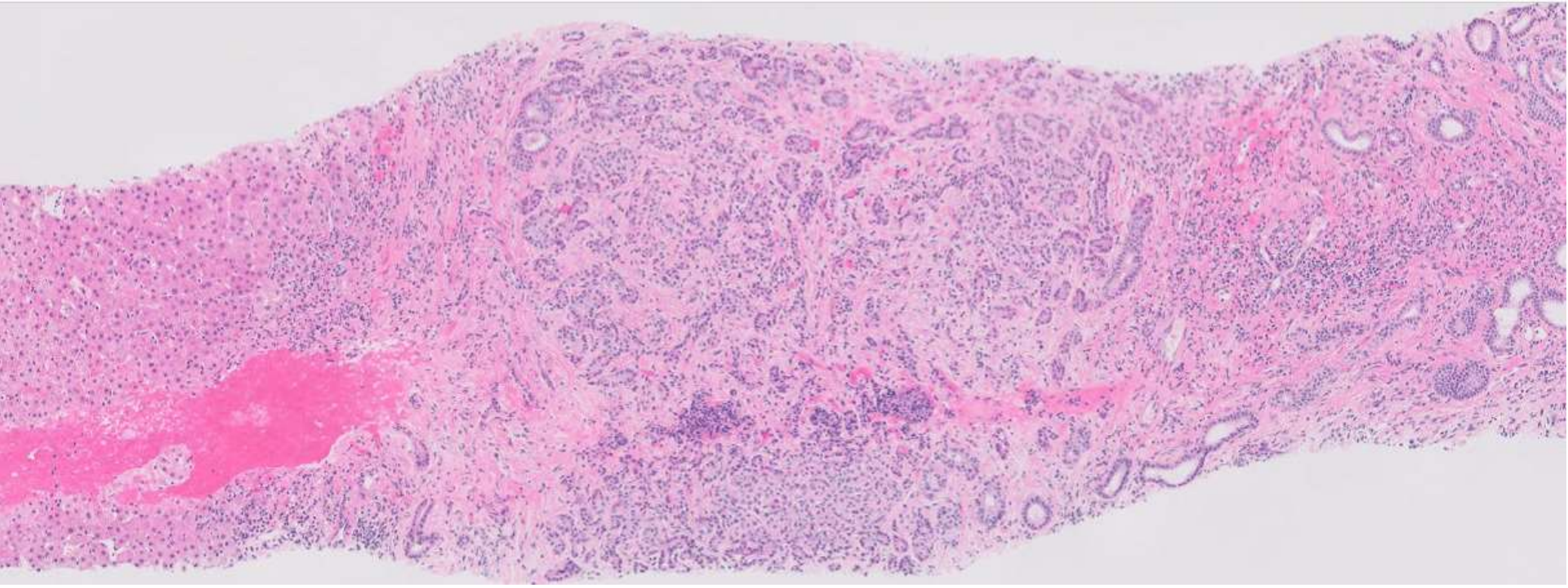

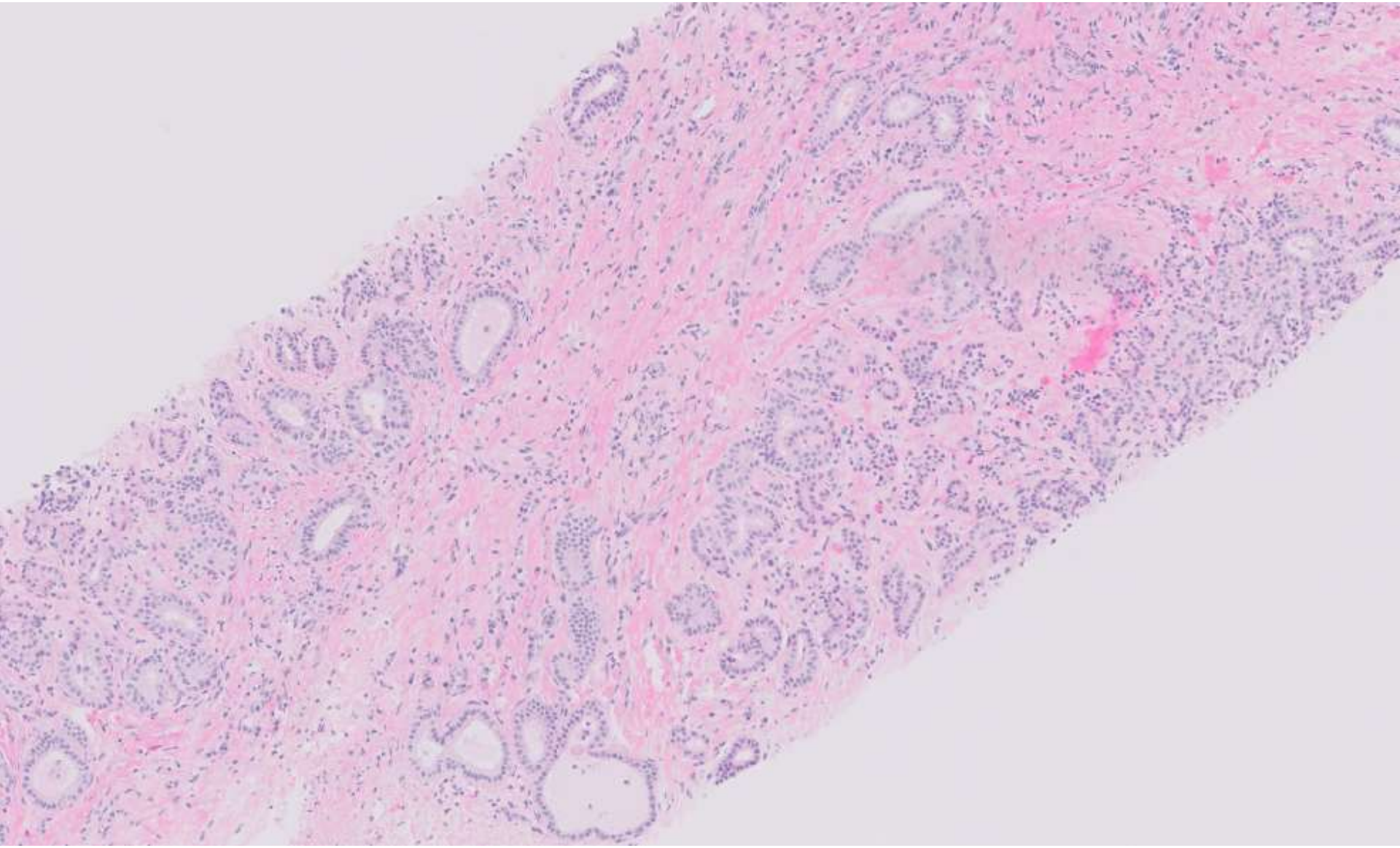

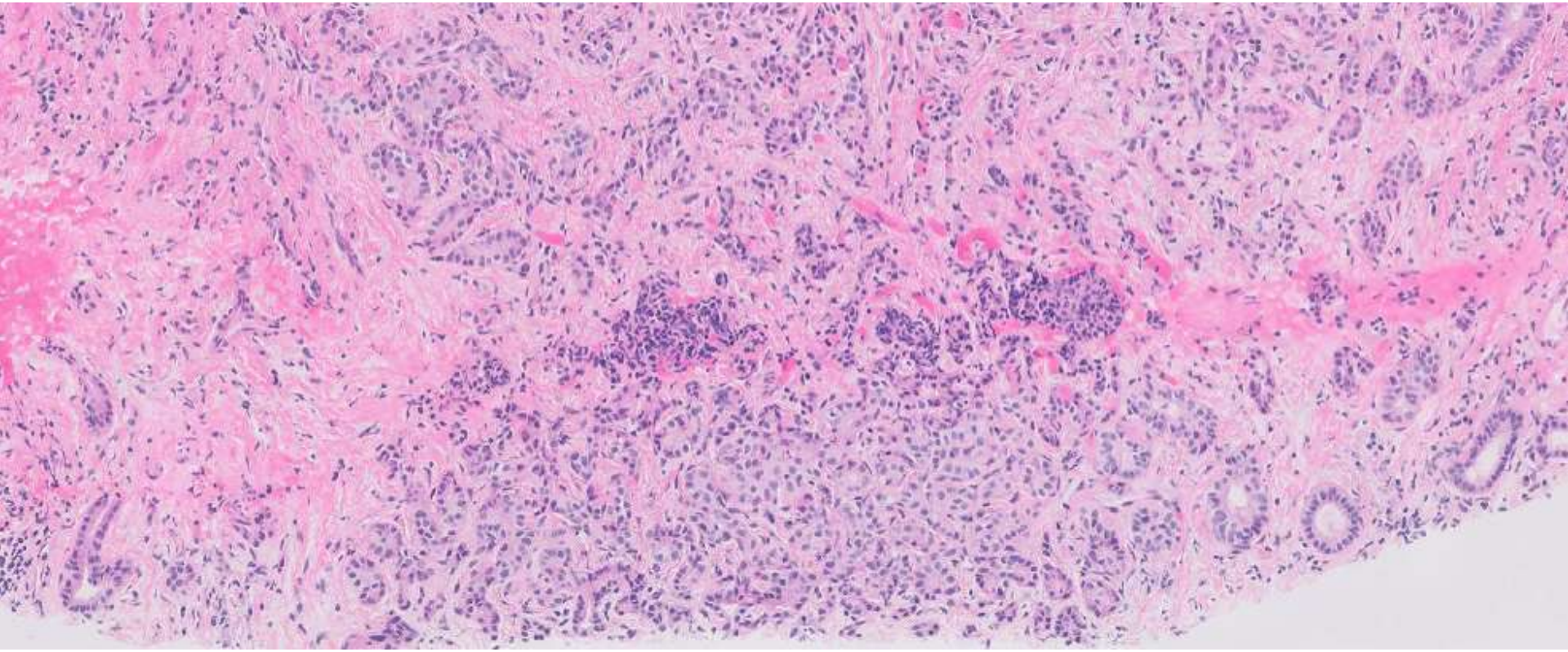

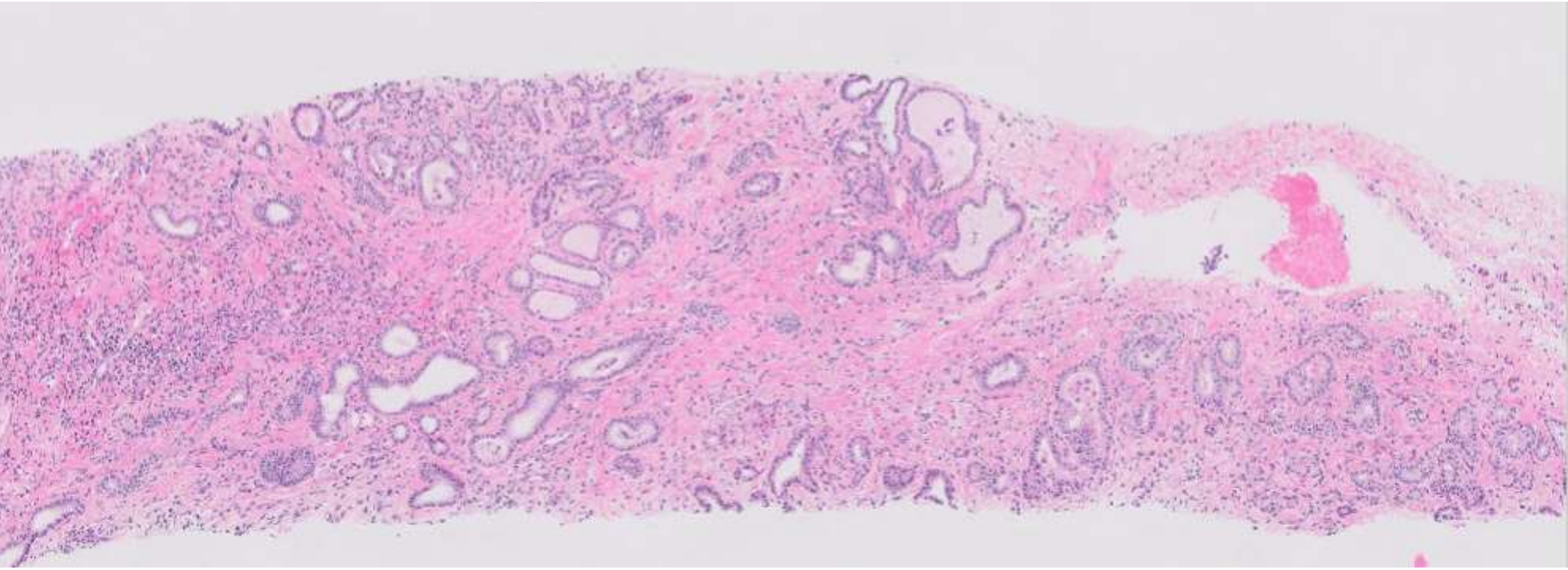

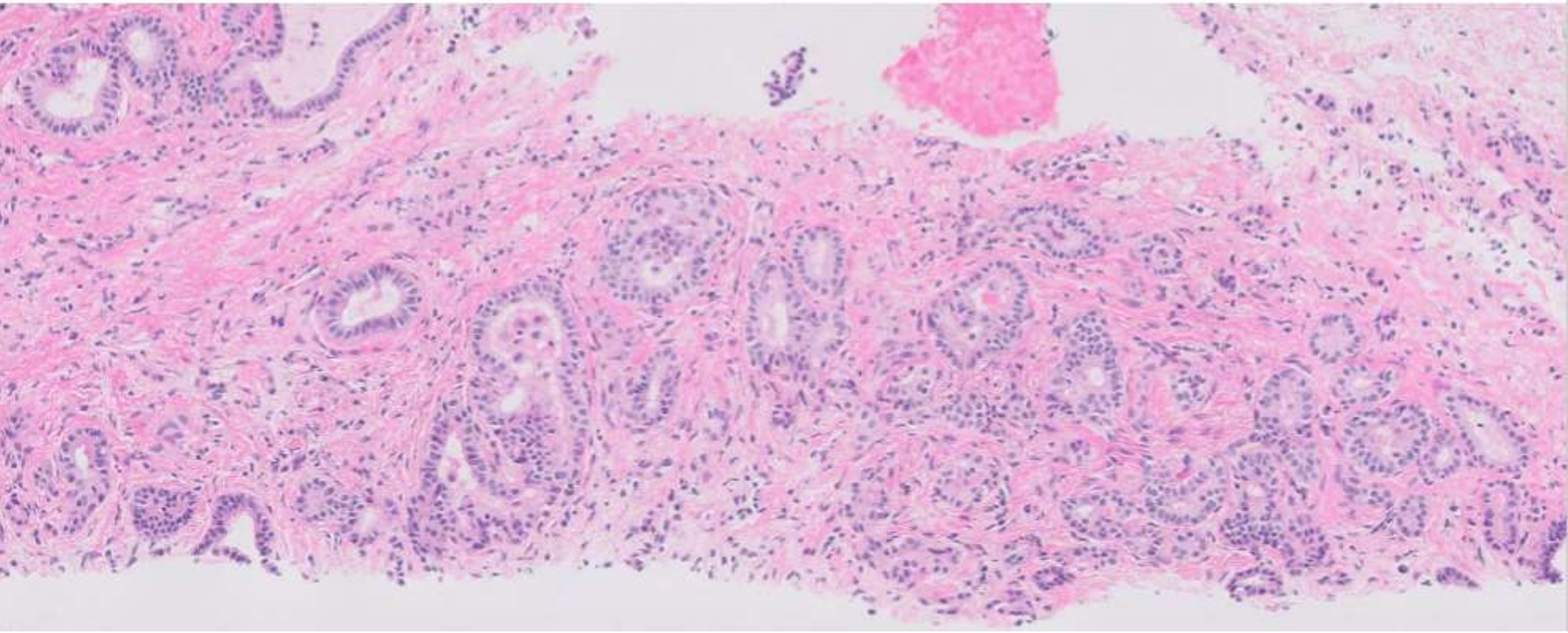

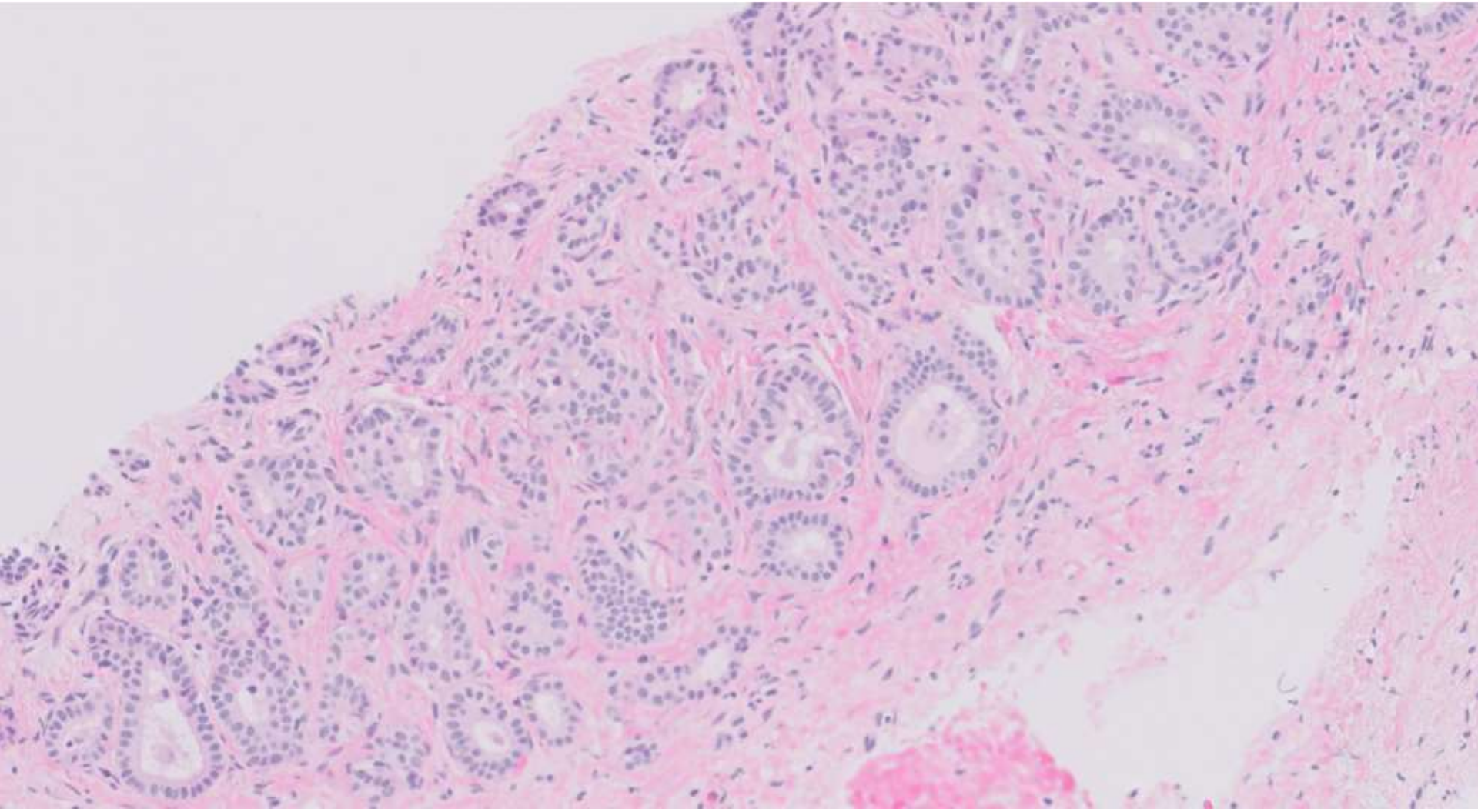

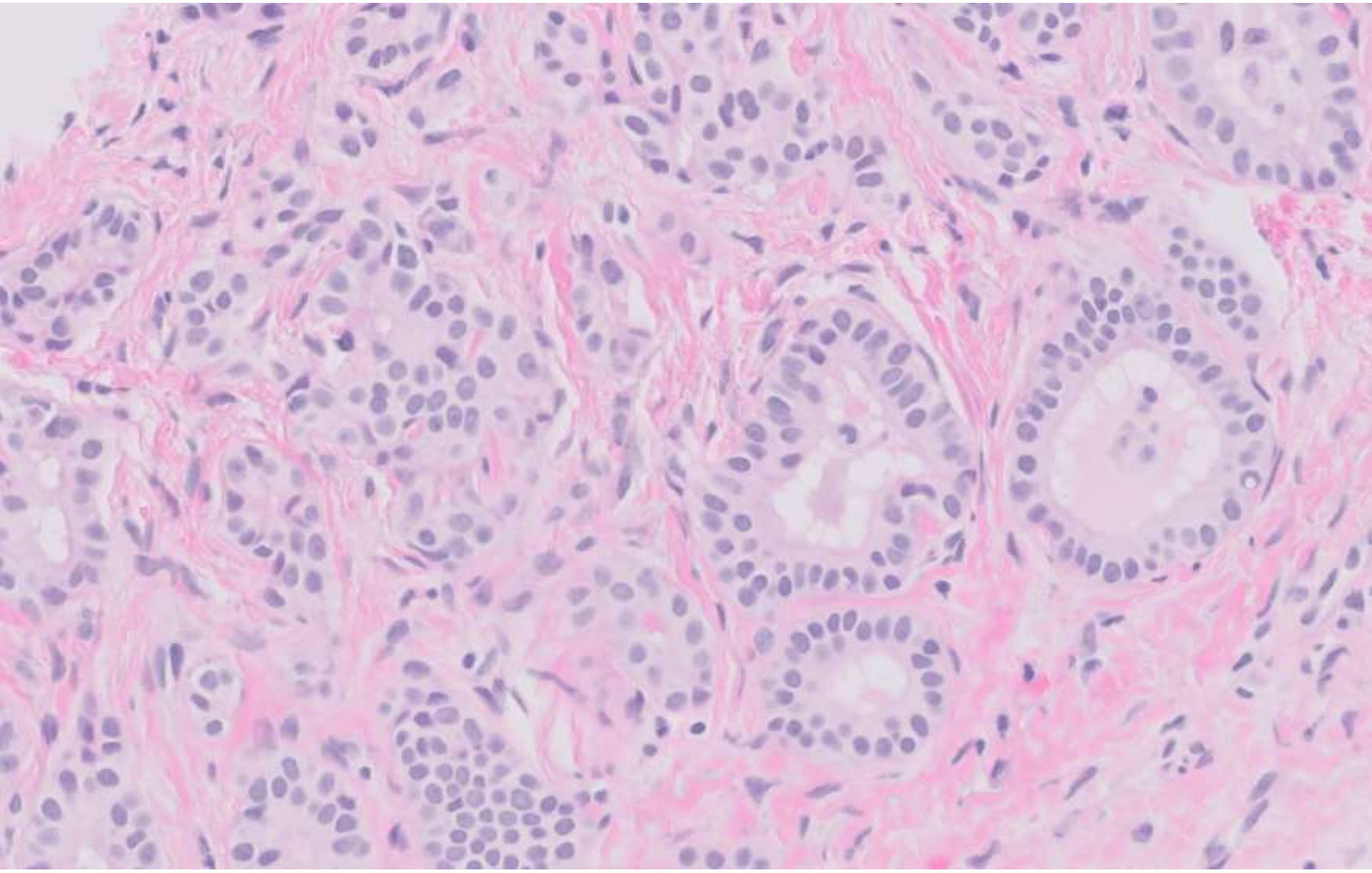

Ki-67

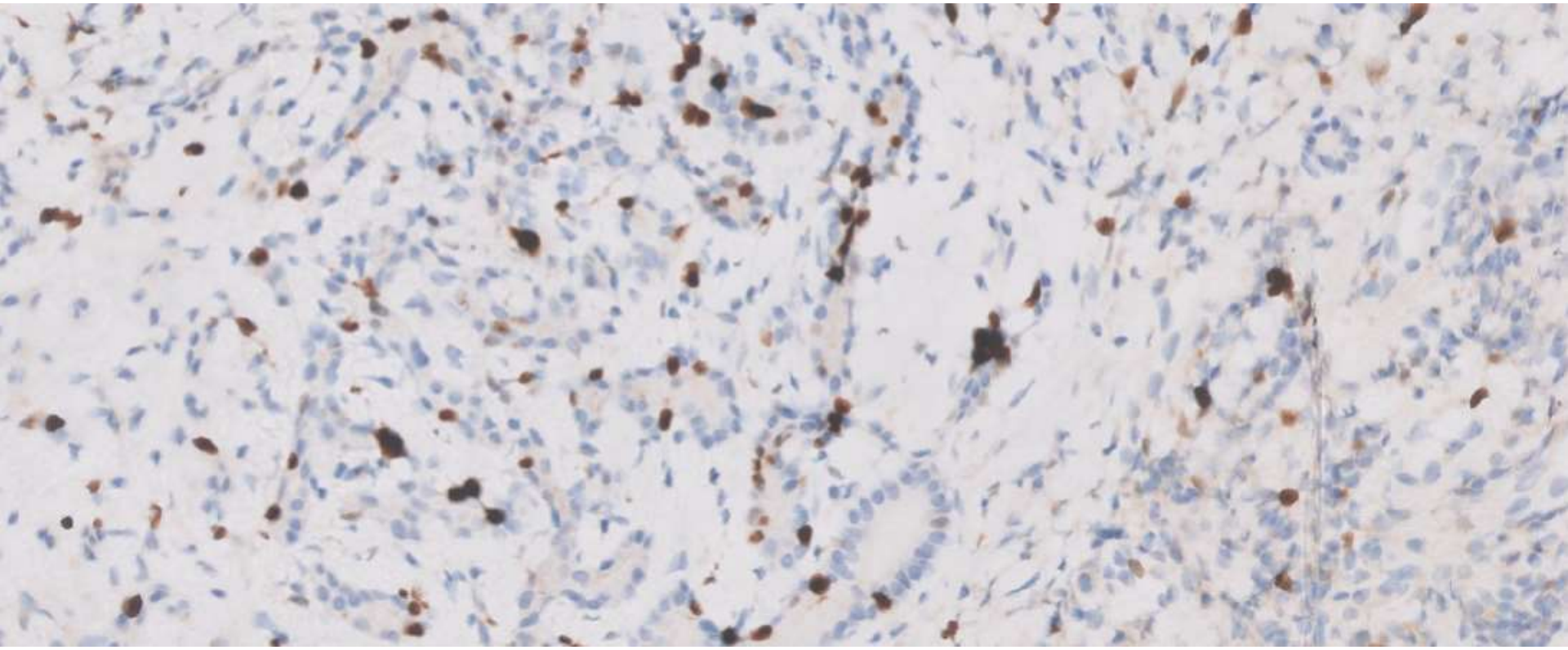

p53

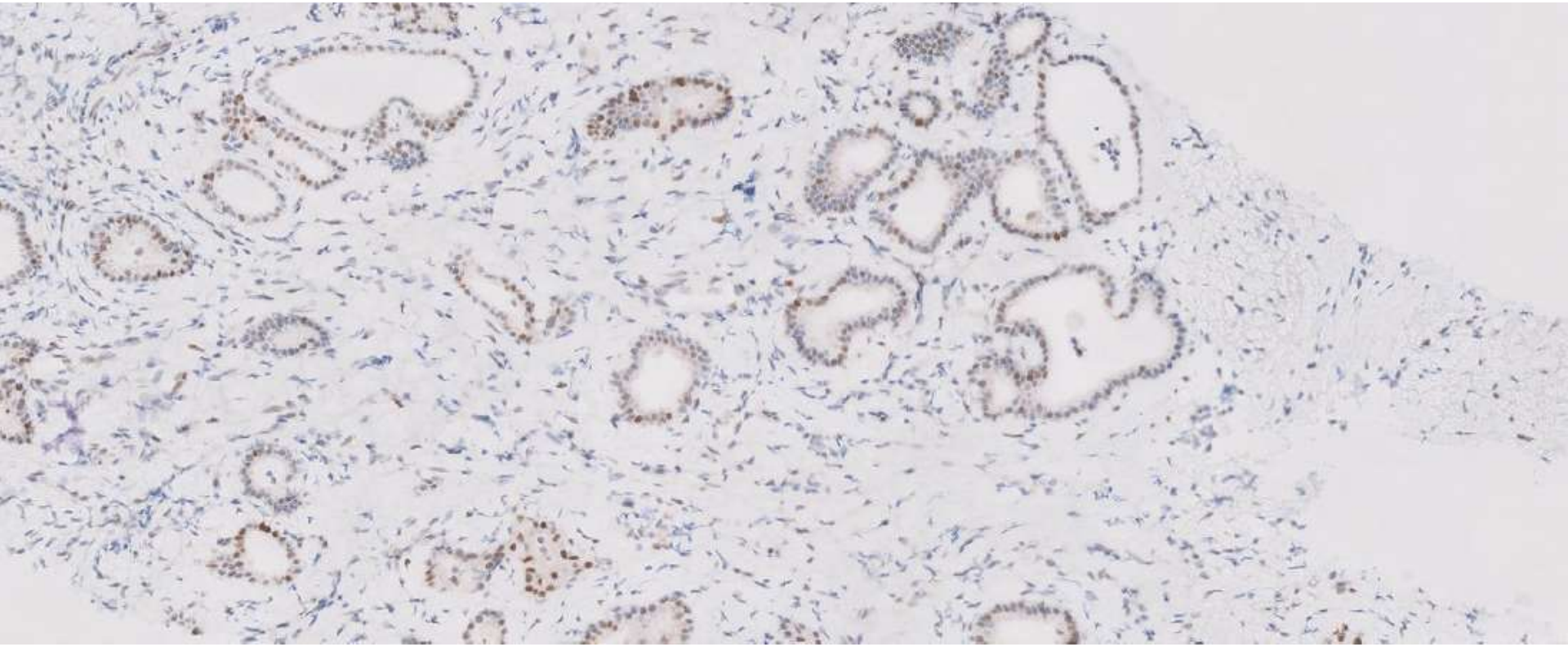

Case: S23-0406

Differential Diagnosis

- Benign biliary proliferation
- Well differentiated intrahepatic cholangiocarcinoma
- Metastatic adenocarcinoma

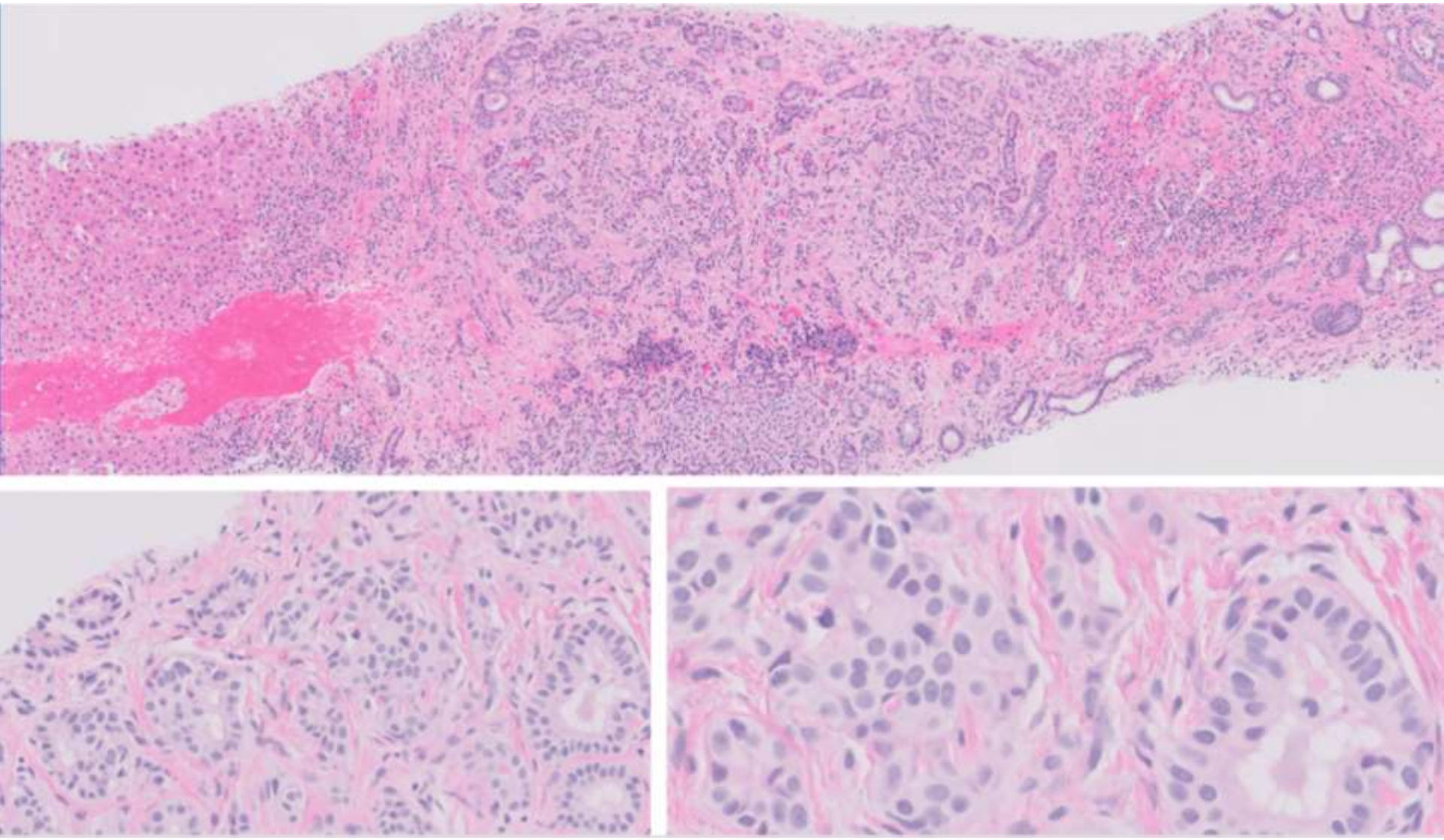

Benign biliary vs. iCCA

Tumor	IHC
Benign biliary lesions	Ki-67<5% p53: wild-type
iCCA	Ki-67 >20% Diffuse strong p53

Ki-67

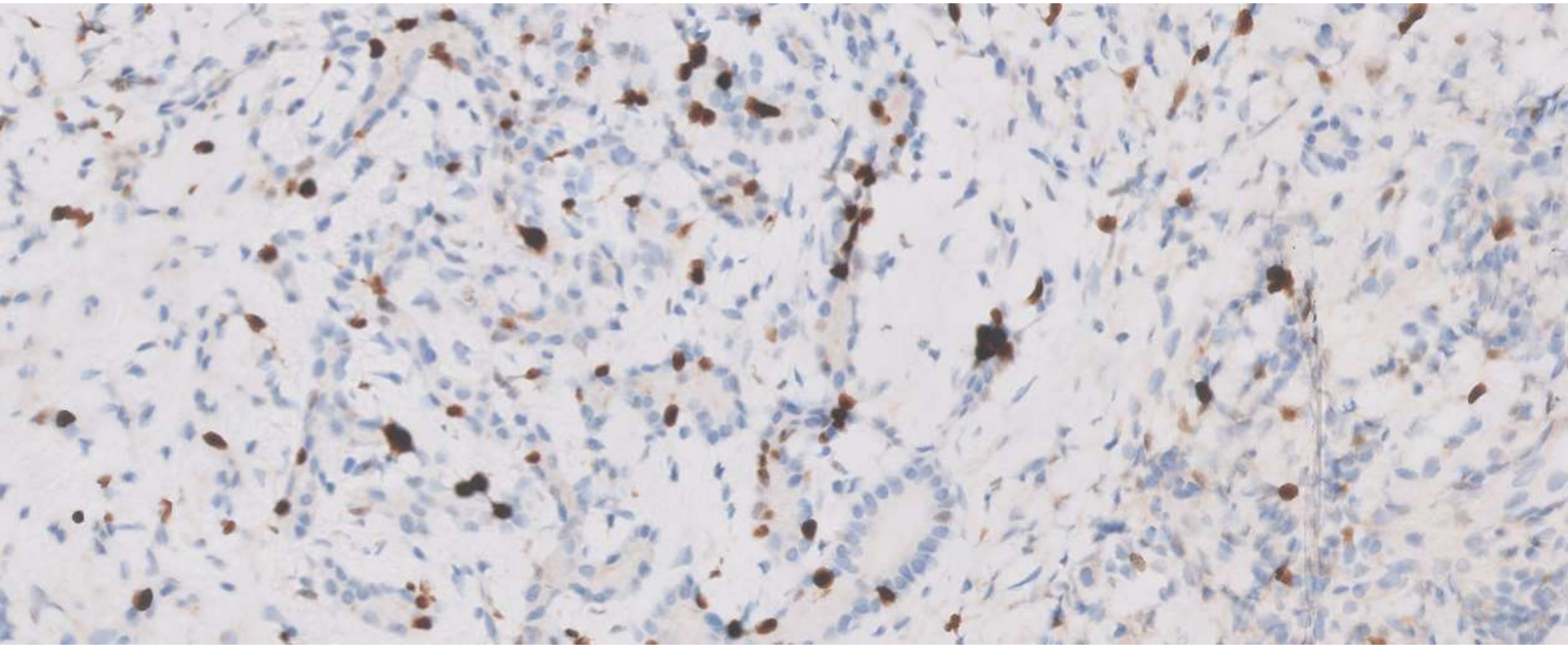

p53

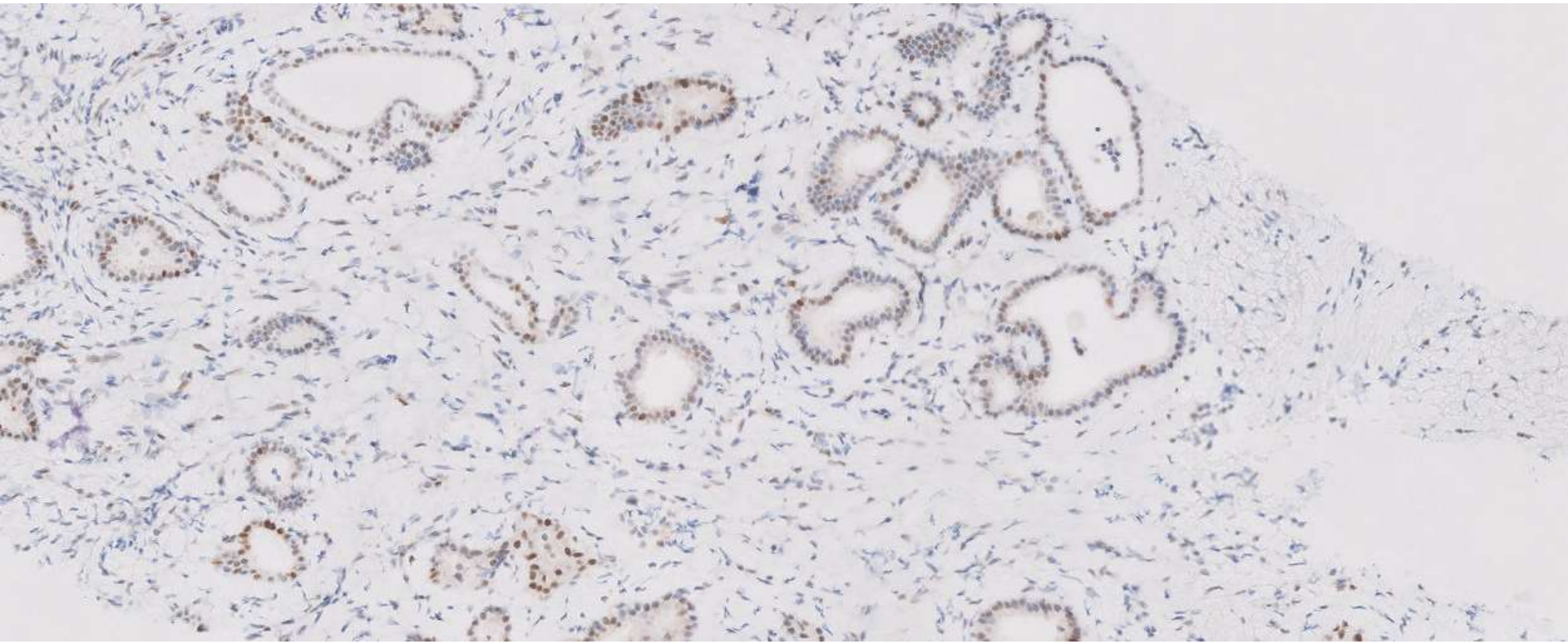

IHC based on mutational profile

Tumor	Genomic changes
Bile duct adenoma	*BRAF* V600E mutation: 50-80%
iCCA	*BAP1*: 7-29% *ARID1A*: 7-36% *DPC4*: 3-5%

Pujals, Histopathol 2015
Angkathunyakul, Histopathol 2017
Hornick, AJSP 2005
Misumi Histopathol 2017

VE1 antibody (*BRAF* V600E mutation)

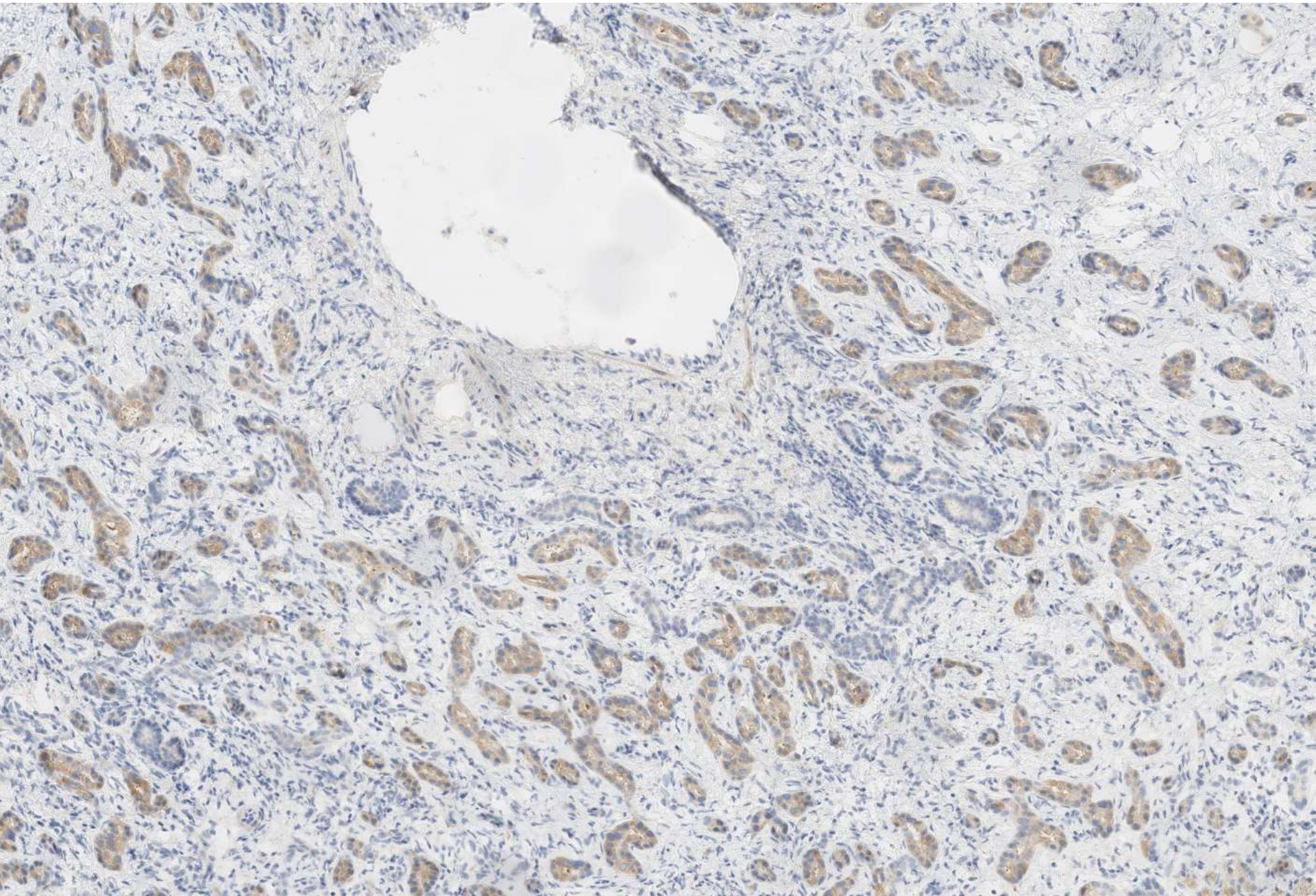

BRAF

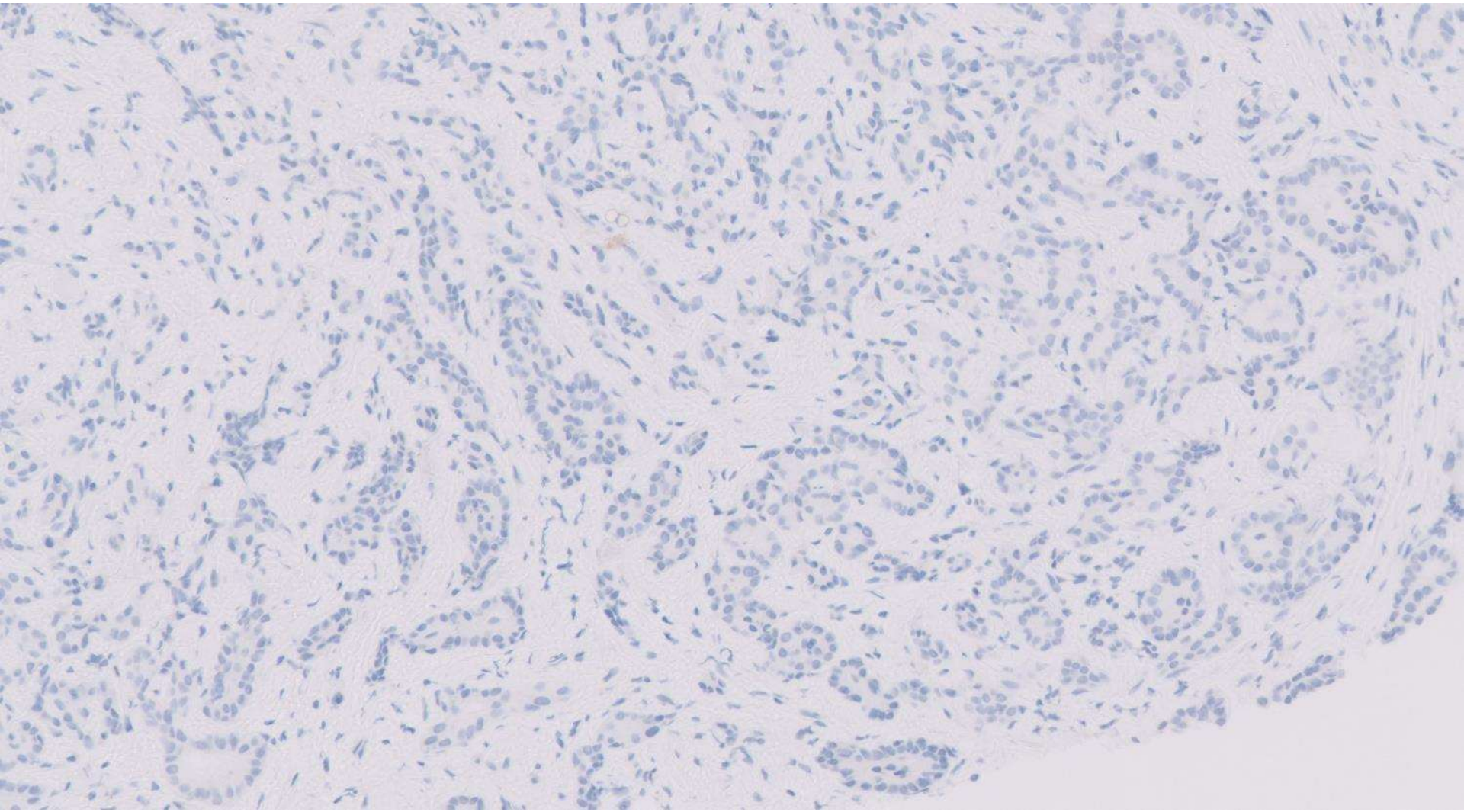

BAP1 loss in iCCA

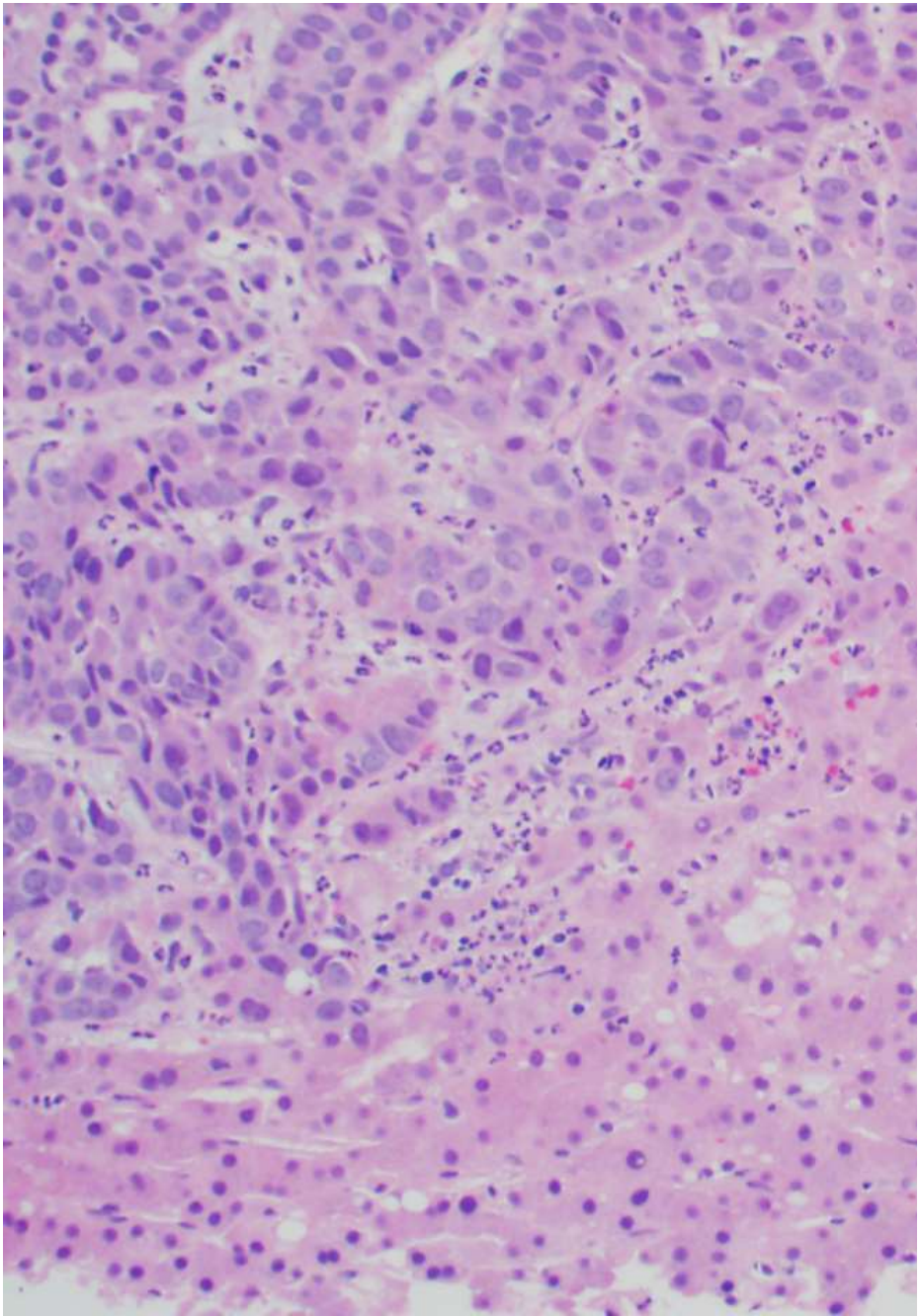

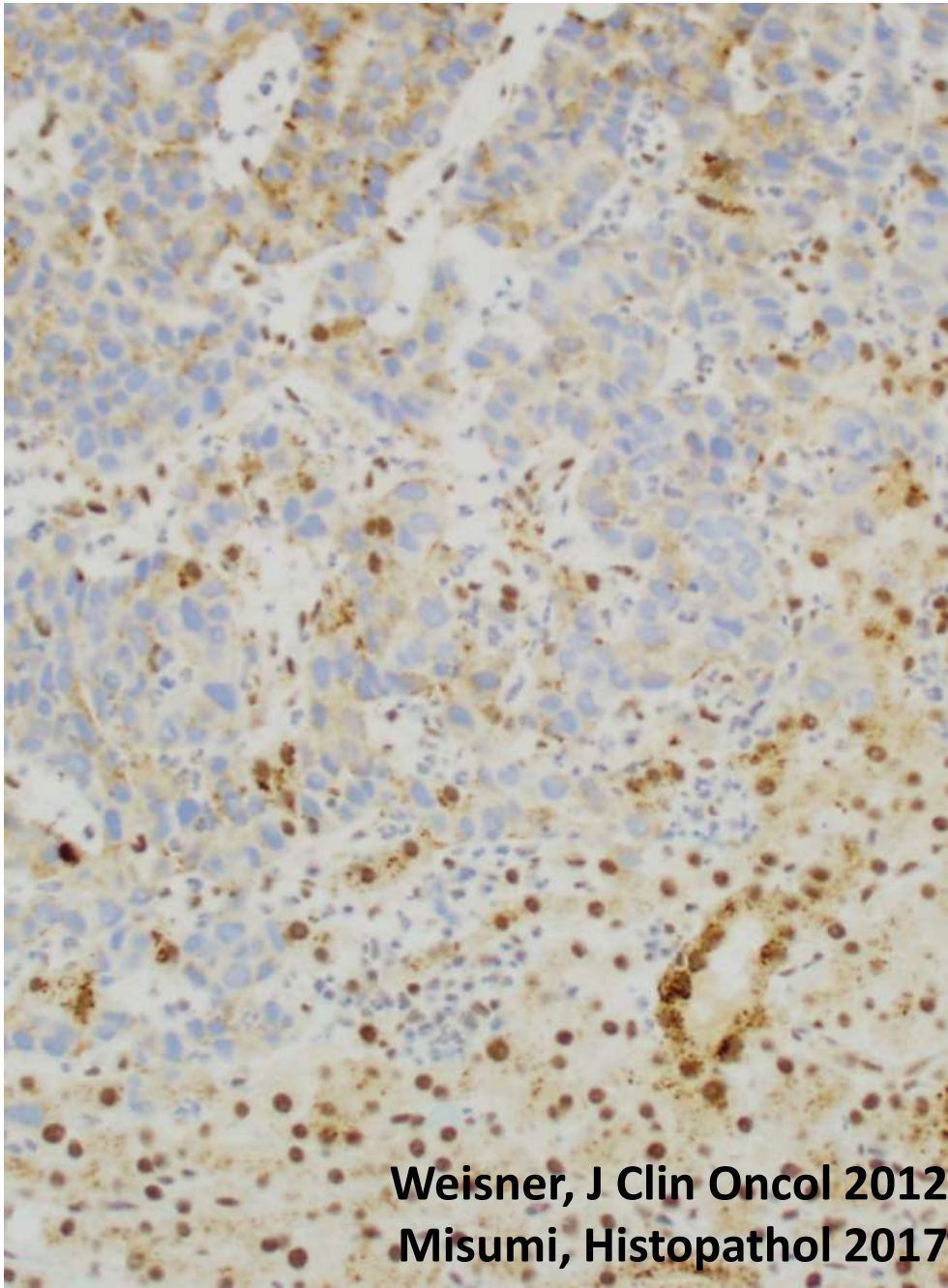

Weisner, J Clin Oncol 2012
Misumi, Histopathol 2017

BAP1

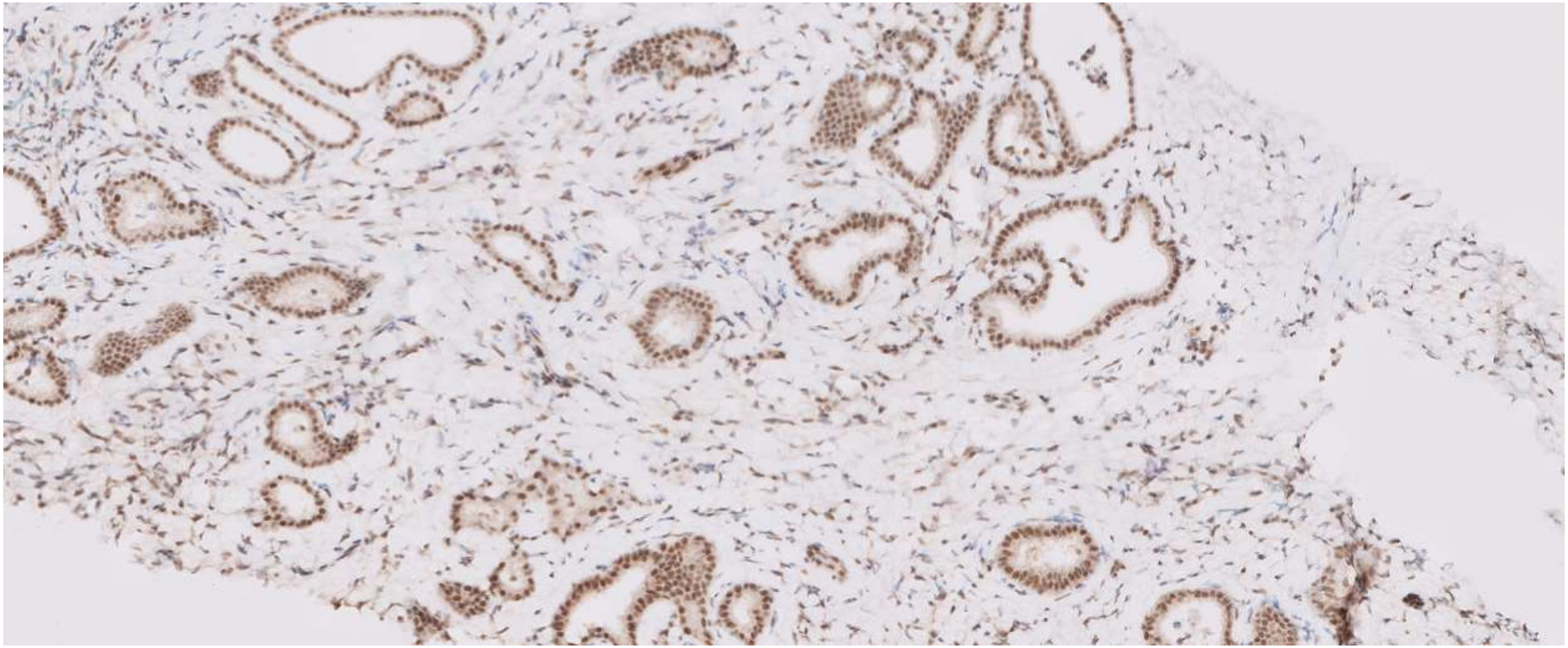

ARID1A

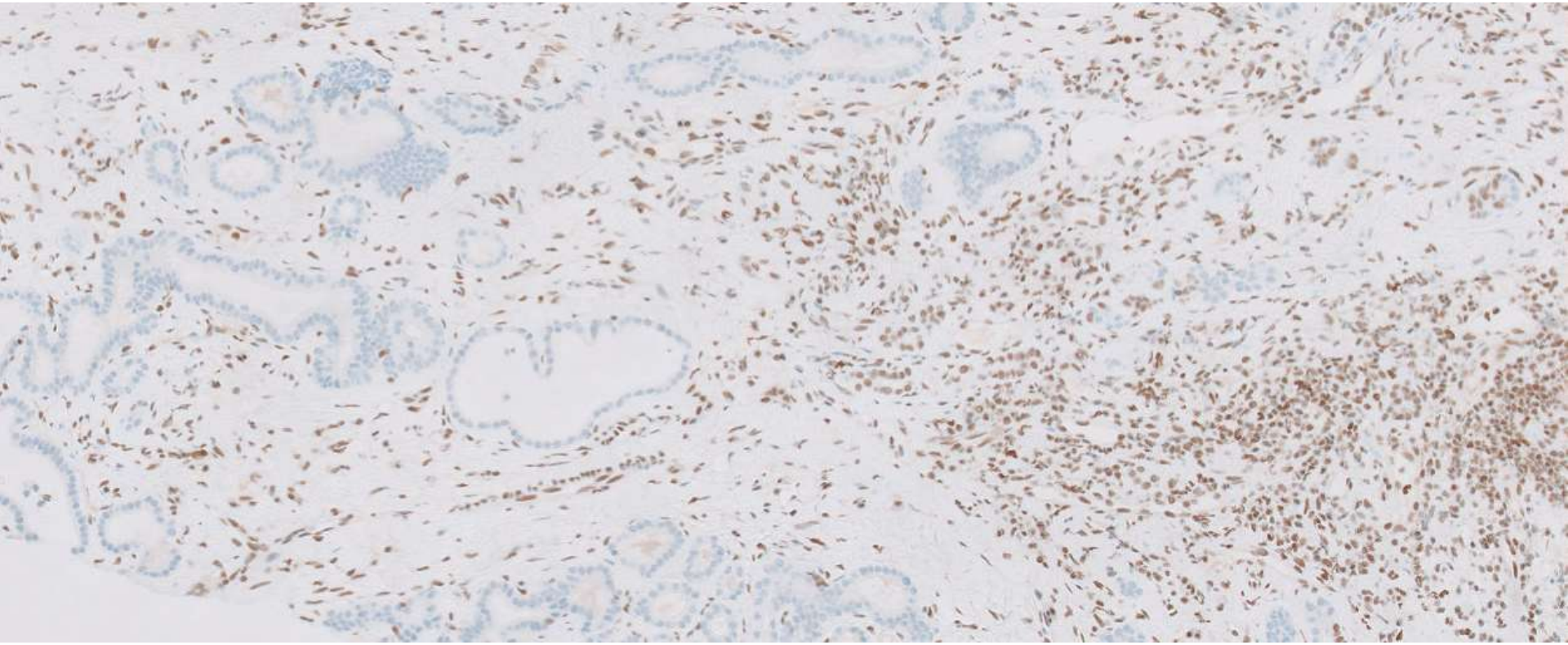

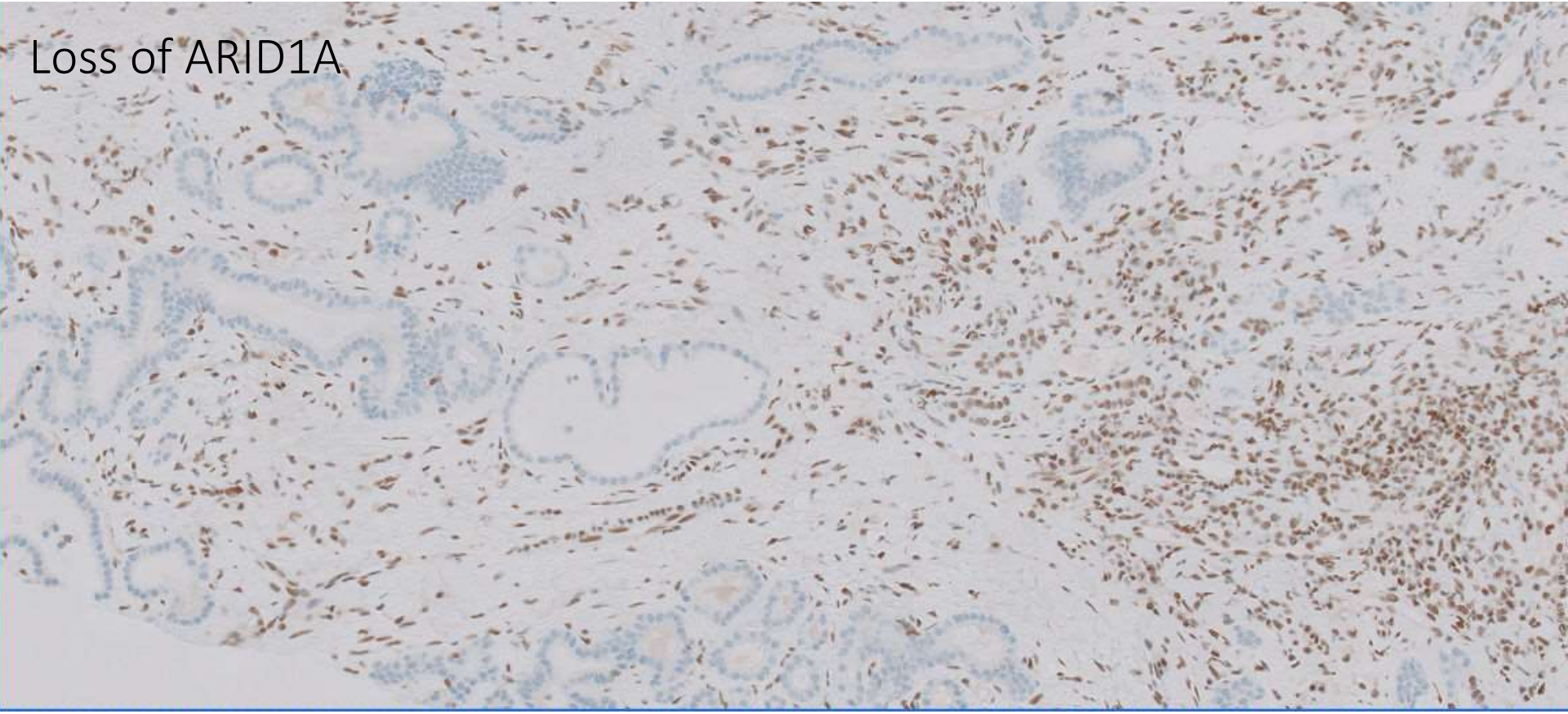

Genomic analysis

- *ARID1A*, *NF1* mutations
- Multiple copy number changes

Chung/Park, Gut Liver 2022

iCCA subtypes: WHO 2019

- Ductal plate malformation pattern
- Subtype of small duct type of intrahepatic cholangiocarcinoma

› Am J Surg Pathol. 2019 Mar;43(3):352-360. doi: 10.1097/PAS.0000000000001201.

Cholangiolocellular Carcinoma With "Ductal Plate Malformation" Pattern May Be Characterized by ARID1A Genetic Alterations

Motoko Sasaki [1], Yasunori Sato [1], Yasuni Nakanuma [1 2]

Affiliations + expand

PMID: 30520820 DOI: 10.1097/PAS.0000000000001201

Abstract

Cholangiolocellular carcinoma (CLC) is a unique subtype of primary liver carcinoma, which sometimes coexists with hepatocellular carcinoma (HCC), cholangiocarcinoma and combined hepatocellular-cholangiocarcinoma (cHCC-CCA). "Ductal plate malformation" (DPM)-pattern of primary liver carcinoma, which resembles biliary lesions in Caroli disease and von Meyenburg complex, is sometimes associated with CLC. We examined genetic alterations of hTERT promoter (hTERT), IDH1 or 2 (IDH1/2), KRAS, ARID1A, PBRM1, ARID2, BAP1, p53 and their association with histologic features such as proportion of CLC and DPM-pattern in 77 patients with primary liver carcinoma diagnosed as cHCC-CCA or CLC. Primary liver carcinomas were histologically subdivided into 29 CLC-predominant (CLC component >80%), 31 with CLC (5% to 80%) and 17 without CLC (<5%). CLC-predominant group was characterized by older age, male-predominant and smaller tumor size. Genetic alterations were detected in hTERT (25%), ARID1A (21%), PBRM1 (20%), ARID2 (3%), BAP1 (1%), p53 (46%), KRAS (5%), and IDH1/2 (8%). ARID1A alteration was more frequent in CLC-predominant group, compared with other groups ($P<0.05$) and was correlated with the degree of DPM-pattern ($P<0.01$). Alterations of hTERT and p53 were less frequent in CLC-predominant group compared with "with CLC group" ($P<0.05$). hTERT mutation was less frequent in carcinomas with DPM-pattern ($P<0.01$). PBRM1 alteration was more frequent in CLC with focal HCC subgroup and without CLC group compared with other groups ($P<0.05$). CLC may be a distinct subgroup of primary liver carcinoma, which is different from cHCC-CCA, based on clinicopathologic and genetic alterations. ARID1A alterations may characterize CLC with DPM-pattern and could be a diagnostic immunohistochemical marker for small CLCs with DPM-pattern.

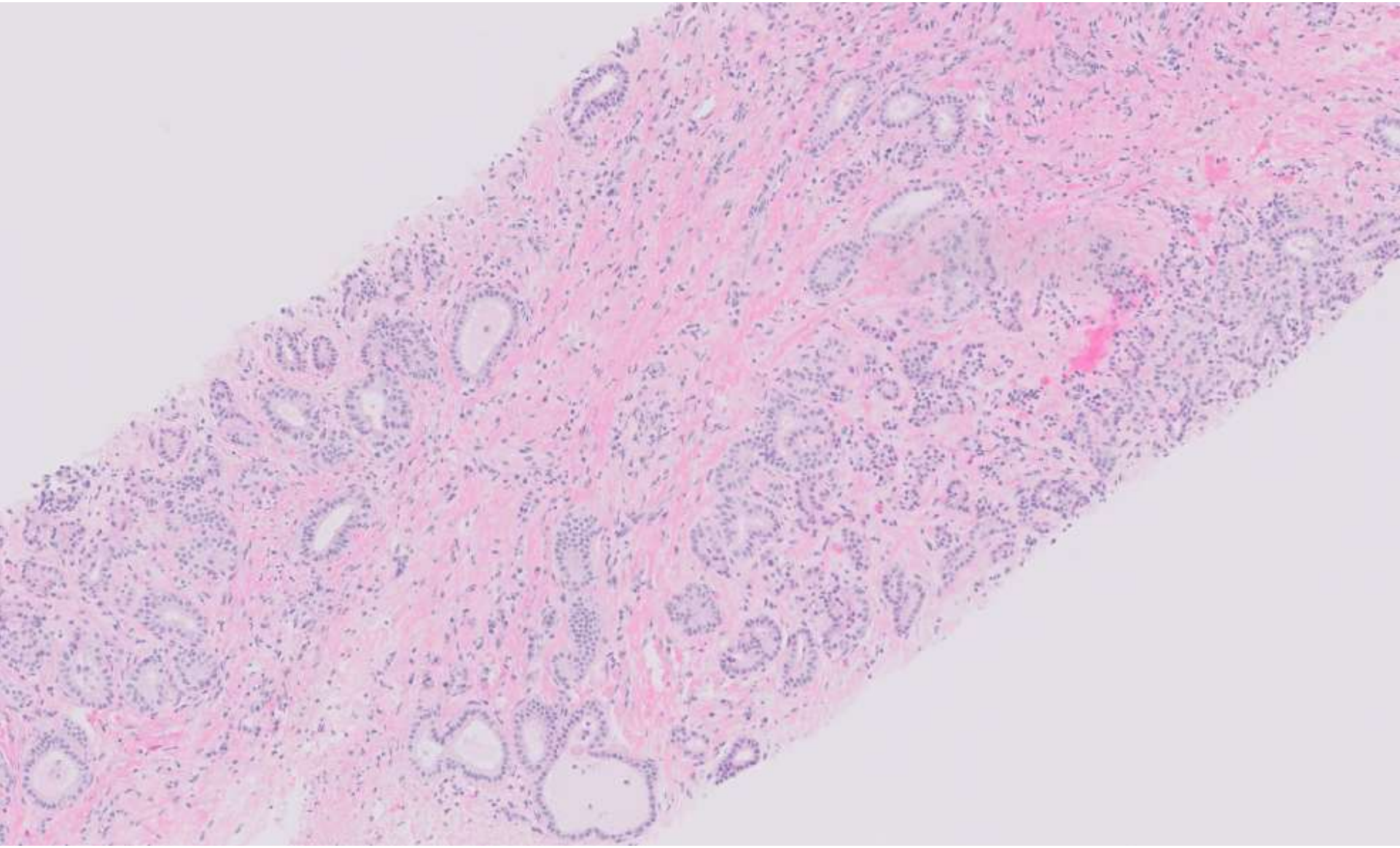

Benign biliary vs. iCCA

Summary of ancillary stains

IHC	Favors CCA
Ki-67	Ki-67> 20%
p53	Diffuse strong p53
BRAF V600E	Typically negative (often positive in BDA)
BAP1 ARID1A DPC4	Loss

iCCA vs. metastatic adenocarcinoma

Genetic change	iCCA	Biliary AC	GB	PDAC	Eso/Gastric
***IDH* mutations**	19-36%	0-7%	0	<1%	<1%
***BAP1* mutation**	7-29%	0-10%	0	<1%	3%
***FGFR2* fusion**	6-50%	0-5%	20%	0	2-9%
PBRM1 mutation	11-17%	5%	20%	4-6%	<1%
SMAD4 mutation	0-4%	10-25%	0	35-60%	8%

Intrahepatic cholangiocarcinoma

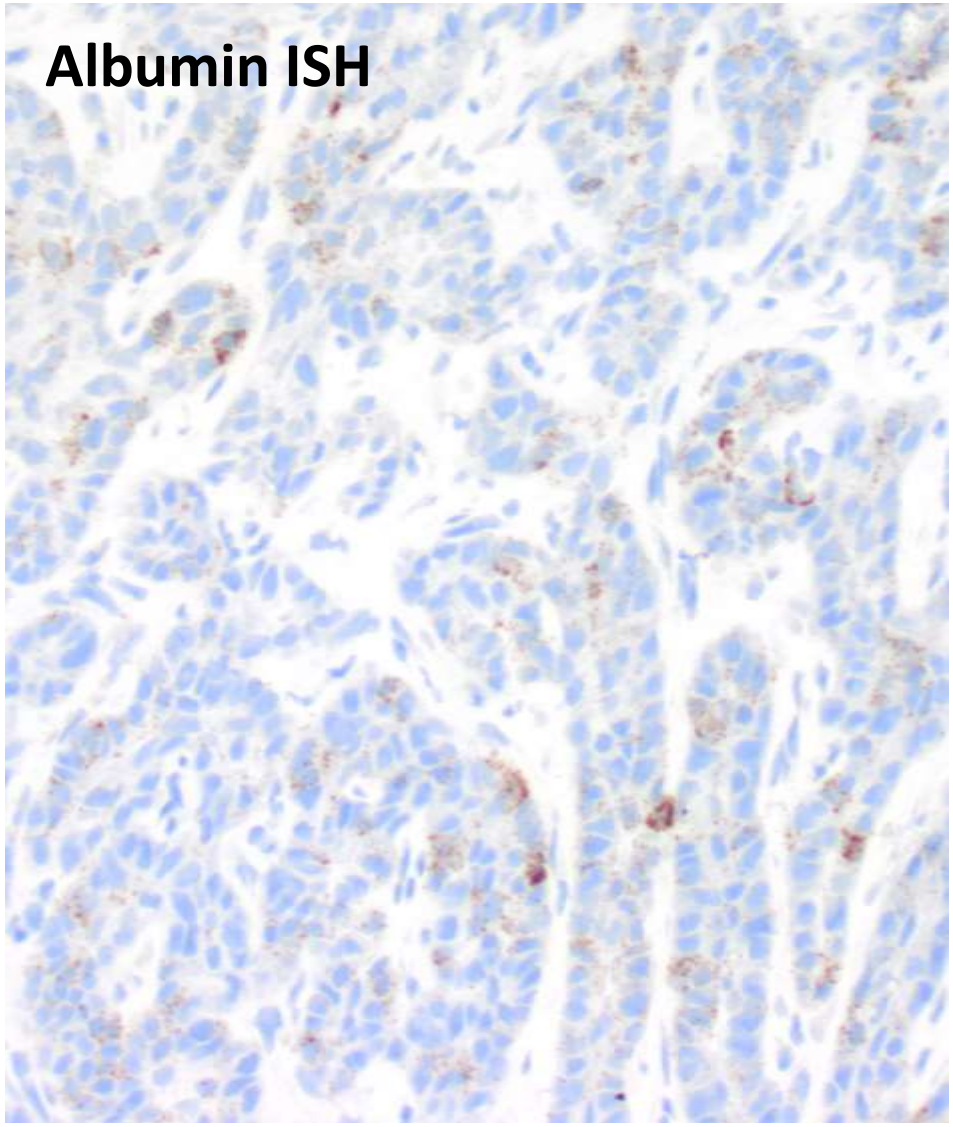

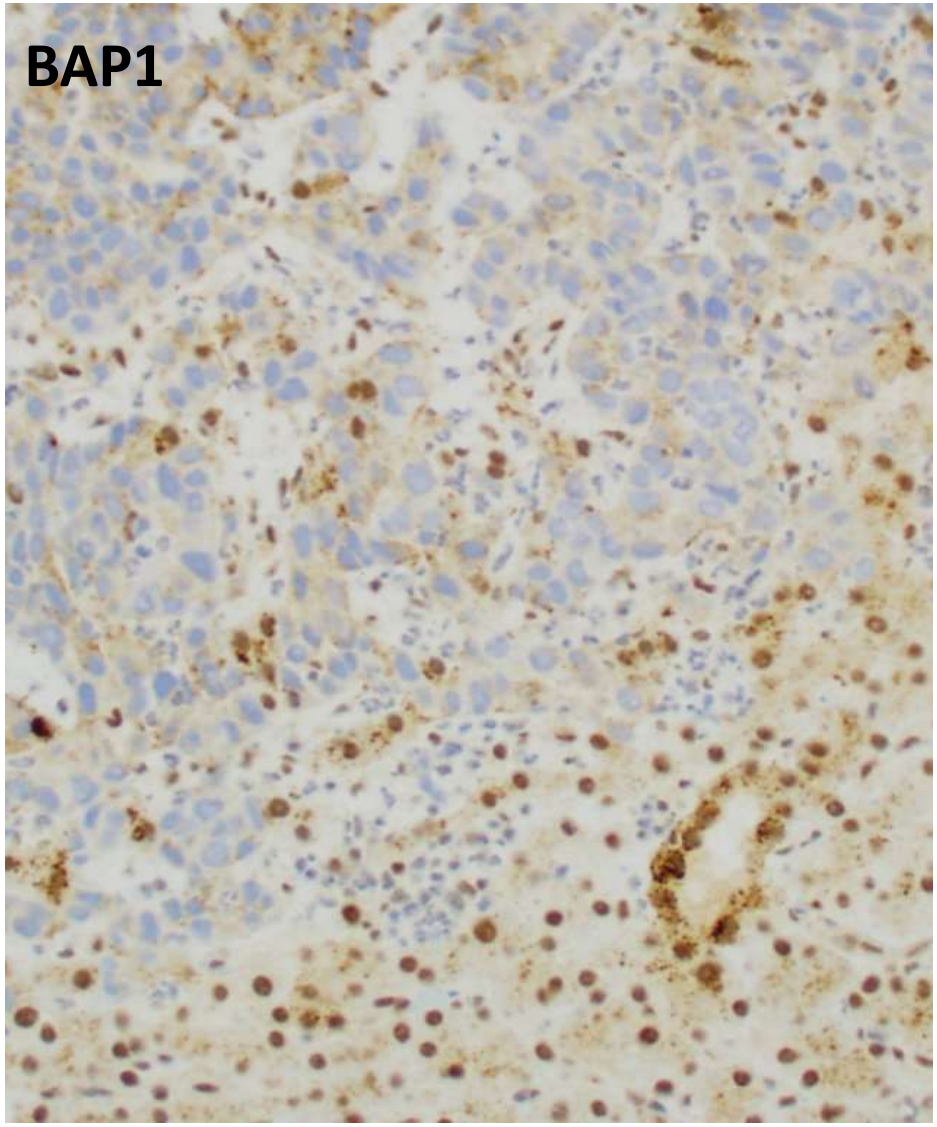

23-0407

Ingold Huang/Linlin Wang; UCSF

Female infant with neutropenia. Bone marrow biopsy submitted.

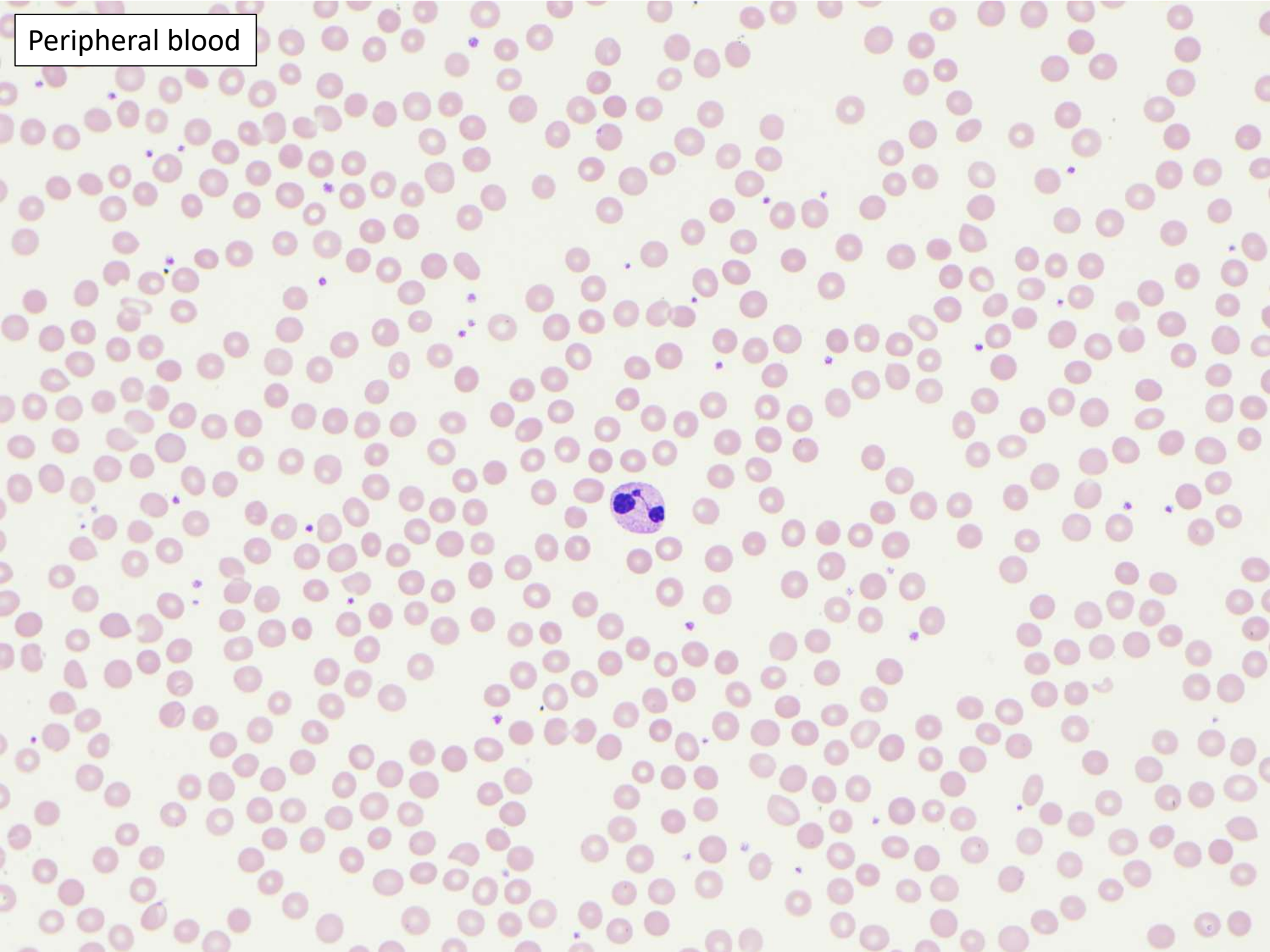
Peripheral blood

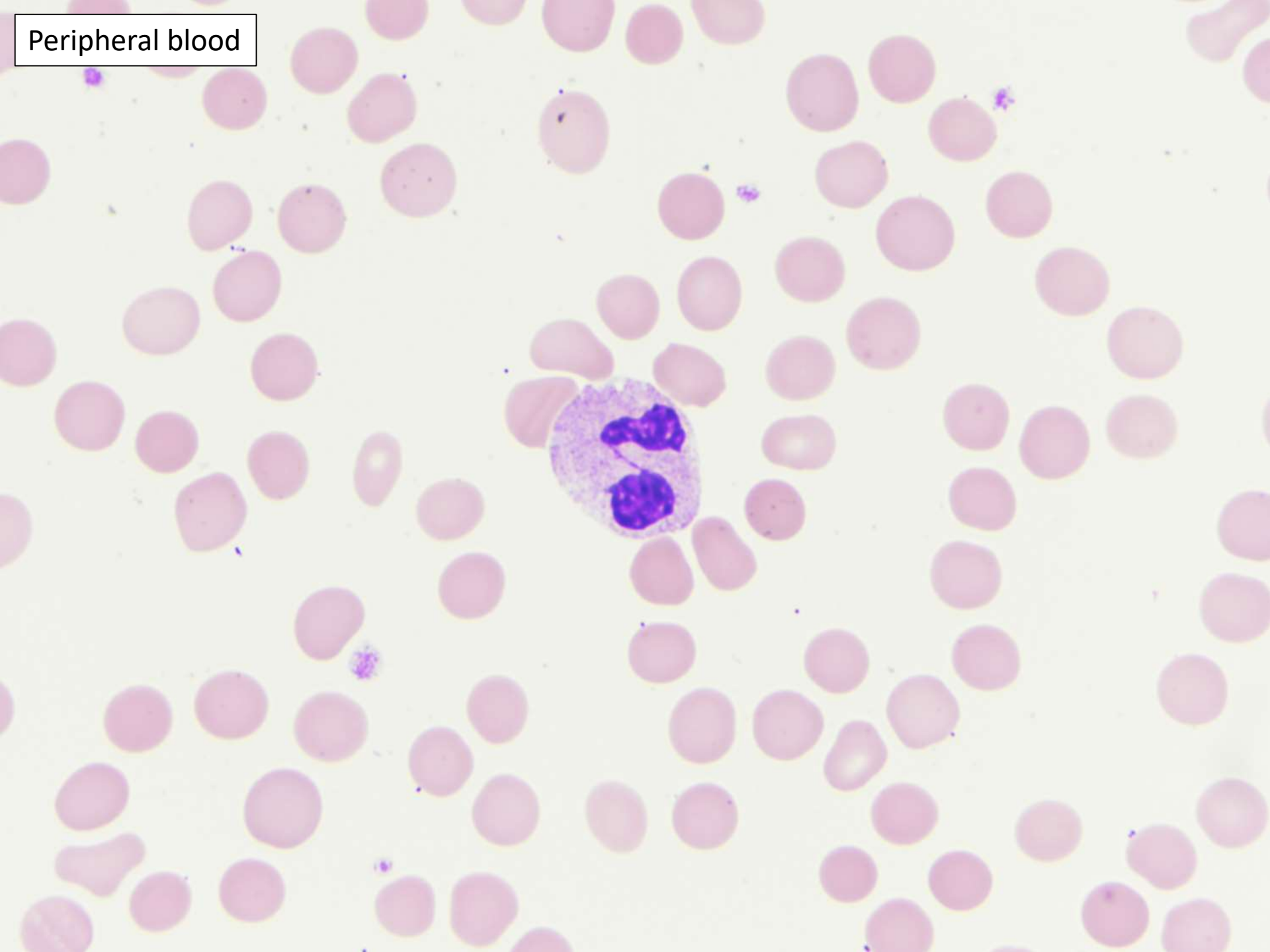
Peripheral blood

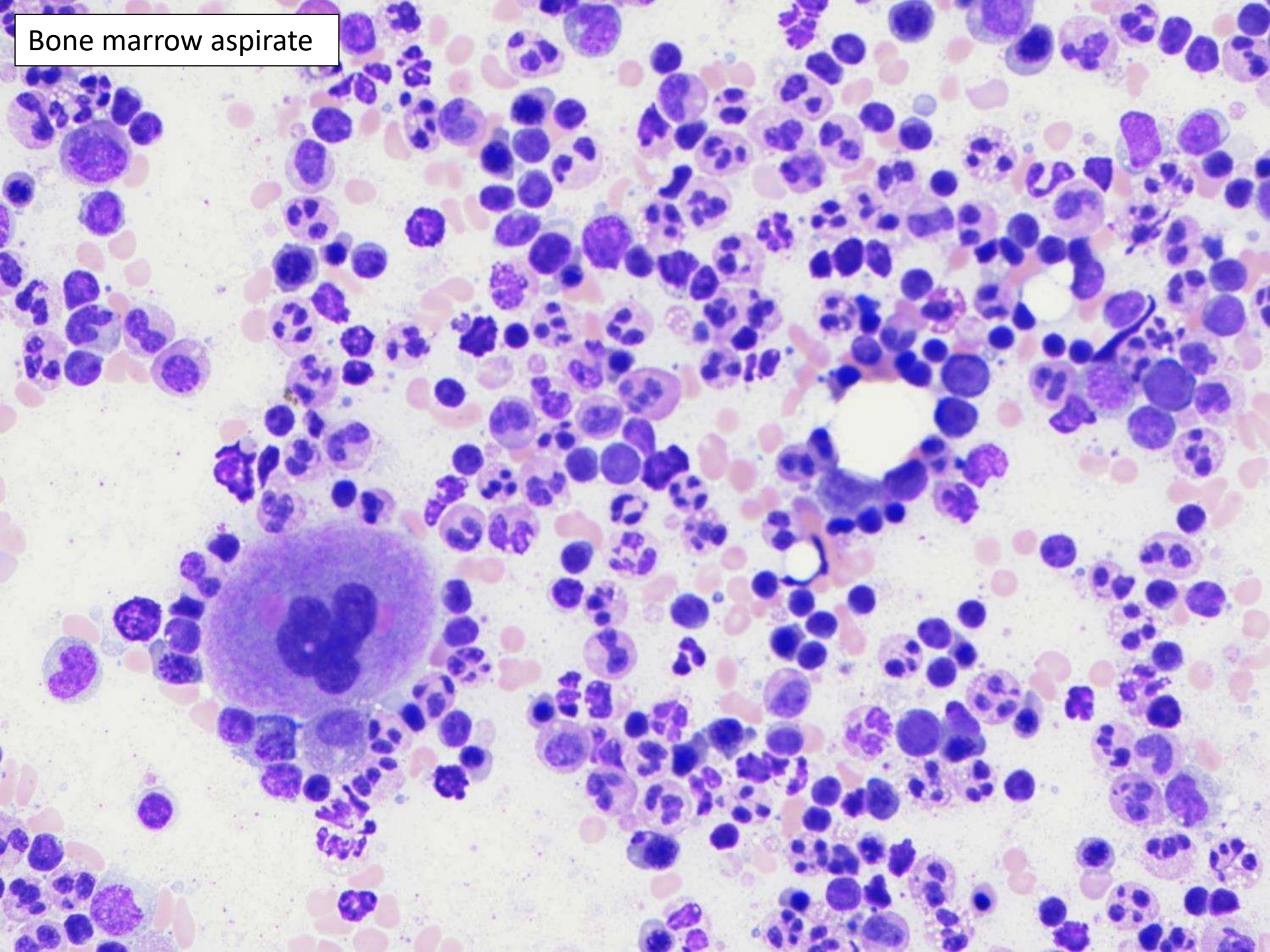
Bone marrow aspirate

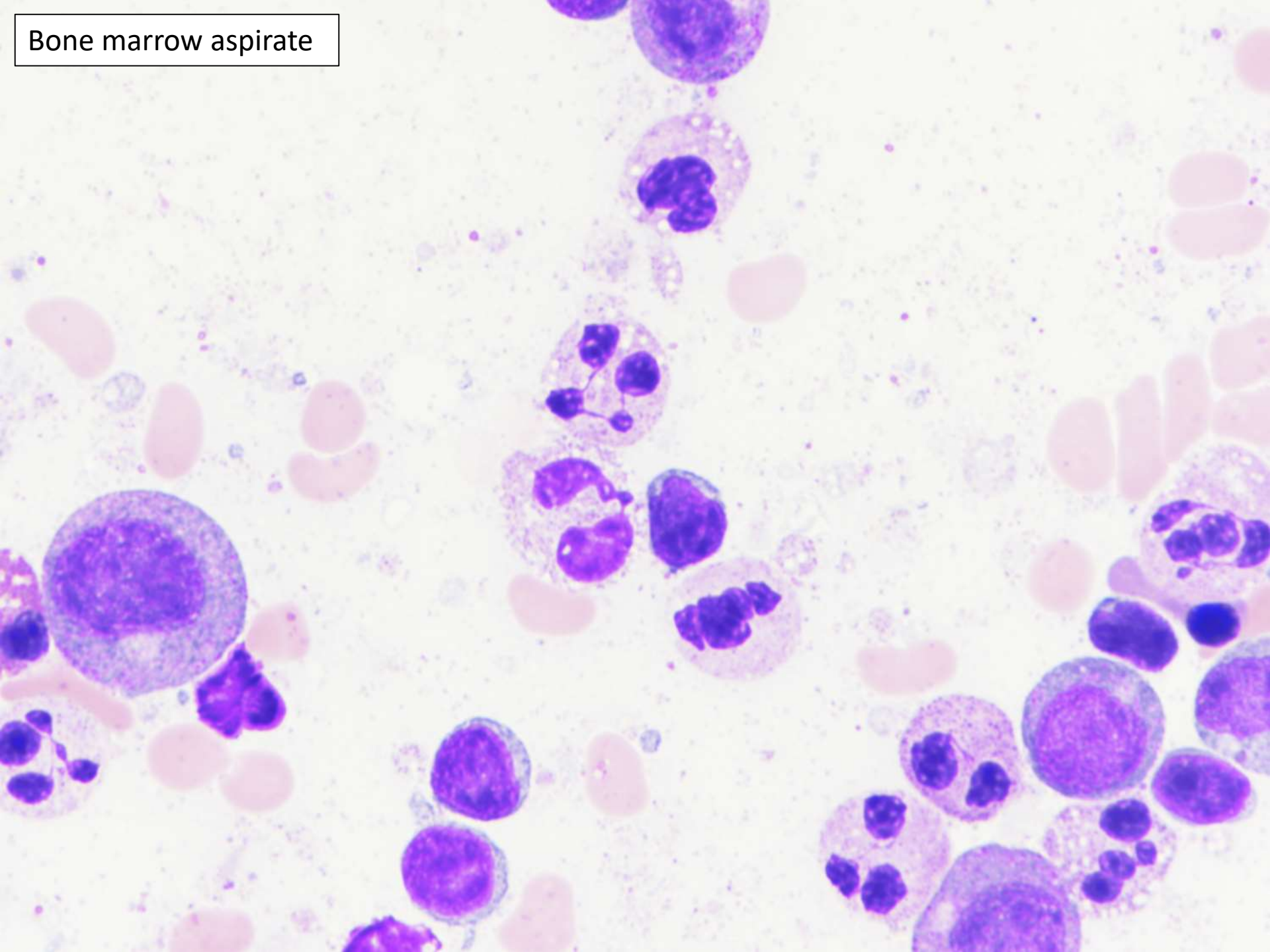
Bone marrow aspirate

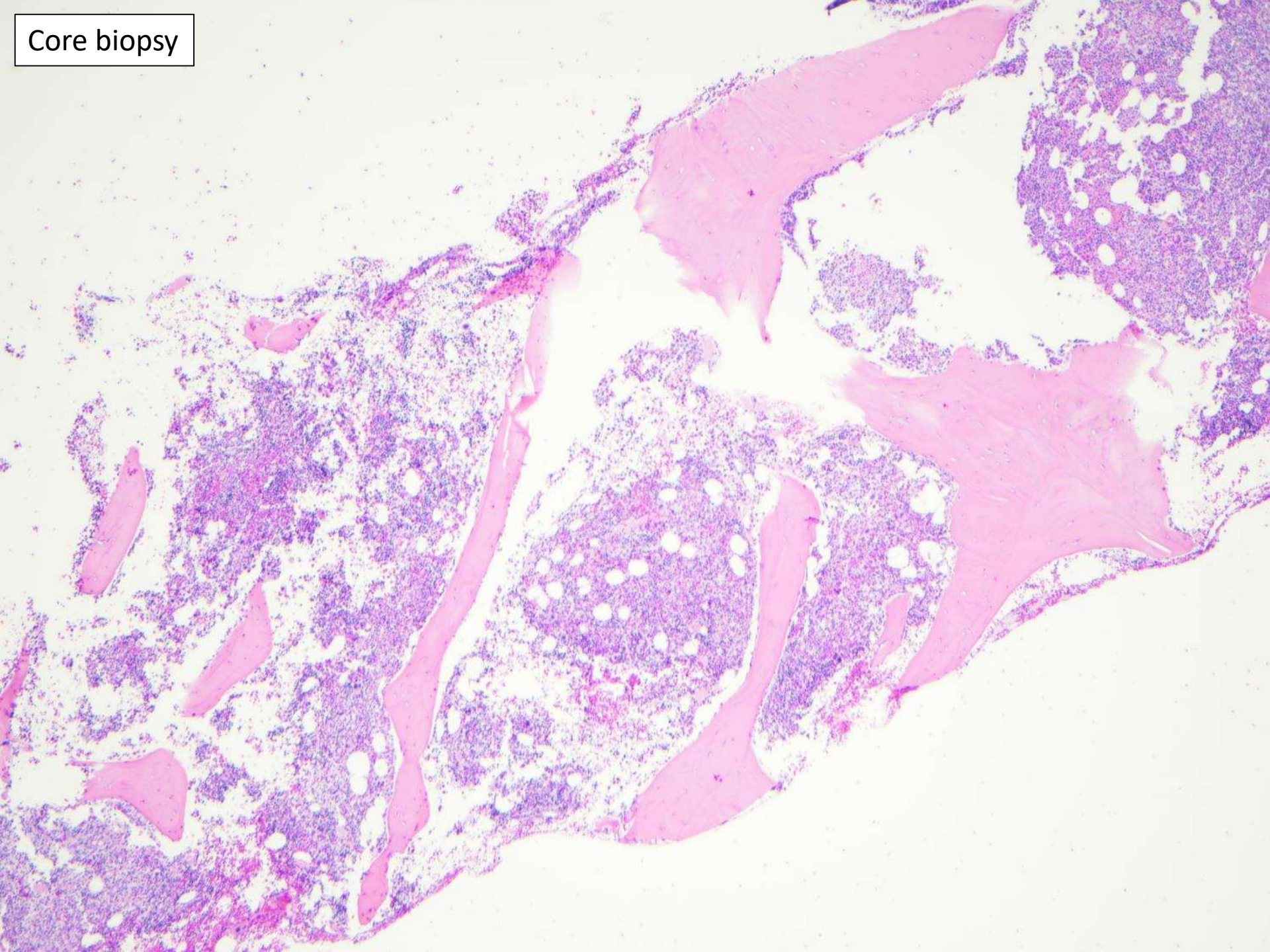
Core biopsy

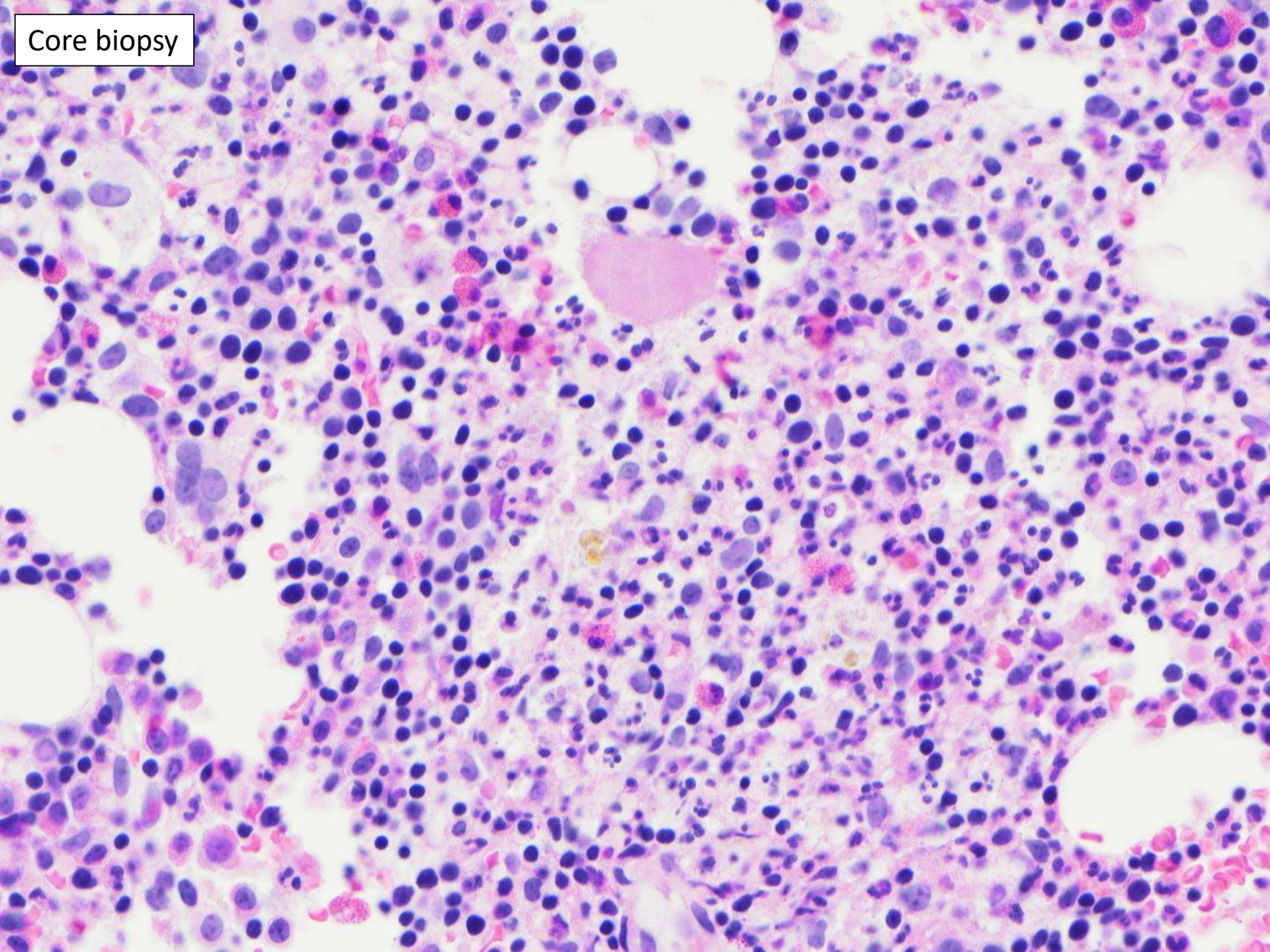
Core biopsy

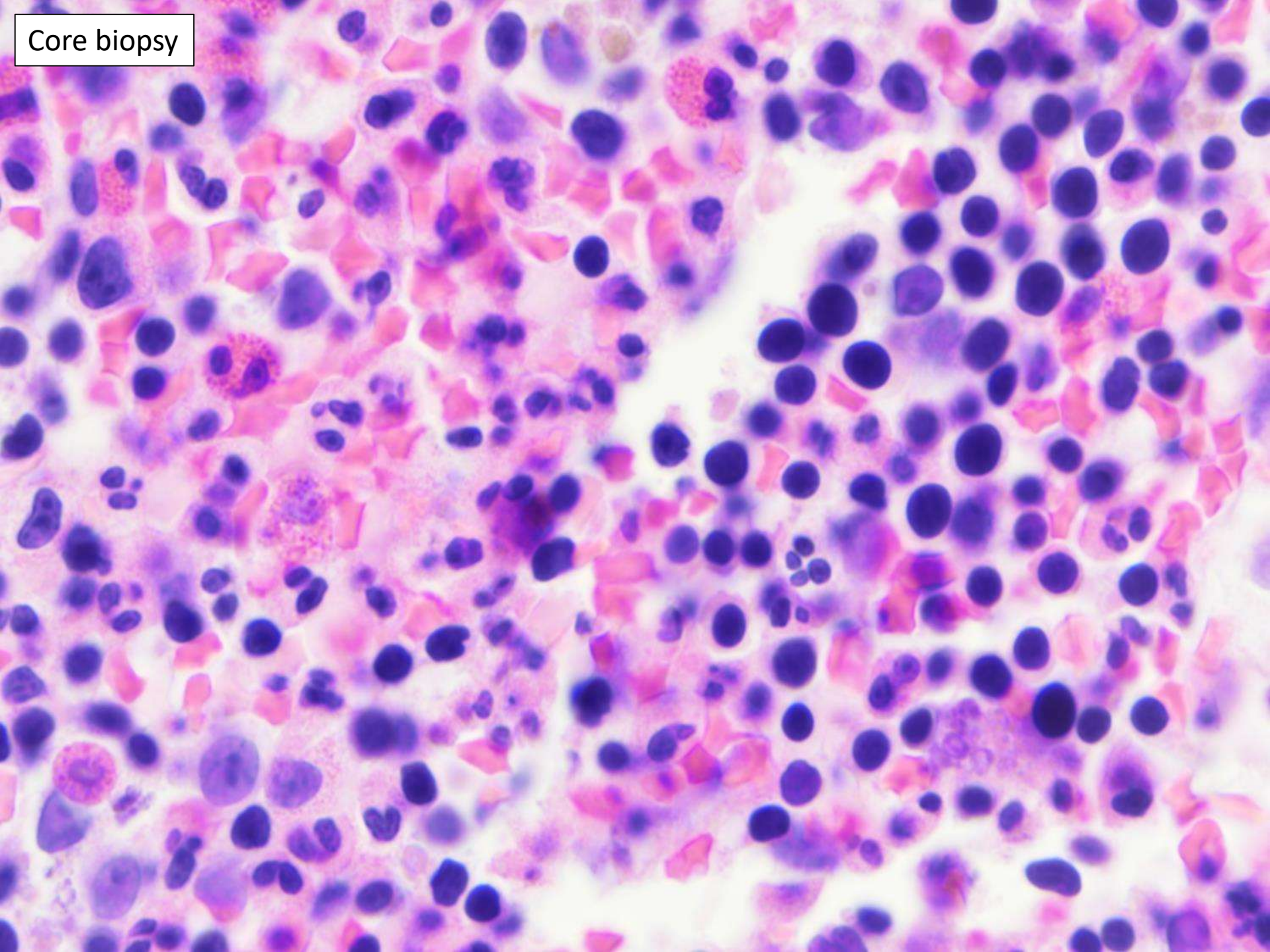
Core biopsy

Differential diagnosis

- Primary immunodeficiency syndrome
- Autoimmune disease
- Toxin/medication
- Malignancy (low on differential given age)

CBC and other labs

- **WBC**: 0.9 x10E9/L ↓ (4.5-15.5 x10E9/L)
  - **Neuts**: 0.26 x10E9/L ↓ (1.5-8.5 x10E9/L)
  - **Lymphs**: 0.32 x10E9/L ↓ (1.2-8 x10E9/L)
  - **Monos**: 0.18 x10E9/L (0-1.4 x10E9/L)
  - **Eos**: 0.08 x10E9/L (0-1.1 x10E9/L)
  - **Basos**: 0.02 x10E9/L (0-0.3 x10E9/L)
- **Hgb**: 11.8 g/dL (11.2-13.5 g/dL)
- **MCV**: 81 fL (75-87 fL)
- **Plt**: 290 x10E9/L (140-450 fL)

- **IgG (serum)**: 276 mg/dL ↓ (463-1236 mg/dL)
- **IgA (serum)**: 41 mg/dL (25-154 mg/dL)
- **IgM (serum)**: 37 mg/dL ↓ (43-196 mg/dL)

Morphology of myelokathexis

Myelokathexis: retention of myeloid cells in bone marrow

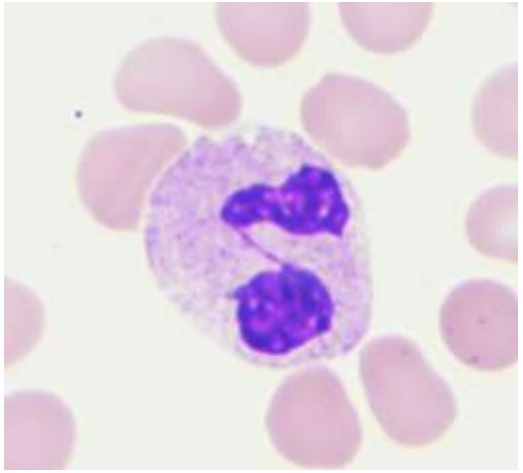

<u>Neutrophil morphology</u>

- Increased mature forms
- Widely separated nuclear lobes
- Elongated filaments
- Cytoplasmic vacuoles
- Subset of neutrophils with senescence/apoptosis

WHIM syndrome

- W= Warts
- H = Hypogammaglobulinemia
- I = Infections
- M = Myelokathexis

(diagnostic if all 4 present)

- Rare primary combined immunodeficiency syndrome

Genetic basis of WHIM syndrome

- Caused by autosomal dominant gain-of-function mutations in *CXCR4*
- *CXCR4* codes for chemokine receptor involved in myeloid and B-cell development and localization

CXCR4 mutation ⇨ Retention of defective neutrophils & B-cells ⇨ WHIM

Our patient

- ❑ Warts
- ✓ Hypogammaglobulinemia
- ✓ Infections
- ✓ Myelokathexis

Molecular testing

CXCR4 heterozygous mutation (S388X, 1013 C → A)

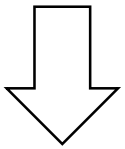

Diagnosed with WHIM syndrome

Management of WHIM syndrome

Treatment

- Treat infections as they occur.
  - Rarely fatal or require hospitalization.
  - May consider prophylactic antibiotics for cases with frequent infections.
- Vaccination
- Leukocyte-mobilizing agents: G-CSF, plerixafor
- IVIG

Cure

- Allogeneic stem cell transplant (4 cases)
- Gene therapy being explored

Patient follow-up

- Now in late adolescence
- Once admitted for cellulitis without bone involvement (resolved)
- Otherwise no serious infections requiring hospitalization
- Recurrent ear/sinus/upper respiratory infections
- Decreased infections and improved growth with IVIG

23-0408

Ankur Sangoi; El Camino Hospital

Adult M presents with BPH, undergoes TURP.

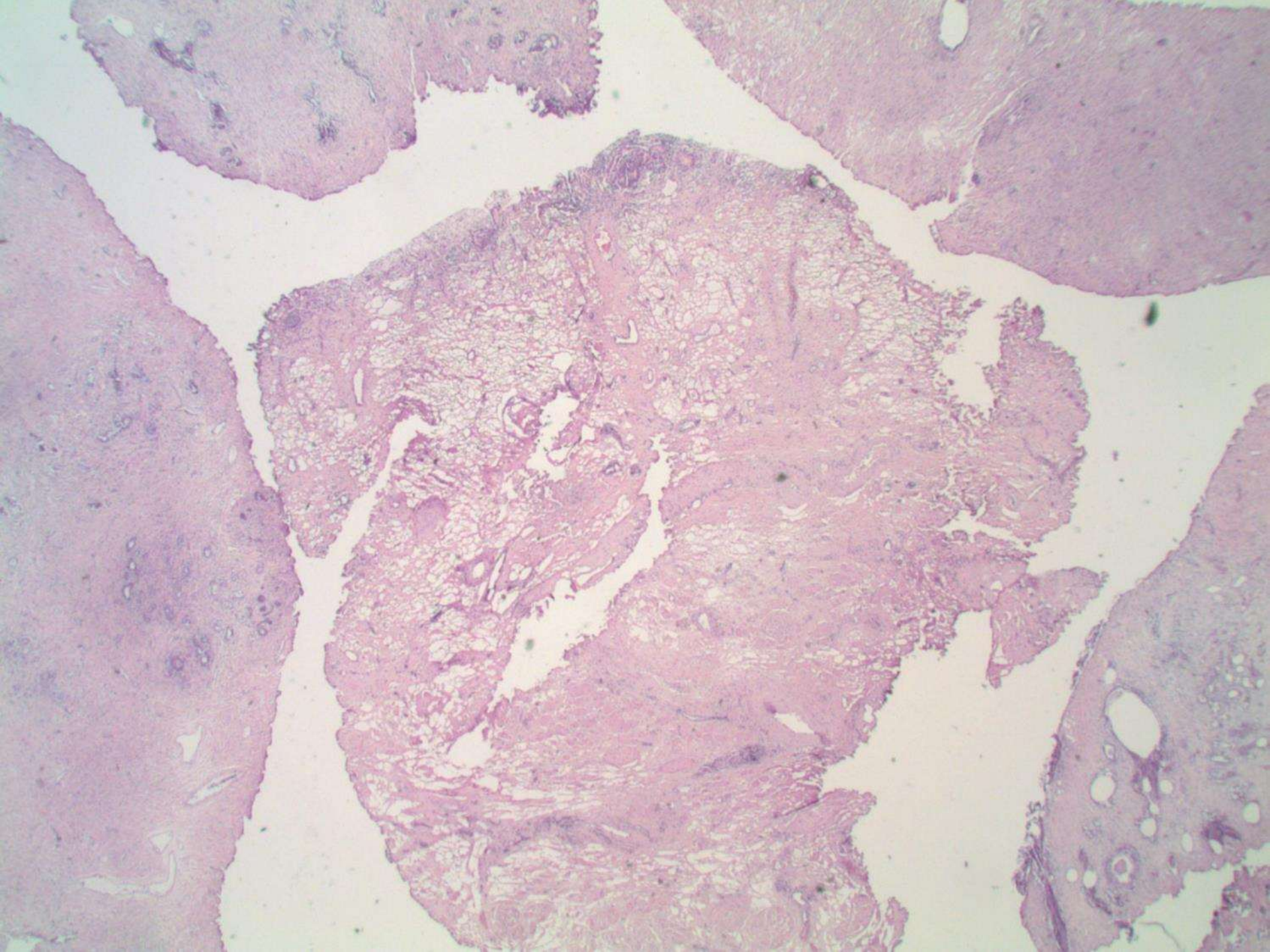

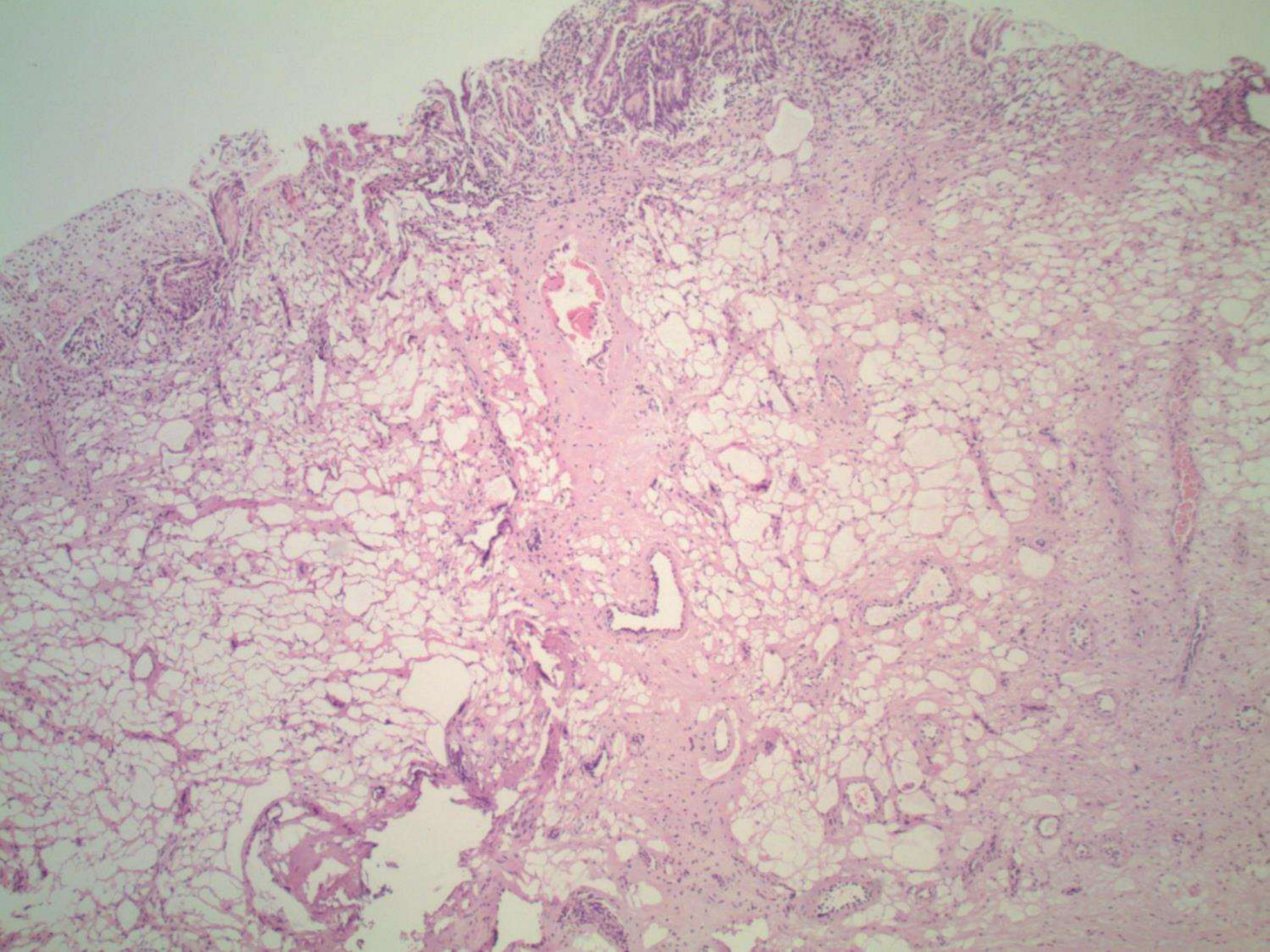

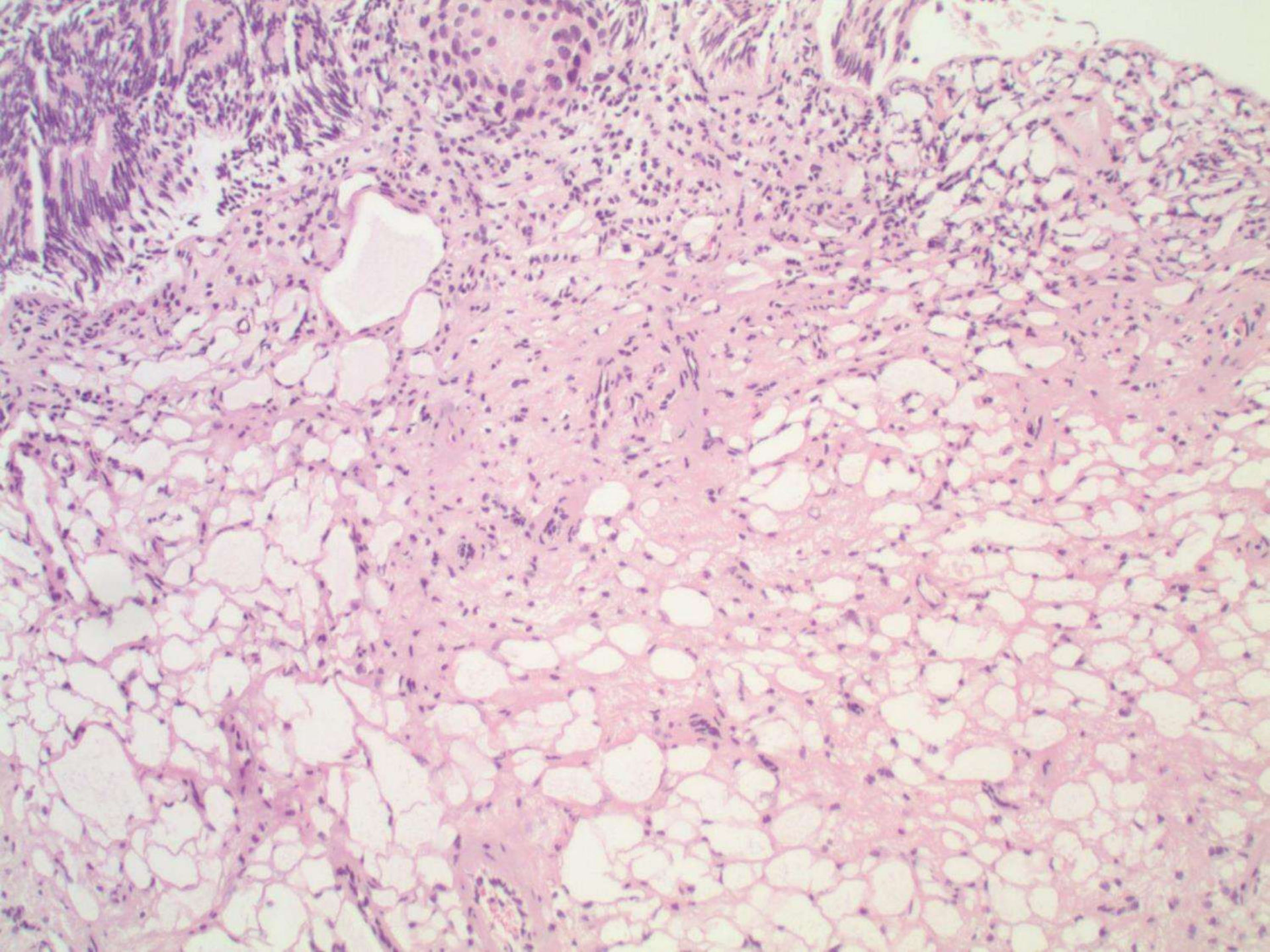

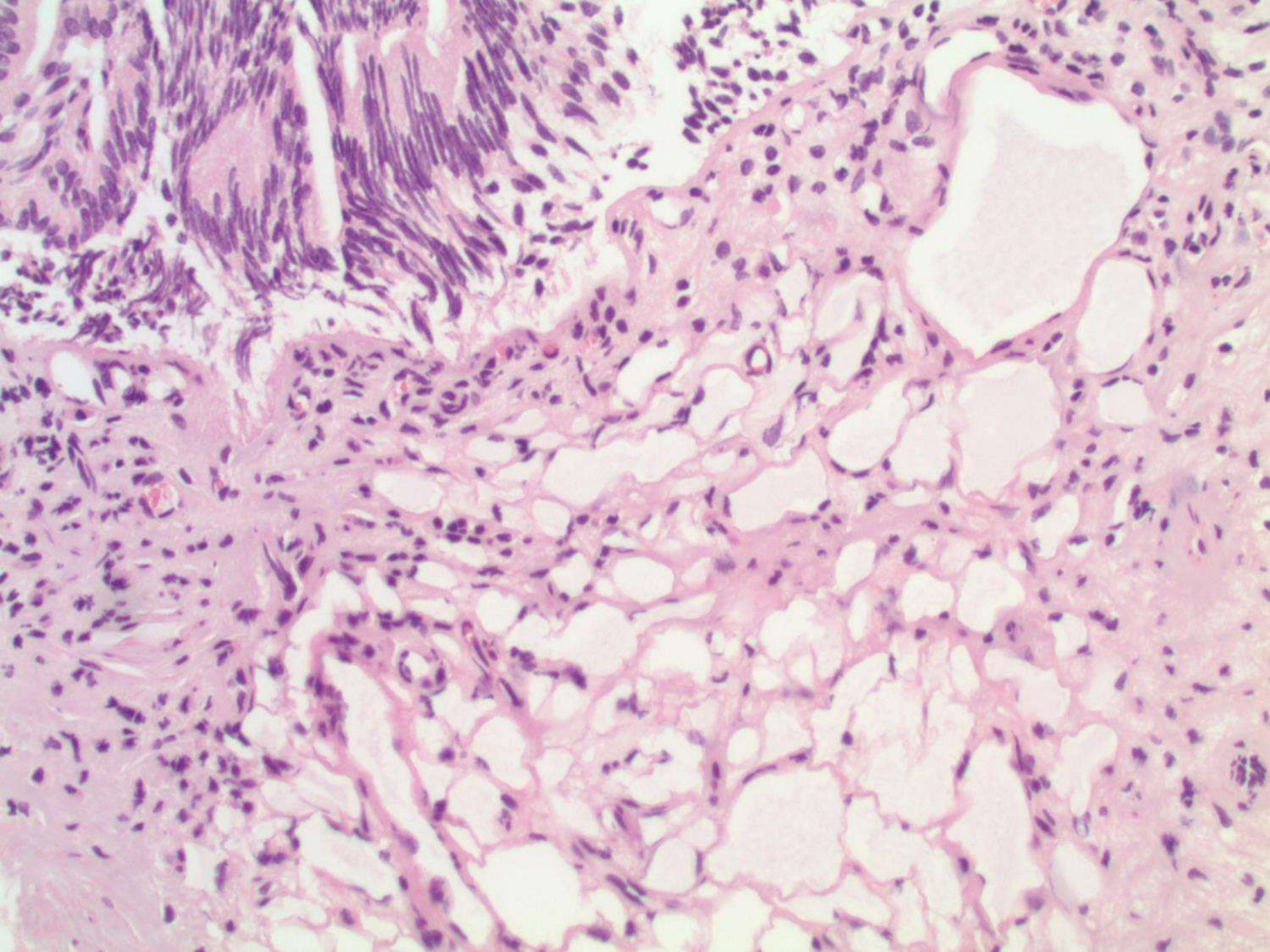

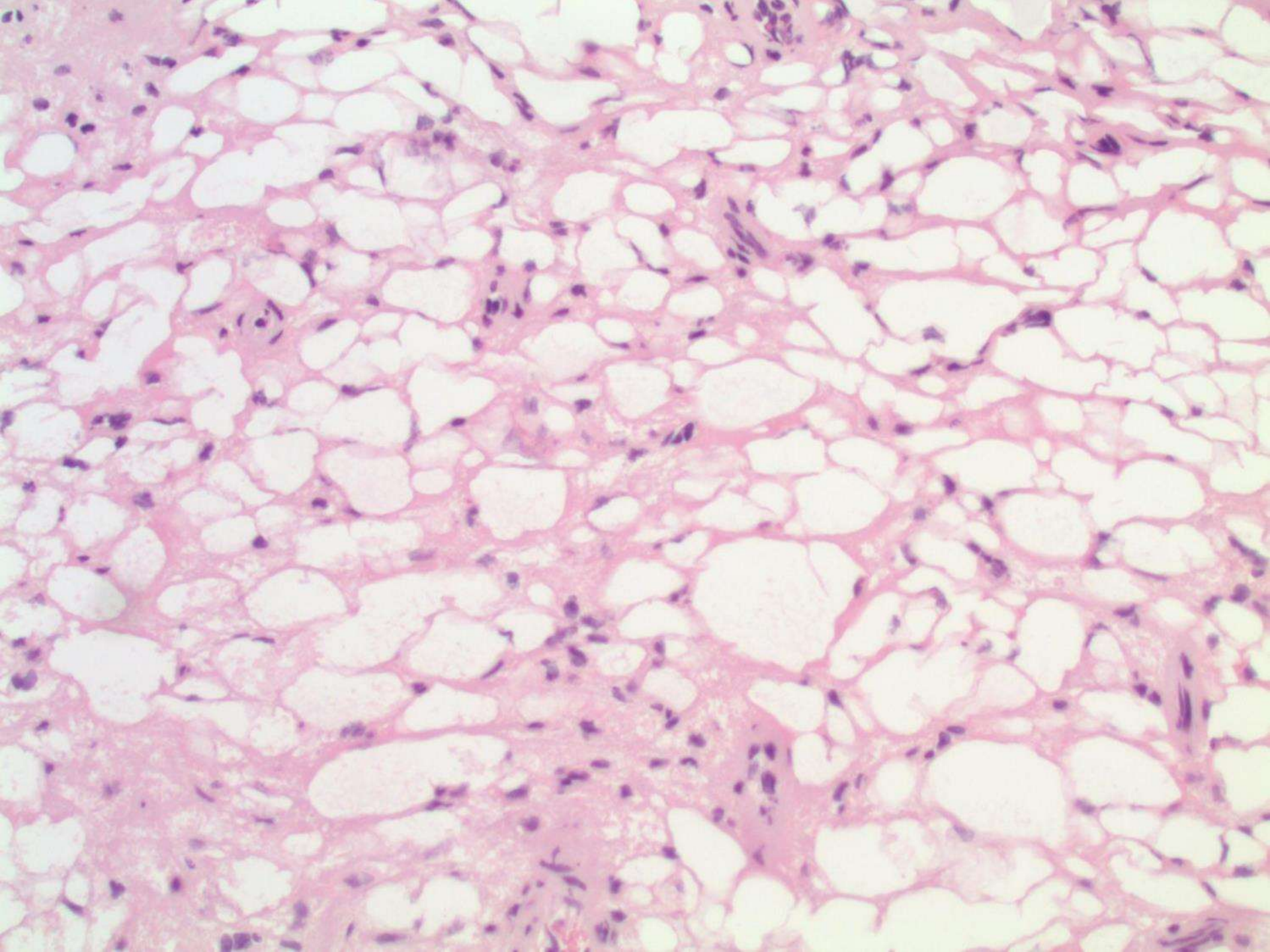

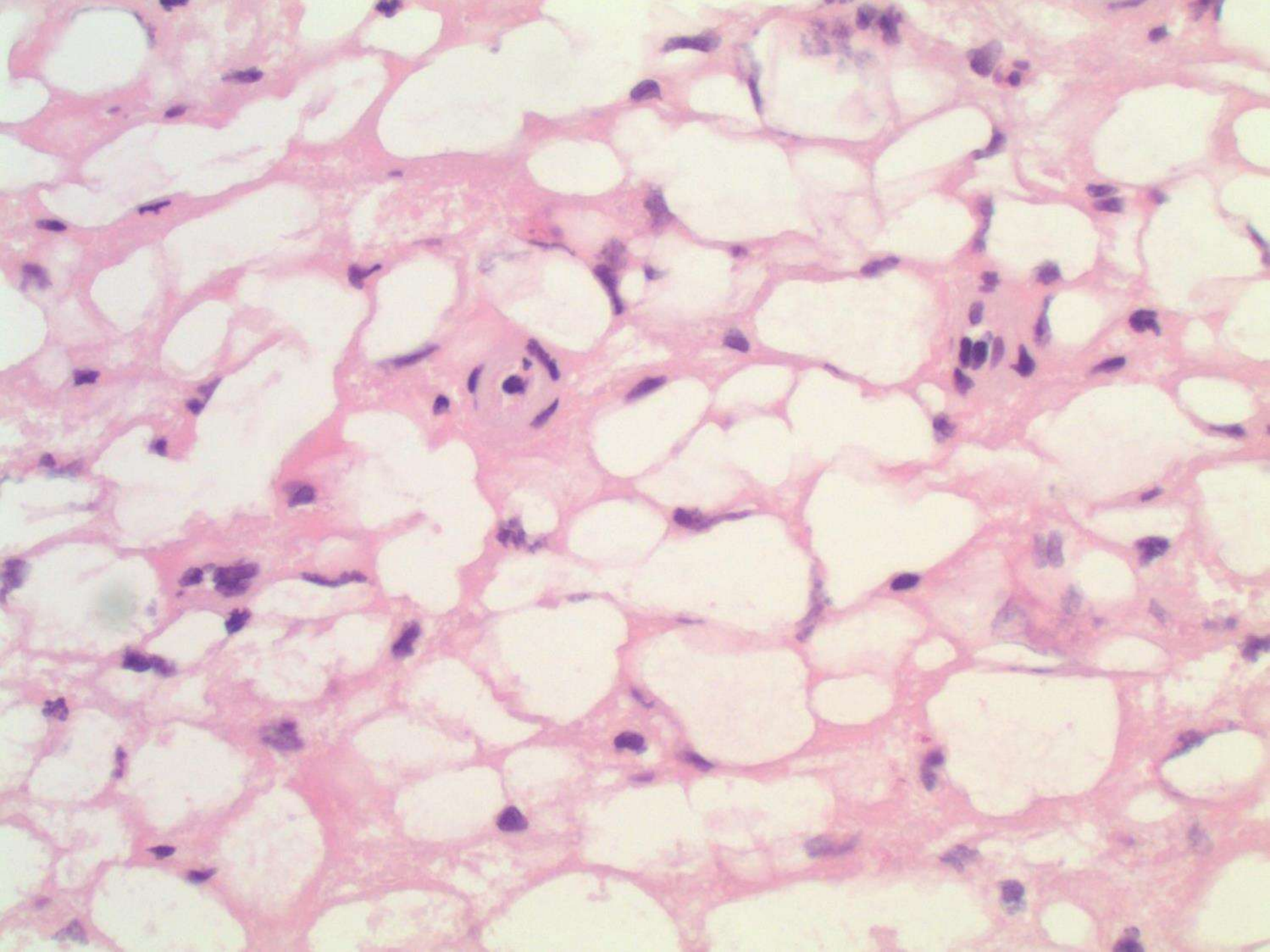

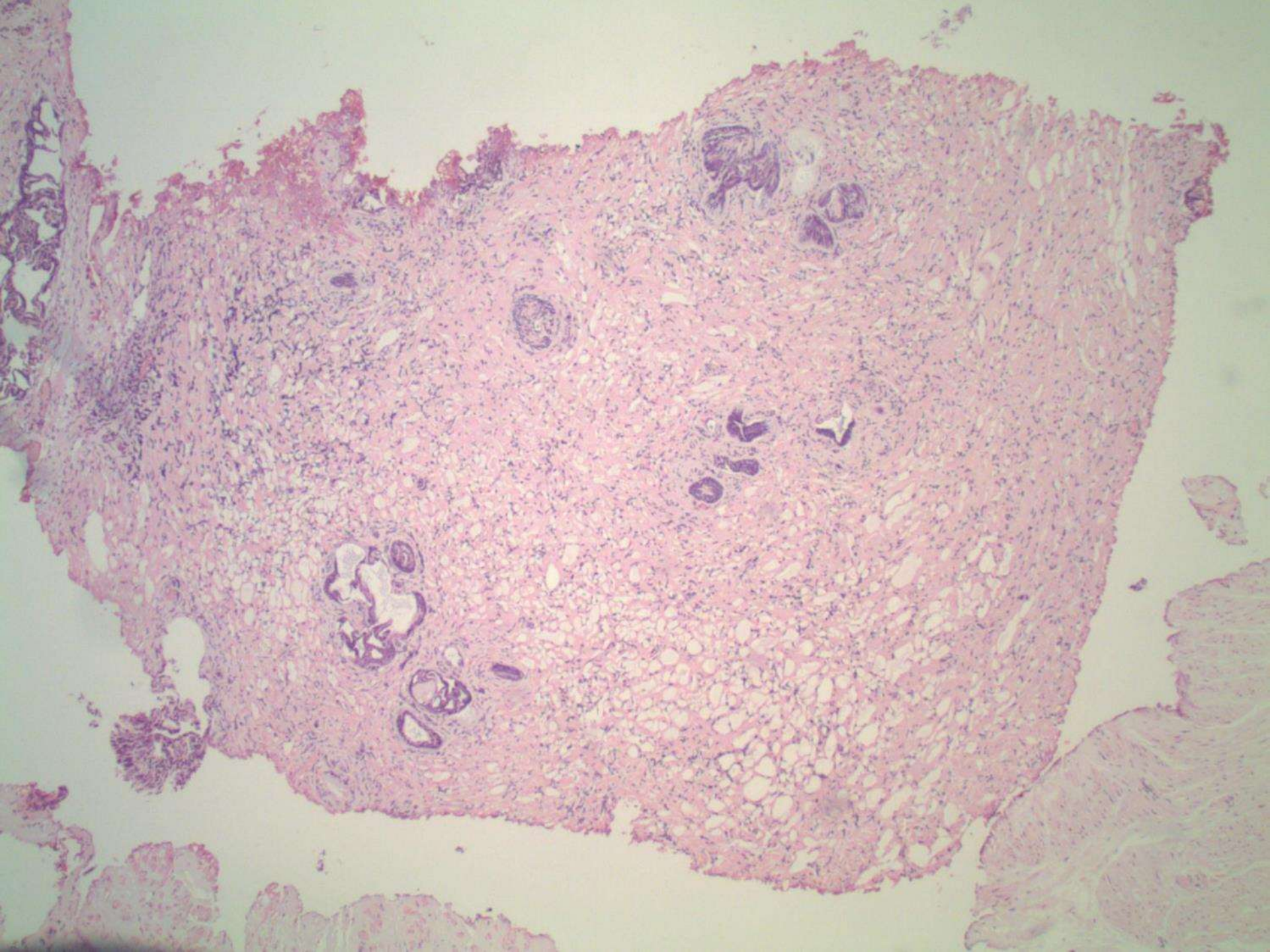

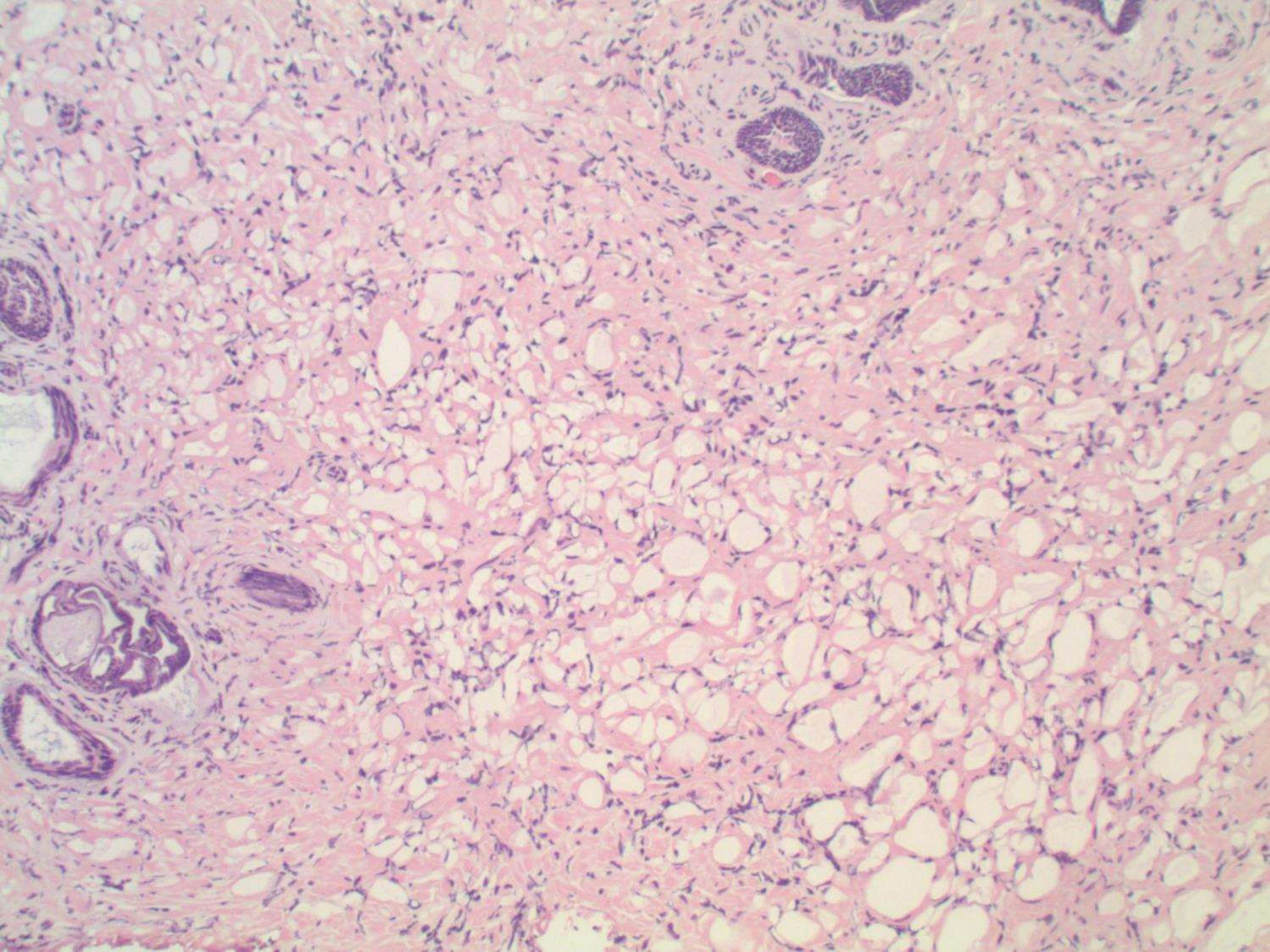

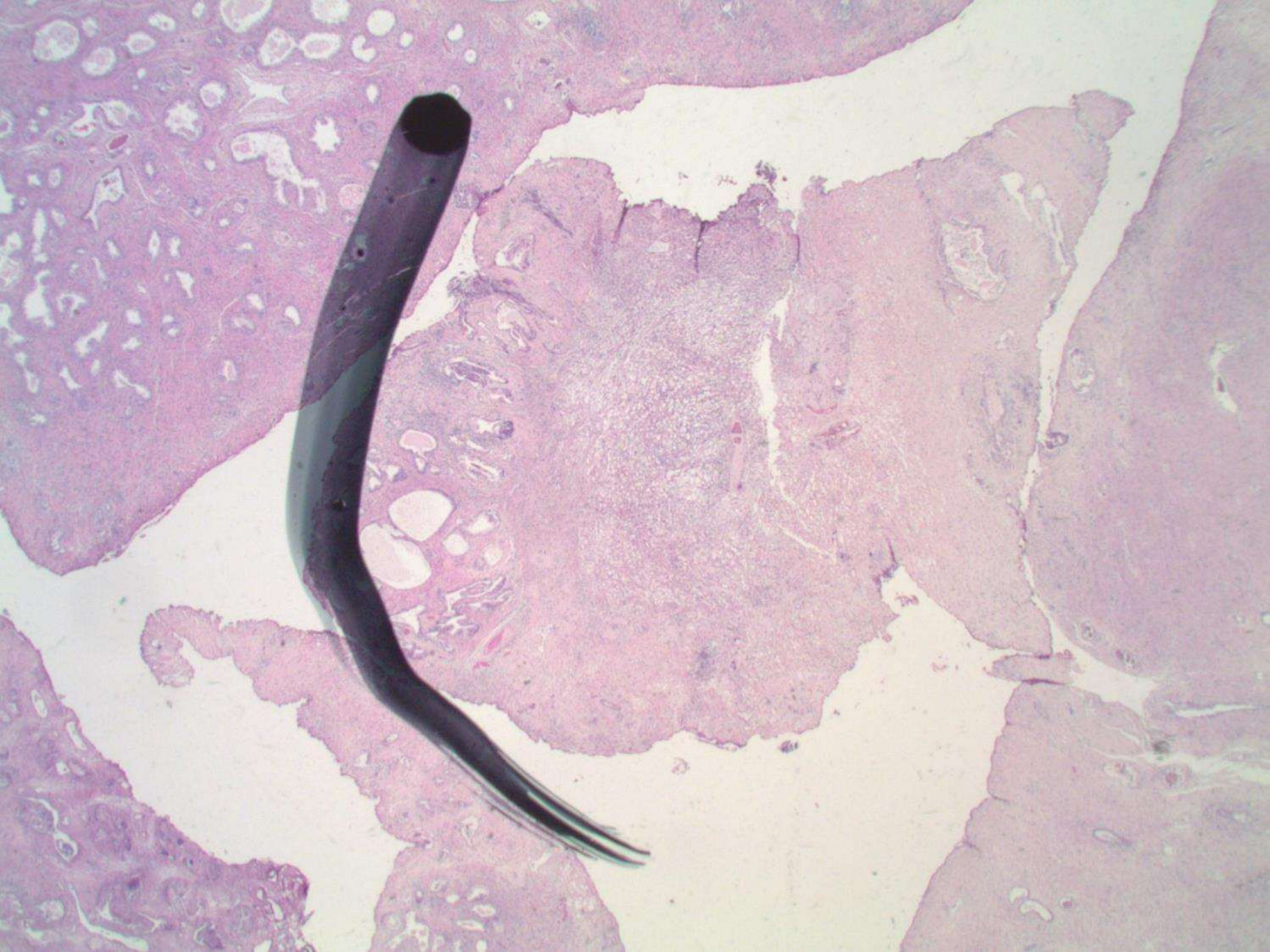

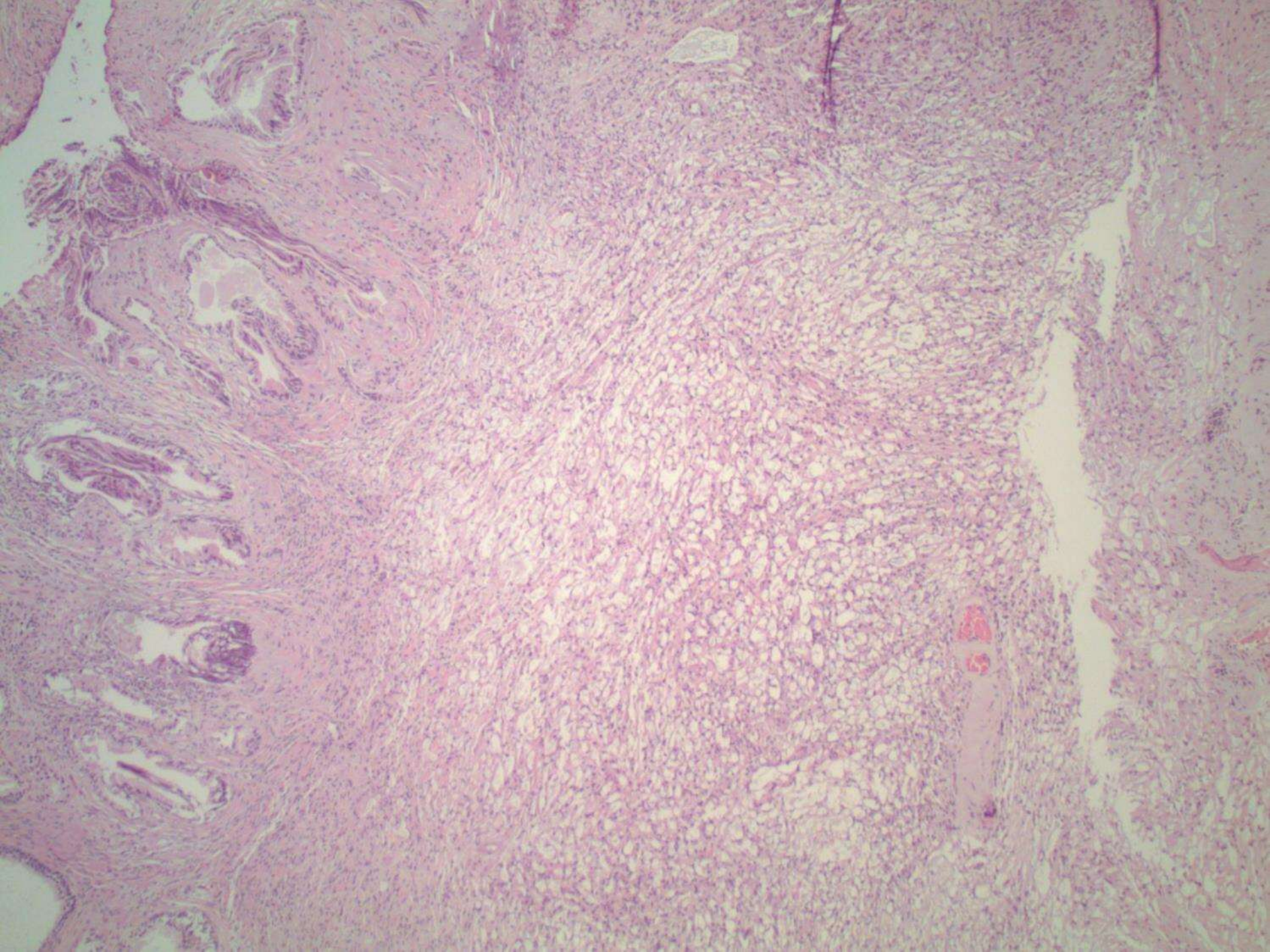

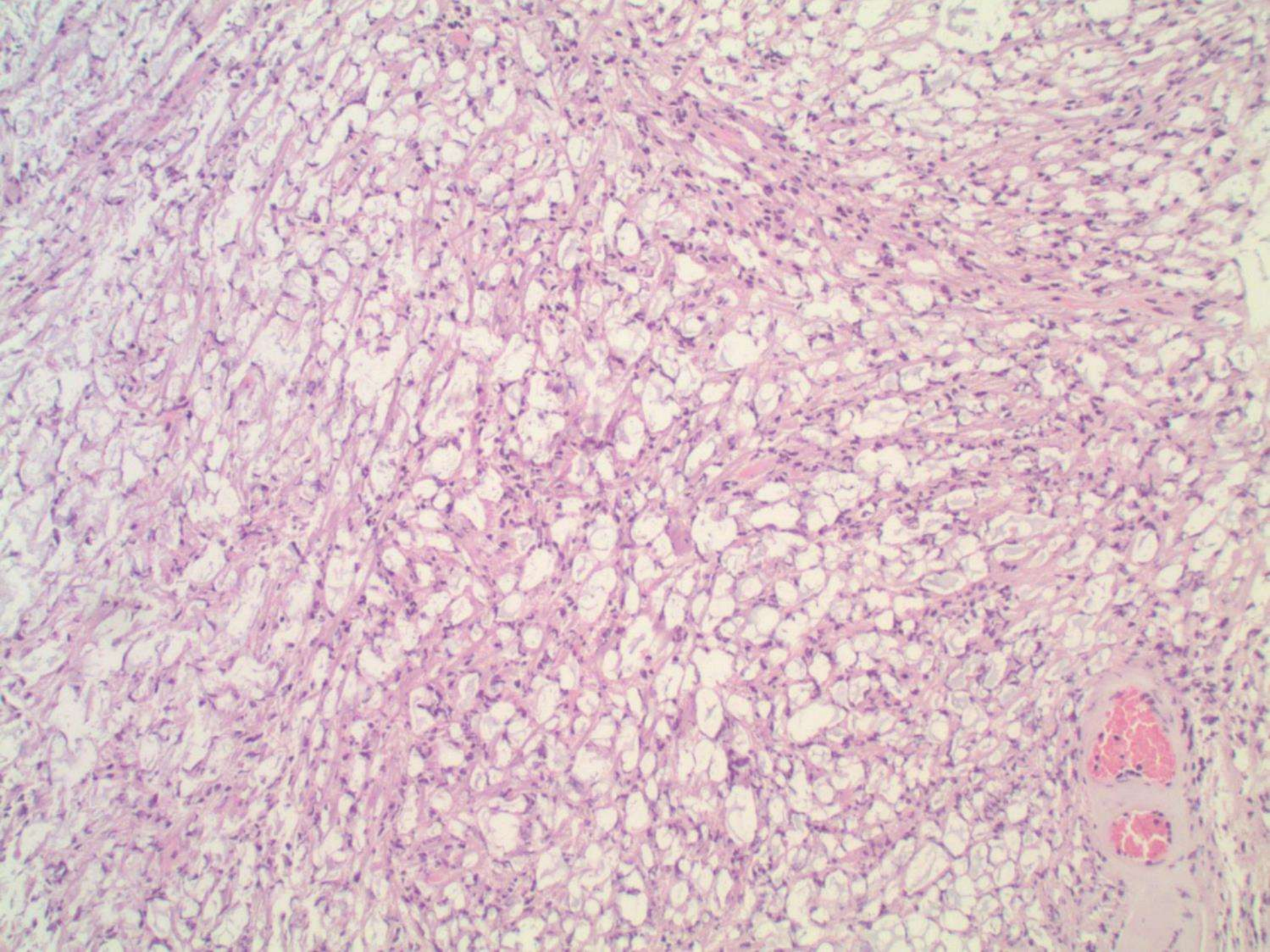

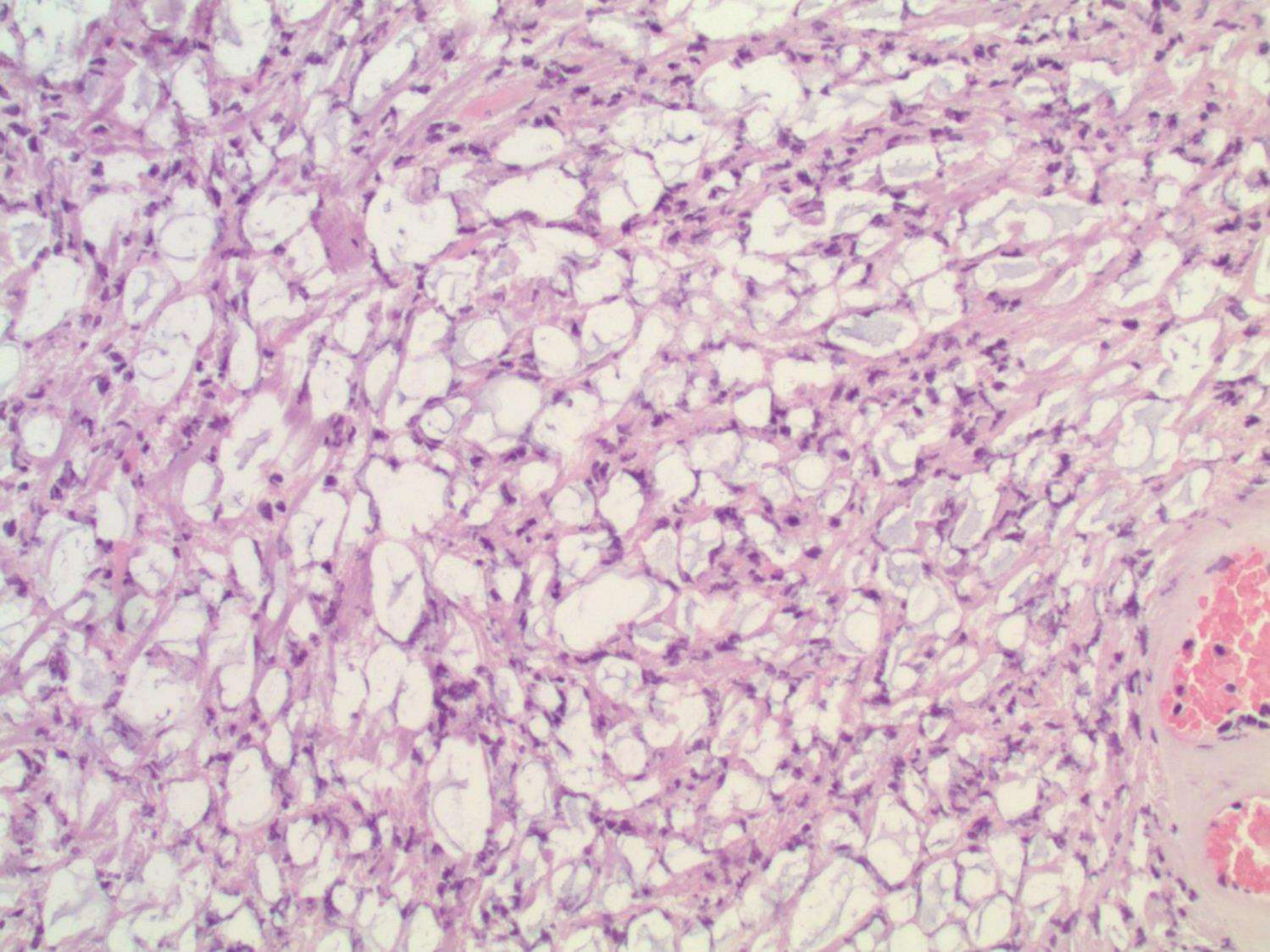

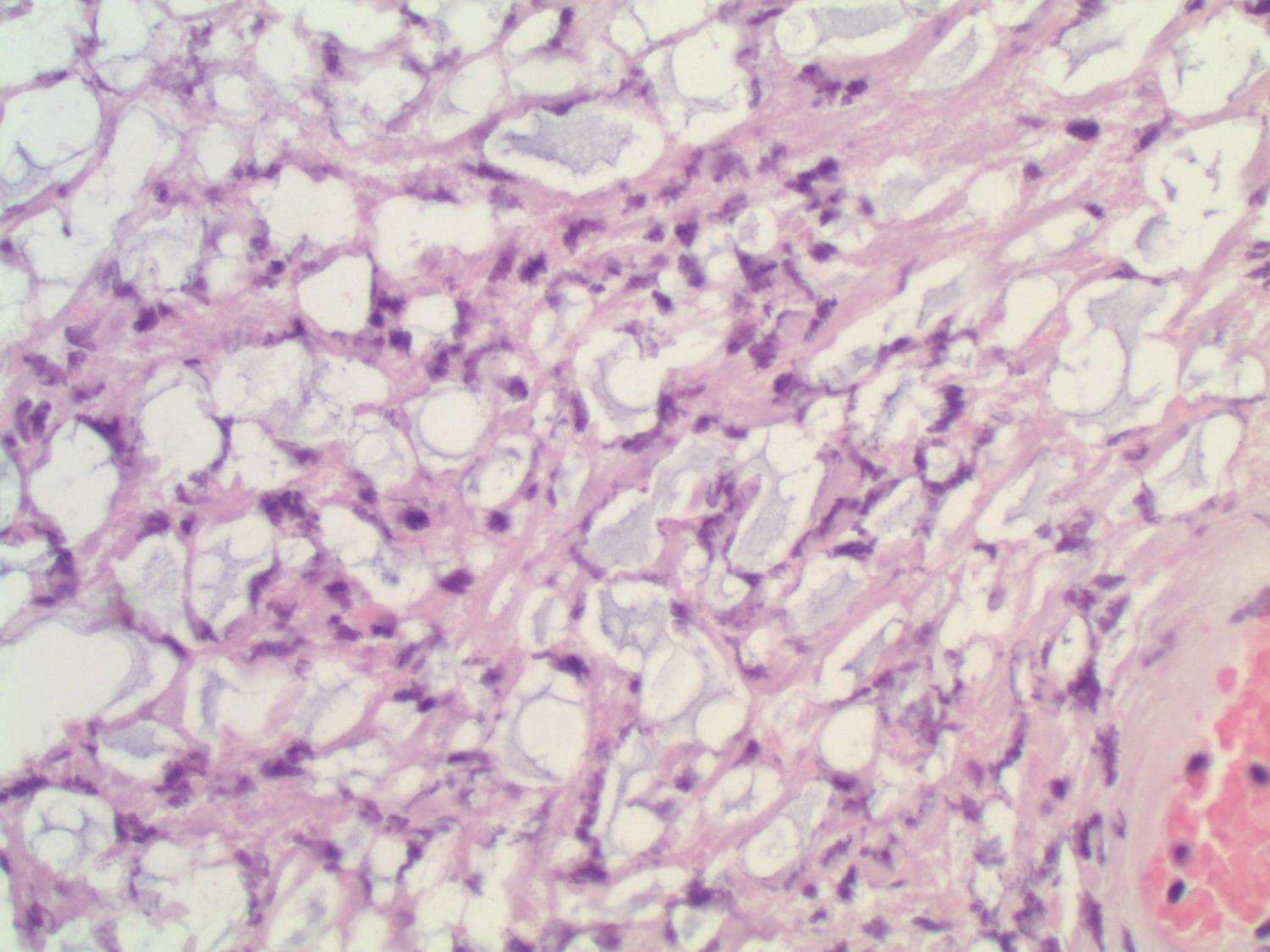

DDx

- **Lymphathic/vascular neoplasm**
- **Fat cells**
- **Inflammatory cells**
- **Nephrogenic adenoma**
- **Adenocarcinoma**
  - Signet ring prostatic adenocarcinoma
  - Signet ring urothelial adenocarcinoma
  - Metastatic signet ring adenocarcinoma
- **Artifact**

IHC:
cystic spaces

- **NEGATIVE:**
  - ERG
  - S100
  - CD45
  - AE1/AE3

International Journal of Surgical Pathology
1–9

DOI: 10.1177/10668969221133349
journals.sagepub.com/home/ijs
SAGE

Artifactual Cystic Spaces in Prostatic Transurethral Resections and Related Specimens: A Potential Diagnostic Confounder

Ankur R. Sangoi, MD[1], Mahmut Akgul, MD[2] and Sean R. Williamson, MD[3]

Abstract

Aims. Histopathologic benign mimickers of prostate cancer have mostly focused on glandular mimics, with non-glandular mimics mainly limited to inflammatory conditions. While there is a paucity of literature recognizing small cystic (presumably artifactual) spaces in transurethral resection specimens, in some instances they can become florid enough to mimic vascular or epithelial neoplasms. Herein, we detailed histologic, immunophenotypic, and clinicopathologic findings in a large series of specimens showing prominent diagnostically confounding cystic spaces. *Methods and Results.* Sixty specimens were obtained (50 transurethral resections, 7 aquablations, 3 laser enucleations), from 17 different surgeons. Seven specimens had concurrent genitourinary pathology (4 prostatic adenocarcinoma, 1 solitary fibrous tumor, 1 prostatic atypia, 1 urothelial carcinoma in situ). The extent of cystic change among overall tissue examined ranged from 1 mm-8 mm (mean 3.4 mm), with luminal content of cystic spaces characterized as empty (72%), both empty and fluid-like (17%), and both empty and mucin-like (11%; mucin histochemical stain was negative on all specimens). Notable differences in degree of tissue cautery artifact or inflammation was not found. Immunohistochemistry performed on 30 specimens showed cystic spaces negative for S100, ERG, pankeratin, and CD45. *Condusion*. Although artifactual in nature, in some instances small cystic spaces encountered in prostatic transurethral resections and more novel related procedures can become florid enough to warrant recognition as a potential diagnostic confounder of vascular or epithelial neoplasms.

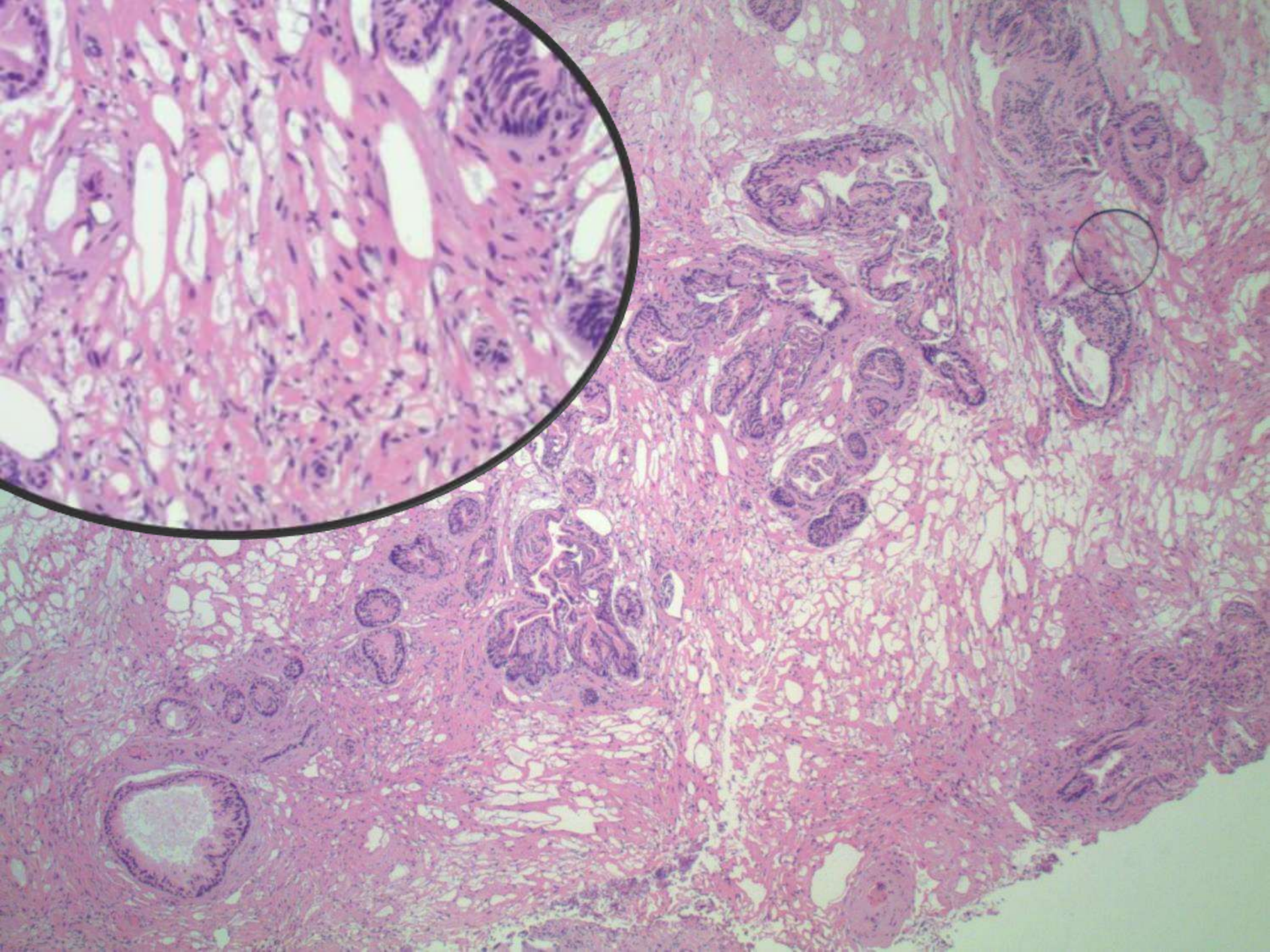

the real PITFALL:

H&E

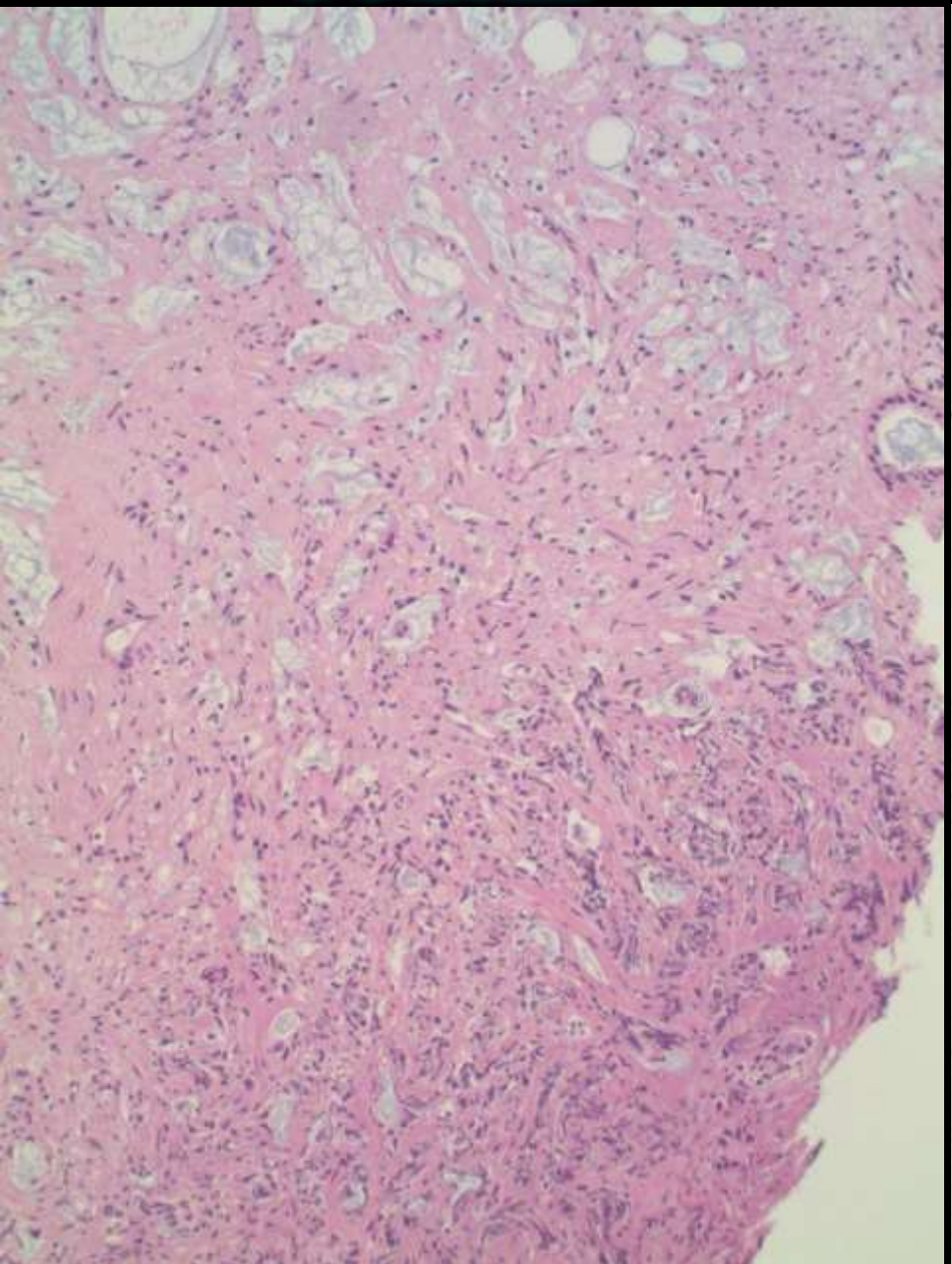

NKX3.1

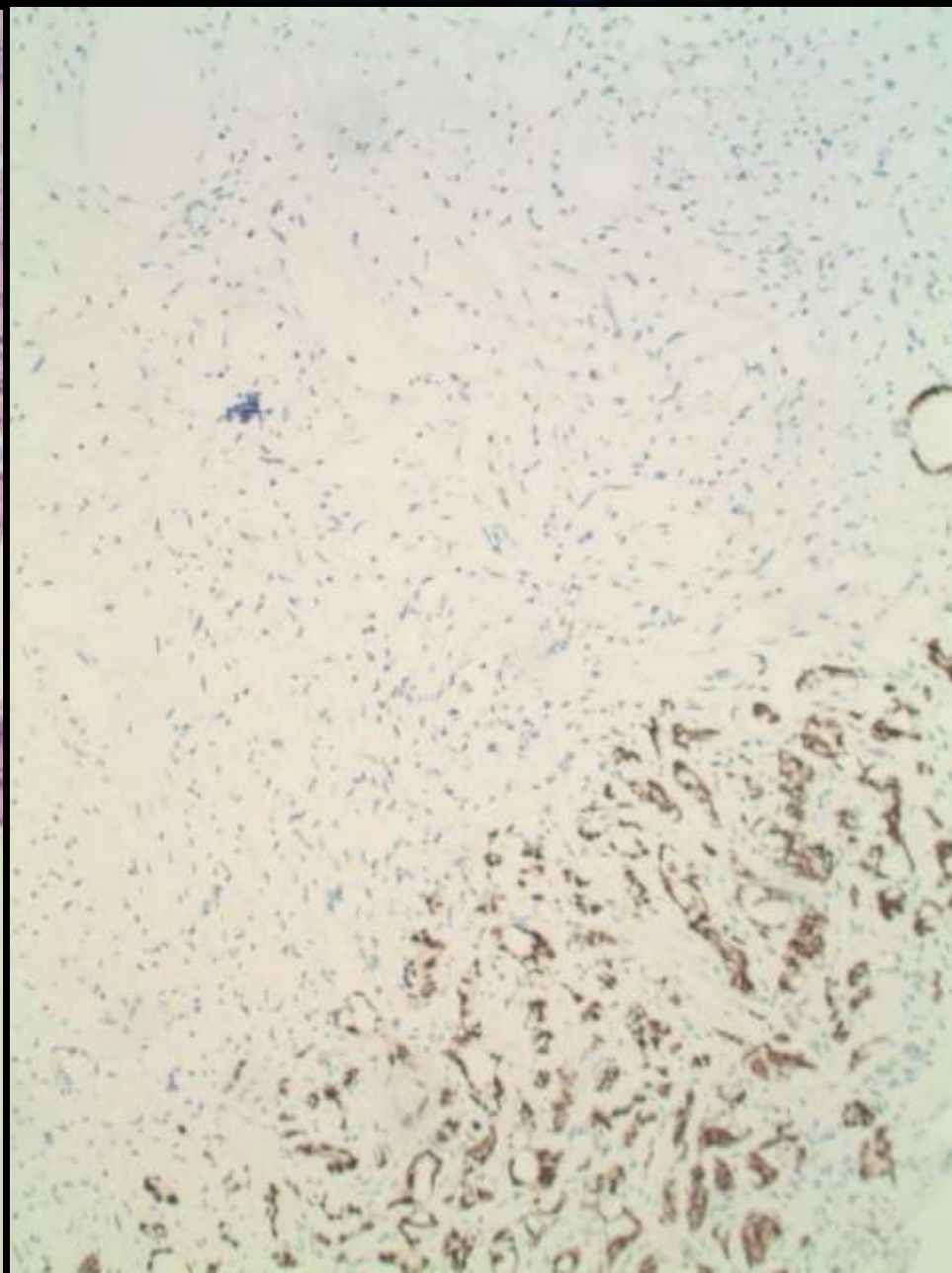

H&E

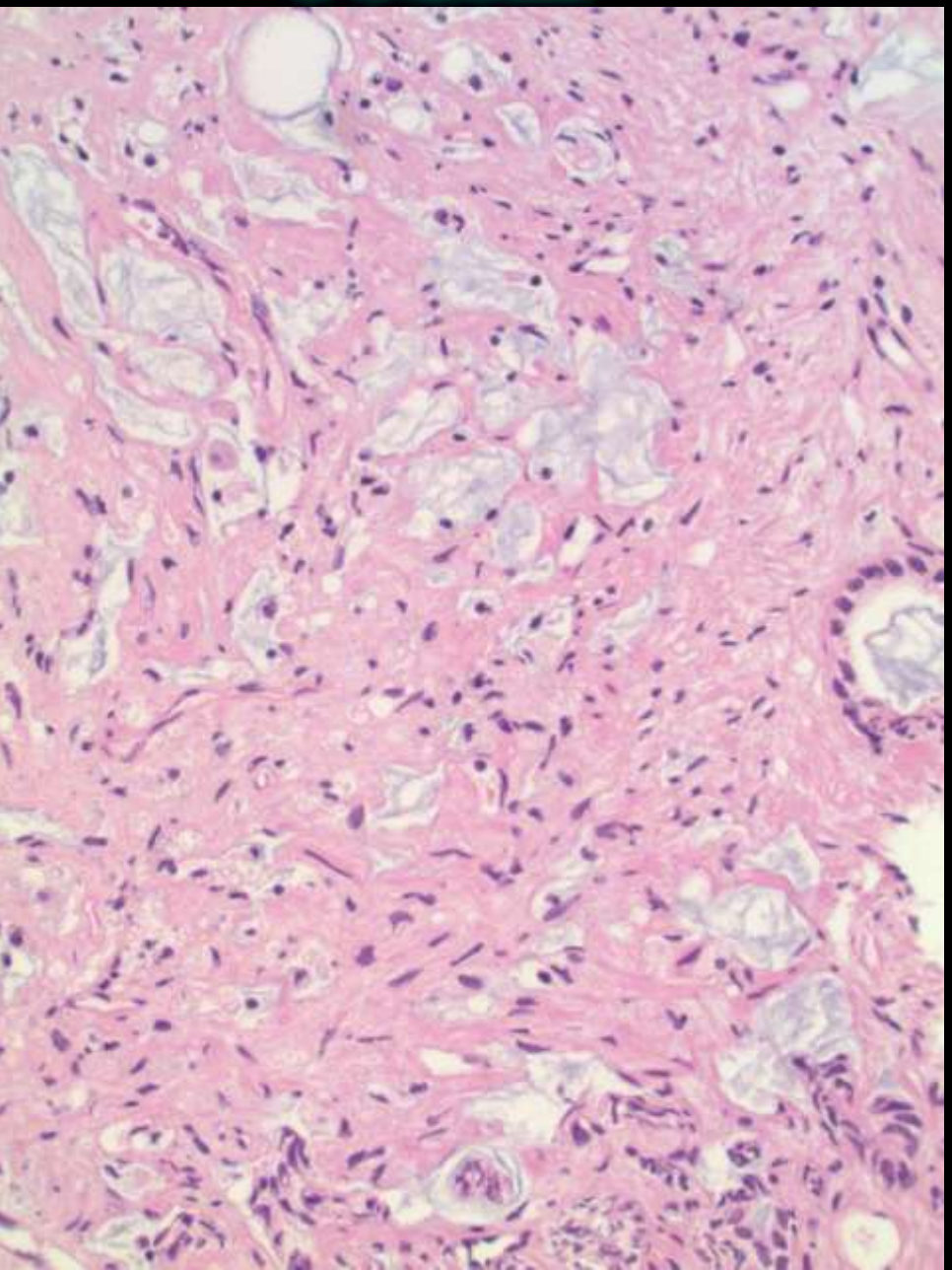

NKX3.1

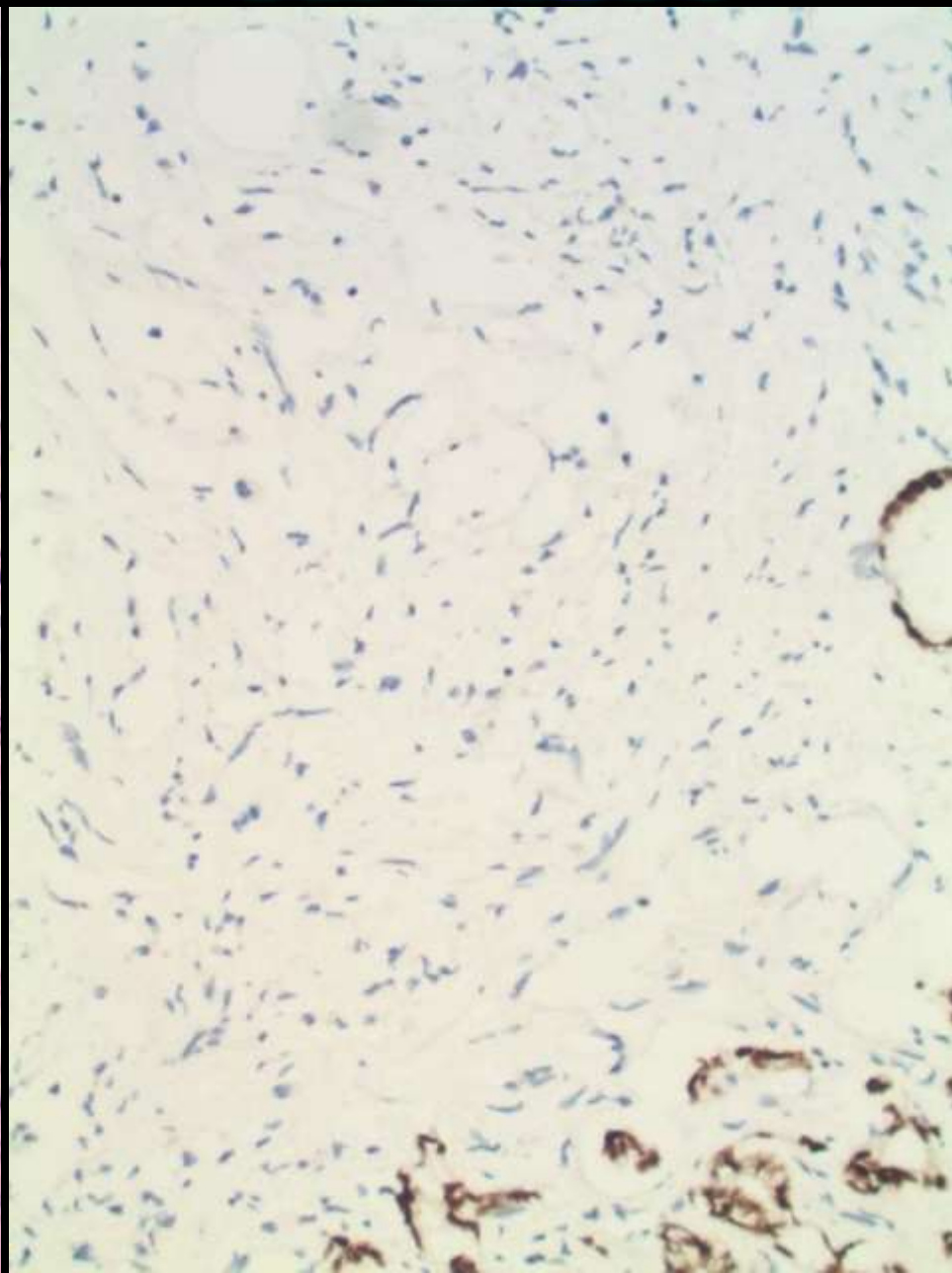

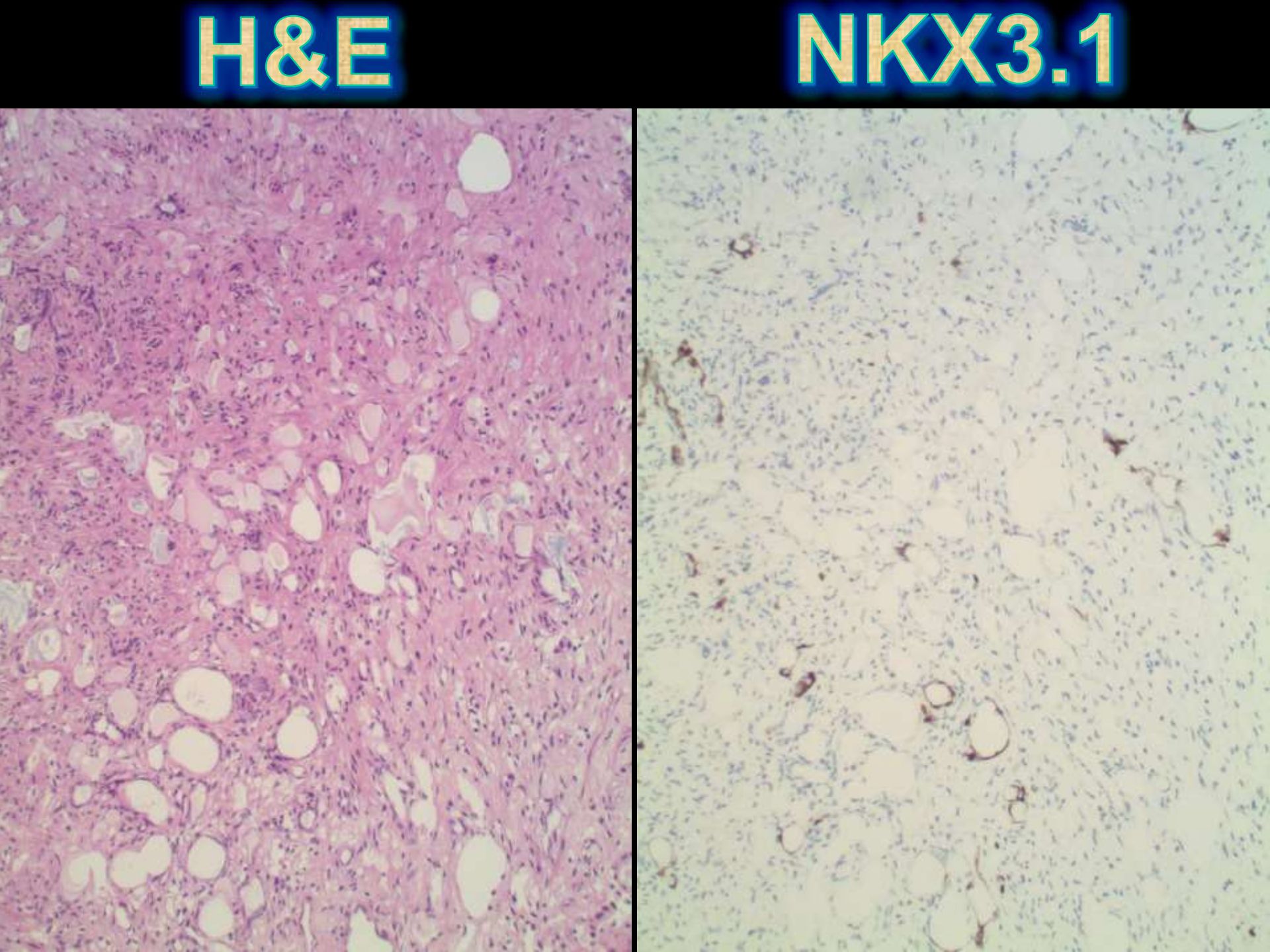
H&E
NKX3.1

H&E

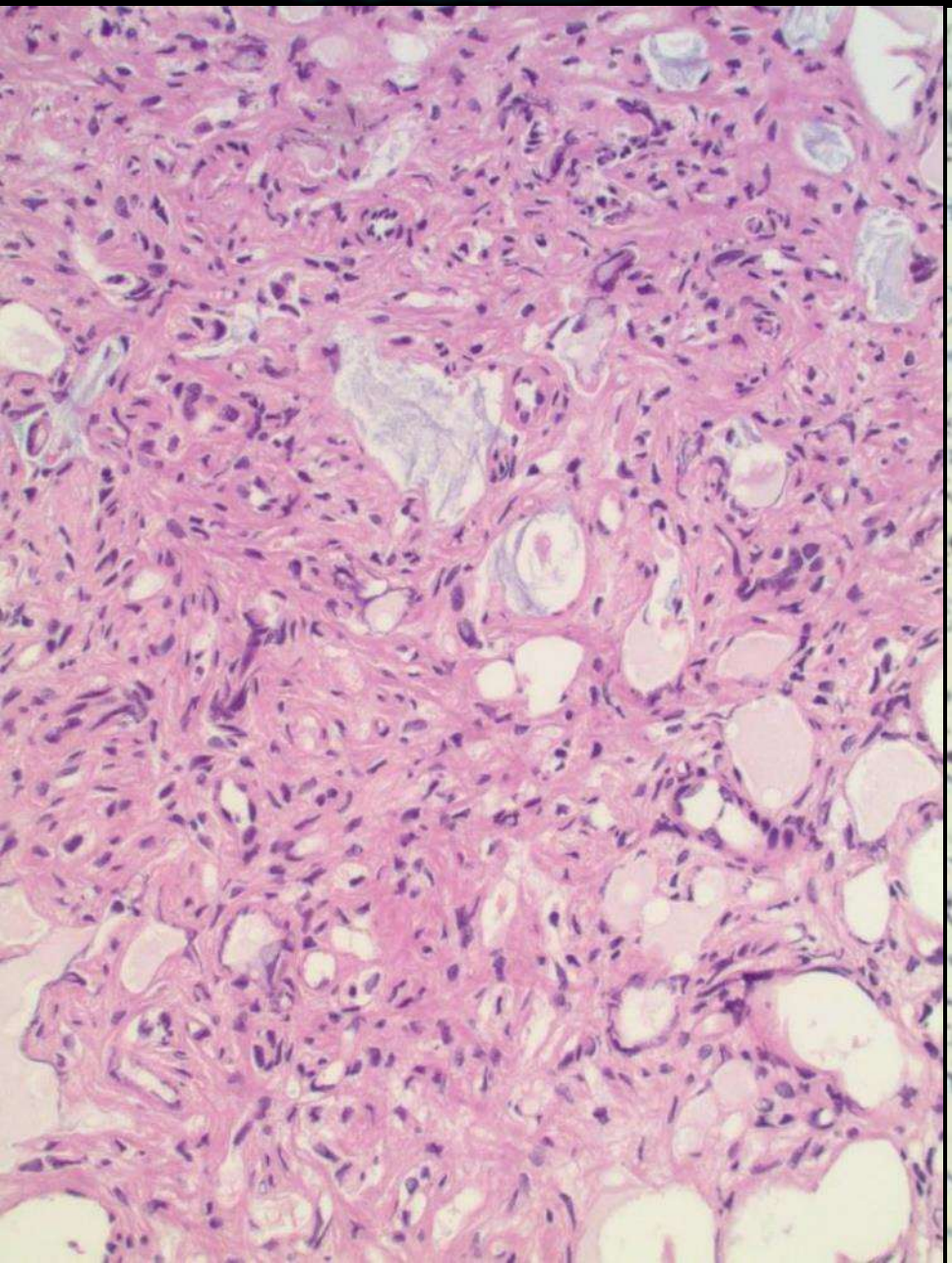

NKX3.1